國立臺灣大學理學院海洋研究所

博士論文

Institute of Oceanography

College of Science

National Taiwan University

Doctoral Dissertation

西北太平洋秋刀魚族群動態與資源評估

Population dynamics and stock assessment of Pacific saury in the Northwestern Pacific Ocean

許蓁

Jhen Hsu

指導教授：張以杰 博士

Advisor: Yi-Jay Chang Ph.D.

中華民國 114 年 1 月

January, 2025

doi:10.6342/NTU202500253

國立臺灣大學博士學位論文
口試委員會審定書

PhD DISSERTATION ACCEPTANCE CERTIFICATE
NATIONAL TAIWAN UNIVERSITY

西北太平洋秋刀魚族群動態與資源評估

Population dynamics and stock assessment of Pacific saury in the Northwestern Pacific Ocean

本論文係許蓁 D07241002 在國立臺灣大學海洋研究所完成之博士學位論文，於民國 114 年 1 月 9 日承下列考試委員審查通過及口試及格，特此證明。

The undersigned, appointed by the Institute of Oceanography on 9, January, 2025 have examined a PhD dissertation entitled above presented by Jhen Hsu D07241002 candidate and hereby certify that it is worthy of acceptance.

口試委員 Oral examination committee:

張以忠

（指導教授 Advisor）

徐志隆　李明安　劉光明

施水銘　謝志豪　黃文卉

系主任/所長 Director: 黃千芬

doi:10.6342/NTU202500253

謝辭

這五六年的時光，內心充滿感激，難以言表。感謝張以杰老師的耐心教導，給予我最正確的學術觀念及寶貴機會，諄諄教誨，以身作則，刀子嘴豆腐心，支持也鼓勵我挑戰自己，增強自己的實力。回頭看這段時光，張老師真的替我開啟了另一道窗，點點滴滴難以言語，感激不盡。感謝 Prof. Punt 在西雅圖時提供了我一個良好的學術環境，在許多我有疑惑之處給予我更清楚的觀念，每一個親切問候都讓我在異鄉的日子多了溫暖。另外，感謝給予我論文寶貴意見的各位委員們：孫志陸老師、李明安老師、劉光明老師、張水鍇老師、黃文彬老師以及謝志豪老師。謝謝孫老師一直以來的鼓勵，還有和師母在生活的關心，不管是在西雅圖或台北；謝謝李老師支持我到台大讀書，我永遠都忘不了老師背著臭豆腐罐頭到西雅圖給我，那個感動永遠忘不了；謝謝劉老師每次的親切問候；謝謝水鍇老師從我碩班到博班口試都沒有缺席；謝謝黃老師一路上在 NPFC 看著我成長。謝謝 Zac 在研究上給予我的好榜樣，一起去濟州島開會時，當我爬山喘不過氣來時，拍拍我要年輕人加油！謝謝蕭仁傑老師，除了鼓勵我外，平常也會給我滿滿的關懷幫助，默默的給我加油打氣。謝謝研究室學弟妹和其他伙伴們：緒邦、坤佑、柏凱、偉哲、正宇、鉦浩、竹珈、昀韋、織宜和冠淳；書妤、李克、子維和呂姐，和大家一起共事，是我博班中最珍貴的資產，我跟著各位一起成長，在互相加油打氣中度過了很多困難，和大家的互動中學習到更多，在我失望絕頂時給予我最及時的溫暖打氣，在 413 的日子真的非常感謝各位，這個難得的緣分和回憶，我很珍惜！感謝 Punt 實驗室的夥伴們：Albi、Grant、Sabrina、Enrico、Juliette、Vale、Lee Qi、Kristin、Terrance、Anna、Han 以及 Kai san, Toshi san, and Jim 在研究上的專業意見。謝謝大學以來不離不棄的長桌會議成員：怡柔、短玎、姵妤、旅瑄和又今，聽著你們的生活總能替我分散一點壓力。謝謝謝瑀、允信、尚融、敬淳和高小姐，因為你們讓我更有勇氣念博班，和你們一起的回憶很單純快樂。謝謝美瑾，在我總是找不人可以講話時，永遠說你有空，可以聽我說，給予我不一樣的想法和意見。謝謝涵晴、東協、尉任學長、施總及漁業署給我的支持和疼愛。謝謝從小到大的好晴人－開薇、冠蓁、郁婕，即使不常見面，但不管我去哪總有你們的暖心。謝謝爸媽給我最無後顧之憂的支持，提供我很好的環境跟教育，鼓勵我正向思考，您們一直不斷學習的精神是我的好榜樣。謝謝我兩位好妹妹：許藁和許葭，可愛的劉奶糖和奕為，生活的打打鬧鬧，讓我在壓力中多了很多調劑。謝謝你總是我最溫暖及穩定的力量。最後，謝謝我自己能秉持著一直堅持下去的信念，這段求學過程雖然充滿挑戰，但能看見自己的成長與蛻變，是我永遠不會後悔的選擇。這不是終點，而是新的開始。我會秉持初衷，繼續在學術道路上精進，期待未來的每一步，謝謝每位支持我的人。

許藁 Jan, 21, 2025

doi:10.6342/NTU202500253

Acknowledgments

At this significant milestone of completing my Ph.D., I am filled with profound gratitude for the guidance and support I have received throughout this journey. I extend my deepest appreciation to my advisor, Dr. Yi-Jay Chang, whose mentorship has shaped my academic path and opened new horizons. I am equally grateful to Professor André E. Punt for providing an enriching research environment during my time at the University of Washington.

My sincere thanks to my committee members - Professors Chih-Lu Sun, Ming-An Lee, Kwang-Ming Liu, Shui-Kai Chang, Wen-Bin Huang, and Chih-hao Hsieh - for their valuable insights and guidance. I particularly thank Professor Jen-Chieh Shiao for his continuous encouragement and support throughout my studies.

The collaborative spirit and friendship of my colleagues have been invaluable. I am grateful to my labmates in Room 413. I also thank the members of the Punt lab - Albi, Grant, Sabrina, Enrico, Juliette, Vale, Lee Qi, Kristin, Terrance, Anna, and Han. And other Professors - Toshi-san, Kai-san, and Jim - for enriching my research experience.

To my friends, family, and particularly my parents and sisters, your unwavering support and encouragement have been my foundation throughout this journey. While this marks the completion of my doctoral studies, I look forward to continuing my academic pursuits with the same passion and dedication.

doi:10.6342/NTU202500253

Table of contents

摘要 ..... **i**

Abstract ..... **ii**

General introduction **1**

1. Chapter 1 − Numerical approach for estimating the probable distribution of steepness **8**

Abstract 8

1.1. Introduction 9

1.2 Material and methods 12

1.3. Results 18

1.4. Discussion 21

1.5. Conclusions 25

2. Chapter 2 − Evaluation of the influence of spatial treatments on catch-per-unit-effort standardization with fishery application and simulation study **26**

Abstract 26

2.1. Introduction 28

2.2. Materials and methods 31

2.3. Results 45

2.4. Discussion 50

2.5. Conclusions 55

3. Chapter 3 − Investigating the drivers of spatial distribution shifts by using spatio-temporal modelling approach **57**

Abstract 57

3.1. Introduction 58

3.2. Materials and methods 60

3.3. Results 66

3.4. Discussion 68

doi:10.6342/NTU202500253

4. Chapter 4 − Stock assessment and addressing the impacts of uncertainty on recovery 73
Abstract 73
4.1. Introduction 74
4.2. Materials and methods 75
4.3. Results 81
4.4. Discussion 84
4.5. Conclusion 87
5. Chapter 5 − Summary and recommendations 89
5.1. Summary 89
5.2. Recommendations 90
References 95
Tables 114
Figures 125
Appendix tables 166
Appendix figures 169
Curriculum Vitae 184

doi:10.6342/NTU202500253

List of tables

Table 1.1. Mean values of the life history parameters used to calculate distributions of stock-recruitment steepness for the Pacific saury 114
Table 1.2. The mean values for main life history parameters are multiplied by and their coefficient of variation for the five scenarios for the Pacific saury 115
Table 2.1. Summary statistics of Ad hoc, Binary, Spatial 1, Spatial 0.1 GLMMs, and VAST fitted to Pacific saury CPUE data. 116
Table 2.2. Summary of the explanatory power and overall influence for each variable considered in the Ad hoc, Binary, Spatial 1, Spatial 0.1 GLMMs, and VAST by using the Pacific saury data.. 117
Table 3.1. Mechanisms and quantitative tests of each hypothesized driver that may affect the distribution of Pacific saury in the Northwestern Pacific Ocean..... 118
Table 4.1. Descriptions of fisheries catch, abundance indices, and length composition data included in the model for the Pacific saury stock assessment..... 119
Table 4.2. Life history and recruitment parameters for the Pacific saury assessment model. 120
Table 4.3. Fishery-specific selectivity assumptions for the Pacific saury stock assessment. 121
Table 4.4. Estimated reference points derived from the Stock Synthesis model for Pacific saury. 122
Table 4.5. Projected results of Pacific saury spawning stock biomass and catch during 2023 – 2027 under deterministic projection. 123
Table 4.6. Projected results of Pacific saury spawning stock biomass and catch during 2023 – 2027 under stochastic projection. 124

doi:10.6342/NTU202500253

List of figures

Figure 1.1. General design of the simulation study. 125
Figure 1.2. The daily natural mortality of fish in the early-life phase. 126
Figure 1.3. The biological information is used to derive the distribution of steepness 127
Figure 1.4. Empirical probability density distribution of stock-recruitment steepness saury. 128
Figure 1.5. Estimated stock-recruitment curve. 129
Figure 1.6. The elasticity of steepness for baseline life-history parameter values. 130
Figure 1.7. Boxplots of steepness under the five environmental scenarios. 131
Figure 2.1. The resulting area stratifications with boxplots of observed CPUEs. 132
Figure 2.2. Annual trends of the relative standardized abundance indices. 133
Figure 2.3. Annual influence of each variable for each spatial treatment. 134
Figure 2.4. The coefficient-distribution-influence (CDI) plot of the spatial random effect for spatially stratified models. 135
Figure 2.5. The coefficient-distribution-influence (CDI) plot of the spatial random effect for the VAST model. 136
Figure 2.6. The coefficient-distribution-influence (CDI) of the year × spatial interaction random effect for spatially stratified models. 137
Figure 2.7. The coefficient-distribution-influence (CDI) plot of spatio-temporal random effect for the VAST model. 138
Figure 2.8. Time series of relative error (RE) in the index of abundance. 139
Figure 2.9. The boxplots of performance metrics for each spatial treatment. 140
Figure 3.1. The spatial distribution of knots and mesh used to fit the spatio-temporal model. 141
Figure 3.2. The magnitude of 2-dimensional spatial autocorrelation. 142
Figure 3.3. Spatiotemporal distributions of the log-transformed density. 143
Figure 3.4. The time-series of the index of relative abundance from VAST. 144
Figure 3.5. The time-series of the estimated centroids of gravities (COGs). 145
Figure 3.6. Estimated log-density in 2001, 2006, 2010, and 2017 from the best model. 146
Figure 3.7. The estimated centroids-of-gravity (COGs) during 2001 – 2017 . 147

doi:10.6342/NTU202500253

Figure 4.1. The spatial boundary of Pacific saury assessment. 148
Figure 4.2. Catches, abundance indices, and length composition in the stock assessment.. 149
Figure 4.3. Time-series of catches during 1980 – 2022 by the fleets. 150
Figure 4.4. Time-series of relative standardized CPUEs during 1980 – 2022. 151
Figure 4.5. Length composition data by fisheries. 152
Figure 4.6. The flowchart of the stochastic projection for the Pacific saury. 153
Figure 4.7. Fit to the early and late Japan, Taiwan and Korea indices..... 154
Figure 4.8. Fit to Russia, China and Japanese biomass survey indices. 155
Figure 4.9. Results from a runs test for each CPUE index. 156
Figure 4.10. The estimated selectivity curve for each fleet. 157
Figure 4.11. The estimated selectivity curve for each survey. 158
Figure 4.12. Aggregate length composition data for stock assessment. 159
Figure 4.13. The quarterly residuals for Japan and Taiwan length composition data..... 160
Figure 4.14. Results from a runs test for each length composition time series. 161
Figure 4.15. Profiles of the relative-negative log-likelihoods for the virgin recruitment in log-scale. 162
Figure 4.16. Estimated time-series of total biomass, spawning biomass, recruitment, and instantaneous fishing mortality.. 163
Figure 4.17. Forecasted spawning biomass and catch under three fishing mortality scenarios using a deterministic approach. 164
Figure 4.18. Forecasted spawning biomass and catch under three fishing mortality scenarios using a stochastic approach. 165

doi:10.6342/NTU202500253

摘要

秋刀魚（*Cololabis saira*）為西北太平洋海域重要之國際漁業資源，其短壽命的生活史特性使族群時空動態易受環境變遷影響。近年來漁獲量持續下降，本研究建構完整之資源評估理論架構，針對秋刀魚族群動態進行方法學改善，以期對此資源有更全面之掌握。本研究從四個面向探討影響秋刀魚資源評估之關鍵要素：首先，運用演化生態學和生殖生物學之數值模擬分析，評估族群加入量（recruitment）之韌性（resilience），此方法解決漁業資源評估常因缺乏可靠且長期的產卵親魚量與入添量數據，而導致族群韌性估計存在高度不確定性之挑戰。結果顯示陡度（steepness）中位數為0.82（80%可能範圍：0.59 − 0.93），代表即使族群產卵親魚量降至未開發時之20%，仍可維持相對高比例的加入量。敏感度分析指出，陡度受幼生死亡率、平均體重、成長和性成熟體長等因素影響最顯著，而不利的環境條件可能透過影響這些參數而降低族群韌性。其次，應用廣義線性混合模型（Generalized Linear Mixed Models，GLMMs）評估不同空間處理方法對單位努力漁獲量（catch-per-unit-effort，CPUE）標準化之影響。研究發現豐度主要受時空效應影響，可能源於漁撈活動或魚群分布之時空變動。在實際漁業資料和模擬研究中，向量自回歸時空模型（Vector Autoregressive Spatio-Temporal，VAST）均優於傳統空間分區方法。當遇優先採樣情況，空間集群分析法中之Spatial1（魚類密度權重低）可作為VAST之替代方案。第三，運用VAST評估秋刀魚之時空動態。結果顯示族群分布重心在2013年後明顯由日本沿岸向公海東移，2017年更出現豐度顯著下降及進一步東移現象。研究發現此分布變化無法單由海洋環境因子或氣候變異指數解釋，推測可能與種間競爭、公海漁獲壓力增加或複雜海洋動態等因素相關。最後，開發秋刀魚年齡結構模型，並考慮諸多未確定性來源與加入量的過程誤差（process error）進行未來族群量預測。評估結果顯示近年產卵親魚量降至歷史低位，低於最大可持續生產量水準（SSB_{MSY}）。儘管目前漁獲死亡率仍低於F_{MSY}，預測結果顯示可能需要更保守的漁獲狀況以利資源恢復。其中，採用$0.5F_{MSY}$情境顯示最高機率維持資源量於SSB_{MSY}以上。本研究深化了對秋刀魚族群動態的理解，並改進了資源評估方法。研究成果強調在發展有效漁業管理策略時，應充分考量環境變異性、空間分布型態及參數不確定性之重要性。研究成果除可為西北太平洋秋刀魚之永續經營提供科學基礎外，所建立之方法論架構亦可作為其他類似漁業資源評估改進之參考。

關鍵字：秋刀魚、韌性、空間異值性、時空模型、未確定性、年齡結構模型、資源評估

doi:10.6342/NTU202500253

Abstract

Pacific saury (*Cololabis saira*) is an important international fishery resource in the Northwestern Pacific Ocean. Its short-lived life history characteristics make its population dynamics particularly susceptible to environmental changes. In response to recent declining catches, this study developed a comprehensive stock assessment framework, advancing methodological approaches to better understand Pacific saury population dynamics. This study systematically investigated four critical aspects of Pacific saury stock assessment. First, this study employed numerical simulation analyses integrating evolutionary ecology and reproductive biology to evaluate population recruitment resilience. This approach addressed a fundamental challenge in fisheries assessment: the high uncertainty in resilience estimation due to limited long-term data on spawning stock biomass and recruitment. Results suggested a median steepness of 0.82 (80% probable range 0.59, 0.93), indicating substantial recruitment capacity even when spawning biomass decreases to 20% of its unexploited level. Sensitivity analyses identified survival rate of early-life stages, mean body weight, growth, and length at maturity as key determinants of steepness, with unfavorable environmental conditions potentially compromising population resilience through these parameters. Second, this study evaluated the impact of spatial treatments on catch-per-unit-effort (CPUE) standardization using Generalized Linear Mixed Models (GLMMs). The analysis demonstrated that abundance was predominantly influenced by spatiotemporal effects, likely reflecting temporal shifts in fishing activities and fish distribution patterns. The Vector Autoregressive Spatio-Temporal (VAST) model consistently outperformed traditional methods in both empirical and simulation studies. For scenarios involving preferential sampling, the Spatial1 approach (incorporating low fish density weighting) emerged as a viable alternative to VAST. Third, the VAST analysis of spatiotemporal dynamics indicated a significant eastward shift in Pacific saury's distribution from Japanese coastal waters to the high seas after 2013, followed by further abundance declines and eastward movement in 2017. Notably, these distributional changes could not be adequately explained by oceanic environmental factors or climate variability indices, suggesting potential influences from interspecific competition, increased high-seas fishing pressure, or complex oceanographic processes. Finally, this study developed an age-structured model incorporating multiple

doi:10.6342/NTU202500253

uncertainty sources and recruitment process error for forecast projections. The assessment indicated a historical low in recent spawning stock biomass, falling below SSB_{MSY}. Despite current fishing mortality remaining below F_{MSY}, projections suggested the need for more conservative harvest rates to facilitate stock recovery, with the $0.5F_{MSY}$ scenario showing the highest probability of maintaining stock above SSB_{MSY}. This research enhances the understanding of Pacific saury population dynamics while advancing stock assessment and management methodologies. The findings highlighted the importance of integrating environmental variability, spatial distribution patterns, and parameter uncertainty into effective fisheries management strategies. Beyond its application to Pacific saury, the established methodological framework provides valuable insights for improving stock assessments of similar fisheries worldwide.

Keywords: Pacific saury, resilience, spatial heterogeneity, spatio-temporal modelling, uncertainty, age-structured model, stock assessment

doi:10.6342/NTU202500253

General introduction

The stock assessment process serves as a comprehensive framework for evaluating fish population dynamics, playing a critical role in supporting sustainable fisheries management (Beverton and Holt, 1957). This framework integrates several elements, including diverse data sources and advanced modelling approaches, to deliver a comprehensive and holistic understanding of stock status, ensuring informed decision-making for effective fishery management. Key inputs include catch data, which encompass commercial, recreational, and bycatch information; biological parameters such as natural mortality, growth, maturity, and recruitment; and indices of relative abundance derived from surveys, fishery catch-per-unit-effort (CPUE), and age or size distribution data. These datasets inform population models that estimate time-series trends in fish biomass and fishing mortality, complemented by advanced models that account for habitat, climate variability, ecosystem interactions, and anthropogenic stressors. The ultimate goal of the stock assessment process is to determine the status of the stock - assessing whether it is overfished or experiencing overfishing − and to generate forecasts that inform the establishment of annual catch limits to promote long-term sustainability. Although significant progress has been made in stock assessment methodologies, ongoing advancements in quantitative fisheries modelling, such as improved standardization of indices of relative abundance and refinement of stock assessment methods, continue to enhance the accuracy and reliability of each element within the process. These efforts aim to further optimize the integration of data sources, models, and inputs, ensuring that the stock assessment framework remains robust and adaptive to evolving scientific and management needs.

Pacific saury (*Cololabis saira*) is a highly migratory small pelagic fish species of significant commercial importance, distributed from coastal to open waters across the North Pacific Ocean (Hubbs and Wisner, 1980). With a short lifespan of two years (Suyama et al., 2006), Pacific saury undergoes seasonal migrations between subarctic and subtropical regions (Fukushima, 1979). Spawning occurs in subtropical waters from autumn to spring, over an extensive area (Iwahashi et al., 2006; Fuji et al., 2021). During spring, larvae and juveniles migrate northward, growing as they reach subarctic areas by

doi:10.6342/NTU202500253

late summer (Kosaka, 2000). By winter, the species migrates southward to subtropical spawning grounds (Miyamoto et al., 2019; Fuji et al., 2021). The spawning season lasts approximately 10 months, with winter being the peak period, characterized by the largest mature adult size range and highest larval densities (Kosaka, 2000; Suyama, 2002; Watanabe and Lo, 1989). The main fishing grounds for Pacific saury are located in the Northwestern Pacific Ocean during summer and autumn (Kosaka, 2000). The species is commercially harvested by Japan, Russia, Korea, China, Taiwan, and Vanuatu, with total annual catches fluctuating over the past three decades, from a peak of 629,576 tons in 2014 to a low of 332,886 tons in 2022 (NPFC, 2023a). While Japan and Russia primarily fish within their exclusive economic zones (EEZs), other countries operate in the high seas of the Northwestern Pacific Ocean. Due to its short lifespan, the fishery predominantly targets one-year-old individuals.

To promote the sustainability of Pacific saury fisheries, regional organizations such as the North Pacific Fisheries Commission (NPFC) implement management measures, including catch quotas, regulation of fishing vessels, and monitoring requirements to mitigate ecosystem impacts and maintain long-term fishery viability (NPFC, 2023b). Despite these efforts, including comprehensive stock assessments using surplus production models, the Pacific saury population has experienced declining biomass in recent years (NPFC, 2019). Addressing this issue requires an improved understanding of how Pacific saury responds to environmental changes and the adoption of enhanced stock assessment approaches, such as age-structured models. These advancements are essential to ensure that management strategies remain effective in maintaining the adaptive capacity of Pacific saury populations.

This dissertation focuses on improving the methodology of elements within the stock assessment process, using Pacific saury in the Northwestern Pacific Ocean as a case study. This study aims to develop and evaluate improved methods for understanding fish and fisheries dynamics, ultimately contributing to more effective fisheries management. Five chapters are organized into this study, each presenting advanced modelling approaches designed to reduce uncertainty by quantifying the impacts of various factors and improving the stock assessment of Pacific saury.

doi:10.6342/NTU202500253

Chapter 1 − Numerical approach for estimating the probable distribution of steepness

The first chapter focuses on the biological component of the stock assessment process, specifically investigating the stock-recruitment relationship for Pacific saury. Stock resilience, often represented by the steepness of the stock-recruitment relationship, is a critical factor in determining stock size, yield, and management objectives. When overexploitation reduces population size, the stock's ability to recover, or resilience, becomes vital for successful restoration. Steepness (*h*; Mace and Doonan, 1988; Francis, 1992) is a commonly used measure of stock resilience, but its estimation is often uncertain due to limited data availability and high variability. Previous studies have shown that misspecifying the steepness value or range can significantly affect stock assessment results and delay the rebuilding of depleted fish stocks (Brodziak and Legault, 2005; Piner et al., 2011). Additionally, directly estimating stock resilience is often impractical, as it requires extensive data collection on spawning biomass and recruitment, which is resource-intensive and challenging to obtain. Since steepness is closely tied to the evolutionary ecology and reproductive biology of a fish stock, understanding its nature is crucial for effective management (Morgan, 2008; Mangel et al., 2013). Numerical approaches offer a practical alternative for estimating steepness by using life history parameters of fish species (e.g., He et al., 2006; Mangel et al., 2010). However, environmental changes, such as climate variability, can alter key life history traits (e.g., growth and maturity, Doney et al., 2012), introducing further uncertainty in resilience estimates and potentially impacting sustainable catch levels.

This chapter aims to address the knowledge gap regarding the variability of steepness in small pelagic fish, such as Pacific saury, in response to environmental changes. Using an individual-based simulation approach, this study estimates the empirical probability distribution of baseline steepness for Pacific saury, identifies the role of life history parameters in determining steepness, and evaluates the impacts of environmental changes on its estimation. Additionally, the study provides a practical framework that can be applied to estimate the steepness of other small pelagic fish species, contributing to improved stock assessment and management strategies.

doi:10.6342/NTU202500253

Chapter 2 − Evaluation of the influence of spatial treatments on catch-per-unit-effort standardization with fishery application and simulation study

The second chapter examines the abundance element of the stock assessment process, with a particular focus on the impact of spatial treatments on the standardization of CPUE. Commercial fishery-dependent CPUE data are commonly used as a relative abundance index in fisheries where regular surveys are impractical (Hilborn and Walters, 1992; Maunder and Punt, 2004). However, raw CPUE data must undergo standardization to address the spatial and temporal variability in fishing behavior and gear configuration (Campbell, 2004; Maunder and Punt, 2004; Maunder et al., 2006). Additionally, preferential sampling and the non-random spatial distribution of fish can cause certain fishing locations to disproportionately influence estimated fish abundance (Rose et al., 1991; Conn et al., 2017; Ducharme-Barth et al., 2022). Therefore, it is important to adjust for the spatial heterogeneity of CPUE data for standardization purposes. The ad hoc grid-based strata are commonly used (e.g., Quinn et al., 1982; Nakano, 1998), but constructing objective and appropriate spatial strata is challenging and may introduce biases into the relative abundance index. Developing and evaluating alternative methods for defining spatial strata objectively can help mitigate biases associated with ad hoc stratification.

This chapter aims to evaluate the effect of various spatial treatments on CPUE standardization using data from the Pacific saury fishery as a case study. Generalized Linear Mixed Models (GLMMs) were employed to compare the statistical performance of four different spatial treatments (i.e., Ad hoc, Binary, Spatial clustering, spatio-temporal modelling approaches), and influence plots were used to assess the impact of explanatory variables. Additionally, a simulation was developed to test the four spatial treatments under two contrasting sampling scenarios − random and preferential. The results of this study are relevant to other fisheries with similar data and provide guidance on the appropriate handling of spatial effects in CPUE standardization.

Chapter 3 − Investigating the drivers of spatial distribution shifts by using spatio-temporal modelling approach

The third chapter further explore the abundance element of the stock assessment process, focusing on the drivers of spatial distribution shifts using a geostatistical modeling

doi:10.6342/NTU202500253

approach. Species distribution models are widely used to analyze the relationship between fish density and environmental variables (e.g., Chang et al., 2019) and to project spatial distribution patterns under climate change scenarios. However, the risks associated with misspecifying environmental relationships within species distribution models have been rarely assessed (e.g., Thorson et al., 2017). In addition, shifts in the spatial distribution of fish populations can be driven by various unmodeled spatiotemporal processes, including prey abundance, complex oceanographic features such as eddies and fronts caused by the mixing of water currents, and interactions with other species (e.g., competition and predation). The effects of these unmodeled processes on fish distribution shifts remain largely unquantified. A recent advancement in spatio-temporal modelling, such as the Vector-Autoregressive Spatiotemporal model (VAST; Thorson, 2019), provides more precise and accurate predictions of species abundance and distribution by accounting for both environmental variables and unobserved spatiotemporal processes, including species interactions and fishing pressure. Spatio-temporal modelling approach has demonstrated superior performance compared to traditional approaches in predicting species distribution and abundance (e.g., Shelton et al., 2014; Thorson et al., 2015). However, the potential biases resulting from misspecified environmental relationships in species distribution models remain underexplored.

This chapter aims to enhance our understanding of the spatiotemporal dynamics of Pacific saury in the Northwestern Pacific Ocean by applying the spatio-temporal modelling approach. The specific objectives are to evaluate the interannual dynamics of Pacific saury during the fishing season, quantify shifts in their spatial distribution over time, and identify the underlying causes of these changes. The analysis leverages data collected by the NPFC Small Scientific Committee (NPFC SSC), offering the most comprehensive spatiotemporal coverage available for this fishery.

Chapter 4 − Stock assessment and addressing the impacts of uncertainty on recovery

The fourth chapter focuses on the population modeling and management advice components of the stock assessment process. A fisheries stock assessment model is developed by incorporating multiple data sources (e.g., biological information and relative abundance) to evaluate fish population or stock status, forming the foundation for effective

doi:10.6342/NTU202500253

fishery management. Understanding and predicting population changes in fish species require careful consideration of numerous factors, including environmental conditions, biological traits, and human impacts (e.g., Hollowed et al., 2013; Szuwalski et al., 2016; Free et al., 2019). Commonly, harvest plans are designed to guide the recovery of overexploited fish populations by using stock assessment models to forecast biomass. However, these models often fail to account for uncertainties in parameters and recruitment, which are crucial for capturing real-world variability. This can lead to overly simplistic and potentially misleading predictions, particularly when deterministic projections are used instead of stochastic approaches. Deterministic projections assume fixed outcomes based on average conditions, whereas stochastic projections incorporate variability and uncertainty, providing a more realistic range of potential outcomes.

Modern stock assessment approaches emphasize the explicit representation and estimation of uncertainty, enabling this uncertainty to be factored into management decision-making processes (Patterson et al., 2001). Given the complexity of fish population dynamics, there is an increasing demand for advanced fisheries management strategies that can accommodate various sources of uncertainty − particularly process error in recruitment estimates. This highlights the need for comprehensive assessment methods that integrate diverse data sources and account for both natural variability and management interventions when predicting population trajectories (e.g., Punt et al., 2024).

This chapter aims to develop an age-structured population model for Pacific saury, advancing beyond the current Bayesian surplus production model approach. The analysis utilizes the Stock Synthesis framework, which enables the integration of multiple sources of uncertainty, including estimated parameters (e.g., selectivity and catchability) and process errors (e.g., recruitment deviations). By employing this comprehensive modelling approach, this study seeks to enhance our understanding of Pacific saury population dynamics and provide more robust management recommendations for the species in the Northwestern Pacific Ocean.

Chapter 5 − Summary and recommendation

This chapter synthesizes the key findings of this dissertation, uniting insights from the four interconnected research components to provide a cohesive narrative on advancing the

doi:10.6342/NTU202500253

assessment and management of Pacific saury in the Northwestern Pacific Ocean. This chapter offers a comprehensive summary of the preceding studies and presents actionable recommendations to enhance the sustainable management and conservation of this vital species. The overarching goal of this research has been to refine methodologies for assessing and managing Pacific saury populations by integrating environmental variability, spatial dynamics, and uncertainty. By examining stock-recruitment resilience, exploring the spatial treatment on standardization CPUE, spatiotemporal distribution dynamics, and age-structured population modelling, this dissertation has significantly advanced the understanding of Pacific saury population dynamics while identifying critical shortcomings in existing management frameworks.

Building on these findings, this chapter underscores the key conclusions from each study and translates them into practical recommendations. It focuses on three pivotal areas: integrating spatial dynamics into stock assessments, addressing multi-species interactions and trophic relationships, and developing robust Management Strategy Evaluation (MSE) frameworks that account for climate variability and ecosystem-wide considerations. By tackling these challenges, the recommendations aim to equip policymakers, researchers, and fishery managers with the tools necessary to balance ecological sustainability with economic objectives. Ultimately, this chapter emphasizes the importance of adaptive, ecosystem-based approaches to fisheries management. In the context of environmental change and escalating anthropogenic pressures, these strategies are essential to ensuring the long-term resilience of Pacific saury populations and the broader marine ecosystems they inhabit.

doi:10.6342/NTU202500253

1. Chapter 1 − Numerical approach for estimating the probable distribution of steepness

Abstract

Determining how resilient a stock-recruitment relationship is to environmental variation is crucial for fisheries management. Steepness is a key factor characterizing the resilience of a fish stock and, hence, for establishing management reference points. This study estimates the distribution of steepness for Pacific saury using a simulation approach based on evolutionary ecology and reproductive biology and how it changes in response to environmental change. The median estimated steepness is 0.82 (80% probable range 0.59, 0.93) based on the best available biological information, which suggests that Pacific saury can produce a relatively high proportion of unfished recruitment when depleted 20% of unfished spawning biomass. Elasticity analysis indicates that steepness for Pacific saury is most sensitive to the survival rate of early-life stages, mean body weight, growth, and length-at-maturity. Environmental change could substantially impact steepness, with unfavorable conditions related to survival rates, length-at-maturity, mean body weight, and growth potentially leading to a reduction in resilience. Understanding these impacts is crucial for the assessment and management of Pacific saury. The numerical simulation approach provides an analytical tool applicable for calculating the steepness distribution in other small pelagic fishes influenced by increases in sea surface temperature due to global warming.

Keywords: Resilience, stock-recruitment relationship, steepness, life history parameters, climate change

doi:10.6342/NTU202500253

1.1. Introduction

Steepness (*h*, Mace and Doonan, 1988; Francis, 1992) is essential for understanding the status of exploited fishery resources. Steepness quantifies the expected reduction in recruitment from an unfished stock when the spawning biomass is reduced to 20% of its unfished level in a stable environment. Higher steepness values characterize populations that are more resilient (higher regenerative capacity) to harvesting, making it fundamental to the calculation of biological reference points. Misspecification of the steepness can substantially impact the assessment results and rebuilding timelines for the depleted fish stocks (Brodziak and Legault, 2005; Brodziak and Piner 2010; Piner et al., 2011). However, steepness is one of the most uncertain parameters in stock assessment modeling due to a lack of data on the biological parameters of the stock-recruitment relationship (SRR) and the considerable variability in recruitment due to factors other than spawner abundance. Furthermore, simulations (e.g., Conn et al., 2010; Lee et al., 2011) have shown that steepness is likely to be poorly estimated within an integrated stock assessment model due to a lack of informative data on spawners and recruitment. Therefore, the steepness is often pre-specified in stock assessments, or a prior distribution is placed on this parameter (Punt and Hilborn, 1997).

Several studies have explored the estimation of steepness, given its importance to assessment and management. For example, Myers et al. (1999) applied linear mixed modeling to a stock-recruitment data set of over 700 fish species and taxa to estimate steepness and its associated uncertainty. Wiff et al. (2018) compiled estimates of steepness and life history parameters (e.g., asymptotic length and size-at-50% maturity) from stock assessment reports for 42 fish stocks and proposed a meta-analysis for predicting steepness using generalized linear models. Their analysis revealed that pelagic species tend to have higher steepness values ($0.58 - 0.86$) in comparison to demersal species ($0.54 - 0.77$). Thorson et al. (2020) developed a data-integrated life history model for combining life history parameters based on the database, *FishBase* (Froese, 1990) and stock-recruitment information (the RAM database; Myers *et al.*, 1995) to simultaneously predict life history and steepness parameters (R package: *FishLife*). Their findings suggested a general pattern for bony fishes (class Actinopterygii) with a steepness value of 0.74. Although the meta-analyses can offer a practical and objective way to determine steepness, they have potential

doi:10.6342/NTU202500253

weaknesses, such as the lack of representativeness in the chosen stocks, the inherent measurement errors in estimates of both spawners and recruitment, and the absence of independence among the multiple stock responses to environmental variations (Brodziak et al., 2015). In addition, accurate estimation of steepness requires data that span a wide range of spawning abundance because the precision of steepness estimates is poor if data on spawning abundance and recruitment are only available when spawning abundance is high (or low) relative to the unfished level. Furthermore, the large amount of variability in recruitment caused by factors other than spawner abundance obscures the SRR, especially for small pelagic fish (Crone et al., 2019).

The concept of the steepness of SRR is closely related to analytical approaches to quantify the probable values of steepness from evolutionary ecology and life history parameters have been developed (e.g., He et al., 2006; Mangel et al., 2010). Brodziak et al. (2015) extended the method of Mangel et al. (2010) by accounting for uncertainty about each life history parameter to estimate a distribution for steepness. Brodziak et al. (2015) found that variation in parameters determining growth, the length-at-weight relationship, maturity and early-life stage mortality had an important influence on steepness for the striped marlin (*Kajikia audax*). However, this study did not consider the joint impacts of covariation in correlated life history parameters such as the expectation of a negative correlation between the asymptotic length and the Brody growth coefficient (i.e., Ricker, 1975; Quinn and Deriso, 1999; Helser and Lai, 2004). This study expands the methods of Brodziak et al. (2015) to analyze the joint impacts on Pacific saury steepness produced by changes in the mean and variance of associated sets of life history traits, such as growth and maturity parameters, under environmental change scenarios.

The Pacific saury (*Cololabis saira*) is a migratory small pelagic fish widely distributed across the North Pacific Ocean, with a significant presence in the Northwestern Pacific (Fukushima, 1979). This species is characterized by a short life span of approximately two years (Suyama et al., 2006) and holds substantial regional commercial value, primarily harvested by stick-held dip net fisheries. Since 2015, Pacific saury has been internationally managed by the NPFC, an intergovernmental organization dedicated to ensuring its long-term conservation and sustainable use. Currently, Pacific saury in the

doi:10.6342/NTU202500253

North Pacific is treated as a single stock management unit (NPFC, 2023b), with stock assessments conducted using a Bayesian surplus production model (NPFC, 2023b). However, surplus production models may have limitations in accurately describing and predicting population dynamics, as they aggregate the effects of recruitment variability and population changes (Pella and Tomlinson, 1969), potentially hindering the exploration of time-varying dynamics. To address these challenges and improve management outcomes, the NPFC has prioritized the development of age-structured models for Pacific saury to better monitor population dynamics and achieve sustainable fishery management goals (NPFC, 2023b). One critical parameter for age-structured models, steepness, remains unknown for this species, highlighting a key gap in current assessments. The life history parameters of Pacific saury are known to be influenced by environmental factors due to its short life-span. For example, Oozeki and Watanabe et al. (2003) found that larval Pacific saury had very low survival rates (less than 10%) when exposed to unfavorable environmental conditions, particularly sea surface temperatures (SSTs) outside the range of 14 to 23°C while Ichii et al. (2018) found that an increase in SST and chlorophyll-a concentration during the spawning season would lead to faster growth of the early-life stage of the Pacific saury. Fuji et al. (2021) reported that the spawning activity of Pacific saury was mainly driven by SST-spawning adults actively spawned in areas with 16 − 21°C, whereas smaller adults spawned in areas with 14 − 16°C. Recent years have seen changes in the life history traits of Pacific saury due to the emergence of unfavorable environmental conditions (e.g., decreased body weight; Kakehi et al., 2022). These changes may be one of the factors contributing to the decline in the Pacific saury population, even though it is not overexploited (NPFC, 2023b). Understanding the probable range of steepness in response to changes in life history parameters due to environmental changes is therefore crucial as this may have a large impact on resilience.

This study introduces a Monte Carlo simulation approach to estimate the probable distribution of steepness for Pacific saury based on life history parameters and a density-dependent relationship between recruitment and population size. The primary goal is to derive an empirical probability distribution for steepness under prevailing environmental conditions and to assess the relative influence of life history traits on steepness estimation. Additionally, the study explores the potential impacts of climate-induced changes on the

doi:10.6342/NTU202500253

regenerative capacity of Pacific saury. By addressing a critical knowledge gap, this research not only advances understanding of Pacific saury dynamics but also offers a practical and adaptable methodology for estimating steepness in other small pelagic fish species facing similar environmental challenges.

1.2 Material and methods

1.2.1. Stock-recruitment model for Pacific saury

This study employed the age-structured simulation model developed by Mangel et al. (2010) to estimate a distribution for steepness in Pacific saury, using life history parameters as the foundation for the analysis. The recruitment dynamics of female Pacific saury in this simulation model were assumed to follow a Beverton-Holt SRR. This SRR is commonly applied to species with life history characteristics similar to those of Pacific saury, such as the Japanese anchovy (Ichinokawa et al., 2017) and Japanese sardine (Furuichi et al., 2020). The expected recruitment of age-0 (defined as the recruited age) individuals to the population in year t, denoted as $N(0,t)$, is given by the following equation:

$$N(0,t) = \frac{\alpha_s SB(t)}{1+\beta SB(t)} \tag{1.1}$$

where $SB(t)$ is female spawning biomass during year t, α_s is the number of new individuals/spawning biomass under steady state (the slope at-the-origin parameter), and β is the density-dependent parameter. Steepness value (h) for the Beverton-Holt SRR was described by Mangel et al. (2010, 2013) as:

$$h = \frac{\alpha_s SPR_0}{4+\alpha_s SPR_0} \tag{1.2}$$

where SPR_0 is the expected spawning biomass-per-recruit in the absence of fishing.

This study assumes that the early-life survival rate varies at the “population” level, while reproductive success (i.e., egg production) is considered at the “individual” level.

doi:10.6342/NTU202500253

These uncertainties are incorporated to calculate a probability distribution for steepness, following the methodology outlined by Mangel et al. (2010, 2013). The approach utilizes a Monte Carlo simulation to generate *j* (= 500) populations, resulting in *j* values for α_s. A frequency distribution for steepness, constrained between 0.2 and 1, is then created from the simulated αs values, based on Equation 1.2. The general process for the simulation study is illustrated in **Figure 1.1**.

To address individual variability, each population consists of "*i*" fish that differ in terms of the values for their growth-related (PM01; PM02 in **Table 1.1**) and reproductive ecology parameters (PM03 in **Table 1.1**). The simulation of the distributions for these parameters was based on the recent literature for Pacific saury (see Section *1.2.3*). The values in **Table 1.1** are predominantly derived from data collected between the 2000s and early 2010s within the Northwest Pacific Ocean, representing the most current and comprehensive biological information available. The age structure of the population *j* was obtained using survival-to-age distributions based on randomly sampled natural mortality rates at different ages (PM04 in **Table 1.1**). Individual fish survivorship within each population was determined by randomly sampling from the population-specific survivorship curves, with interpolation applied using a uniformly distributed random variable (Step ① in **Figure 1.1**).

1.2.2. Slope at the origin

The number of new individuals per spawning biomass for population *j*, $\alpha_s(j)$, is calculated by multiplying the expected early-life survival rate (L_s) by the sum of the egg production of all individuals (i.e., age 0 to the maximum age: a_{max}) and dividing by total spawning biomass (Mangel *et al*., 2010; 2013) (Step ② in **Figure 1.1**):

$$\alpha_s(j) = \frac{L_s \sum_i N_s E(W(a_{i,j}))}{\sum_i W(a_{i,j})} \tag{1.3}$$

where $W(a_{i,j})$ is the body mass of the i^{th} fish in the j^{th} population, $E()$ is batch fecundity as a function of body mass, and N_s is the number of spawning events.

doi:10.6342/NTU202500253

The early-life survival rate (L_s) is based on the allometric relationship between body mass and natural mortality during the early-life stages. The duration of the early-life stage (D_{ELS}) for Pacific saury is defined as the number of days required for an egg to develop into the smallest observed size of 12 cm knob length (KnL), as determined from mid-trawl survey data (Suyama et al., 2012). This size is considered the end of the early-life phase, which includes the egg, larval, and part of the juvenile stages, marking the point at which the individual enters the population as a recruit (i.e., age-0 fish). D_{ELS} is calculated from the Gompertz growth curve based on the age corresponding to 12 cm KnL. Growth during D_{ELS} days for Pacific saury is expressed as the daily increase in the fish biomass (W_{ELS}), which is modelled as an exponential function with a constant daily rate of increase in body mass (K_{ELS}) from the initial egg weight ($W_E = 1.3 \times 10^{-4}$ g; Nakaya et al. (2011)) to the final early-life stage (D_{ELS} = 120 days) (**Table 1.1**). The daily growth pattern is expressed as: $W_{ELS}(d) = W_E \times \exp(K_{ELS} \times day)$, where $K_{ELS} = \log(W(D_{ELS})/W_E)/ D_{ELS}$. The average weight at D_{ELS} is calculated using the mean length at D_{ELS} calculated from the Gompertz growth curve and the length-at-weight function (**Table 1.1**).

The survival rates of Pacific saury during the early-life stage are characterized by a decrease in natural mortality as body mass increases following McGurk (1986). Typically, the early-life phase is associated with higher natural mortality rates, which tend to decrease once the fish reaches a critical weight. McGurk (1986) developed the two functions for calculating the natural mortality rate based on the dry weight body mass of the early-life stage (dw_{ELS}), i.e., whether it is below (egg and larval stage) or above (a part of the juvenile stage) the critical weight (w_c = 0.00504 g). The survival rate function for the egg and larval stage (M_{EL}) and the juvenile stage (M_J) are $M_{EL}(d) = 2.2\times10^{-4} dw_{ELS}(d)^{-0.85}$ and $M_J(d) = 5.26\times10^{-3} dw_{ELS}(d)^{-0.25}$, respectively, where d denotes day. The dry weight of W_{ELS} was adjusted by $0.2W_{ELS}(d)$ by McGurk (1986). This study integrated the daily weight-dependent natural mortality rate calculated from McGurk (1986) with the results of a survival experiment for Pacific saury during the egg and larval stage conducted by Nakaya et al. (2011) (**Figure 1.2**). The patterns of daily natural mortality rates between the two studies were similar, verifying the applicability of McGurk's (1986) daily natural mortality model for the early-life stages of Pacific saury. This study examined the weight-based mortality function proposed by McCoy and Gillooly (2008) (**Figure 1.2**). However, when

doi:10.6342/NTU202500253

fitting these mortality functions to the observed mortality data of Nakaya et al. (2011), this study found a smaller residual sum of squares (RSS) for McGurk's (1986) method (46.63 for McGurk; 63.44 for McCoy and Gillooly). Therefore, this study used McGurk's approach was adopted, as it demonstrated a better fit for estimating Pacific saury mortality during the early-life stage. The quantification of uncertainty in early-life survival (PM05 in **Table 1.1**), which varies at the "population" level, is detailed in Section *1.2.3*.

1.2.3. Simulation analysis

The Monte Carlo simulation involved individuals experiencing varying growth and natural mortality rates, length-at-weight relationships, and reproductive parameters, while the survival rate for the early-life stage varied by population (**Figure 1.3**). A total of 250 simulations[1] for each of 500 populations consisting of 1,000 individual fish were used to create a distribution for *h*, which was then approximated by a beta probability density function (Step ③ in **Figure 1.1**; Mangel et al., 2010; 2013). The resulting distribution for steepness spanned an interval from 0.2 to 1.0 with an increment of 0.01.

Two approaches were employed to represent uncertainty in the life history parameters used to calculate the baseline distribution for steepness, which reflected the prevailing environmental conditions. A common coefficient of variance (CV = 0.2) was applied when generating parameters for the baseline analysis, with sensitivity to this value explored to assess the relative impact of each parameter on steepness.

1) The parameters of the growth function (L_{inf}, K, t_0) and of the length-weight relationship (a, b) are likely to be highly correlated (Chen, 1996; Chang et al., 2009). For these parameters, the mean parameter values (PM01; PM02 in **Table 1.1**) were used to calculate the expected values for L_t and W_t, after which independent multiplicative lognormal error (mean 1 and CV of 0.2) was multiplied by these predicted values. The underlying curves (PM01) and (PM02) were then fitted to the generated values using the *optim*() function in the R environment (R Core Team,

[1] An analysis showed that there was little sensitivity of distribution of steepness for the baseline assumptions to the number of simulations (100, 200, 250, 500), populations (100 to 1,000), and individuals (1,000 to 1,500) (**Figure S1.1**).

doi:10.6342/NTU202500253

2022), enabling the calculation of model parameters for further analysis.

2) The remaining parameters were sampled independently from probability distributions with means given in **Table 1.1** and a CV of 0.2 (Mangel et al., 2010; Kai and Fujinami, 2018). Specifically, the annual natural mortality values by age (M_0 and M_1) were modeled using gamma distributions (Mangel et al., 2010), while the early-life parameters (M_{EJa}, M_{EJb}, M_{Ja}, M_{Jb}, D_{ELS}, and W_E) and reproductive parameters (L_{50}, r, T_B, E_G, and SL) were modeled using lognormal distributions.

1.2.4. Comparison of estimated baseline steepness with the outcomes of previous meta-analyses

The baseline distribution for steepness was compared to the steepness values predicted from the meta-analyses conducted by Wiff et al. (2018) and Thorson (2019). Wiff et al. (2018) compiled 42 estimates of h and other life history parameters from data collected between the 1950s and 2000s. They used a linear model that utilized the ratio of relative length at maturity (L_{50}/L_{inf}) as the explanatory variable (Table 1 in Wiff et al., 2018) to predict the mean steepness value. However, the uncertainties of the related coefficients were not provided in their study, so the uncertainty of the estimated steepness value cannot be calculated. In contrast, *FishLife* utilized taxonomic relatedness and field measurements from the global dataset *FishBase* (Froese, 1990) to fit an evolutionary model of life history (Thorson et al., 2017).

A hierarchical model for steepness, as outlined by Thorson, (2020), was fitted to stock-recruitment data from the original RAM database (Myers et al., 1999). This package also estimates uncertainty based on the quantity and quality of the records. For Pacific saury, the life history information in *FishBase* was gathered during the mid-1990s to early-2000s. This study then compared the Beverton-Holt SRR curve formulated in terms of steepness derived from various estimations, including those from our study, Wiff et al. (2018), and Thorson (2020) (See **Figure S1.2**).

1.2.5. Elasticity analysis

doi:10.6342/NTU202500253

An elasticity analysis was conducted using the parameter values in **Table 1.1** to identify which life history parameters have the greatest impact on the distribution of steepness. Elasticity, a unit-independent measure of parameter sensitivity, is particularly useful for assessing the effects of parameters with different units and scales. This analysis indicates whether an increase in a parameter leads to an increase (positive elasticity) or a decrease (negative elasticity) in steepness. The magnitude of the elasticity quantifies the extent of the change, showing whether a parameter's increase leads to a large or small change in steepness. For example, an elasticity, $e(\theta_j)$, of X indicates that a 1% change in life history parameter j results in roughly an X% change in steepness. The elasticity for each parameter ($e(\theta_j)$) was calculated as:

$$e(\theta_j) = \frac{\partial h}{\partial \theta_j}(\underline{\theta})\frac{\theta_j}{h} \tag{1.4}$$

where h and θ_j are steepness and the j^{th} life history parameters, respectively. The partial derivative of steepness as a function of $\underline{\theta_j}$ was numerically calculated by using a first-order central-difference approximation.

1.2.6. Evaluating the impact of environmental change on the steepness

The potential impact of environmental change on steepness for Pacific saury was examined through four scenarios, which quantified how variations in the main life history parameters of Pacific saury − such as growth, body weight, maturity, early-life stage survival, and annual natural mortality − could influence steepness under changing environmental conditions. These life history parameters are known to be responsive to environmental changes, with increased water temperatures expected to reduce the size and survival rates of early-life stages, thereby decreasing the population growth rate (Anderson and Gillooly, 2020; Savage et al., 2004). For example, the life history parameters (growth, length-at-weight, and maturity) for the Pacific sardine (*Sardinops sagax*), a small pelagic fish with similar characteristics to the Pacific saury, vary by approximately 5% across various environmental conditions (Dorval et al., 2015). Similarly, Kakehi et al. (2022) observed a

doi:10.6342/NTU202500253

decline of around 5% in the weight of age-1 saury during 2019 and 2020 compared to the levels observed between 2003 − 2018. This decline in body weight contributed to delayed age-1 saury spawning migrations and a reproductive decline in recent years (2019 − 2020), attributed to environmental change. Considering the potential impact of environmental shifts on the life history of saury and other small pelagic fishes, the mean values of the life history parameters were varied by ± 5% in the four scenarios (2 − 5; **Table 1.2**) to mimic changes in the mean values of life history parameters under different environmental conditions. In addition, the impact of different CVs for the main life history parameters on estimated steepness values for Pacific saury was examined.

This study assumes that the Pacific saury population experienced favorable environmental conditions in Scenarios 2 and 3, leading to faster growth, increased body weight, higher survival rates during the early-life stage, earlier maturity, and lower annual natural mortality (Huret et al., 2019; Albo-Puigserver et al., 2021). These improved conditions reflect an environment that supports enhanced individual growth and reproductive success, resulting in more robust population dynamics. In contrast, this study assumed that the Pacific saury faced unfavorable conditions in Scenarios 4 and 5, leading to lower growth, smaller body weight, lower survival during the early-life phase, delayed maturity, and higher annual natural mortality (**Table 1.2**). This study also examined how the variability of the main life history parameters affected steepness for Pacific saury under alternative environmental conditions. This study considered CVs of 0.2 in Scenarios 2 and 4 and 0.4 in Scenarios 3 and 5, respectively (**Table 1.2**). The remaining life history parameters ($T_{B,}$ E_G, S_L, D_{ELS}, and W_E) were generated as for the baseline scenario (**Table 1.1**).

1.3. Results

1.3.1. The distribution of steepness for Pacific saury for the baseline conditions

The distribution of steepness for Pacific saury was calculated under prevailing environmental conditions (Scenario 1) and was not symmetrical (**Figure 1.4**). Instead, it exhibited left-skewed with a median value of 0.82 and an 80% probable range (0.59, 0.93). The mean steepness was 0.79 with a CV of 0.18, and the parameters of the fitted beta

doi:10.6342/NTU202500253

density were 6.45 and 1.78 (**Figure 1.4**). These findings suggest that the SRR of Pacific saury is likely highly resilient to declines in spawning potential. The SRR curves derived from the mean value of baseline steepness of this study were compared with those derived from the meta-analysis of Wiff et al. (2018) and *FishLife* (**Figure 1.5**). The meta-analysis approach of Wiff et al. (2018) led to a smaller mean steepness value for Pacific saury (0.56) than that obtained in this study. In addition, the estimated mean of the steepness distribution of this study was higher than the estimate of 0.70, and the 80% confidence interval (0.42, 0.98) was obtained from *FishLife* (**Figure S1.2**; Thorson, 2019). The uncertainty in the steepness value estimated from *FishLife* was larger, including most of the baseline steepness distribution and the estimate of steepness using the Wiff et al. (2018) method.

1.3.2. Relative importance of life history parameters on steepness

The elasticities of steepness for the life history parameters differed in both direction and magnitude among parameters (**Figure 1.6)**. The elasticity analysis showed that over half (53%) of the life history parameters had negative elasticity. The shape parameter of maturity-at-length (r), the exponent parameter for the survival rate for juveniles (M_J), and the annual mortality of age-1 fish (M_1) had negligible effects on steepness ($e(r)$ = 0.04%, $e(M_J)$ = -0.04%, $e(M_1)$ = -0.09%). In contrast, the survival rate of the egg and larval stages (M_{EL}), the exponent parameter of the length-at-weight relationship (b), and the asymptotic length parameter (L_{inf}) had substantial impacts on steepness, with elasticities for these parameters larger than 3% ($e(M_{EL})$ = -8.89%, $e(b)$ = 3.70%, $e(L_{inf})$ = 3.30%).

Among the three parameters with substantial influences on steepness, the largest negative elasticity was found for the survival rate of the egg and larval stages (M_{EL}). The exponent parameters of the length-at-weight relationship (b), which is a measure of the fish's body weight, had a smaller but still important effect on the steepness. The female length at 50% maturity (L_{50}), annual mortality of age-0 fish (M_0), and the duration of the early-life stage (D_{ELH}) had moderate effects on steepness, with elasticities larger than 1%. These parameters led to a negative elasticity, with the size of the elasticities being -2.06% for L_{50}, -1.85% for M_0, and -1.44% for D_{ELH}. The elasticities for the remaining six parameters showed that the growth coefficient (K), scale parameter of length-at-weight (a),

doi:10.6342/NTU202500253

batch fecundity (E_G), numbers of spawning seasons (SL), annual mortality of age-1 fish (M_1), the average time between spawning events (T_B), and the time at inflection parameter of Gompertz growth function (t_0) have less important effects on steepness, with elasticities from -0.69 to 0.41%.

1.3.3 Impacts of environment-driven changes in life history parameters on the steepness

The steepness values and their corresponding CVs under five scenarios are shown in **Table S1.1**. The five scenarios are composed of different means and CVs for the main life history parameters (growth, length-at-weight, maturity, survival rate in the early-life stage, and annual natural mortality), and represent potential environmental effects. The median value of the steepness distributions ranged from 0.33 to 0.97, and the CV ranged from 0.08 to 0.49 across five scenarios (**Figure 1.7** and **Table S1.1**).

As expected, steepness was higher when the environment was more favorable, with faster growth rates, larger body weight, higher survival rate in the early-life stage, smaller maturity size, and lower natural mortality (Scenarios 2 and 3) compared to unfavorable environments (Scenarios 4 and 5). The median values of steepness for Scenario 2 and 3 were highest (0.97), and the CVs were lowest (0.05 and 0.08, respectively). The median value of steepness (0.33) derived from Scenario 4, which had the highest uncertainty for the main life history parameter (CV = 0.4), resulted in the lowest median for steepness (0.33) and the CVs of estimated steepness values for Scenarios 4 and 5 were higher than other scenarios (**Figure 1.7**). These results indicated that moderately positive effects of the favorable environment on the estimated steepness (Scenarios 2 and 3) led to 13% changes compared to the baseline scenario (Scenario 1) (**Table S1.1**).

A substantially negative effect of unfavorable environment on the estimated median steepness (Scenario 4 and 5) resulted in -60% and -49% changes compared to the baseline scenario (Scenario 1) (**Table S1.1**). Overall, the results of this study suggest that either the value or variation of main life history parameters could have an impact on the estimated steepness value of the Pacific saury under the potential environmental variability, in particular under unfavorable environments.

doi:10.6342/NTU202500253

1.4. Discussion

1.4.1. The resilience of Pacific saury under changing environmental conditions

This study developed a numerical simulation approach that incorporated principles of evolutionary ecology and reproductive biology to evaluate a probable range of steepness values for Pacific saury under five environmental conditions. The results indicated that the median steepness value under prevailing environmental conditions (Scenario 1) was 0.82, suggesting that Pacific saury is likely to exhibit high resilience to exploitation. In comparison, the mean steepness values for Atlantic herring (*Clupea harengus*) and Pacific sardine (*Sardinops sagax*) were estimated to be 0.85 and 0.82, respectively, based on a meta-analysis by Myers et al. (1999). These values are consistent with the median steepness calculated for Pacific saury, further supporting the biological plausibility of the distribution. The similarities between these species, which share life history traits such as fast growth, low maturity at age, and short longevity, reinforce the biological relevance of the steepness values derived in this study.

The elasticity analysis revealed that changes in survival rates during the egg and larval stages had the largest negative impact on steepness, while changes in fish body weight had a significantly positive effect on steepness for Pacific saury. Yatsu, (2019) found that reduced zooplankton abundance and unsuitable sea surface temperatures (SST) have contributed to lower survival rates during the early-life stages of Pacific saury since 2016. Similarly, Kakehi et al. (2021) noted that low body weight in Pacific saury delayed the spawning season in 2019－2020, as individuals continued to feed for growth instead of migrating to spawn. This delay compressed spawning timing and likely reduced reproductive success. Therefore, the baseline steepness value may not accurately reflect the current unfavorable environmental conditions, which have contributed to a decline in stock resilience in recent years.

Beyond Pacific saury, similar challenges in recruitment and recovery due to shifts in life history characteristics have been observed in other small pelagic fish species. For example, McGowan et al. (2021) reported that Pacific herring (*Clupea pallasii*) struggled with recruitment and recovery, influenced by factors such as diminished total spawning,

doi:10.6342/NTU202500253

delayed spawning timing, and restricted spawning areas. Similarly, Koenigstein et al. (2022) suggested that the failure of Pacific sardine (*Sardinops sagax*) to recover after 2014, coupled with reduced egg production and lower adult food availability, has led to a decline in sardine abundance. These studies emphasize that many fish stocks are affected by fluctuations in productivity, which in turn influence their recovery capabilities. This study advocates for considering shifts in fish productivity within the broader context of fisheries management, such as the use of dynamic reference points (Berger, 2019).

The findings from this study indicate that steepness can decrease under unfavorable environmental conditions, suggesting that variations in life history parameters during such conditions may significantly reduce the resilience of Pacific saury to exploitation. Moreover, unfavorable conditions may introduce greater uncertainty in steepness estimates. In contrast, Scenarios 2 and 3, which represent favorable environmental conditions, show more optimistic steepness values. This study evaluated the potential impacts of environmental variability on life history parameters and the resilience of Pacific saury. As fish productivity is often strongly influenced by environmental factors (e.g., Szuwalski et al., 2016; Holt and Michielsens, 2020), and considering that assuming steepness as unity in stock assessment models is biologically implausible (Brodziak et al., 2005; Mangel et al., 2010; Miller and Brooks, 2021), our study contributes to developing a more comprehensive framework for assessing the impact of stock size on recruitment under varying environmental conditions and density-dependent effects (e.g., Watanabe, 1991; Nakaya et al., 2011).

While the simplifying assumption of steepness being unity has been and will likely continue to be used in stock assessments, this study proposes that the steepness distributions under different scenarios (see Section *1.3.3*) could be integrated into future Pacific saury assessments. This would be particularly valuable if an age-structured model is employed for assessment, allowing for a better understanding of the influence of steepness on abundance and reference points, particularly in the context of environmental variability.

1.4.2. Comparing the steepness estimation with meta-analysis

doi:10.6342/NTU202500253

The comparison of steepness values across different methods underscores among-method variation as a significant source of uncertainty. The meta-analysis by Wiff et al. (2018) estimated the mean steepness for Pacific saury to be 0.56, which is smaller than the lower bound of the 95% confidence interval (0.59) derived from the baseline analysis. However, it is important to recognize that the stocks included in the Wiff et al. (2018) meta-analysis were primarily from the southeastern Pacific Ocean and the southwestern Atlantic Ocean, covering the period from 2002 to 2012. As a result, the relationship between life history and steepness observed in that study may be more regionally and temporally specific and may not accurately represent Pacific saury in the Northwestern Pacific. Furthermore, the meta-analysis by Wiff et al. (2018) relied on only two life history parameters, while steepness is influenced by several life history factors (Myers et al., 1999; Mangel et al., 2010; Brodziak et al., 2015). Therefore, the steepness prediction from Wiff et al. (2018) may not fully capture the complexity of steepness estimation for Pacific saury in its specific ecological context.

In contrast, a global meta-analysis conducted by *FishLife* examined the relationships between life history parameters and steepness using extensive datasets for both life history parameters (sourced from *FishBase*) and stock-recruit estimates (from the RAM database). The mean steepness value for Pacific saury derived from *FishLife* was 0.70, which is lower than the value obtained from the baseline analysis (0.79). However, the 80% probability interval for steepness in the baseline analysis (0.59, 0.93) includes 0.70, suggesting that the estimates are not inconsistent. The lower mean steepness value estimated by *FishLife* may be influenced by the period during which the life history data for Pacific saury were collected, which spans the mid-1990s to early-2000s.

1.4.3. The relative importance of life history on Pacific saury's steepness

The results of the elasticity analysis indicate that steepness for Pacific saury is most sensitive to parameters related to growth, body weight, and the survival rates of the egg and larval stages. For instance, increases in growth rate and body weight enhance reproductive output, while higher survival rates for egg and larval stages lead to greater productivity and overall resilience. This study utilized estimates of early-life survival rates

doi:10.6342/NTU202500253

for teleosts from McGurk's (1986) meta-analysis to characterize egg-to-juvenile survival for Pacific saury. Given the significant impact of early-life survival on steepness, as indicated by the elasticity analysis, it would be beneficial to update McGurk's dataset with more recent data on larval fish survival rates. Nonetheless, a similar pattern of daily natural mortality rates was observed between the meta-analytic estimates and rearing experiments (Nakaya et al., 2011) for Pacific saury.

Moreover, this study is based on the best available life history parameters (e.g., growth curve, age-specific maturity, and weight-length relationships) to calculate the probable distribution of steepness. However, the spatial and temporal coverage of the data used to estimate these parameters was limited to a specific offshore region of Japan (e.g., Kosaka, 2000; Suyama et al., 2015). To improve the accuracy and representativeness of the steepness estimates, it is recommended to enhance the spatial and temporal coverage of biological data, enabling more comprehensive life history parameters for Pacific saury.

1.4.4. Density-dependent effect of the stock-recruitment relationship

The exact nature of SRR is usually unclear due to considerable variability in recruitment caused by factors other than spawner's abundance, such as environmental conditions and observation errors in the stock-recruitment data (S-R data) (Hilborn and Walters, 1992; Conn et al., 2010; Subbey et al., 2014). However, recent studies have provided evidence supporting the presence of density-dependent effects of the SRR for small pelagic fishes. For example, Szuwalski et al. (2019) selected the time series of recruitment and spawning stock biomass from the RAM Legacy Stock Assessment Database, which consisted mainly of assessment results in North America, Europe, and Oceania (Ricard et al., 2012) to identify the density-dependent response of SRR for 14 stocks in 28 forage fish stocks. In addition, Kurota et al. (2020) examined the correlation of SRR using the stock and recruitment data from 28 Japanese fisheries stock, which are characterized by many small pelagic fishes, such as sardine, anchovy, mackerel, and herring. They reported that the spawner abundance was significantly related to recruitment in 17 of the 23 Japanese fisheries.

doi:10.6342/NTU202500253

Despite these findings, the shape of the SRR for Pacific saury remains unknown. To advance our understanding, future studies should focus on estimating the SRR using qualitative data from real-world scenarios. This could include developing more accurate abundance indices for recruitment and improving the reliability of abundance indices for adult Pacific saury, which would help clarify the SRR for this species.

1.5. Conclusions

A lack of reliable long-term stock and recruitment data for fish stocks results in high uncertainty when estimating steepness, a key parameter for assessment and management. This study developed a numerical approach based on population biology as an alternative way to estimate steepness. It outlined a framework to quantify how variability in life history parameters, driven by environmental conditions, could impact steepness. This is particularly relevant as resilience may vary in response to factors such as sea surface temperature (SST) changes linked to global warming. The importance of considering environmental variability and its effects on stock productivity is increasingly recognized as a priority for fisheries management (Szuwalski et al., 2016). This study contributes to understanding the impacts of life history variability on steepness estimates for Pacific saury. Unfavorable environmental conditions could reduce growth, body weight, and survival rates during the egg and larval stages, which in turn diminishes the resilience of Pacific saury populations.

An implication of this study is that our results could provide a foundation for a baseline steepness value in the development of an integrated age-structured model, while also identifying how steepness values may shift in response to environmental variability. This highlights the need to account for environmental effects on resilience when conducting stock assessments and calculating management reference points for Pacific saury.

doi:10.6342/NTU202500253

2. Chapter 2 − Evaluation of the influence of spatial treatments on catch-per-unit-effort standardization with fishery application and simulation study

Abstract

Fishery-dependent catch-per-unit-effort (CPUE) data often exhibit spatial heterogeneity over space and time, which means that the spatial treatment in statistical models used to standardize CPUE is critically important. This study evaluated several spatial treatments to standardize CPUE data using Generalized Linear Mixed Models (GLMMs). Results include a real-world application and a simulation based on the Taiwanese stick-held dip net fishery for Pacific saury in the Northwestern Pacific Ocean. This study compared the performance of three spatially stratified approaches in GLMMs (spatially stratified GLMMs), (i) Ad hoc; (ii) Binary (binary recursive area partitioning based on model selection criteria); and (iii) Spatial clustering (partitioning of grids into discrete strata based on the spatial proximity and average CPUE in each grid), to a spatio-temporal GLMM (VAST). An influence analysis was constructed to quantify discrepancies between unstandardized and standardized indices that assisted in identifying the annual influence of explanatory variables in GLMMs. This study developed a simulation to corroborate the results from the case study and evaluated the four spatial treatments using data generated from two contrasted, random and preferential, sampling scenarios. Results from the real-world application indicated that VAST was statistically superior to the other approaches, based on conditional deviance explained, conditional Akaike Information Criterion, and five-fold cross-validations. The influence analysis indicated that the interaction of year and spatial effect or spatio-temporal variable had a major influence on the standardized CPUE. Both simulation scenarios showed that VAST performed the best, with the lowest model error (measured by root mean square error) and bias, for estimating relative abundance indices. Although the spatial clustering approach created a flexible shape for the area strata, the simulation results under preferential samplings showed that clustering with a stronger emphasis placed on average CPUE could lead to bias in estimated abundance indices. However, spatial clustering that balanced average CPUE with spatial proximity could be a reasonable alternative if it is not possible to apply a spatio-temporal approach. The

doi:10.6342/NTU202500253

importance of conducting influence analysis and the greater performance of a spatio-temporal approach are highlighted.

Keywords: CPUE standardization, simulation-testing, influence analysis, spatio-temporal modelling approach, area stratification, Pacific saury

doi:10.6342/NTU202500253

2.1. Introduction

Commercial catch-per-unit-effort (CPUE) data are often standardized for use as an index of relative abundance, particularly in fisheries where a regular survey has not been feasible (Hilborn and Walters, 1992; Maunder and Punt, 2004). To effectively use CPUE as a relative abundance index, raw CPUE data must conduct standardization to account for variations in spatial and temporal factors such as gear configuration, fishing power, and fishing behavior (Campbell, 2004; Maunder and Punt, 2004; Maunder et al., 2006). The non-random nature of spatial distributions of fish density can also cause CPUE data from preferred fishing grounds to exert a disproportionate effect on the estimated fish abundance (i.e., preferential sampling: Rose et al., 1991; Conn et al., 2017; Ducharme-Barth et al., 2022). Therefore, adjusting for the spatial heterogeneity of CPUE data is essential for CPUE standardization. The confounding effect of spatial heterogeneity has commonly been addressed by the inclusion of categorical grids (e.g., 5° × 5° grids) or area strata within Generalized Linear Models (GLMs), Generalized Additive Models (GAMs), and Generalized Linear Mixed Models (GLMMs) used for CPUE standardizations (Maunder and Punt, 2004). In theory, the area strata are assumed to represent spatial heterogeneity in fish density, which may be treated as categorical variables in the standardization model to adjust for differences in CPUE associated with each stratum. Ideally, an appropriate area stratum is a region where fish density is homogeneous (Bishop, 2006), but in the reality this is seldom the case. Many studies take ad hoc sets of grids as the area strata in standardizing CPUE analysis, or use area strata defined using either the spatial distribution of nominal CPUE and fishing effort or oceanographic conditions (e.g., Quinn et al., 1982; Nakano, 1998). However, it is difficult to construct appropriate area strata objectively using an ad hoc approach, and spatial misspecification in the CPUE standardization process could potentially result in a biased index of relative abundance (Bishop, 2006).

Several spatially stratified approaches have been developed to define objective criteria for the area stratifications in standardizing fishery CPUE. For example, a binary recursive partitioning approach was developed to automatically stratify the study area based on information criteria (e.g., Akaike or Bayesian Information Criteria, AIC or BIC) (Ichinokawa and Brodziak, 2010). This approach created area stratifications more effectively than the area strata determined in an ad hoc manner and achieved better GLM

doi:10.6342/NTU202500253

fits to the CPUE data of North Pacific swordfish (*Xiphias gladius*). However, the binary recursive partitioning approach is limited to generate rectangular area strata due to its binary partitioning nature. In the real world, the distribution of fish density is unlikely to be structured as rectangular shapes. Ono et al. (2015) proposed an alternative area stratification approach known as spatial clustering to improve upon the rectangular area strata shape seen in Ichinokawa and Brodziak (2010). The spatial clustering approach applies a *k*-medoids algorithm to cluster grids of CPUE data according to the similarity of the spatial proximity and average CPUE of grids. This approach creates a flexible shape rather than a rectangular shape for the area strata which may better match the population structure inferred from the CPUE data. Ono et al. (2015) also suggested, based on simulation experiments, that the spatial clustering approach could reduce bias in abundance indices compared to the ad hoc approach, but this would not be expected to occur if the spatial distribution of fishing grounds had shifted over time.

The spatial effect in conventional GLMs for CPUE standardization assumes that the adjacent strata/grids are independent of each other. However, the variation of fish abundance and availability is often continuous and correlated with biotic and abiotic environmental factors over space (i.e., spatially structured). Therefore, it seems appropriate to incorporate spatial autocorrelation into a standardization model as a continuous covariate to more reasonably reflect the spatial heterogeneity of fish distributions (Thorson et al., 2015; Thorson and Barnett, 2017). Recent years have seen the emergence of spatio-temporal models (e.g., Vector-Autoregressive Spatiotemporal, VAST; Thorson, 2019) for standardizing CPUE data (e.g., Xu et al., 2019; Maunder et al., 2020; Ducharme-Barth et al., 2022), because this approach could provide a more sophisticated treatment of spatial variation by accounting for not only the long-term spatial autocorrelation (i.e., spatial autocorrelation that is constant over time) but also the spatio-temporal autocorrelation (i.e., spatial autocorrelation that is specific to each year of the study period) in the CPUE standardization. Specifically, a spatio-temporal approach allows for the spatial and spatio-temporal effects to be treated as a continuous Gaussian Markov random field, which may yield more precise, biologically reasonable, and interpretable estimates of abundance than common area strata factors in GLMs (Shelton et al., 2014; Thorson et al., 2015).

doi:10.6342/NTU202500253

Multiple comparative studies (Grüss et al. 2019; Zhou et al. 2019) have shown the benefits of using spatio-temporal models for standardizing CPUE data relative to other regression models. Grüss et al. (2019) used a simulation experiment to show that VAST minimized residual variance over space without defining the area strata in advance and usually had the lowest error, bias, and most appropriate levels of coverage relative to the eight other linear models considered. Zhou et al. (2019) showed similar results when comparing a spatio-temporal approach to GLMs and GAMs. However, the Grüss et al. (2019) and Zhou et al. (2019) studies only considered a fixed ad hoc area stratification (10 areas and 7 areas, respectively) *a priori* to CPUE standardization. Consequently, it was not possible to evaluate whether their area stratification approaches were appropriate and sufficient to standardize CPUE. To our knowledge, there has not been a study which explicitly compares the performance of different spatial treatments (Ad hoc, Binary, Spatial clustering, and spatio-temporal approaches) where a consistent model structure with the same sets of covariates has been applied.

Most CPUE standardization studies have concentrated on removing the effects of predictors to obtain an unbiased index of abundance. Few studies have focused on understanding the differences between standardized and unstandardized CPUE indices (Holdsworth et al., 2017; Hoyle et al., 2019; Feenstra et al., 2019). Bentley et al. (2012) suggested that it is necessary when conducting an explanatory analysis (e.g., R package *influ*; https://github.com/trophia/influ) to explore how the CPUE standardization model removes confounding effects by including each explanatory variable in models rather than simply accepting the relative abundance index arising from a model. Furthermore, although considering the interaction effect of year and area in GLMs is a common way to standardize spatiotemporal patterns in CPUE data, the influence analysis of the interaction effect has rarely been examined.

Given the identified gaps in the literature, the analytical objective was to evaluate the effects of spatial treatments on CPUE standardization, using a consistent model structure and with the same sets of covariates within a GLMM framework. This objective was achieved by using the CPUE data of a commercially important migratory species, Pacific saury (*Cololabis saira*), as an example. The Pacific saury fishery in the

doi:10.6342/NTU202500253

Northwestern Pacific Ocean exploited by the Taiwanese stick-held dip net vessels provides an example of spatial heterogeneity of CPUE data, with more than 98,000 fishery operations recorded during 1994－2019 over a large geographical range (Chang et al., 2019). This study employed a GLMM framework, incorporating year effects, spatial and spatio-temporal variation terms, a vessel effect, and the influence of oceanographic conditions (such as sea surface temperature). The study then compared the statistical performance of four spatial treatment approaches (three area stratification methods and a spatio-temporal model) by evaluating metrics such as conditional deviance explained, conditional AIC, and performing repeated five-fold cross-validation 10 times. Additionally, influence plots (Bentley et al., 2012) were utilized to illustrate how the GLMM framework mitigates confounding effects of explanatory variables. A simulation study was also conducted, employing two contrasting spatial sampling scenarios to assess whether different spatial treatments could lead to model misspecification in CPUE standardization. Although this study was developed with Pacific saury in mind, its methodology and findings are broadly applicable to other fisheries with similar data, offering valuable insights into the appropriate treatment of spatial effects in CPUE standardization analyses.

2.2. Materials and methods

2.2.1. Pacific saury fishery dataset and data filtering

This study utilized Pacific saury fishery logbook data from Taiwanese stick-held dip net vessels operating in the Northwestern Pacific Ocean (mainly 35 − 49°N and 140 − 173°E) during the main fishing season (August to November) between 1997 and 2019. The daily logbook data contained catch (in metric tons), vessel identification (vessel ID), effort (number of hauls), and the location of sets by latitude-longitude at a resolution of 0.25°. These records were provided by the Overseas Fisheries Development Council of Taiwan. Since Pacific saury are targeted by vessels fishing at night using lamps to attract schools of fish, the dataset does not contain any zero catches. Data filtering was applied to remove incomplete and insufficient data, such as sets missing information on date, vessel ID, or location, resulting in a final dataset of 98,738 fishing operations, after eliminating 2% of the original sets.

doi:10.6342/NTU202500253

2.2.2. Spatially stratified GLMMs

The application of GLMMs has been one of the most frequently employed modelling approaches for CPUE standardization (Maunder and Punt, 2004). GLMMs (Pinheiro and Bates, 2000) extend the GLM method by allowing some of the explanatory variables in the linear predictor to be treated as random variables. This flexibility makes GLMMs particularly valuable in accounting for complex interactions, such as the year × spatial interaction, which is common in CPUE standardization (Miyabe and Takeuchi, 2003; Forrestal et al., 2019; Grüss et al., 2019). Various studies have indicated that the spatial and temporal distribution of Pacific saury could be affected by changes in sea surface temperatures (SST; Chang et al., 2019; Hsu et al., 2021). Specifically, a fishery-independent survey for Pacific saury showed that it prefers a habitat with SST between 7 − 15°C (Hashimoto et al., 2020). Consequently, this study incorporated SST and its squared value (SST^2) as continuous variables in the GLMM standardization models to account for the possibility of CPUE peaking at intermediate SST levels (Thorson and Barnett, 2017; Hashimoto et al., 2019). Additionally, the use of light (e.g., number or power of lights) is an important factor influencing catchability in the Pacific saury fishery, as fishermen rely on fishing lamps to attract fish schools at night. However, this study did not have direct information on light usage in the Taiwanese logbook data for the stick-held dip net fishery. As a proxy for fishing power, vessel ID was used as a covariate in the CPUE standardization process, a common approach in fisheries research (Punt et al., 2000; Glazer and Butterworth, 2002; Battaile and Quinn, 2004).

Two metrics of fishing effort − haul numbers and fishing days − could be used to define the CPUE from the Pacific saury logbook dataset. However, these metrics were not consistently reported throughout the study period. Haul data, which were first recorded in 2003, were missing from 48% of the logbook records between 2003 and 2006. As a result, fishing effort defined by the number of fishing days allowed for a longer period of analysis (1997 − 2019).

Despite the advantage of having a longer period of data, using the fishing day definition of effort could potentially lead to hyperstability (Hilborn and Walters, 1992). This could occur if an increase in daily hauls was used to maintain a consistent daily catch

doi:10.6342/NTU202500253

rate when fish abundance was low, potentially distorting the true relationship between effort and catch. To evaluate this concern, we developed standardized indices using both effort definitions (**Figure S2.1**). Since the trends were similar between the two metrics, CPUE based on fishing days (metric tons per day) was ultimately used throughout the analysis.

Positive CPUE data were assumed to follow either a lognormal or gamma distribution (Ortiz and Arocha, 2004); the lognormal distribution was assumed in the current study for positive CPUE data following Ichinokawa and Brodziak (2010) and Winker et al. (2013). An exploratory analysis did not indicate that the current analysis was sensitive to the choice of error distribution as the standardized CPUE indices and deviance explained (e.g., conditional R^2) were similar for the two error distributions within the GLMM considered. The residual frequency distributions of the two error assumptions derived from the five GLMMs indicated no violation of the assumed statistical distributions. Accordingly, we normalized the CPUE response by the natural logarithm transformation, *log*(*CPUE*), which is a common procedure in CPUE standardization (Winker et al., 2013; Grüss et al., 2019). To focus on comparing the influences of various spatial treatments on the CPUE standardization, we only included five explanatory variables in the GLMMs, and we did not conduct any model selection procedure. However, the statistical significance of each variable was examined. Explanatory variables considered in the GLMMs included *Year*, *Area* (see section *2.2.3*), *Vessel*, quadratic water temperature effects (*SST* and SST^2), and the interaction of year and spatial effects (*Year*×*Area*; to take into account vessel targeting behavior or fish distribution shift). *SST* and SST^2 were treated as continuous variables while the remaining covariates were treated as factors. This study fits GLMMs to standardize CPUE for Pacific saury as described in the following equation (Ono et al., 2015; Thorson et al., 2015):

$$\log(p_i) = \beta_{Year(i)} + \beta_{Area(i)} + \beta_{Year(i)\times Area(i)} + \beta_{Vessel(i)} + \beta_{SST(i)} \times SST_{(i)} + \beta_{SST^2(i)} \times SST^2{}_{(i)} \quad (2.1)$$

where p_i is the predictor for observations i (metric tons/day), and β is the estimated coefficient of its subscript (e.g., *Year*, *Area*, etc.) for observation i. This study treated the

doi:10.6342/NTU202500253

year effect, area effect, and quadratic water temperature effects as fixed effects. The vessel and the year × spatial interaction were treated as random effects. Model fitting was carried out with the "*lmer*" functions provided in the R statistical platform (Bates et al., 2015; R Core Team, 2021).

2.2.3. Spatial treatments in the spatially stratified GLMMs

Three area stratification approaches were used in the GLMMs (i.e., spatially stratified GLMMs) for standardizing Pacific saury CPUE data. These alternative area stratifications are described below:

(i) Ad hoc approach

The definition of the four area strata was modified based on Huang et al. (2007; 2020) which grouped the $1^o \times 1^o$ grids of Pacific saury CPUE data based on the bathymetric (depth) contours derived from the Centenary Edition of the GEBCO (General Bathymetric Chart of the Oceans) Digital Atlas (IOC-IHO-BODC, 2003). This approach is currently used for the CPUE standardization of Pacific saury by the North Pacific Fisheries Commission (Huang et al., 2021; Hashimoto et al., 2020).

(ii) Binary recursive partitioning approach

The binary recursive partitioning method, developed by Ichinokawa and Brodziak (2010), is an algorithm that systematically divides the study area into multiple strata through sequential, recursive steps. This method was used to partition Pacific saury CPUE data using a three-step process. First, the algorithm divided the entire study domain into all possible pairs of strata, using a fixed spatial resolution (0.25°) defined by a grid of evenly spaced dividing lines. Second, a generalized linear mixed model (GLMM; see Section *2.2.2*) was employed to fit the CPUE data for each possible stratification. Third, the Akaike Information Criterion (AIC; Burnham and Anderson, 2002) was used to identify the stratification with the best model fit among the options. This process was repeated recursively, refining the strata until no further AIC improvements could be achieved by adding additional strata. To maintain consistency and comparability across stratification approaches, the maximum number of strata was limited to six.

doi:10.6342/NTU202500253

(iii) Spatial clustering approach

The spatial clustering method used a k-medoids algorithm to divide the 0.25° × 0.25° grids of Pacific saury CPUE into distinct area strata, considering both spatial proximity and average CPUE within each grid (Ono et al., 2015). The process began by calculating the Euclidean distance and the difference in mean CPUE values between grid pairs. Next, a *k*-medoids clustering analysis (Kaufman and Rousseeuw, 1990) was performed, where medoids represent the grid points within each cluster that have the lowest average dissimilarity to other points in the same cluster. To adjust the clustering process, the dissimilarity matrix was multiplied by a weighting factor *w*, which emphasized (or de-emphasized) the influence of spatial proximity relative to differences in fish population density (Ono et al., 2015). This approach resulted in irregularly shaped strata, aligning them more closely with the population distribution patterns inferred from the CPUE data.

Following the approach of Ono et al. (2015), this study set two weighting factors, w =1 and w = 0.1, to illustrate two shapes for the stratified area, namely "Spatial 1" and "Spatial 0.1". The "Spatial 1" approach assigns equal weight to spatial proximity and average fish density. The "Spatial 1" configuration assigns equal weight to spatial proximity and average fish density, while the "Spatial 0.1" configuration reduces the weight of spatial proximity, making a one-unit difference in spatial coordinates 100 times less influential than a one-unit change in population density. The *k*-medoids clustering analysis was conducted using the *pam*() function from the cluster package in R (Maechler et al., 2014). To determine the optimal number of area strata, a visual inspection of the inflection point in the change of AIC values was performed as the number of clusters increased. The number of clusters (ranging between 2 and 6 strata) corresponding to this inflection point was selected as the optimal solution.

2.2.4. Spatio-temporal GLMM

The spatio-temporal modelling approach used herein was adapted from the R package *VAST* (version 3.2.2 of the *VAST* R package) (https://github.com/James-Thorson-NOAA/VAST) developed by Thorson et al. (2015). By default, VAST implements a delta-generalized linear mixed modelling framework, where the probability distribution for the

doi:10.6342/NTU202500253

catch is decomposed into two components representing the probability of encounter and the expected catch rate, given that catch occurs (Thorson, 2019). This study only included the positive catch rate (i.e., observed CPUE) component because the Pacific saury dataset did not contain zero CPUE data. This model structure is possible in *VAST* by specifying the user-controlled vector for observation models as ObsModel = 1 (the distribution for positive catch rates is lognormal) and 3 (the encounter probability equals 1 for any year) in VAST and by turning off all model structure associated with the probability of encounter component (e.g., FieldConfig = c("Omega1"= 0, "Epsilon1"= 0, "Omega2"= 1, "Epsilon2"= 1) & OverdispersionConfig = c("Eta1"= 0, "Eta2"= 1)). The positive catch rate was approximated using a lognormal GLMM with a log-link function and linear predictors, which included Gaussian random fields to model the spatial and spatio-temporal effects. The assumption of using a log-transformed positive catch rate in VAST has been commonly used (e.g., Xu et al., 2019; Grüss et al., 2019; Sculley and Brodziak, 2020). Other positive continuous distributions such as the Gamma distribution could also be considered.

VAST requires the specification of spatial knots (*s*), which are points used to estimate the correlations for spatial and spatio-temporal effects. This study specified 100 spatial knots to approximate the spatial and spatio-temporal autocorrelated variations. This approach differs from the default configuration in VAST, where spatial knots are allocated with density proportional to the sampling intensity through a *k*-means algorithm (e.g., Xu et al., 2019; Grüss et al., 2019; Sculley and Brodziak, 2020). However, previous studies (e.g., Ducharme-Barth et al., 2022) have suggested that a uniform allocation of knots across a pre-defined spatial domain might be preferable over a proportional allocation based on fishing intensity using *k*-means. As a sensitivity, this study developed two standardized indices using both knot configurations (**Figure S2.2**). The trend observed between both knot configurations was similar, but the coefficients of variation (CVs) for the standardized indices derived from the uniform knot distribution were higher than those from the proportional knot distribution (**Figure S2.3**). Given the similarity of standardized indices, this study used the proportional knot distribution for the comparison to other spatial treatments in this study. Additionally, an exploratory analysis was conducted to confirm that the results remained qualitatively similar when using different numbers of spatial knots

doi:10.6342/NTU202500253

(100, 150, and 200 knots). The logarithmic prediction of the standardized Pacific saury CPUE is described below:

$$\log(p_i) = \beta(t_i) + \omega(s_i) + \varepsilon(s_i, t_i) + \delta(v_i) + \sum_{j=1}^{n_j} \gamma(j) X(s_i, t_i, j) \quad (2.2)$$

where $p(i)$ is the predictor for observation i (metric tons/day), $\beta(t_i)$ is the intercept for year t_i as a fixed effect and independent among years, $\omega(s_i)$ is the time-invariant spatial variation at location s_i (i.e., each of the 100 knots), and $\varepsilon(s_i,t_i)$ is the time-varying spatio-temporal variation for location s_i in year t_i, and $\delta(v_i)$ is the vessel effect as a mean-zero random effect with a standard deviation of one (Thorson, 2019). In addition, $\gamma(j)$ is the j_{th} catchability covariate $X(s_i, t_i, j)$ on location s_i in year t_i (i.e., the impact of SST on daily observed Pacific saury CPUE; Hashimoto et al., 2020), n_j is the number of catchability covariates. The marginal likelihood of fixed effect parameters is calculated with Template Model Builder using the Laplace approximation to integrate across random effect parameters (Kristensen et al., 2016), and fixed effect parameters are then estimated by maximizing the marginal likelihood within the R computing environment (R Core Team, 2021). Convergence was checked by ensuring that the absolute value of the final gradient of the log-likelihood function at the maximum likelihood estimate was less than 0.001 for all parameters and that the Hessian matrix of the likelihood function was positive definite.

2.2.5. Statistical performance

The conditional R^2 (Nakagawa and Schielzeth, 2013) and conditional AIC (Greven and Kneib, 2010) were calculated to evaluate the performance of five GLMMs applied to Pacific saury CPUE data. These models included the Ad hoc, Binary, Spatial 1, Spatial 0.1 GLMMs, and VAST. To further compare model performance, repeated five-fold cross-validation was conducted (Winker et al., 2013; Shono, 2014). A stratified random sampling approach, using years as strata, was applied during cross-validation to maintain the dataset's structure, as the year effect was a key variable. Within each year stratum, the data were randomly sampled without replacement. For each cross-validation iteration,

doi:10.6342/NTU202500253

80% of the data served as “training data” to fit the model, while the remaining 20% was used as “testing data” to predict CPUE based on the covariate information. The statistical performance of the five GLMMs was assessed by averaging the explained deviances (R^2) and Pearson’s correlation coefficients derived from the observed and predicted CPUE values in the testing data. To ensure robust evaluation, the five-fold cross-validation process was repeated 10 times. The average values of R^2 and Pearson’s correlation coefficients across the 10 replicates were used to determine the overall performance of each GLMM.

2.2.6. Standardized abundance indices

Standardized abundance indices derived from spatially stratified GLMMs (Ad hoc, Binary, Spatial 1, and Spatial 0.1) were calculated in two steps. First, CPUE was predicted with fitted GLMMs for all combinations of years and areas. This study then used the mean of the assumed normal distribution of the year × spatial random effect (i.e., zero) to impute the missing year × spatial values to derive the standardized CPUE for each year and area (Campbell, 2015):

$$\hat{CPUE}_{Area,Year} = \exp\left(\beta_{Year} + \beta_{Area} + \beta_{Year\times Area}\right) \tag{2.3}$$

A bias-corrected estimate for the standardized CPUE in each year and area was calculated as $\exp\left(\hat{CPUE}_{Area,Year} + \hat{\sigma}^2/2\right)$, where $\hat{\sigma}^2$ is the estimated model standard deviation (residual standard error) (Maunder and Punt, 2004). In the second step, this study calculated the standardized abundance indices, with and without area weighting, and compared their difference(s) for each spatially stratified GLMM. The index without the area weighting was computed by using an equal weight for each area (i.e., arithmetic mean). The area-weighted index ($\hat{CPUE}_{Year}$) was obtained by summing over all stratified areas within a year ($\hat{CPUE}_{Area,Year}$) following Campbell (2015):

doi:10.6342/NTU202500253

$$\hat{CPUE}_{Year} = \sum_{Area=1}^{n_s} SA_{Area} \times \hat{CPUE}_{Area,Year} \quad (2.4)$$

where n is the number of area strata (which differ among various area stratification approaches); SA_{Area} is the proportion of the surface area for a given *Area* to the whole studied domain.

Unlike the spatially stratified approaches, the explicit spatial correlation modelled in VAST was used to predict the Pacific saury density across all spatial cells in this study area. The standardized abundance index in year t across the studied area was described as follows:

$$\hat{CPUE}(t) = \sum_{n_s=1}^{n_s} SA(s) \times \exp\left(\beta(t) + \omega(s) + \varepsilon(s,t)\right) \quad (2.5)$$

where n_s is the number of knots s; $\beta(t)$ is the year effect in t year; $\omega(s)$ is the spatial effect at s knot; $\varepsilon(s,t)$ is the spatio-temporal effect at s knot in t year, and $SA(s)$ is the surface area of the triangulated mesh associated with knot s. Annual relative abundance indices without area weighting were also calculated for VAST. The bias-correction estimator within VAST (Thorson and Kristensen, 2016) was employed to account for retransformation bias when predicting the abundance.

Uncertainties about the annual relative abundance indices deriving from the three spatially stratified GLMMs were estimated based on the method used by Campbell (2015; see section *2.2.6* for details). For VAST, the uncertainty of the predicted index was computed using a generalization of the delta method (Thorson et al., 2015; Thorson and Barnett, 2017). Each of the standardized abundance indices was then normalized to its mean value over the studied period (1994 - 2019). This normalization step allows for easier comparison across the different models and ensures that the indices are on the same scale. Normalizing to the mean period helps to highlight trends and variations over time,

doi:10.6342/NTU202500253

regardless of absolute magnitude, making it easier to detect patterns and assess the relative abundance of Pacific saury over the study period (Winker et al., 2013; Kai et al., 2017).

2.2.7. Quantifying the influence of explanatory variables

To quantify the influence of each explanatory variable on the difference between standardized CPUE and the unstandardized arithmetic mean of observed CPUE for each year, we applied the influence analysis method outlined by Bentley et al. (2012). This approach calculates the annual influence of an explanatory variable by combining the model coefficients with changes in the distribution of CPUE data over time, as visualized in the Coefficient Distribution-Influence (CDI) plot (Bentley et al., 2012).

To calculate such a measure of influence, the normalized coefficient associated with an explanatory variable (ρ) was calculated as:

$$\rho = \sum_{i=1}^{n} \alpha_i \Big/ n \tag{2.6}$$

where α_i is the estimated coefficient of a variable (factor) corresponding to observation i, and n is the number of CPUE observations. Then, the annual influence value for a variable in year y (AI_y) was the exponentiation of the mean difference between the coefficients corresponding to all observations in that year and the normalized coefficient for a multiplicative GLMM (since the log-link function was used, i.e., $AI_y = \exp(\delta_y)$):

$$\delta_y = \left(\frac{\sum_{i=1}^{n_y} \alpha_i - \rho}{n_y} \right) \tag{2.7}$$

where n_y is the number of observations in year y. If the AI_y value for a variable is larger than one, it implies that adding this variable to the model will make the standardized CPUE

doi:10.6342/NTU202500253

less than the unstandardized CPUE in year *y*. Conversely, an AI_y value less than one indicates that adding the variable will make the standardized CPUE higher than the unstandardized CPUE in year *y*. If AI_y equals one, the variable has no impact on the difference between unstandardized and standardized CPUE in year *y*.

The overall influence metric of a variable across all years ($\overline{AI}$) was calculated as:

$$\overline{AI} = \exp\left(\frac{\sum_{y=1}^{y=m} \delta_y}{m}\right) - 1 \tag{2.8}$$

where *m* is the number of years.

The CDI plot, first introduced by Bentley et al. (2012), integrates information on normalized coefficient values, changes in the data record's distribution, and the resulting *AI* values into a single visualization (see **Figure 2.4** for an example). Specifically, the top panel of the CDI plot displays the normalized coefficients for a variable along with their standard errors. The bottom-left panel uses bubbles to represent the annual distribution of data records across levels of the variable, while the bottom-right panel shows the *AI* values for the variable over time. When extending the CDI plot to VAST, this study grouped the 100 spatial knots into 20 "grouped" knots based on their coefficients, arranged from low to high, to simplify the visualization of the spatial random effect's data distribution and coefficients. A CDI plot was then generated for these grouped knots. Since knots with similar coefficients correspond to spatial areas with similar levels of predicted abundance, this grouping enabled the identification of index changes driven by shifts in sampling effort between areas of high or low estimated abundance. Additionally, exploratory analysis revealed that spatial knots within the same group were generally located close to each other geographically.

Although the year × spatial interaction was modeled as a random effect (i.e., assumed to be normally distributed with a mean of zero), its influence could still be assessed by analyzing patterns in the coefficients that deviate from their overall average. To better understand the information captured by the year × spatial interaction coefficients

doi:10.6342/NTU202500253

across years, we adapted the CDI plot method of Bentley et al. (2012). Specifically, we visualized the normalized coefficients of the year × spatial interaction (represented as solid, colored circles in the top panel) by area. The AI_y value for the year × spatial interaction in year y (displayed in the bottom-right panel) was calculated in the same manner as for a factor variable. For the spatio-temporal effect in VAST, the CDI plot also utilized 20 grouped knots, simplifying the visualization while retaining spatial resolution. This approach allowed for a clearer examination of the interaction's contributions to variability in CPUE across both time and space. In this study, influence analysis was applied solely to explain the difference between the standardized index without area weighting and the unstandardized index. This limitation was due to the fact that the area-weighting process operates independently of the estimated coefficients and the distributional changes in CPUE observations over time.

2.2.8. Evaluation using simulated data

Simulation testing is a powerful tool for evaluating the performance of CPUE standardization methods (Ono et al., 2015; Grüss et al., 2019; Ducharme-Barth et al., 2022). The key advantage of this approach is that the simulated abundance trends are known, allowing the standardization methods to be tested based on their ability to accurately predict "true" abundance trends. However, abundance indices derived from fishery-dependent CPUE data are prone to bias due to the non-random nature of fisheries' spatial distributions - a phenomenon known as "preferential sampling" (Clark and Mangel, 1979; Rose and Leggett, 1991; Rose and Kulka, 1999; Swain and Sinclair, 1994).

To address this, this study developed a simulation framework incorporating two spatial sampling scenarios - random and preferential spatial sampling patterns - to evaluate which spatial treatments could effectively account for spatial heterogeneity in the data and produce unbiased results relative to the true value. Simulated Pacific saury data, reflecting conditions in the Northwestern Pacific Ocean, were generated and analyzed using both spatially stratified GLMMs (i.e., Ad hoc, Binary, and Spatial clustering approaches) and VAST. The models were fit to the simulated CPUE data under the two sampling scenarios: (i) random spatial sampling and (ii) preferential spatial sampling. The resulting total

doi:10.6342/NTU202500253

abundance estimates were then compared with the true abundance values to assess model performance.

(i) Sampling patterns

The spatial domain of the simulation covered the spatial extent of the fishing ground for Pacific saury from 140 − 170°E and from 35 − 50°N (Hsu et al., 2021). Following the approach by Thorson et al. (2015), true biomass was simulated by fitting a VAST model without effects of vessel and sea surface temperature to generate a base biomass distribution of Pacific saury $B(s,t)$ (metric tons/day) from 1997 to 2019, where s denotes a cell of 0.25° spatial resolution (7,023 cells in the spatial domain) and t denotes the yearly time step (illustrated in **Figure S2.4**a). The biomass summed across all 0.25° spatial cells over the whole spatial domain for the year t was referred to as the "true" index (T_t). For each of the different spatial sampling patterns (i.e., random and preferential sampling; **Figure S2.4**b-c), observation error η was incorporated to produce the "observed" data $\hat{d}(s,t)$ at each spatial cell s and year t:

$$\hat{d}(s,t) = B(s,t) \times e^{\eta} \tag{2.9}$$

$$\eta \sim Normal(0, 0.2) \tag{2.10}$$

In the random sampling pattern, each spatial cell s had an equal probability of being selected, regardless of the underlying Pacific saury density distribution. In contrast, the preferential sampling pattern followed the principle that fishers are more likely to fish in areas with higher fish densities (Allen and McGlade, 1986; Hilborn and Walters, 1987). For both the random and preferential sampling scenarios, 300 spatial cells were sampled per time step, with replacement. Exploratory analysis confirmed that a total of 300 observations was sufficient to recover the "true" abundance index under the random sampling pattern. For the preferential sampling pattern, however, the probability of selecting a spatial cell s ($P_{pref,s}$) in a given year was proportional to the simulated fish density (Ducharme-Barth et al., 2022):

doi:10.6342/NTU202500253

$$P_{pref,s} = \frac{(B_s)^{\varphi}}{\sum_{n_s=1}^{n_s}(B_s)^{\varphi}} \tag{2.11}$$

where the probability exponent φ controls the magnitude of preferential sampling. When φ = 0 all spatial cells have an equal probability of being sampled (e.g., random sampling). This study set φ = 8 to impose a very strong degree of preferential sampling (extreme preferential sampling, Ducharme-Barth et al., 2022). Both fishing effort sampling patterns were simulated 40 times, resulting in a total of 80 datasets that were used to estimate abundance indices. It should be noted that the defined area strata in the Binary and Spatial clustering approaches and knot configurations in VAST would differ slightly among simulation runs since the simulated data varied with each iteration.

(ii) CPUE standardization and performance evaluation

Model performance in all simulations was evaluated relative to the "true" index. Prior to assessing model performance, each of the derived indices with area weighting (both estimated and true indices) was rescaled to a mean of 1 by dividing by its overall mean, respectively. Model performance was assessed based on three metrics: (1) the relative error metric in year y (RE_y); (2) the root mean squared error (RMSE) and (3) the bias metric described below.

The relative error in each year was calculated as (Ono et al., 2015):

$$RE_y = \frac{(\hat{I}_y - T_y)}{T_y} \tag{2.12}$$

where $\hat{I}_y$ and T_y are the estimated and true indices in year y.

The measurement of model error was calculated as below (Stow et al., 2009; Ducharme-Barth et al., 2022):

doi:10.6342/NTU202500253

$$RMSE = \sqrt{\frac{\sum_{y=1}^{n} (\hat{I}_y - T_y)^2}{n}} \quad (2.13)$$

where n is the number of years. A higher RMSE represents a greater error in the estimated index of abundance.

The bias metric we considered was the coefficient β of the following the linear model (Thorson et al., 2015; Grüss et al., 2019; Ducharme-Barth et al., 2022):

$$\hat{I}_y = \alpha + \beta \times T_y + \varepsilon_y \quad (2.14)$$

$$\varepsilon_y \sim Normal(0, \sigma_\varepsilon^2) \quad (2.15)$$

where α is the intercept, and β is the slope parameter from a linear model between the true index T_y and the estimated index of abundance $\hat{I}_y$. A β of 1 is indicative that changes in the true index are reflected accurately by the estimated index (i.e., unbiased), while a β greater than 1 (lower than 1) indicates that $\hat{I}_y$ underestimates (overestimates) changes in the true index (Wilberg et al., 2010; Thorson et al., 2015). This study also examined if the best model selected by conditional AIC and conditional R^2 in the simulation test could provide the least biased representation of the true index pattern.

2.3. Results

2.3.1. Area stratifications and knots configuration

The geographic boundaries and variability of observed CPUE for the area strata, as determined by the area stratification approaches, are shown in **Figure 2.1**. The studied area was divided into four strata by both the ad hoc method and the binary recursive algorithm (**Figure 2.1**a and c). The optimal number of clusters (i.e., five area strata) for the Spatial 1 and Spatial 0.1 approaches was determined using the inflection point in the change of AIC values (results not shown). The area strata in the Spatial 1 approach were less patchy

doi:10.6342/NTU202500253

compared to those in the Spatial 0.1 approach, which was due to the greater emphasis on spatial proximity relative to the observed CPUE differences (**Figure 2.1**e and h). For each area stratification approach, the mean observed CPUE across the strata differed significantly (ANOVA test, $p < 0.001$) (**Figure 2.1**b, d, f, and g). In the VAST model, the 100 spatial knots were distributed in proportion to the density of observations, resulting in fewer knots at the periphery of the spatial domain. Model convergence was confirmed as the Hessian matrix was positive definite and the maximum gradient component was smaller than 0.001. Most of the higher observed CPUE values were found in areas where more spatial knots were distributed (**Figure 2.1**i). This outcome was expected, given the decision to allocate spatial knots based on the density of fishery-dependent samples, and suggests that preferential sampling may be present in the Pacific saury data.

2.3.2. Comparison of the statistical performance

All explanatory variables considered in the GLMMs were statistically significant (likelihood-ratio test, $p < 0.005$) (**Table S2.1**). The year × spatial random-effect coefficients for each GLMM have been assessed to follow a normal distribution (Shapiro-Wilk test; $p > 0.05$). In general, the VAST model demonstrated higher conditional R^2 and lower conditional AIC values than the spatially stratified GLMMs (**Table 2.1**). Additionally, results from the testing data in the five-fold cross-validation showed that VAST achieved the highest mean values for deviance explained (mean conditional R^2 = 65%) and Pearson's correlation coefficient (mean $\rho = 0.54$) compared to the other GLMMs (**Table 2.1**). Overall, VAST outperformed the other models, providing the best fit to the data, while the Ad hoc GLMM performed the poorest. Aside from VAST, the two spatial clustering GLMMs also performed better than the other spatially stratified models, based on both the goodness-of-fit and five-fold cross-validation results (**Table 2.1**).

2.3.3. Trends in nominal and standardized indices

Trends in nominal and standardized indices for Pacific saury without area-weighting illustrated large fluctuations (**Figure 2.2**a). The annual trends of nominal and standardized CPUE were generally consistent from 1997 to 2008, with the exception of the Binary

doi:10.6342/NTU202500253

GLMM in 2000. From 2009 to 2014, both nominal and standardized CPUE showed an increasing trend, although the standardized CPUE displayed significant interannual variability. Both nominal and standardized CPUE showed a decreasing trend during 2015 − 2019. The CVs of annual relative abundance indices derived from the Binary GLMM (0.23 − 0.33) and VAST (0.10 − 0.21) showed a decreasing temporal trend while the CVs from the other GLMMs were relatively stable in the late time period (**Figure 2.2**b).

The area-weighted abundance indices calculated from all GLMMs displayed less variation than the indices without area weighting. This study compared the derived abundance indices with and without the area-weighting approach from the spatially stratified GLMMs (**Figure S2.5**). For the Ad hoc and Spatial 1 GLMMs, each area strata had a similar surface area (i.e., similar spatial weighting) which caused the derived weighted standardized abundance indices to be very similar to the un-weighted indices (**Figure S2.6**a, and c). However, the abundance indices derived from the Binary and Spatial 0.1 GLMMs received more weighting from Area III and Area IV, respectively, leading to slight divergences between the weighted and unweighted standardized abundance indices (**Figure S2**.6b and d).

2.3.4. Influence of explanatory variables on annual relative abundance indices

The AI plots of the GLMMs, which illustrate the influence of each variable on the differences between standardized and unstandardized CPUE, are shown in **Figure 2.3**. AI values for the spatial and year × spatial effects varied across the five GLMMs, while the AI values for the vessel and quadratic SST effects exhibited consistent trends among the models. This outcome highlights the importance of spatial treatment in the GLMMs (for example, see **Figure 2.2**a). The substantial discrepancy between annual relative abundance indices compared to the unstandardized CPUE during 2009 − 2014 could be explained by the larger variation of the AI values for the year × spatial effect (0.81 − 1.45) and the increasing AI values of the vessel effect (0.94 − 1.10) over the time period. The influence of vessel effect showed an obvious increasing trend in recent years (**Figure 2.3**). Higher AI values for the vessel effect (1.15 − 1.27) compared to the spatial and year × spatial

doi:10.6342/NTU202500253

effects (spatio-temporal effect) (0.80 − 1.24) during 2015 − 2019 led to the annual standardized CPUE being lower than the unstandardized CPUE.

Overall, the influence of each variable indicated that the spatial, year × spatial interaction, and vessel effects had greater overall influence on the annual relative abundance indices than the quadratic SST effect (the overall influence of SST was nearly one) (**Table 2.2**). Although the spatial and vessel effects exhibited greater explanatory power (conditional R^2) than the year × spatial effect in the spatially stratified GLMMs, their influence on the difference between standardized and unstandardized CPUE was less than that of the year × spatial effect. This suggests that a variable with higher explanatory power (e.g., spatial and vessel effects) does not necessarily have a greater influence on the difference between standardized and unstandardized CPUE.

2.3.5. Exploration of the spatial treatments in influencing annual relative abundance indices

The composite CDI plots of the spatial effects for spatially stratified GLMMs are shown in **Figure 2.4**, while the spatial random effect for VAST is depicted in **Figure 2.5**. The AI values of the spatial effects for the spatially stratified GLMMs were greater than one (vertical line in the bottom-right panel of **Figure 2.4**) before 2000, except for the Spatial 0.1 GLMM. This was because a larger proportion of the data was distributed in area strata (Area I for Ad hoc, Area III for Binary, and Area I for Spatial 1) with coefficients (spatial effects) larger than one (horizontal line in the top panel of **Figure 2.4**). In contrast, for the Spatial 0.1 GLMM, a higher proportion of the data was concentrated in Area I, which had a coefficient lower than one, resulting in AI values of the spatial effect being below one from 1998 to 2000. During 2006 - 2014, the data were uniformly distributed across all area strata for all spatially stratified GLMMs, and as a result, the AI values of the spatial effect remained stable around one. Since 2015, the AI values of the spatial effect were consistently below one for all spatially stratified GLMMs, as a larger proportion of data shifted to area strata with smaller coefficients (Area IV for Ad hoc, Area II for Binary, Area V for Spatial 1, and Areas II and V for Spatial 0.1). For the VAST model, the AI values of the spatial random effect were above one before 2004, as a greater proportion of

doi:10.6342/NTU202500253

the data was distributed in grouped knots (knots 17 − 20) with coefficients larger than one (**Figure 2.5**).

The composite CDI plot of the year × spatial effect for spatially stratified GLMMs is shown in **Figure 2.6**. A substantially higher AI value for the year × spatial effect was observed in 2000 for the Binary GLMM and in 2006 for all spatially stratified GLMMs, respectively. This was due to a greater proportion of data being distributed in Area III with a high coefficient (3.30) in 2000 for the Binary GLMM and in Areas III, II, IV, and V in 2006 for the Ad hoc (2.33), Binary (3.95), Spatial 1 (2.30), and Spatial 0.1 (1.63) GLMM, respectively. The CDI plot of the spatio-temporal effect for the VAST model is shown in **Figure 2.7**. Higher AI values were observed in 2006 and 2007 for VAST, as the coefficients were generally higher for those years. A lower AI value was also observed in 2015, resulting from a higher proportion of the data shifting to the grouped knots 1 − 3 with lower coefficients.

2.3.6. Results of simulation test

Relative errors (REs) from the simulation results indicated that the VAST model produced relative abundance indices that closely matched the "true" index (REs fluctuated around zero overtime without an apparent trend) for both sampling scenarios compared to other GLMMs (**Figure 2.8**). VAST also exhibited the lowest mean RMSE and the least bias (i.e., close to one) under both random and preferential sampling scenarios (**Figure 2.9**). In contrast, the Ad hoc and Binary GLMMs generally exhibited larger REs over time (exceeding or nearing ± 20%) (Figure 2.8a), higher mean RMSE values (0.14 and 0.13), and less accurate estimates of the relative abundance index (mean bias = 1.02 and 0.97), compared to the other approaches under the random sampling scenario (**Figure 2.9**a). Notably, the Spatial 1 and 0.1 GLMMs generally performed similarly to VAST under the random sampling scenario. However, the Spatial 0.1 GLMM displayed a temporal trend in REs with considerable variation (**Figure 2.8**i), the largest model error (mean RMSE = 0.18), and the highest bias (overestimation; mean bias = 0.89) compared to other GLMMs under the preferential sampling scenario (**Figure 2.9**b). Overall, all GLMMs exhibited higher model errors (i.e., larger mean RMSE) under the preferential sampling scenario compared

doi:10.6342/NTU202500253

to the random sampling, though a pattern of larger mean bias was not observed (although the standard deviation of bias increased) (**Figure 2.9**).

The model selection criteria (i.e., conditional R^2 and conditional AIC) evaluated from the simulation results, along with RMSE and bias, consistently showed that VAST was the best model under both sampling scenarios (**Figure S2.7**). However, under the preferential sampling scenario, the Spatial 0.1 GLMM had a greater value for the conditional R^2 and a lower conditional AIC value than the Ad hoc and Binary GLMMs (**Figure S2.7**b). It was also the most inaccurate and biased representation of the true index based on the simulation results of RE, RMSE, and bias metrics. This suggests that model selection criteria did not consistently align with the model performance in fitting the true index.

2.4. Discussion

This study employed an influence analysis to assess the standardization effects of explanatory variables included in the five GLMMs using Pacific saury fishery data. A key finding was the growing influence of the vessel effect observed in recent years, which suggests a temporal shift in catchability within the Taiwanese stick-held dip net fishery. Since catchability often fluctuates over time in many fisheries (Wilberg et al., 2010), failing to account for such variations in CPUE standardization could lead to errors, including overestimating the Pacific saury abundance index in more recent years. Additionally, this study extended the original *influ* package to accommodate the interaction between year × spatial effects in spatially stratified GLMMs, as well as the spatio-temporal effects in the spatio-temporal model (VAST). The year × spatial or spatio-temporal interaction was identified as the most influential effect, with large coefficients and substantial interannual variation. This led to significant fluctuations in the annual abundance index (AI) values, as shown in the influence plots. Notably, the year × spatial interaction in the spatially stratified GLMMs exhibited substantial AI values for the years 2000 and 2006 (**Figure 2.3**b). These spikes in influence suggest that the spatial structure assumed for those years may have been mis-specified, resulting in extreme estimated coefficients and potentially biased results for those years. This underscores the importance of carefully evaluating spatial assumptions

doi:10.6342/NTU202500253

and their impact on CPUE standardization models, particularly in years where model performance may be compromised.

The results of this study also indicated that the variable with the greatest explanatory power in terms of deviance explained (such as the vessel or area variable in the Pacific saury example) did not necessarily have the most significant influence on the difference between unstandardized and standardized CPUE. Overall, we conclude that the difference between standardized and unstandardized CPUE in the Pacific saury fishery can primarily be attributed to modeled changes in fishing locations or shifts in fish distribution over time (Hashimoto et al., 2020; Hsu et al., 2021). Additionally, there was evidence of a shift in the fleet toward more efficient vessels, as reflected in the influence plot and overall influence metric for the vessel variable. This study highlighted the extended influence analysis, particularly the application to spatial and year × spatial interaction effects (spatio-temporal effects in VAST), as an effective tool for evaluating whether the spatial structure assumed in the model can capture patterns in the spatial heterogeneity of the CPUE data and identify spatial shifts over time under preferential sampling.

In the real-world application using Pacific saury fishery data, VAST demonstrated superior performance compared to other GLMMs in terms of conditional AIC values, deviance explained (as measured by conditional R^2), and results from five-fold cross-validation (mean conditional R^2 and Pearson's correlation coefficient). Additionally, under both random and preferential sampling scenarios, VAST showed better performance, with lower model error (the smallest RMSE) and bias (bias value close to one) compared to the other spatially stratified GLMMs. This is due to VAST's ability to efficiently model how fish density varies continuously across space (Kristensen et al., 2014) and describe temporal patterns in density distribution (unexplained variability; Thorson and Barnett, 2017; Hsu et al., 2021; Han et al., 2022) through spatial and spatio-temporal random effects, implemented using a stochastic partial differential equation approach (Lindgren et al., 2011).

This study concluded that a spatio-temporal model, such as the one used in VAST, more effectively captures the spatial heterogeneity of CPUE data, as shown by the simulation results. Moreover, VAST proved to be more robust to deviations from random

doi:10.6342/NTU202500253

sampling than the other GLMMs used in this study. Similar findings from Kai (2019) on pelagic sharks also indicated that including spatio-temporal random effects in a model minimizes residual variability, and that a GLMM with spatial random effects performs better than models with fixed spatial effects. Furthermore, VAST offers a more direct approach for conventional CPUE analysis because it does not require pre-defined area stratification. This study also contributes to a growing body of literature suggesting that spatio-temporal approaches like VAST are more statistically efficient (i.e., they provide greater precision with a given amount of data; **Figure 2.2**b) compared to spatially stratified models (Thorson et al., 2015; Kai, 2019; Grüss et al., 2019; Zhou et al., 2019).

The ad hoc GLMM showed the poorest performance among the spatially stratified GLMMs in terms of conditional R^2, conditional AIC, and five-fold cross-validation results for the Pacific saury fishery data. This study suggests that the use of four area strata, separated in an ad hoc manner based on bathymetric contours, may not adequately capture the spatial heterogeneity of Pacific saury density. This conclusion was supported by the simulation results, which demonstrated that the Ad hoc GLMM consistently had higher model errors in index estimation compared to the Binary and Spatial 1 approaches, regardless of the sampling patterns. Given that many CPUE standardization analyses use an ad hoc approach (e.g., Nakano, 1998; Haltuch et al., 2013), the study emphasizes the need for caution when employing such methods. However, it's worth noting that alternative ad hoc spatial structures (e.g., 5° × 5° grid) exist, and the effectiveness of these methods should be evaluated in the context of the findings from this study in future work.

The binary recursive algorithm, which uses AIC to guide area stratification, was found to be an objective method for defining area strata. However, the simulation results indicated that the Binary GLMM generally performed poorly in index estimation, with larger RMSE and bias. This could be due to the inherent limitations of the binary partitioning approach, which constrains the area strata to rectangular shapes. In contrast, the distribution of fish density is typically irregular and not structured in rectangular patterns. Among the other approaches evaluated, the Spatial 0.1 and Spatial 1 GLMMs demonstrated better performance with higher conditional R^2 and lower conditional AIC compared to the Binary GLMM when applied to Pacific saury fishery data (**Table 2.1**).

doi:10.6342/NTU202500253

The simulation results showed that these spatial clustering approaches performed well under the random sampling scenario. Spatial clustering, which creates more flexible area strata based on the similarity of average CPUE and spatial proximity, was better able to reflect the patchy nature of Pacific saury habitats, which are often associated with features like eddies and SST fronts (Kuroda and Yokouchi, 2017; Ichii et al., 2018). However, the study noted that the Spatial 0.1 GLMM, which is highly density-weighted, exhibited the largest model error and bias under the preferential sampling scenario. This suggests that while spatial clustering can capture habitat patchiness, it may struggle under conditions where preferential sampling biases the data. Additionally, a simulation study by Ono et al. (2015) highlighted that the Spatial 0.1 approach may perform poorly when there is a directional change in fishing grounds over time. This is relevant to the Pacific saury fishery, where studies by Hashimoto et al. (2020) and Hsu et al. (2021) observed a slight eastward shift in the centroid of fishing grounds, likely driven by changes in fish distribution.

This study highlights the inconsistencies between the model selection criteria (conditional R^2 and conditional AIC) and the simulation results for the Spatial 0.1 approach, which suggests that model selection criteria may not always lead to the most unbiased abundance index. This reinforces the importance of using simulation testing in evaluating CPUE standardization methods, as emphasized by previous studies (Ono et al., 2015; Grüss et al., 2019; Ducharme-Barth et al., 2022). Simulation testing provides an additional layer of validation and ensures that models perform well under real-world conditions, especially when spatial-temporal dynamics or preferential sampling are involved. Based on the findings, the study recommends caution in using the highly density-weighted Spatial 0.1 approach in situations where there is a non-random spatiotemporal distribution of fishers relative to fish populations, or when fish distributions shift over time. The Spatial 1 approach, in contrast, was identified as a reasonable alternative when a spatio-temporal analysis cannot be conducted. The flexibility of spatial clustering in the Spatial 1 model allows it to better capture the spatial heterogeneity of the Pacific saury fishery data.

The study also examined the sensitivity of the VAST model's spatial knot structure, where knots were allocated spatially using a *k*-means algorithm in proportion to sampling intensity. While this did not meaningfully affect the mean index, it did impact the

doi:10.6342/NTU202500253

associated uncertainty estimates, with uniform knot distribution leading to larger CVs. The increased uncertainty associated with uniform knot allocation may be a desirable feature when the spatial domain is appropriately specified to match the distribution of the population. However, if the spatial domain is mis-specified (e.g., too broad), this increased uncertainty may be misleading. Prior studies (Grüss et al., 2019; Ducharme-Barth et al., 2022) suggested that a uniform allocation of knots may improve index estimation when applied to spatially-imbalanced data, such as fishery-dependent data. Given the potential impact of different knot configurations on uncertainty estimates and index accuracy, the study recommends that future research explore the effect of various knot allocation strategies in VAST. Investigating this aspect would contribute to further improving the model's performance, particularly in cases where sampling is not evenly distributed across space.

This study highlights an important limitation in the Taiwanese stick-held dip net logbook data, namely the absence of zero catch values, which is a consequence of fishers using fishing lamps to attract Pacific saury schools. The absence of zero catch data, along with the issues related to effort definition (hauls vs. days), can lead to hyperstability in the CPUE standardization. Hyperstability, a phenomenon where standardized CPUE remains high even as abundance declines, can result in overestimating biomass and underestimating fishing mortality. This could be especially problematic for stock assessments and fisheries management, as it may lead to inaccurate conclusions about fishery health (Hilborn and Walters, 1992; Crecco and Overholtz, 1990). The study suggests that the random vessel effect currently included in the models may implicitly capture some of the differences in fishing power across vessels, but it is unlikely to fully account for temporal changes in the fishing power of individual vessels. Temporal changes in fishing power, particularly those influenced by the number or power of fishing lamps, are crucial for more accurate CPUE standardization. This information could be better incorporated into the logbook data to improve the accuracy of CPUE models. This study strongly encourages the collection of key catchability data - such as the number and/or power of fishing lamps - so that this can be explicitly included in future CPUE standardization efforts.

doi:10.6342/NTU202500253

Moreover, this study recommends that future research explore the impact of different treatments for the vessel random effect, such as the inclusion of random covariates in spatially stratified GLMMs or the use of mean-zero random effects with a standard deviation of one in VAST (Xu et al., 2019; Ducharme-Barth et al., 2022). Although the influence analysis in this study suggests that the impact on the mean index is likely similar for these treatments, a more detailed exploration would provide valuable insights into optimizing the vessel random effect treatment for improved model performance.

2.5. Conclusions

This study underscores the importance of CPUE standardization for effective stock assessment, particularly for the Pacific saury fishery, where fishery-dependent CPUE data is often used to evaluate stock status. The findings of this study, along with the simulation experiment, contribute to a broader understanding of how spatial treatments within a GLMM framework can impact CPUE index estimation. Specifically, this study suggests that explicitly modeling spatial autocorrelation using Gaussian Markov random fields (GMRFs) in a spatio-temporal framework, such as VAST, provides a more accurate representation of the spatial heterogeneity present in CPUE data. This approach is seen as superior to traditional area stratifications, which can misinterpret fish density distributions when they rely on ad hoc or fixed grid patterns.

The simulation results highlighted that while spatial clustering approaches, particularly the highly flexible Spatial 0.1 treatment, can define spatial strata with great flexibility, they may result in substantial errors and biases when fishing activity is non-random and non-stationary relative to fish distribution. A less extreme approach, such as Spatial 1, offers a reasonable alternative when spatio-temporal modeling is not feasible. In addition to focusing on the resulting abundance indices, this study also emphasizes the importance of examining how explanatory variables impact the standardized CPUE index. The influence analysis, extended to the spatio-temporal framework of VAST and including diagnostics for the year × spatial interaction term, provided valuable insights into model components and their effects on CPUE standardization. This methodology represents an

doi:10.6342/NTU202500253

innovative tool for evaluating CPUE models, offering a more comprehensive understanding of the underlying data and assumptions.

Ultimately, the methodologies and tools presented in this study have broader applicability to other fisheries with similar data structures. By emphasizing the value of spatially explicit modeling and influence diagnostics, this study contributes to a growing body of research on improving CPUE standardization, and its findings should be considered valuable in future stock assessments across diverse fisheries. The study positions the spatio-temporal framework and associated tools as essential elements of modern CPUE standardization analyses.

doi:10.6342/NTU202500253

3. Chapter 3 − Investigating the drivers of spatial distribution shifts by using spatio-temporal modelling approach

Abstract

Pacific saury (*Cololabis saira*) is both a significant fisheries resource and an ecologically important species in the Northwestern Pacific Ocean. While evidence suggests that its distribution is influenced by environmental variability, the relative contributions of environmental factors versus unmodeled spatiotemporal processes remain unexplored. To address this, fisheries data from members of the North Pacific Fisheries Commission were analyzed using a geostatistical modeling approach to examine interannual changes in the spatiotemporal distribution of Pacific saury during the fishing season (May − December) from 2001 to 2017. The study aimed to assess the influence of local environmental variables (e.g., sea surface temperatures), regional variables (e.g., Southern Oscillation Index), and unmodeled spatiotemporal variables (e.g., species interactions). The results revealed an eastward shift in the centroid of Pacific saury's distribution after 2013, with a further shift and a decline in relative abundance by 2017. Interestingly, no single local or regional environmental variable, nor any combination of these, could fully explain this distributional shift. Instead, the shift was primarily attributed to unmodeled spatiotemporal factors. This highlights the need for further research to quantitatively understand the underlying mechanisms driving these changes. While environmental data will become more widely available in the future, this study cautions that before projecting Pacific saury's distribution in the context of climate change or other environmental factors, it is essential to first assess whether the proposed driving variables adequately explain the variability observed in historical distribution data.

Keywords: Pacific saury, spatiotemporal modelling approach, spatiotemporal dynamics, distribution shift, stick-held dip net fisheries

doi:10.6342/NTU202500253

3.1. Introduction

Pacific saury (*Cololabis saira*) is a small, migratory pelagic fish that is widely distributed across the vast expanses of the Northwestern Pacific Ocean (Fukushima, 1979). This species is of significant commercial value in the region, primarily harvested by stick-held dip net fisheries. Since 2015, Pacific saury has been managed on an international level by the NPFC, an intergovernmental organization dedicated to ensuring the sustainable exploitation of the resource. Offshore fishing vessels from Japan and Russia mainly operate within their respective exclusive economic zones, while distant-water vessels from China, Korea, and Taiwan predominantly fish in the high seas west of 165°E in the Northwestern Pacific Ocean.

Factors that may influence the distribution of Pacific saury have attracted considerable scientific and practical interest, as expected given its international commercial importance. The life span of Pacific saury has been estimated to be 2 years (Suyama et al., 2006). During this short life span, the population exhibits migrations between the subtropical and subarctic zones (Fukushima, 1979; Suyama et al., 2012; Miyamoto et al., 2019), and its spatial distribution appears to be affected by environmental variability in the Northwestern Pacific Ocean (Tseng et al., 2013; Chang et al., 2019; Hua et al., 2020). The specific local environmental variables previously investigated for possible effects on Pacific saury abundance and distribution have included sea surface temperature (SST; Watanabe et al., 2003; Hashimoto et al., 2020), sea surface height (SSH; Kuroda and Yokouchi, 2017), sea surface salinity (Takasuka et al., 2014), chlorophyll-*a* concentration (chl-*a*; Tseng et al., 2013) or net primary production (Chang et al., 2019), and sea surface temperature gradient (SSTG) (Hua et al., 2020). In addition, regional environmental and climatological variability (e.g., quantified by the NINO3.4 index [El Niño/Southern Oscillation indicator] and Pacific Decadal Oscillation, PDO) might also affect the distribution and density of Pacific saury (Tian et al., 2003, 2004; Chang et al., 2019). Although several studies have suggested the potential to forecast shifts of the Pacific saury distributions using local/regional environmental variables, these studies have not demostrated that such variables explain a substantial portion of historical distribution shifts. For example, Tseng et al. (2011) observed a noticeable poleward shift in potential Pacific saury habitats driven by increasing SST. Chang et al. (2019) proposed that the suitable

doi:10.6342/NTU202500253

fishing grounds of Pacific saury could be predicted six months into the future by using a habitat suitability (HSI) model including local environmental variables such as SST, SSH, SSS, and NPP. Hua et al. (2020) reported that the SSTG could explain a substantial portion of the fish density variations and provide a way to forecast saury fishing grounds based on the weight-based HSI analysis. Despite these findings, while many studies have identified statistically significant relationships between environmental variables and fish density, the relative importance of each variable in explaining the spatial shifts of Pacific saury remains uncertain.

The spatial distribution of Pacific saury is likely influenced by a variety of unmodeled spatiotemporal processes − factors that are either unobserved or challenging to observe. Previous research has suggested that changes in Pacific saury migration may be driven by fluctuations in prey abundance, particularly copepods (Neocalanus spp.), or by complex oceanographic conditions such as eddies and fronts formed by the mixing of the Kuroshio and Oyashio currents, which can trap Pacific saury's prey (Tadokoro et al., 2005; Saitoh et al., 1986; Tseng et al., 2014). Furthermore, shifts in the distribution of Pacific saury may also be influenced by species interactions, such as competition or predation (Glaser, 2015; Ito et al., 2013). However, the impact of these unmodeled spatiotemporal processes on Pacific saury's shifting distribution remains largely unquantified. Recent studies have proposed that integrating simple species distribution models (SDMs) with geostatistical modeling approaches like VAST (i.e., Vector-Autoregressive Spatiotemporal; Thorson, 2019) could provide a more detailed understanding of these processes. This approach allows for the decomposition of sampling variation into biologically meaningful components, leading to more precise and accurate predictions of species abundance and distribution than traditional SDMs (e.g., Shelton et al., 2014; Thorson et al., 2015). Specifically, VAST accounts for both environmental factors and unmodeled spatiotemporal processes - such as species interactions, complex oceanographic conditions, and fishery harvest − when estimating species abundance and distribution, offering a more comprehensive treatment of spatiotemporal variation compared to conventional models.

doi:10.6342/NTU202500253

Given the promising capabilities of VAST for estimating species distributions and the growing need to understand the spatiotemporal dynamics of Pacific saury in the Northwestern Pacific Ocean, the objectives of this study were: (i) to assess the interannual spatiotemporal dynamics of Pacific saury during the fishing season (May − December) from 2001 to 2017 using VAST, based on data collected by the NPFC SSC, which provides the most comprehensive spatial-temporal coverage currently available; (ii) to quantify the extent of the shift in Pacific saury's spatial distribution over time; and (iii) to determine whether changes in Pacific saury's spatial distribution can be attributed to local and/or regional environmental variables or to unmodeled spatiotemporal processes.

3.2. Materials and methods

3.2.1. Fishery and environmental data

The study area covered the Northwestern Pacific Ocean between 35 − 50°N and 140 − 170°E. Fishery data containing the catch (in metric tons) and effort (in operating days) of stick-held dip net fisheries from the members of NPFC (China, Japan, Korea, Russia, Taiwan, and Vanuatu) were collected in the fishing season (May to December) during 1994 − 2017. The dataset was aggregated by year and month with a spatial resolution of 1°×1° in latitude and longitude. The data were selected from 2001 to 2017 to fully cover an extensive spatial range with consistent fishing effort distribution by all members of NPFC (**Figure S3.1**). This study assumes this dataset covers the main habitat of the Pacific saury stock exploited in the Northwestern Pacific Ocean during May and December in the studied period. This study also considered the local (e.g., SST) and regional environmental variables (i.e., SOI, and PDO indices) that have been most commonly used to examine possible effects on the density and distribution of Pacific saury (Tian et al., 2004; Chang et al., 2019; Hashimoto et al., 2020; Hua et al., 2020). Local environmental variables included SST (°C); SSH (m), and chl-*a* (in $mg \times m^{-3}$). These local monthly environmental data were obtained from the Asia-Pacific Data Research Center (APDRC) (http://apdrc.soest.hawaii.edu/data/data.php) and Copernicus Marine Environment Monitoring Service (CMEMS) Global ARMOR3D L4 Reprocessed dataset (http://marine.copernicus.eu/). The PDO and SOI during 2001 − 2017 were obtained from the NOAA National Climatic Data Center (NCDC) (https://www.ncdc.noaa.gov/).

doi:10.6342/NTU202500253

3.2.2. Spatiotemporal model structure

VAST (version 12.2.0) was applied to fishery-dependent data (Xu et al., 2019; Sculley and Brodziak, 2020), represented as catch-per-unit-effort (CPUE; metric tons per operating day per square degree), to estimate the spatiotemporal dynamics of Pacific saury in the Northwestern Pacific Ocean. *VAST* is an R package that implements a spatiotemporal generalized linear mixed model (GLMM) framework, which is publicly available online (https://github.com/James-Thorson/VAST). The fishing activities analyzed in this study took place across more than 250 unique 1° × 1° spatial grids. For computational efficiency, the *k*-means method was employed to cluster all observed data into 100 spatial knots. It was assumed that both spatial and spatiotemporal random effects for a grid cell were derived from the closest knot in space. The predicted results were confirmed to be qualitatively similar regardless of the number of spatial knots within the spatial range. The knots were allocated spatially with a density proportional to the sampling intensity based on the observed data. The ensemble of knots, referred to as the mesh (**Figure 3.1**a), was used to approximate spatial and spatiotemporal variation, allowing the spatiotemporal models to predict density at unsampled locations using the correlations among knots (Shelton et al., 2014). After determining the locations of the 100 knots, they were fixed while model parameters were estimated. Subsequently, 0.1° × 0.1° grid cells were created as extrapolation grids to cover the entire area for predictions based on the fitted model (**Figure 3.1**b).

VAST implements a delta-generalized linear mixed model framework, where the catch probability distribution is decomposed into two components: the probability of encounter and the expected catch rate, conditional on the occurrence of a catch (Thorson, 2019). In this study, only the positive catch rate (i.e., observed CPUE) component was included, as Pacific saury schools are targeted by the stick-held dip net fisheries with a 100% encounter rate, using fish finders and satellite sea surface temperature images. This decision was made by specifying the user-controlled vector for observation models as ObsModel = 1 (lognormal distribution for positive catch rates) and 3 (fixing the encounter probability to 1 for all years) (Thorson, 2019).

doi:10.6342/NTU202500253

The predicted Pacific saury density (i.e., mass of fish in metric ton per day per square degree) was approximated using a spatiotemporal lognormal GLMM with a log-linked linear predictor as follows:

$$p(i) = \beta(t_i) + \omega(s_i) + \varepsilon(s_i, t_i) + \sum_{j=1}^{n_j} \gamma(j) X(s_i, t_i, j) + \sum_{k=1}^{n_k} \lambda(k) Q(i,k) \quad (3.1)$$

where $p(i)$ is the predictor for observation i, $\beta(t_i)$ is the intercept for year t_i as a fixed effect and independent among years, $\omega(s_i)$ is time-invariant spatial variation at knot s_i (i.e., each of the 100 knots), and $\varepsilon(s_i,t_i)$ is time-varying spatial-temporal variation for knot s_i in year t_i (i.e., the interaction of spatial variation and time). In addition, $\gamma(j)$ is the impact of the j_{th} density covariate $X(s_i, t_i, j)$ on knot s_i in year t_i, n_j is the number of density covariates (in the full model, n_j = 8), $Q(i,k)$ is the catchability covariates that explain variation in catchability, $\lambda(k)$ is the estimated impact of catchability covariates for this linear predictor, and n_k is the number of catchability covariates. In this study, the only catchability coefficient was a fleet dummy variable (i.e., n_k = 1).

The spatial and spatiotemporal variation are assumed to have correlations based on the distance from the knots; i.e., nearby densities are more similar than those that are remote. More specifically, spatial variation (ω) is modelled as a Gaussian random field (GRF), which reduces to a multivariate normal distribution (*MVN*) when evaluated at a finite set of knots (Thorson et al., 2015). The spatiotemporal random effect $\varepsilon(,t)$ is fitted independently for each year and is also modelled as GRF:

$$\omega \sim MVN\left(0, \mathbf{R}_{\omega}\right) \quad (3.2a)$$

$$\varepsilon(,t) \sim MVN\left(0, \mathbf{R}_{\varepsilon}\right) \quad (3.2b)$$

where *MVN* is the multivariate normal distribution with expected value 0 for each knot; $\mathbf{R}$ is a covariance matrix for the random field. This study assumed the covariance between two knots s and s' follow the Matérn correlation function:

doi:10.6342/NTU202500253

$$\mathbf{R}_{\omega}(s,s') = \text{Matern}\left(\kappa\left|\mathbf{H}(s-s')\right|\right) \quad (3.3a)$$

$$\mathbf{R}_{\varepsilon_t}(s,s') = \text{Matern}\left(\kappa\left|\mathbf{H}(s-s')\right|\right) \quad (3.3b)$$

where κ determines the rate at which decorrelation drops with increasing distance, and $\mathbf{H}$ is a 2 × 2 linear transformation matrix representing geometric anisotropy (a condition where spatial correlation varies with both and distance and direction; see Thorson et al., 2015). The marginal likelihood of fixed effect parameters is calculated with Template Model Builder using the Laplace approximation to integrate across random effect parameters (Kristensen et al., 2016), and fixed effect parameters are then estimated by maximizing the marginal likelihood within the R computing environment (R Core Team, 2021). The standard errors of estimated parameters and model outputs were calculated using the generalization of the delta method. Convergence was verified by confirming that the absolute value of the final gradient of the log-likelihood function at the maximum likelihood estimate was below 0.0001 for all parameters, and by ensuring that the Hessian matrix of the likelihood function was positive definite.

3.2.3. Density covariates

Five density covariates were retained in the best (i.e., most parsimonious) model, which was selected through backward model selection using the Akaike Information Criterion (AIC) (Akaike, 1974) during the preliminary analyses. A variable was excluded from the model if its removal led to a lower AIC compared to the full model for each batch (**Table S3.1**):

$$X(s,t) = \left(\text{SST}(s,t), \text{SST}^2(s,t), \text{chl-}a(s,t), \text{SOI}(s(N),t), \text{SOI}(s(E),t)\right) \quad (3.4)$$

where SST(s,t) is the linear effect of sea surface temperature associated with knot s and year t, SST^2(s,t) is temperature-squared (i.e., a quadratic effect of temperature), chl-a (s,t) is the concentration of chlorophyll-a. SOI (s(N),t), and SOI (s(E),t) are the interaction of northward (latitudinal) or eastward (longitudinal) direction with the annual trend of SOI index (Thorson et al., 2017b). The low correlations among the density covariates (Pearson's correlation coefficients ranging from -0.03 ─ 0.13), and the nonlinear

doi:10.6342/NTU202500253

relationship between SST and SST^2 indicated that the multicollinearity is not an issue for the best model.

3.2.4. Derived index of relative abundance

The index of relative abundance in year *t*, computed using an area-weighted approach, $B(t)$, was obtained by scaling the predicted density by the total area associated with the knots (Thorson et al., 2015):

$$B(t) = \sum_{s=1}^{n_s} a(s) \times \exp\left(\beta(t) + \omega(s) + \varepsilon(s,t) + \sum_{j=1}^{n_j} \gamma(j) X(s,t,j)\right) \quad (3.5)$$

where *a(s)* is the area associated with modelled knot *s*.

3.2.5. Calculating the centroid of gravity

To summarize the distribution shift for Pacific saury during the studied period, this study calculated a model-based estimate of the yearly (t) centroid of gravities (COG_t) from the predicted relative abundance throughout the whole spatial domain (Thorson et al., 2017b):

$$COG_t = \sum_{s=1}^{n_s} \frac{\hat{B}_t \times Z_s}{\hat{B}_t} \quad (3.6)$$

where Z_s is the northing or easting value for knot s in the Universal Transverse Mercator (UTM) coordinate in kilometers (km), and $\hat{B}_t$ is the predicted relative abundance in the year t.

3.2.6. Counterfactual model exploration

The spatiotemporal random fields, $\varepsilon(s, t)$, and the covariates, $X(s, t, j)$, in VAST are used to account for changes in spatial distribution over time. The spatiotemporal random fields represent unmodeled spatiotemporal processes, capturing residual patterns that cannot be explained by the fixed effects (i.e., covariates). To assess the relative importance of local and/or regional environmental variables versus unmodeled spatiotemporal variables in

doi:10.6342/NTU202500253

explaining the spatial distribution shift of Pacific saury, a counterfactual analysis (Thorson et al., 2017b; Perretti and Thorson, 2019) was conducted.

This study examined three hypotheses regarding changes in the distribution of Pacific saury over time: (i) a single local or regional environmental variable; (ii) multiple local and regional environmental variables; and (iii) unmodeled spatiotemporal variables. These hypotheses are not mutually exclusive, and the aim was to estimate the proportion of variance in the center of gravity (COG) of Pacific saury explained by each variable. To achieve this, the fixed and random effects were extracted from the best model, with some fixed to zero to exclude individual processes. For each counterfactual model, the time series of northward and eastward COG, estimated without the subset of parameters, were compared to the COG derived from the full model. An exploratory run confirmed that setting both environmental variables and unexplained variation to zero resulted in no variance in COG, suggesting that all estimated variation in COG could be attributed to either of these two processes. A detailed description of the counterfactual models follows below:

(i) Single local or regional environmental variable

To examine the relative effect of a single local (i.e., SST, SST^2, chl-*a*) or regional (i.e., SOI index with northing and easting) environmental variables, the intercept was fixed at the average level across time, and any variation of the spatiotemporal random effect was removed. Only one of the estimated single local variables or a regional environmental variable was retained at a time to predict relative abundance and recalculate the COG. Descriptions of the mechanism and the quantitative test for the hypothesis of the distribution shift are provided in **Table 3.1**.

(ii) Multiple local and regional environmental variables

The intercept was fixed at the average level over time, and the variation from the spatiotemporal random effect (i.e., set at zero) was removed to examine the relative effect of multiple local and regional environmental variables. Combinations of local and regional environmental variables were then set to their estimated values, which were used to predict the relative abundance for all knots, and recalculate the COG.

doi:10.6342/NTU202500253

(iii) Unmodelled spatiotemporal variables

To examine the relative effect of the unmodelled spatiotemporal processes (which was not explained by any local/regional environmental variables), any effects from the local/regional environmental variables were eliminated, and the steps above were followed to recalculate relative abundance and COG.

3.3. Results

3.3.1 Spatiotemporal dynamics of Pacific saury

VAST fitted the data robustly, as demonstrated by the goodness of fit of the best model (deviance explained = 69%). The time series of residuals across knots were centered around zero (**Figure S3.2**), and the spatial distribution of residuals showed no significant spatial patterns, except for 2005 and 2006 (**Figure S3.3**). All environmental variables included in the best model were statistically significant (likelihood ratio test, $p < 0.001$). The estimate of the standard deviation for the spatiotemporal random effect (0.543) was significantly greater than that of the spatial random effect (0.283), highlighting the heterogeneity in the spatial distribution of Pacific saury density over time. The geometric anisotropy of spatial correlation for Pacific saury density is shown in **Figure 3.2**.

The correlation ellipse (representing the 10% correlation distance) was oriented from east to west, indicating that the spatial and spatiotemporal correlations of Pacific saury density decreased more rapidly latitudinally than longitudinally. The predicted density maps from the best model revealed substantial interannual variation in the density distribution of Pacific saury between 2001 and 2017 (Figure 3.3). During the early years (2001 − 2007), high densities were primarily concentrated near the coastal waters of Japan (140 − 150°E and 38 − 45°N), with the exception of 2005. Since 2010, the area of high density has generally shifted and expanded eastward, with a pronounced eastward shift observed after 2013. From 2015 to 2017, high densities were primarily located in the high seas (150 − 160°E and 40 − 45°N). Notably, the predicted density distribution in 2017 showed a marked departure from previous years, with high densities appearing in the region of 150 − 170°E and 36 − 42°N. Additionally, the predicted time series of annual

doi:10.6342/NTU202500253

density from the best model exhibited a fluctuating pattern, closely mirroring the trends observed in both the nominal CPUE and the predicted relative abundance (**Figure 3.4**).

3.3.2. Time series of COGs of Pacific saury

The trajectories of the northward and eastward COG from the best model (**Figure 3.5**a, b) also indicated an apparent eastward shift in distribution (the maximum difference is 585 km) compared to the north-south direction (146 km) over the years. The eastward COG in 2006 and 2017 reached the historical minimum and maximum easting of 175 km and 760 km, respectively (**Figure 3.5**a). COG has gradually shifted eastward since 2010 and further shifted after 2013. For the north-south direction, the time series of COG indicated relatively persistent regimes in the distribution (**Figure 3.5**b). The 95% confidence intervals of the eastward COGs were wider (CV range = 6.4 − 27.8%) than those of the northward direction (CV range = 0.4 − 1.1%) throughout the study period, reflecting greater spatial variability of density longitudinally than latitudinally.

3.3.3. Relative importance of local/regional environmental vs. unmodelled variables

The predicted density maps for 2001, 2006, 2010, and 2017, representing the years with the most substantial inconsistencies among the counterfactual models, were selected to highlight the relative importance of local/regional environmental variables and unmodelled spatiotemporal processes (**Figure 3.6**). When examining the relative influence of a single local or regional environmental variable, the results revealed that SST alone (including both linear and quadratic SST effects) was unable to account for the interannual variation in density distribution, including the location of high-density areas or year-to-year variability derived from the best model (**Figure 3.6**a, b). This outcome was consistent across other covariates, except for the SOI index when combined with northings, which showed a more noticeable pattern (**Figure S3.4**).

When multiple environmental variables and climatic indices were considered in isolation, the resulting density distribution patterns were similar to those produced by the SOI index with northings (**Figures 3.6**c and **S3.4**e). However, the general patterns in the spatiotemporal variation of Pacific saury density were primarily driven by the unmodelled

doi:10.6342/NTU202500253

spatiotemporal processes (**Figure 3.6**d). While these unmodelled spatiotemporal variables were the dominant contributors, they tended to overestimate density in 2010 and 2017 compared to the effects of other covariates. Investigation of the estimated COG trends under each hypothesized driver clearly confirms that the observed interannual variation in COG was mainly due to unmodelled variation. The COG trends (both easting and northing directions) derived from the unmodelled spatiotemporal variable in isolation were similar to those from the best model in both directions (**Figure 3.7**). SST generated flat COG trends (**Figure 3.7**c, d), which indicated that SST has very limited prediction power for the Pacific saury density. The SOI index with northings contributed to relatively larger fluctuations in COGs than the other local/regional environmental variables (**Figures S3.5** and **S3.6**). This result suggests that the SOI index is the most important factor among the local/regional variables in explaining the interannual spatial distribution patterns (**Figures S3.5**f and **S3.6**f). The COG trends derived from the multiple environmental variables and climatic indices were similar to that by the SOI index with northings (**Figures S3.5**b**,** f and **S3.6**b, f). It should be noted that the COG trends could be balanced out by the offset effects among the local and regional environmental variables, which led to a less varied COG trend along the north-south axis over time (**Figure 3.7**e**,** f).

3.4. Discussion

This study analyzed spatiotemporal dynamics of Pacific saury density in the Northwest Pacific Ocean between 35 − 50°N and 140 − 170°E during 2001 − 2017 by using the *VAST* R package and the extensive fishery dataset collected by the NPFC SSC. This study acknowledged that use of fishery-dependent data collected without a scientific sampling design may lead to the CPUE data from preferred fishing grounds having a disproportionate influence on the predicted density distribution, which is often referred to as preferential sampling (Conn et al., 2017; Gao et al., 2020). However, for Pacific saury, this issue is likely minimal because the dataset analyzed here reflects consistent fishing effort distribution across all NPFC member nations and covers an extensive spatial range over the studied period. Additionally, VAST offers several advantages over non-spatial modeling approaches. Its ability to account for correlated spatial processes, impute densities in unfished areas, and apply an appropriate area-weighting scheme reduces both

doi:10.6342/NTU202500253

bias and variance in density predictions (Thorson et al., 2015). The study also highlights the importance of continued efforts to develop approaches that simultaneously estimate fishers' locational decisions and fish densities, as suggested by Thorson et al. (2017c).

The area of high Pacific saury density and the COG has progressively shifted eastward since 2010, with a more pronounced shift occurring after 2013. This eastward shift in distribution was accompanied by relatively low density in 2017. Similar trends in the eastward distribution shift of Pacific saury after 2010 have also been identified in fishery-independent biomass surveys (Hashimoto et al., 2020). This study found that neither a single local or regional environmental variable nor any linear combination of variables could adequately explain the observed distribution shifts. Instead, the majority of the distribution shift was attributed to unmodelled spatiotemporal variation. This result is consistent with the findings from previous studies using conventional SDMs (e.g., regression-based models) that have attributed a small portion of the data variability in distribution variation for Pacific saury to the investigated environmental effects (e.g., deviance explained <36% in Tseng et al., 2013; <12% in Chang et al., 2019). In contrast, VAST, which conditions on unmodelled spatiotemporal variation represented as random effects (Thorson and Ward, 2013; Shelton et al., 2014), captures residual spatiotemporal patterns that are not explained by fixed effects such as environmental variables. In the future, environmental data should become increasingly available. However, this study cautions that before projecting the Pacific saury distribution resulting from climate change or other environmental phenomena, the first step should be to verify whether the hypothesized driving variables lead to a meaningful proportion of variability in the historical distribution data.

There are several possible mechanisms to explain why the shifts in Pacific saury distribution are attributed to the "unmodelled" spatiotemporal variation. For example, *Neocalanus* copepods are the common zooplankton prey for the Japanese sardine (*Sardinops melanostictus*) and Pacific saury (Tadokoro et al., 2005). Ito et al. (2013) indicated that the increase in the abundance of Japanese sardine could lead to a decrease in the prey plankton density and hence the growth of Pacific saury. It is worth noting that the stock of Japanese sardines increased steadily after 2013 (Furuichi et al., 2020). This study

doi:10.6342/NTU202500253

hypothesizes that the spatiotemporal variation in the density of Pacific saury may be strongly correlated (negative) with the effect of the competitive fish species (i.e., Japanese sardine) on the zooplankton prey of Pacific saury (Matsuda et al., 1992). Although only a single species distribution model was constructed in this study, VAST can analyze data for multiple species simultaneously to infer the spatiotemporal variation in the density of species with similar habitat requirements. Thorson and Barnett (2017) reported that there was a strong covariation in population density among US Pacific Coast rockfishes and thornyheads (*Sebastes* and *Sebastolobus* spp.) using joint species distribution prediction. This study suggests that using this modelling technique may improve estimation of the population density distribution of Pacific saury while considering other correlated fish species when multiple species data are available.

Previous studies have suggested that complex hydrographical dynamics, such as fronts and eddies, may drive spatial distribution shifts of Pacific saury over time. Yasuda and Watanabe (1994) demonstrated that the interannual north-south shift of the Oyashio front is closely associated with the interannual fluctuation of Pacific saury fishing grounds. Similarly, Kuroda and Yokouchi (2017) found that interactions between the Oyashio current and mesoscale eddies after 2010 caused large-scale shifts in favorable potential fishing grounds, moving them from the Hokkaido coast to offshore areas in recent years. Although the spatial distribution of Pacific saury is challenging to explain using local or regional environmental variables alone, this study posits that the potential effects of hydrographical dynamics on distribution shifts may be captured indirectly by the unmodelled spatiotemporal variable included in the model. This highlights the ability of spatiotemporal modeling frameworks, such as VAST, to account for complex environmental processes that are not explicitly represented by fixed effects.

The catches of the Pacific saury were limited to the Japanese EEZ in the early period (2001 − 2007). However, there is an increasing trend of fishing mortality after 2007 attributed to the increase of catches in high-seas areas (NPFC, 2019). This study recommends future research to integrate the spatial information regarding the fishing mortality as a density covariate into the current spatiotemporal model to explore whether the eastward shift of density distribution primarily attributed to the unmodelled variation

doi:10.6342/NTU202500253

can be related to the heterogeneity in fishing intensity. There are several possible explanations for the inability of the effects of local/regional environmental variables to explain Pacific saury distribution shifts. One is that the model could not capture the effect of the local/regional environmental variables due to the insufficient model flexibility. Nevertheless, this study included a quadratic effect of the local environmental variable (SST) and a linear effect of the regional environmental variable (SOI). It is possible that a highly nonlinear model (e.g., spline) may improve the model performance. However, this study cautions that adding more flexible model structures may lead to spurious relationships, which could be mistaken as meaningful (Fourcade et al., 2018). Furthermore, previous studies indicated that the abundance and the suitable spawning ground of the Pacific saury exhibited interannual-decadal variation due to regime shifts (Ichii et al., 2017; Liu et al., 2019). Including the interactions of environmental variables and an additional dummy variable or spatially-varying coefficient models (Thorson, 2019) may increase the estimated importance of some environmental variables, although this was outside the scope of this study. Chang et al. (2019) indicated that habitat preferences and suitable habitat areas of Pacific saury differed between size classes (e.g., medium- and large-sized). The age/size aggregated model with the spatiotemporal random effects used in this study may balance out the estimated importance of local or regional environmental variables. This study recommends that adding (currently unavailable) age/size data may provide additional information to better understand the ontogenetic habitat preferences combined with changes in size/age structure of Pacific saury and improve the estimated importance of the environmental variables (Kristensen et al., 2014; Kai et al., 2017; Barbeaux and Hollowed, 2018).

Understanding the spatial dynamics of fisheries is essential for effective management and conservation of migratory oceanic pelagic species in practical applications (Sibert and Hampton, 2003). Gaining insights into spatiotemporal dynamics enables the use of spatially explicit stock assessment models in future research. This is particularly important because the current Bayesian surplus production model employed by the NPFC to assess Pacific saury does not incorporate spatial structure in population dynamics. Punt (2019) highlighted that integrating spatial modeling approaches during

doi:10.6342/NTU202500253

data pre-processing (e.g., Cao et al., 2017; Kai et al., 2017) is a viable strategy to account for spatial structure in assessment models. Although this study generated a time series of density indices using VAST, it did not focus on applying the standardized relative abundance index for stock assessment purposes. The calculation of an annual standardized index requires careful consideration of confounding factors such as seasonal effects, vessel-specific influences, and changes in target species that may affect catchability. Future research should prioritize simulations exploring the benefits of spatiotemporal modeling under various scenarios of fish abundance trends and the spatial-temporal distribution of fish and fishing effort. Additionally, assessing the performance of standardized indices is critical to enhancing confidence in stock assessment outcomes. Finally, monitoring the eastward shift of the Pacific saury density "hotspot" (i.e., center of gravity, or COG) over time is crucial. Hotspots are often key elements in conservation strategies, particularly when designing spatial protections such as time-area closures for harvested species. Tracking changes in hotspot locations over time has significant implications for the effectiveness of spatial protections, emphasizing the importance of following these shifts to inform adaptive management strategies.

doi:10.6342/NTU202500253

4. Chapter 4 − Stock assessment and addressing the impacts of uncertainty on recovery

Abstract

This study developed an age-structured stock assessment model for Pacific saury (*Cololabis saira*) in the western North Pacific Ocean using Stock Synthesis, incorporating data from 1980 to 2022. The assessment revealed that the spawning stock biomass has declined to historically low levels (31,655.4 mt) in recent years (2020 − 2022), falling below SSB_{MSY} (42,611.8 mt), while current fishing mortality (F_{2022} = 1.42) remains below F_{MSY} (2.61). To evaluate potential recovery strategies, both deterministic and stochastic projections were conducted for 2023-2042 under three fishing mortality scenarios: $0.5F_{MSY}$, $0.75F_{MSY}$, and F_{MSY}. Although deterministic projections showed stable trajectories, stochastic projections incorporating parameter uncertainty and recruitment variability revealed substantial fluctuations in both biomass and catch predictions. The $0.5F_{MSY}$ scenario demonstrated the highest probability (100%) of maintaining stock above SSB_{MSY} during 2023 − 2027, compared to declining probabilities under $0.75F_{MSY}$ (84.9% to 75.5%) and F_{MSY} (50.5% to 75.8%) scenarios. These findings suggested that lower fishing mortality rates may facilitate faster population recovery while considering uncertainty in future stock status. Furthermore, this study highlighted the importance of incorporating environmental variables and parameter uncertainty in future projections to better account for climate change impacts, in order to provide more robust management advice for this environmentally sensitive species.

Keywords: age-structured model, future projections, stochastic projection, uncertainty, management, Pacific saury

doi:10.6342/NTU202500253

4.1. Introduction

Small pelagic fish present unique challenges for stock assessment and management due to their complex biological properties. These species are characterized by dramatic population fluctuations that can occur even without commercial exploitation, with boom-bust cycles spanning multiple years and varying by orders of magnitude in biomass (McClatchie et al. 2017; Salvatteci et al. 2018). These fluctuations are mainly driven by recruitment success or failure, attributed to their relatively short lifespans and high reproductive output (Essington et al. 2015; Szuwalski and Hilborn 2016; Checkley et al. 2017). Environmental factors play a crucial role in determining their distribution, growth, and survival within highly dynamic and productive ecosystems (Fiechter et al. 2015; Checkley et al. 2017). Given the inherent unpredictability of marine ecosystems, and small pelagic fish populations in particular, combined with our inability to fully understand their population dynamics underscores the need for precaution when determining catch levels for these species (Pikitch et al., 2014).

The recovery of overexploited fish populations has traditionally been managed through harvest scenarios that inform sustainable management strategies (Safina et al., 2005). Typically, harvest scenario advice relies on stock assessment model projections fitted to fisheries and biological data to forecast biomass values over the near term ($1-5$ years; e.g., Kuriyama et al. 2020). These forecasts depend on recent estimates of biological processes, such as stock-recruit relationships and growth patterns, assuming relative stability in these parameters over the projected timeframe (i.e., deterministic projection). However, this assumption warrants re-evaluation given changing environmental conditions and their impact on small pelagic fish populations. Furthermore, several uncertainties from model parameters, such as selectivity and catchability, is rarely considered in future projections to reflect the realistic fishery variability (i.e., stochastic projection).

Pacific saury (*Cololabis saira*) is one of the most commercially important migratory small pelagic fish species in the Northwestern Pacific Ocean, with a distribution ranging from coastal to open waters (Hubbs and Wisner, 1980). The fishing grounds are located in the western part of the North Pacific Ocean, with peak fishing activity occurring during summer and autumn (Kosaka, 2000). The species supports significant commercial

doi:10.6342/NTU202500253

fisheries for multiple countries, including Japan, Russia, Korea, China, Taiwan, and Vanuatu. Over the past three decades, total landings have shown considerable fluctuation, reaching a peak of 629,576 tons in 2014 before declining to 332,886 tons in 2022 (NPFC, 2023a). Despite the implementation of quota management measures by the NPFC in 2019, the Pacific saury population has shown limited signs of recovery. Recent studies have identified environmental changes as a potential factor contributing to reduced recruitment levels (e.g., Kakehi et al., 2020). This environmental influence suggests that even under reduced fishing pressure, recruitment levels may remain low, potentially rendering current quota estimates derived from stock assessments overly optimistic. Currently, the stock assessment of Pacific saury is conducted by using the Bayesian surplus production model with assuming the stationary processes for Pacific saury. However, even the comprehensive stock assessment (surplus production model) and management strategies (TAC) have been conducted, the Pacific saury population has been experiencing depleted biomass in recent years despite conservation measures established by the NPFC. It is urgent that enhanced stock assessment modeling approach (e.g., age-structured model) and consider the various sources of uncertainty to conduct the projection could ensure that management actions maintain the adaptive capacity of populations.

Given these challenges, this study considers various sources of uncertainty from estimated parameters (e.g., selectivity and catchability parameters) and process error (recruitment deviates) using the Stock Synthesis framework (Methot and Wetzel, 2013). Stock Synthesis is an integrated stock assessment method that develops the population dynamics model separately from the model relating monitoring data to model predictions (Maunder and Punt, 2013). The objective of this study is to (i) develop an age-structure model for Pacific saury; (ii) conduct the future projection for both deterministic and stochastic approaches; (iii) evaluate the harvest control strategy performance for nominal fishing mortality levels, 50 percent F_{MSY}, 75 percent F_{MSY}, and 100 percent F_{MSY}.

4.2. Materials and methods

4.2.1. Stock assessment model

(i) Spatiotemporal structure and data used

doi:10.6342/NTU202500253

Based on the general consensus that a single management stock for the Pacific saury is likely in the Northwestern Pacific Ocean (WNPO), this study presented here an assessment of Pacific saury in the WNPO area (**Figure 4.1**). A total of six stick-held dip net fleets of Pacific saury were defined on the basis of NPFC members (Japan, Taiwan, Korea, Russia, China, and Vanuatu). Three types of data were used: fishery-specific catches (in metric ton, mt), relative abundance indices, and length composition data (in cm). The fishery data were compiled for 1980 − 2022, noting that the catch data and length composition data were compiled and modelled on a quarterly basis. All CPUE indices were also modelled as a quarterly index. Available data, sources of data, and temporal coverage of the datasets used in the stock assessment were summarized in **Figure 4.2**. Time series of Pacific saury catches in the WNPO by different fleets from 1980 to 2022 are shown in **Table 4.1** and **Figure 4.3**. In recent decades, annual total catches of Pacific saury increased from 176,364 mt in 1998 to 617,509 mt in 2008, then continuously decreased to 262,639 mt in 2017, except for a high catch in 2014 (629,576 mt). After 2018, catches continued to decline through 2021, with the recent average catch being 110,660 mt during 2020 − 2022.

Relative abundance indices of the WNPO Pacific saury, based on standardized catch-per-unit-effort (CPUE), by fleets were shown in **Table 4.1** and **Figure 4.4**. Visual inspection of all indices showed an overall decreasing trend with the last 7 years (2014 − 2020). The early index of Japan generally increased during 1980 − 1993. The coefficient of variation (CV) for each index was assumed to be equal to the standard error (SE) on the log scale. The CVs were set to 0.26 (the smallest CV value of the biomass survey of Japan) for fits the CPUE index at best.

Quarterly fish length composition data from 1994 − 2020 by fleets were summarized in **Table 4.1**. Length frequency data were compiled using 1-cm length bins from 14 to 35 cm. **Figure 4.5** showed the annual variations of quarterly length compositions by fleets. Most of the fleets caught large (>30 cm) individuals. The aggregated length composition distribution generally showed a single mode around 30 cm for Taiwan, but was mixed mode with two peaks around 27 cm and 30 cm for Japan.

(ii) Model description

doi:10.6342/NTU202500253

The assessment was conducted with Stock Synthesis (SS) version 3.30.20 (Methot and Wetzel, 2013). SS model is a flexible and widely used statistical framework for stock assessment that can be adapted to short-lived species such as sardine, prawn, and squid. These species are characterized by rapid growth, high natural mortality, and significant interannual variability in recruitment due to environmental influences. The SS model is particularly well-suited for short-lived species because it allows for the integration of multiple data sources, including catch-at-age or catch-at-length data, indices of relative abundance, and environmental covariates, to model population dynamics. For short-lived species, SS can incorporate their unique life history traits by using age-structured or length-structured models with high-resolution temporal scales (e.g., monthly or seasonal time steps) to capture rapid changes in population size and structure. The model can account for strong recruitment pulses, environmental variability, and high turnover rates, which are critical for understanding and managing these species effectively.

The SS model for Pacific saury was set up as a single area and single-gender model with four seasons (quarters). Spawning was assumed to occur in February (month 2). The available biological parameters for the WNPO saury stock were used (**Table 4.2**). The maximum age of Pacific saury was set to 2, the age at length L_1 was set to age 0, and the CV of the growth curve was set to 0.2 for young and old fish. The growth curve used a von Bertalanffy growth curve refitted from the Gompertz growth curve by Suyama et al. (2015) for ages 0 − 2. The von Bertalanffy growth coefficient parameter (K) and the maximum length (L_{inf}) were set to 2.02 and 31.45 cm, respectively with the size at age-0 = 0.66 cm. The natural mortality (2.18) of Pacific saury was estimated by using a meta-analytical approach that uses theoretical and empirical models to predict the natural mortality rate as a function of life history parameters (**Table 4.3**). A Beverton-Holt spawner-recruit relationship was used with steepness (h) set at 0.82 (see Chapter 1) and sigmaR (σ_r) set at 0.6.

Initial fishing mortality was estimated for the fleet of Japan during 1980 − 1994 (F1_JPN_early). Main recruitment deviations were estimated from 1978 − 2020. Early recruitment deviations were estimated from 1978 to 1979 as the population was not at equilibrium prior to the start of the model. The population model and the fishery length

doi:10.6342/NTU202500253

data had 22 one cm length bins from 14 – 35+ cm. The population had three age groups from age 0 to 2+. Fishery size data were used to estimate selectivity patterns, which controlled the size distribution of the fishery removals. Survey selectivity patterns mirrored their respective catch fleets (**Table 4.3**). Model estimated time series of total biomass for age 1+ (B_{age1+} in metric tons), female spawning stock biomass (SSB in metric tons), recruitment (R in 1,000s of fish) and fishing mortality (F in $year^{-1}$) were tabulated on an annual basis.

(iii) Model Diagnostics

The model was assumed to have converged if the standard error of the estimated parameters could be derived from the inverse of the negative Hessian matrix. Various convergence diagnostics were also evaluated. A gradient of >0.001 would suggest poorly fit parameter estimates. Parameter estimates hitting bounds of the prior was also indicative of poor model fit. Profiling the likelihood on the virgin recruitment (R_0), where the R0 is fixed at a range of values around the maximum likelihood estimate and then the likelihood is estimated, was used to identify influential data components (Lee et al., 2014). A runs test was used to evaluate randomness in the residuals of the CPUE and length composition data (Carvalho et al., 2021). Residual plots of the observed vs expected data were examined to evaluate goodness-of-fit for the CPUE and length composition data.

Several diagnostics have been evaluated for their utility to identify data conflicts and model misspecification within integrated stock assessment models (Carvalho et al., 2017). However, Carvalho et al. (2017) determined that there was no single diagnostic that worked well in all of the cases they evaluated. Instead, they recommend the use of a carefully selected range of diagnostics that proved to increase the ability to detect model misspecification. Key stock assessments diagnostics identified by Carvalho et al. (2017) and Carvalho et al. (2021) were implemented to evaluate the stock assessment model.

4.2.2. Future projection

Future projections were conducted in SS3 to evaluate the impact of various fishing mortality levels on future spawning stock biomass and yield (catch). The projections spanned from 2023 to 2042 (20 years). Since traditional F_{MSY} targets may be too aggressive

doi:10.6342/NTU202500253

for fish species with high environmental sensitivity and ecosystem importance, this study examined more conservative fishing mortality rates. Specifically, $0.5F_{MSY}$ and $0.75F_{MSY}$ were evaluated as precautionary approaches that provide buffers against recruitment uncertainty, environmental variability, and ecosystem needs, helping to maintain sufficient biomass for both predator requirements and fishery sustainability. The projections evaluated three fishing mortality scenarios: (1) High F scenario: Full F_{MSY}; (2) Moderate F scenario: 75% of F_{MSY} ($0.75F_{MSY}$); (3) Low F scenario: 50% of F_{MSY} ($0.5F_{MSY}$). Each scenario represents varying levels of precautionary management, with specific implications for the sustainability of Pacific saury populations and their role in the ecosystem.

The High F scenario (F_{MSY}) represents a non-precautionary approach, aiming to maximize yield at the level of maximum sustainable yield (MSY). While this strategy may achieve short-term economic benefits, it carries significant ecological risks, particularly for forage species like Pacific saury, which exhibit high recruitment variability and serve as a critical prey resource for dependent predators. Harvesting at F_{MSY} assumes optimal stock productivity and may not adequately account for environmental variability, uncertainties in stock assessments, or the cascading effects of reduced prey availability on the broader ecosystem.

The Moderate F scenario ($0.75F_{MSY}$) introduces a more cautious approach by reducing fishing pressure to 75% of the F_{MSY} level. This scenario reflects a balance between sustaining economic yields and mitigating risks to the stock and ecosystem. It provides a buffer against uncertainties in recruitment and environmental conditions, reducing the likelihood of overfishing while maintaining reasonable levels of harvest. This approach is particularly valuable for species with fluctuating population dynamics, as it allows for more resilient stock recovery under unfavorable conditions.

The Low F scenario ($0.5F_{MSY}$) represents the most precautionary approach and is based on the recommendations of Pitkitch et al. (2018). This strategy prioritizes the ecological role of forage species by maintaining fishing mortality at or below 50% of F_{MSY}. Such a reduction in fishing pressure helps ensure adequate biomass levels to support dependent predators, thereby safeguarding ecosystem stability. It also provides the greatest buffer against uncertainties in stock assessments and environmental variability, reducing

doi:10.6342/NTU202500253

the risk of population collapse. While this approach may result in reduced short-term economic returns, it aligns with ecosystem-based fisheries management principles and enhances the long-term sustainability of both the stock and the broader marine ecosystem.

By evaluating these scenarios, this study highlights the trade-offs between maximizing harvest and ensuring ecological resilience. Adopting the $0.5F_{MSY}$ or $0.75F_{MSY}$ scenarios provides a more sustainable pathway, particularly under the current challenges of environmental change and high uncertainty in recruitment patterns. These precautionary approaches align with modern fisheries management strategies that aim to balance ecological health with economic objectives.

All scenarios were applied to stock estimates beginning in 2023 and projected forward for 20 years through 2042. The future projection routine calculated the future SSB and yield that would occur while the specific fishing mortality, selectivity patterns, and relative fishing mortality proportions depended on the specific fishing mortality scenarios. Although this study provides a 20-year projection, since the life span of Pacific saury is 2 years, this study also focused on calculating the probability of $SSB>SSB_{MSY}$, median catch, and its variation during the first five years (2023 − 2027). The specifications for both deterministic and stochastic future projections are detailed below:

(i) Deterministic projection

The deterministic stock projections for Pacific saury were conducted without recruitment deviations nor log-bias adjustment were applied to the future projections. The absolute future recruitments were based on one deterministic scenario: the expected stock-recruitment relationship and the average recruitment during the historical period (1980 − 2022).

(ii) Stochastic projection

The framework of stochastic projection by considering the model parameters uncertainty and process error was shown in **Figure 4.6**. At the first step, this study applied the SS3 assessment model to both the original dataset and a bootstrapped dataset generated from the original assessment model. Subsequently, a data-generating model produces 100 bootstrap datasets, each of which is fitted using an estimation model that maintains the

doi:10.6342/NTU202500253

same structure as the original SS3 model. This part could consider the uncertainty from estimated model parameters (i.e., R_0, initial fishing mortality, selective parameters by fleets, catchability by indices and recruitment deviations). In addition, the recruitment deviations for the future period are randomly sampled from last 20 years (2003 - 2023) and used to replace the future recruitment deviates.

4.3. Results

4.3.1. Stock assessment results

(i) Model fit and diagnostics

The WNPO Pacific saury model estimated 111 parameters, and had a total likelihood of 1766.34. The inverse Hessian was positive definite, which allowed for the estimation of parameter standard deviations and suggests that the model converged, and the maximum gradient component was 2.03e-05, which is smaller than 0.001. None of the parameter estimates hit a bound. Fits to the abundance indices were generally good, with no substantial divergences between the expected and estimated CPUEs (**Figures 4.7; 4.8**). However, the S1_JPN_early, S2_JPN_late and S3_TWN did not pass the run test (**Figure 4.9**), which suggests that the residuals are not likely random. Estimated selectivity for each fleet and survey was shown in **Figures 4.10 and 4.11**, respectively. Fits to the length composition data suggested that the model predicted size compositions did not match the observations in some years (**Figures 4.12**; **4.13**). Furthermore, the results of the run test indicated that F1_JPN_late and F2_TWN pass the run test (**Figure 4.14**), which suggests that their residuals are likely random. Profiling on R_0 showed that the recruitment estimates were influential in the model results (**Figure 4.15**).

(ii) Stock assessment model outputs

The estimated total biomass of Pacific saury shows substantial variation from 1980 to 2020, fluctuating between 120,000 and 160,000 mt (**Figure 4.16**a). There was a noticeable peak period during 1985 − 1992, when biomass reached its highest levels of around 140,000 − 150,000 mt. After 1992, the biomass declined and has maintained a relatively constant level of around 120,000 − 130,000 mt from 1995 to 2020, with minor fluctuations. Despite some short-term variations, the overall biomass has remained

doi:10.6342/NTU202500253

relatively stable in recent years, showing no significant increasing or decreasing trends since 2000. The estimated SSB of Pacific saury has shown considerable fluctuation over the past four decades, with two notable peaks: a major peak around 1993 − 1995 reaching approximately 330,000 mt, and a smaller peak around 2007 − 2008 reaching about 250,000 mt. Since 2010, there has been a concerning declining trend, with biomass levels dropping to historical lows of around 50,000 mt by 2020. The current biomass is below the limit reference point SSB_{MSY} (**Figure 4.16**b).

Recruitment patterns closely mirror the spawning biomass trends, showing major peaks in the early-to-mid 1990s and moderate peaks in the mid-2000s. Recent recruitment levels have been consistently low, particularly since 2015, indicating potential challenges in population renewal (**Figure 4.16**c). The estimated fishing mortality (F) trend shows an inverse pattern to biomass and recruitment. F levels were relatively low during the high biomass period of the early 1990s (around 0.5 − 1.0 per year) but have increased substantially since the mid-2000s. Recent years show high variability in fishing mortality, with several spikes exceeding the F_{MSY} reference point, particularly around 2015 − 2018 (**Figure 4.16**d). The overall assessment results indicated that the Pacific saury stock is in an overfished based on estimated total biomass below sustainable levels ($B<B_{MSY}$), poor recruitment, and periods of relatively high fishing pressure. This situation suggests the need for improved management measures to promote stock recovery.

(iii) Stock status

The Pacific saury stock has shown significant decline in recent years, with the spawning stock biomass falling to historically low levels of around 50,000 mt by 2020, well below the SSB_{MSY} reference point (42,611.8 mt; SD = 4,798.96 mt; **Table 4.4**). The current SSB in 2022 was estimated at 25,809.9 mt (SD = 4,299.01 mt), and the recent three-year average SSB (2020 - 2022) was 31,655.4 mt (SD = 4,677.77 mt). Both current and recent SSB levels are below SSB_{MSY}, indicating that the stock is in a overfished state based on MSY-reference point.

In contrast, fishing mortality has increased substantially since the mid-2000s, with several periods exceeding F_{MSY} (2.61; SD = 0.04), particularly during 2015 − 2018. The latest fishing mortality (F_{2022}) was estimated at 1.42 (SD = 0.22), which is lower than F_{MSY}.

doi:10.6342/NTU202500253

Although the current fishing pressure is below the MSY-reference point (F_{MSY}), the depleted spawning stock biomass ($SSB_{2022}<SSB_{MSY}$) suggested that rebuilding measures may be necessary to ensure the stock's recovery.

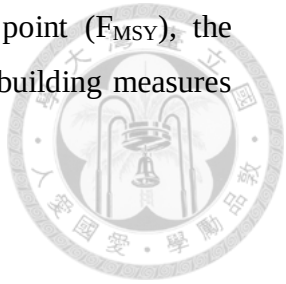

4.3.2. Future projections

(i) Deterministic projections

Based on the deterministic projections for Pacific saury from 2023 to 2042 under three different fishing mortality scenarios ($0.5F_{MSY}$, $0.75F_{MSY}$, and F_{MSY}), both spawning biomass and catch show distinct recovery patterns following their historical decline to low levels by 2020 (**Figure 4.17**). For spawning biomass, the projections indicated recovery to approximately 12,000 mt under $0.5F_{MSY}$ (most conservative scenario), 8,000 mt under $0.75F_{MSY}$ (moderate scenario), and 5,000 mt under F_{MSY}, with all scenarios showing relative stabilization after 2025 (**Figure 4.17**a and **Table 4.5**). The corresponding catch projections demonstrate that the F_{MSY} scenario yields the highest long-term catch at around 40,000 mt, while the $0.75F_{MSY}$ and $0.5F_{MSY}$ scenarios result in lower but stable catches of approximately 28,000 mt and 22,000 mt respectively, with all scenarios showing an initial rapid increase from 2023 to 2025 before stabilizing (**Figure 4.17**b and **Table 4.5**). These projections highlight the clear trade-offs between fishing pressure and stock recovery, indicating that the stock would reach different equilibrium levels depending on the fishing mortality scenarios, with lower fishing mortality leading to higher spawning biomass but lower catches, and vice versa.

(ii) Stochastic projections

Based on the stochastic projections for Pacific saury from 2023 to 2042, which incorporate recruitment variability and parameter uncertainty in the future (shown by gray lines representing individual trajectories), the results demonstrate substantial variability across all fishing mortality scenarios (**Figure 4.18**). Under the $0.5F_{MSY}$ scenario (**Figure 4.18**a-b), the spawning biomass showed a median trajectory (blue line) stabilizing around 12,000 mt, while catches stabilize around 20,000 mt, with stochastic trajectories ranging from approximately 15,000 to 80,000 mt. For the $0.75F_{MSY}$ scenario (**Figure 4.18**c-d), the

doi:10.6342/NTU202500253

median spawning biomass stabilizes at a lower level of about 8,000 mt, with median catches around 40,000 mt and stochastic variations ranging from 20,000 to 120,000 mt. Under the F_{MSY} scenario (**Figure 4.18**e-f), the median spawning biomass shows the lowest stabilization at approximately 5,000 mt, near the SSB_{MSY}, while catches show the highest variability ranging from 20,000 to 160,000 mt with a median around 50,000 mt. In addition, under the $0.5F_{MSY}$ scenario, the probability remains at 100% throughout the recent projection period (2023 − 2027), indicating a high likelihood of maintaining the stock above SSB_{MSY}. With $0.75F_{MSY}$, the probability started at 84.9% in 2023 and showed a gradual decline to 75.5% by 2027. Under the F_{MSY} scenario, the probability fluctuates between 50.5% and 75.8%, with the lowest probability occurring in 2026 (50.5%). These results suggest that lower fishing mortality rates provide higher probability of maintaining the stock above SSB_{MSY}, while fishing at F_{MSY} level results in approximately equal chances of the stock being above or below SSB_{MSY} (**Table 4.6**). In addition, while the median catch increases substantially when moving from $0.5F_{MSY}$ to $0.75F_{MSY}$, there is only a marginal increase when moving from $0.75F_{MSY}$ to full F_{MSY}, suggesting diminishing returns (where increasing fishing effort does not result in proportional increases in catch) in catch rates at higher fishing mortality levels (**Table 4.6**). Overall, the stochastic projections suggested that higher fishing mortality not only leads to lower spawning biomass but also increases the uncertainty in both biomass and catch outcomes, highlighting the increased risks associated with more intensive fishing strategies.

4.4. Discussion

4.4.1. Improve the current stock assessment model for Pacific saury

A persistent challenge in the Pacific saury stock assessment model lies in its difficulty with size composition fitting, particularly for larger fish (**Figure 4.11** and **4.12**). This issue is interlinked with several model components and points to the complex relationship between growth patterns, selectivity assumptions, and natural mortality parameters. In addition, the assumption that the Japanese survey's selectivity pattern (S7_JPN_bio) matches that of the Japanese fishery (F1_JPN) represents a significant simplification that may not reflect reality. Survey vessels and commercial fishing vessels often operate differently, using distinct gear types or fishing methods, which could result in different size selectivity

doi:10.6342/NTU202500253

patterns. This identical selectivity assumption was likely made for model simplicity but might be masking important differences in how these two data sources sample the population. Further complicating matters, the model's dome-shaped selectivity curves showed problematic behavior, with abrupt peaks and declines over the largest size bins.

This pattern suggested potential misspecification in how the model represents the interaction between fishing gear and different fish sizes. The abrupt decline in selectivity for larger fish might not accurately represent the true fishing process, where larger fish might remain equally catchable rather than becoming less vulnerable to capture. These interconnected issues highlighted the need for a more nuanced approach to modeling size-based processes in the Pacific saury assessment. Future improvements might involve developing separate selectivity patterns for surveys and commercial fisheries, reconsidering the appropriateness of dome-shaped versus asymptotic selectivity assumptions, and better integrating our understanding of saury growth and mortality patterns into the model structure.

4.4.2. Poor recruitment condition in the recent years

The persistent low recruitment of Pacific saury in recent years may be driven by environmental factors. From a population dynamics perspective, the significantly depleted spawning stock biomass, which has fallen below the SSB_{MSY}, likely represented a driver of poor recruitment (i.e., Beverton and Holt stock-recruitment relationship). This reduced spawning population represented fewer adults are available to produce eggs and larvae, potentially creating a negative feedback loop where low spawning stock leads to reduced recruitment, which in turn results in even lower future spawning biomass. Kakehi et al. (2022) also found that body weight and condition of adult Pacific saury had significant decreasing trends in 2019 and 2020, indicating that a decrease in the number of eggs laid. In addition, recent years have seen significant alterations in ocean temperature patterns (Takasuka et al., 2016), current systems (Ichii et al., 2018), and primary productivity (copepod community; Miyamoto et al., 2020) in Pacific saury feeding and spawning habitats (Fuji et al., 2021). Changes in the Kuroshio Current system and associated frontal zones, which are critical for saury migration and spawning, may have affected the survival

doi:10.6342/NTU202500253

and growth of eggs and larvae (Oozeki et al., 2004; Nakaya et al., 2010). Furthermore, shifts in water temperature can influence the timing and location of spawning, potentially creating mismatches between larval emergence and optimal feeding conditions (Fuji et al., 2023). These climate-driven changes might also be altering the spatial distribution of suitable habitat for juvenile Pacific saury, forcing them into less optimal areas for growth and survival. Given that environmental variability and its effects on stock productivity and fleet dynamics are increasingly being recognized as a priority for fisheries management (Szuwalski et al. 2016). Future work could conduct sensitivity analysis to identify how steepness values (stock-recruitment relationship; see **Chapter 1**), growth, and selectivity parameters may change given environmental variability (e.g., Harford et al., 2019).

4.4.3. Projections

The stochastic scenarios demonstrated substantial variability around median trajectories, particularly in catch projections, where potential fluctuations significantly exceed deterministic predictions. It should be noted that stochastic projections indicated a 50% probability of Pacific saury population recovery to MSY levels in the short term under the F_{MSY} scenario. However, with current estimated fishing mortality rates approximately at F_{MSY} (0.9) based on surplus production model (NPFC, 2023a), population recovery remains slow even when fishing mortality is restricted below F_{MSY}, suggesting this level may still be insufficient for the population to recover to MSY levels. Therefore, this study suggested that a further reduction in current fishing mortality (e.g., to 0.75 or $0.5F_{MSY}$), coupled with potential future recruitment increases, may facilitate faster population recovery to F_{MSY} levels. In addition to considering various fishing mortality scenarios, future stock assessments should account for multiple sources of uncertainty. Parameter uncertainty, particularly in key biological reference points such as steepness, natural mortality, growth and recruitment, should be incorporated into future analyses to provide more robust projections (e.g., Siple et al., 2019; Wildermuth et al. 2023). These uncertainties could significantly affect our understanding of stock resilience and recovery potential, especially when combined with varying fishing pressure scenarios. Furthermore, future projections for Pacific saury stock assessment should be integrated with forecasted environmental variables, particularly those derived from climate change scenarios (e.g.,

doi:10.6342/NTU202500253

CMIP6 emission scenarios). While environmental variables may not significantly affect the historical assessment outputs due to the dominance of monitoring data, they become crucial when projecting future population states. These projections depend heavily on assumptions about how population parameters will respond to changing environmental conditions (e.g., Punt et al., 2024). The interaction between parameter uncertainty and environmental variability adds another layer of complexity to stock projections, highlighting the need for comprehensive sensitivity analyses that consider both sources of variation simultaneously.

Additionally, future development of a Management Strategy Evaluation (MSE) framework for Pacific saury would be crucial to test the robustness of different harvest scenarios under various uncertainties (Butterworth, 2007; Punt et al., 2014; 2016). Such an MSE should incorporate multiple operating models that capture the range of plausible hypotheses about stock dynamics, including alternative stock-recruitment relationships, varying growth patterns, and different scenarios of environmental influence on recruitment. The framework should also evaluate performance metrics that are relevant to both conservation and socio-economic objectives, such as probability of stock recovery, catch stability, and long-term yield. This would provide a more comprehensive understanding of the trade-offs between different management strategies and help identify harvest control rules that are robust to the inherent uncertainties in Pacific saury population dynamics.

4.5. Conclusion

This study developed an age-structured model for Pacific saury and evaluated various harvest control strategies through both deterministic and stochastic projections. The stock assessment results indicated that the Pacific saury population is currently in a depleted state, with spawning stock biomass falling below SSB_{MSY} and experiencing poor recruitment in recent years. The stochastic projections, which incorporated parameter uncertainty and process error, revealed significant trade-offs between different fishing mortality scenarios ($0.5F_{MSY}$, $0.75F_{MSY}$, and F_{MSY}). The analysis demonstrated that while higher fishing mortality rates potentially yield larger median catches, they also lead to lower spawning biomass and increased uncertainty in both biomass and catch outcomes. Notably, the

doi:10.6342/NTU202500253

projections showed diminishing returns in catch rates at higher fishing mortality levels, with only marginal catch increases when moving from $0.75F_{MSY}$ to full F_{MSY}.

The probability of maintaining the stock above SSBMSY was highest under the $0.5F_{MSY}$ scenario (100%), followed by $0.75F_{MSY}$ (75.5 − 84.9%), while the F_{MSY} scenario showed approximately equal chances of the stock being above or below SSB_{MSY} (50.5 − 75.8%). These findings suggested that more conservative fishing mortality rates ($0.5F_{MSY}$ or $0.75F_{MSY}$) may be more appropriate for managing Pacific saury, particularly given the species' sensitivity to environmental variations and its depleted status. Future stock assessments would benefit from incorporating environmental variables, particularly those derived from climate change scenarios, and conducting comprehensive sensitivity analyses that consider both parameter uncertainty and environmental variability simultaneously.

doi:10.6342/NTU202500253

5. Chapter 5 − Summary and recommendations

5.1. Summary

My study focused on improving the methodology and stock assessment of Pacific saury (*Cololabis saira*) in the Northwestern Pacific Ocean through following interconnected studies. First, this study developed a numerical approach to estimate the stock-recruitment resilience (steepness) of Pacific saury using life history parameters and reproductive biology. This study revealed a median steepness value of 0.82 with an 80% probable range of (0.59, 0.93), suggesting high resilience to fishing pressure under prevailing environmental conditions. However, sensitivity analyses demonstrated that unfavorable environmental conditions could substantially decrease this resilience by affecting growth, body weight, and survival rates of eggs and larvae. This suggested that environmental variation should be considered when estimating steepness for stock assessments. Second, this study evaluated different spatial treatments for standardizing CPUE data under GLMMs. Through both real-world application and simulation studies, the analysis found that a spatio-temporal modelling approach (VAST; i.e., continuous spatial treatment) outperformed traditional methods (i.e., area stratification) in capturing spatial heterogeneity, especially for the preferential sampling (i.e., CPUE data from preferred fishing grounds to exert a disproportionate effect on the estimated fish abundance). In addition, the influence analysis indicated that the interaction between year and spatial effects had major impacts on standardized CPUE indices. The importance of conducting influence analysis and the greater performance of a spatio-temporal approach are highlighted.

Third, the analysis of spatiotemporal dynamics using joint fishery data from several fleets operated in the Northwestern Pacific Ocean during 2001 − 2017 suggested an eastward shift in Pacific saury distribution after 2013, with further shifts and lower abundance in 2017. It should be noted that these distribution changes could not be adequately explained by either local environmental variables (e.g., SST) or regional climate indices (e.g., SOI index). Instead, they were primarily attributed to “unmodelled spatiotemporal processes” (e.g., the biological interaction of other species), highlighting the need to better understand underlying ecological mechanisms. Lastly, building on these

doi:10.6342/NTU202500253

findings, an age-structured stock assessment model was developed incorporating various sources of uncertainty to conduct the forecast projection. The stock assessment suggested that spawning stock biomass of Pacific saury has declined to historically low levels (31,655.4 mt) in recent years, below SSB_{MSY}. Although current fishing mortality remains below F_{MSY}, stochastic projections suggested more conservative harvest rates may be necessary for recovery. The $0.5F_{MSY}$ scenario demonstrated the highest probability of maintaining the stock above SSB_{MSY}. However, considering the trade-off between stock recovery and fishery, this study recommends the $0.75F_{MSY}$ scenario as a more balanced approach. Overall, these studies advanced our understanding of Pacific saury population dynamics and provided improved methods for stock assessment and management. The findings emphasized the importance of considering environmental variability, spatial distribution patterns, and parameter uncertainty in developing effective fisheries management strategies.

5.2. Recommendations

5.2.1. Spatial consideration in stock assessment

The current total allowable catch (TAC) allocation for Pacific saury, as determined by the NPFC, designates 60% for high seas and 40% for Exclusive Economic Zones (EEZs). However, this allocation lacks a robust scientific foundation (NPFC, 2024a). This arbitrary approach fails to account for the intricate spatial dynamics of Pacific saury populations, which exhibit complex migration patterns and significant spatial variability in growth and abundance across temporal and spatial scales.

As highlighted in Chapter 2, the arbitrary spatial stratification with rectangular shape does not effectively reflect the heterogeneous distribution of Pacific saury density. It is because that the Pacific saury population exhibits dynamic spatiotemporal characteristics may be driven by complex interactions among oceanographic conditions, food availability, and reproductive strategies (Chang et al., 2019; Fuji et al., 2021; Miyamoto et al., 2020). These factors challenge the traditional assumption of a homogeneously structured stock, underscoring the need for more scientifically informed

doi:10.6342/NTU202500253

and adaptive management approaches to better align with the biological and ecological realities of Pacific saury.

The complex nature of Pacific saury populations necessitates sophisticated analytical methods that go beyond traditional management frameworks. Integration of spatial processes into stock assessments, particularly through spatial data disaggregation, reveals critical insights into population dynamics (e.g., Carruthers et al., 2011; Cardinale et al., 2023). This advanced methodological approach allows scientists to detect subtle variations in key biological parameters - recruitment, growth, and mortality rates - which might be overlooked by conventional assessment methods. The resulting spatially structured population models provide a more nuanced and complete picture of Pacific saury population structure by accounting for both spatial distribution patterns and demographic diversity. From a management perspective, these insights can inform more adaptive and spatially explicit conservation strategies (Kapur et al., 2021). Compared to traditional quota systems reliant on broad administrative boundaries, spatially-resolved management approaches offer several advantages: enhanced ecological precision, improved monitoring capabilities, and more targeted intervention strategies (e.g., TAC; Punt, 2019).

5.2.2. Multi-species stock assessment

Currently, the NPFC conducts a regular assessment of Pacific saury every year to monitor its stock status, and has implemented an interim hockey-stick harvest control rule (HCR) to set the TAC with using B_{MSY} as the target reference point to recover the stock to MSY levels (NPFC, 2024b). However, like other small pelagic fish species, Pacific saury exhibits rapid growth, short life span, high recruitment variability, and complex schooling behavior. These biological traits, combined with their sensitivity to environmental conditions and role as a forage species, make traditional single-species management approaches insufficient for sustainable management (e.g., McClatchie et al. 2017; Forrest et al. 2023). Therefore, manager should consider to implement a hockey stick HCR with a biomass limit of no less than 40% of unfished biomass (B_0), and fishing mortality should not exceed 50% of F_{MSY}. This approach would help maintain adequate population levels for dependent predators while still allowing for sustainable commercial harvest. More

doi:10.6342/NTU202500253

specifically, Pitkitch et al. (2018) found that predators highly dependent on forage fish (for 50 percent or more of their diet) are common, occurring in three-fourths of marine ecosystems examined. These dependent predators are more sensitive to changes in forage fish abundance than less-dependent species. This study recommends that regular monitoring of both Pacific saury populations and their predators (e.g., blue shark, albacore, chub mackerel; Yatsu, 2019) also should be conducted to assess ecosystem impacts, and spatial management measures may be needed to prevent localized depletion in important feeding areas.

In addition, to effectively manage Pacific saury, it is essential to account for interactions with other forage fish species, such as Japanese sardine (*Sardinops melanostictus*), chub mackerel (*Scomber japonicus*), and Japanese anchovy (*Engraulis japonicus*), which generally spawn in subtropical waters from winter to spring (Takasuka et al., 2008; Kanamori et al., 2019; Fuji et al., 2021). Forage fish species often exhibit compensatory responses when another species is depleted (Yatsu, 2019). For example, Chapter 3 highlighted that unmodelled factors, such as species interactions, play a significant role in driving distribution shifts of Pacific saury. Similarly, Fuji et al. (2023) demonstrated that after 2013, the expansion of Japanese sardine into colder waters coincided with an observed shift in Pacific saury distribution to colder waters - but only in areas where sardines were present. This distributional shift was absent east of 180° longitude, where sardines were not observed, suggesting that interspecific competition likely influences the spatial distribution of small pelagic fish.

When one forage fish species is heavily exploited, competing species may increase in abundance by capitalizing on the reduced competition for food resources. For example, reduced Pacific saury populations due to fishing pressure could potentially benefit Japanese sardine populations by alleviating competition for zooplankton prey (Yamamoto and Katayama, 2012; Miyamoto et al., 2020). Therefore, management strategies should not focus on Pacific saury in isolation but should incorporate trophic interactions and competition with other forage fish species, such as Japanese sardine, through multi-species assessments. This approach would help maintain a balanced ecosystem among forage fish species while ensuring sustainable harvest levels for all.

doi:10.6342/NTU202500253

5.2.3. Management Strategy Evaluation

Management Strategy Evaluation (MSE) is a crucial tool for testing and refining fisheries management strategies to ensure long-term sustainability, especially in the face of the inherent uncertainties in marine ecosystems (Butterworth and Punt, 1999; Punt, Butterworth, et al., 2016; Rademeyer et al., 2007). These uncertainties, such as fluctuating fish stocks, environmental changes, and data limitations − pose significant challenges for predicting future conditions. MSE offers a structured framework that allows for the assessment of how different management strategies perform under various scenarios. By addressing biological, environmental, and data uncertainties, MSE helps evaluate the robustness of these strategies. Furthermore, it plays a critical role in preventing overfishing by evaluating strategies under worst-case scenarios and supports adaptive management by ensuring that strategies can evolve in response to changing conditions. In addition, MSE facilitates the balancing of competing objectives and informs decision-making by providing evidence-based insights for policymakers and stakeholders. Ultimately, MSE enhances fisheries management by ensuring that strategies remain effective, transparent, and sustainable.

In Chapter 1, this study presented potential steepness values for Pacific saury under various environmental conditions. Small pelagic fish steepness is often assumed to be high, but low steepness could have serious implications for collapses, recovery from fishing, and population variability. Therefore, future MSE analyses should incorporate the uncertainty associated with steepness as one of the critical sources of uncertainty. In Chapter 4, an age-structured model was developed, which could serve as a starting point for constructing the population dynamics model for Pacific saury in MSE. Additionally, Chapter 4 considered only a constant HCR, future MSE analyses should explore a performance of various HCRs across multiple scenarios that account for environmental uncertainty, varying recruitment patterns, and species interactions. Specifically, the framework should evaluate HCRs with dynamic unfished biomass (B_0) reference points (Berger, 2019; Bessell-Browne et al., 2022), as these have been shown to reduce the frequency of fishery closures while maintaining sustainable biomass levels across varying recruitment scenarios.

doi:10.6342/NTU202500253

Given the transboundary nature of Pacific saury, the MSE framework also should evaluate management procedures that can be practically implemented through international cooperation (such as NPFC). Performance metrics can extend beyond traditional single-species objectives to include ecosystem considerations, such as maintaining adequate forage base for predators and ensuring economic stability and achieving management objectives for multiple species (e.g., Schiano et al. 2023; Kaplan et al. 2021; Pérez-Rodríguez et al. 2022), particularly Japanese sardine (Fuji et al., 2023). These studies also highlighted the need for sufficient basic biological knowledge of both predators and prey to inform ecosystem models in support of MSE strategies. To enhance the practical utility of the MSE, regular updates with new information (e.g., competitors and predator relative abundance indices) and refined models (e.g., spatio-temporal modelling approach) should be incorporated as part of an adaptive management approach (e.g., Moosa and Butterworth, 2024). This would allow management strategies to evolve as our understanding of Pacific saury's response to environmental changes improves and as new challenges emerge in the fishery.

doi:10.6342/NTU202500253

References

Akaike, H. (1974). A new look at statistical model identification. *IEEE Transactions on Automatic Control*, AC-19, 716–723.

Albo-Puigserver, M., Pennino, M. G., Bellido, J. M., Colmenero, A. I., Giráldez, A., Hidalgo, M., & Coll, M. (2021). Changes in life history traits of small pelagic fish in the western Mediterranean Sea. *Frontiers in Marine Science*, 8, 570354.

Allen, P. M., & McGlade, J. M. (1986). Dynamics of discovery and exploitation: the case of the Scotian shelf groundfish fisheries. *Canadian Journal of Fisheries and Aquatic Sciences*, 43(6), 1187–1200.

Anderson, D., & Gillooly, J. (2020). Predicting egg size across temperatures in marine teleost fishes. *Fish and Fisheries*, 21, 1027–1033.

Bates, D., Maechler, M., Bolker, B., & Walker, S. (2015). Fitting linear mixed-effects models using lme4. *Journal of Statistical Software*, 67, 1–48.

Battaile, B. C., & Quinn II, T. J. (2004). Catch per unit effort standardization of the eastern Bering Sea walleye pollock (*Theragra chalcogramma*) fleet. *Fisheries Research*, 70, 161–177.

Barbeaux, S. J., & Hollowed, A. B. (2018). Ontogeny matters: Climate variability and effects on fish distribution in the eastern Bering Sea. *Fisheries Oceanography*, 27, 1–15.

Bentley, N., Kendrick, T. H., Starr, P. J., & Breen, P. A. (2012). Influence plots and metrics: Tools for better understanding fisheries catch-per-unit-effort standardizations. *ICES Journal of Marine Science*, 69, 84–88.

Berger, A. M. (2019). Character of temporal variability in stock productivity influences the utility of dynamic reference points. *Fisheries Research*, 217, 185–197.

Bessell-Browne, P., Punt, A. E., Tuck, G. N., Day, J., Klaer, N., & Penney, A. (2022). The effects of implementing a "dynamic B0" harvest control rule in Australia's Southern and Eastern Scalefish and Shark Fishery. *Fisheries Research*, 252, 106306.

Bishop, J. (2006). Standardizing fishery-dependent catch and effort data in complex fisheries with technology change. *Reviews in Fish Biology and Fisheries*, 16, 21–38.

Brodziak, J., & Legault, C. M. (2005). Model averaging to estimate rebuilding targets for overfished stocks. *Canadian Journal of Fisheries and Aquatic Sciences*, 62, 544–562.

doi:10.6342/NTU202500253

Brodziak, J., & Piner, K. (2010). Model averaging and probable status of North Pacific striped marlin, *Tetrapturus audax*. *Canadian Journal of Fisheries and Aquatic Sciences*, 67, 793–805.

Brodziak, J., Mangel, M., & Sun, C. L. (2015). Stock-recruitment resilience of North Pacific striped marlin based on reproductive ecology. *Fisheries Research*, 166, 140–150.

Burnham, K. P., & Anderson, D. R. (2002). A practical information-theoretic approach. Model selection and multimodel inference. Second edition. Springer, New York. 488 pp.

Butterworth, D. S., & Punt, A. E. (1999). Experiences in the evaluation and implementation of management procedures. *ICES Journal of Marine Science*, 56(6), 985–998.

Butterworth, D. S. (2007). Why a management procedure approach? Some positives and negatives. *ICES Journal of Marine Science*, 64, 613–617.

Campbell, R. A. (2004). CPUE standardisation and the construction of indices of stock abundance in a spatially varying fishery using general linear models. *Fisheries Research*, 70, 209–227.

Campbell, R. A. (2015). Constructing stock abundance indices from catch and effort data: Some nuts and bolts. *Fisheries Research*, 161, 109–130.

Cao, J., Thorson, J. T., Richards, R. A., & Chen, Y. (2017). Spatiotemporal index standardization improves the stock assessment of northern shrimp in the Gulf of Maine. *Canadian Journal of Fisheries and Aquatic Sciences*, 74, 1781–1793.

Cardinale, M., Zimmermann, F., Søvik, G., Griffiths, C. A., Bergenius Nord, M., & Winker, H. (2023). Spatially explicit stock assessment uncovers sequential depletion of northern shrimp stock components in the North Sea. *ICES Journal of Marine Science*, 80, 1868–1880.

Carruthers, T. R., McAllister, M. K., & Taylor, N. G. (2011). Spatial surplus production modeling of Atlantic tunas and billfish. *Ecological Applications*, 21(7), 2734–2755.

Carvalho, F., Punt, A. E., Chang, Y. J., Maunder, M. N., & Piner, K. R. (2017). Can diagnostic tests help identify model misspecification in integrated stock assessments? *Fisheries Research*, 192, 28–40.

Carvalho, F., Winker, H., Courtney, D., Kapur, M., Kell, L., Cardinale, M., et al., (2021). A cookbook for using model diagnostics in integrated stock assessments. *Fisheries Research*, 240, 105959.

doi:10.6342/NTU202500253

Chang, Y. J., Lan, K. W., Walsh, W. A., Hsu, J., & Hsieh, C. H. (2019). Modelling the impacts of environmental variation on habitat suitability for Pacific saury in the Northwestern Pacific Ocean. *Fisheries Oceanography*, 28, 291–304.

Checkley Jr, D. M., Asch, R. G., & Rykaczewski, R. R. (2017). Climate, anchovy, and sardine. *Annual Review of Marine Science*, 9, 469–493.

Chen, Y. (1996). A Monte Carlo study on impacts of the size of subsample catch on estimation of fish stock parameters. *Fisheries Research*, 26, 207–223.

Clark, C. W., & Mangel, M. (1979). Aggregation and fishery dynamics: Theoretical study of schooling and the purse seine tuna fisheries. *Fisheries Bulletin*, 77, 317–337.

Conn, P. B., Williams, E. H., & Shertzer, K. W. (2010). When can we reliably estimate the productivity of fish stocks? *Canadian Journal of Fisheries and Aquatic Sciences*, 67, 511–523.

Conn, P. B., Thorson, J. T., & Johnson, D. S. (2017). Confronting preferential sampling when analysing population distributions: Diagnosis and model-based triage. *Methods in Ecology and Evolution*, 8, 1535–1546.

Crecco, V., & Overholtz, W. J. (1990). Causes of density-dependent catchability for Georges Bank haddock, *Melanogrammus aeglefinus*. *Canadian Journal of Fisheries and Aquatic Sciences*, 47(2), 385–394.

Crone, P. R., Maunder, M. N., Lee, H., & Piner, K. R. (2019). Good practices for including environmental data to inform spawner-recruit dynamics in integrated stock assessments: Small pelagic species case study. *Fisheries Research*, 217, 122–132.

Diggle, P., Ribeiro, P. (2007). Geostatistics, M.-b. Springer Series in Statistics. Springer.

Doney, S. C., Ruckelshaus, M., Emmett Duffy, J., Barry, J. P., Chan, F., English, C. A., & Talley, L. D. (2012). The effects of climate change on marine ecosystems. *Annual Review of Marine Science*, 4, 11–37.

Dorval, E., McDaniel, J. D., Macewicz, B. J., et al. (2015). Changes in growth and maturation parameters of Pacific sardine, *Sardinops sagax*, collected off California during a period of stock recovery from 1994 to 2010. *Journal of Fish Biology*, 87, 286–310.

Ducharme-Barth, N. D., Grüss, A., Vincent, M. T., Kiyofuji, H., Aoki, Y., Pilling, G., Hampton, J., & Thorson, J. T. (2022). Impacts of fisheries-dependent spatial sampling patterns on catch-per-unit-effort standardization: A simulation study and fishery application. *Fisheries Research*, 246, 106169.

doi:10.6342/NTU202500253

Essington, T. E., Moriarty, P. E., Froehlich, H. E., Hodgson, E. E., Koehn, L. E., Oken, K. L., et al. (2015). Fishing amplifies forage fish population collapses. *Proceedings of the National Academy of Sciences*, 112, 6648–6652.

Feenstra, J., McGarvey, R., Linnane, A., Haddon, M., Matthews, J., Punt, A. E. (2019). Impacts on CPUE from vessel fleet composition changes in an Australian lobster (*Jasus edwardsii*) fishery. *New Zealand Journal of Marine and Freshwater Research*, 53, 292–302.

Fiechter, J., Rose, K. A., Curchitser, E. N., & Hedstrom, K. S. (2015). The role of environmental controls in determining sardine and anchovy population cycles in the California Current: Analysis of an end-to-end model. *Progress in Oceanography*, 138, 381–398.

Forrest, R. E., Kronlund, A. R., Cleary, J. S., & Grinnell, M. H. (2023). An evidence-based approach for selecting a limit reference point for Pacific herring (*Clupea pallasii*) stocks in British Columbia, Canada. *Canadian Journal of Fisheries and Aquatic Sciences*, 80, 1071–1083.

Forrestal, F. C., Schirripa, M., Goodyear, C. P., Arrizabalaga, H., Babcock, E. A., Coelho, R., Ingram, W., Lauretta, M., Ortiz, M., Sharma, R. (2019). Testing robustness of CPUE standardization and inclusion of environmental variables with simulated longline catch datasets. *Fisheries Research*, 210, 1–13.

Francis, R. I. C. (1992). Use of risk analysis to assess fishery management strategies: A case study using orange roughy (*Hoplostethus atlanticus*) on the Chatham Rise, New Zealand. *Canadian Journal of Fisheries and Aquatic Sciences*, 49, 922–930.

Free, C. M., Thorson, J. T., Pinsky, M. L., Oken, K. L., Wiedenmann, J., & Jensen, O. P. (2019). Impacts of historical warming on marine fisheries production. *Science*, 363, 979–983.

Froese, R. (1990). FISHBASE: An information system to support fisheries and aquaculture research. *Fishbyte*, 8, 21–24.

Fuji, T., Kurita, Y., Suyama, S., & Ambe, D. (2021). Estimating the spawning ground of Pacific saury, *Cololabis saira*, by using the distribution and geographical variation in maturation status of adult fish during the main spawning season. *Fisheries Oceanography*, 30, 382–396.

Fuji, T., Nakayama, S. I., Hashimoto, M., Miyamoto, H., Kamimura, Y., Furuichi, S., ... & Suyama, S. (2023). Biological interactions potentially alter the large-scale distribution pattern of the small pelagic fish, Pacific saury, *Cololabis saira*. *Marine Ecology Progress Series*, 704, 99–117.

doi:10.6342/NTU202500253

Fukushima, S. (1979). Synoptic analysis of migration and fishing conditions of saury in the northwest Pacific Ocean. *Bulletin of the Tohoku Regional Fisheries Research Laboratory*, 41, 1–70.

Furuichi, S., Yasuda, T., Kurota, H., Yoda, M., Suzuki, K., Takahashi, M., & Fukuwaka, M. A. (2020). Disentangling the effects of climate and density-dependent factors on spatiotemporal dynamics of Japanese sardine spawning. *Marine Ecology Progress Series*, 633, 157–168.

Gao, J., Thorson, J. T., Szuwalski, C., & Wang, H. Y. (2020). Historical dynamics of the demersal fish community in the East and South China Seas. *Marine and Freshwater Research*, 71(9), 1073–1085.

Glaser, S. M., Waechter, K. E., & Bransome, N. C. (2015). Through the stomach of a predator: Regional patterns of forage in the diet of albacore tuna in the California Current System and metrics needed for ecosystem-based management. *Journal of Marine Systems*, 146, 38–49.

Glazer, J. P., & Butterworth, D. S. (2002). GLM-based standardization of the catch per unit effort series for South African west coast hake, focusing on adjustments for targeting other species. *African Journal of Marine Science*, 24, 323–339.

Greven, S., & Kneib, T. (2010). On the behavior of marginal and conditional AIC in linear mixed models. *Biometrika*, 97, 773–789.

Grüss, A., Walter III, J. F., Babcock, E. A., Forrestal, F. C., Thorson, J. T., Lauretta, M. V., Schirripa, M. J. (2019). Evaluation of the impacts of different treatments of spatio-temporal variation in catch-per-unit-effort standardization models. *Fisheries Research*, 213, 75–93.

Haltuch, M. A., Ono, K., & Valero, J. L. (2013). Status of the U.S. Petrale Sole Resource in 2012. Pacific Fishery Management Council, Portland, Oregon.

Han, Q., Grüss, A., Shan, X., Jin, X., & Thorson, J. T. (2021). Understanding patterns of distribution shifts and range expansion/contraction for small yellow croaker (*Larimichthys polyactis*) in the Yellow Sea. *Fisheries Oceanography*, 30, 69–84.

Harford, W. J., Sagarese, S. R., & Karnauskas, M. (2019). Coping with information gaps in stock productivity for rebuilding and achieving maximum sustainable yield for grouper–snapper fisheries. *Fish and Fisheries*, 20(2), 303–321.

Hashimoto, M., Kidokoro, H., Suyama, S., Fuji, T., Miyamoto, H., Naya, M., & Kitakado, T. (2020). Comparison of biomass estimates from multiple stratification approaches in a swept area method for Pacific saury, *Cololabis saira*, in the western North Pacific. *Fisheries Research*, 1–12.

doi:10.6342/NTU202500253

Hashimoto, M., Naya, M., Suyama, S., Nakayama, S.I., Fuji, T., Miyamoto, H., Kawabata, A., & Nakatsuka, S. (2021). Standardized CPUE of Pacific saury (*Cololabis saira*) caught by the Japanese stick-held dip net fishery up to 2020. NPFC-2021-SSC PS07-WP07.

Hashimoto, M., Nishijima, S., Yukami, R., Watanabe, C., Kamimura, Y., Furuichi, S., Ichinokawa, M., & Okamura, H. (2019). Spatiotemporal dynamics of the Pacific chub mackerel revealed by standardized abundance indices. *Fisheries Research*, 219, 105315.

He, X., Mangel, M., & MacCall, A. (2006). A prior for steepness in stock-recruitment relationships, based on an evolutionary persistence principle. *Fishery Bulletin-National Oceanic and Atmospheric Administration*, 104.

Helser, T. E., & Lai, H. L. (2004). A Bayesian hierarchical meta-analysis of fish growth: with an example for North American largemouth bass, *Micropterus salmoides*. *Ecological Modelling*, 178, 399–416.

Hilborn, R., & Walters, C. J. (1992). Quantitative Fisheries Stock Assessment and Management: Choice, Dynamics and Uncertainty. Chapman & Hall, New York.

Hilborn, R., & Walters, C. J. (1987). A general model for simulation of stock and fleet dynamics in spatially heterogeneous fisheries. *Canadian Journal of Fisheries and Aquatic Sciences*, 44, 1366–1369.

Holdsworth, J. C., & Saul, P. J. (2017). Striped marlin catch and CPUE in the New Zealand sport fishery 2013-14 to 2015-16. *New Zealand Fisheries Assessment Report, 18*, 27.

Hollowed, A. B., Barange, M., Beamish, R. J., Brander, K., Cochrane, K., Drinkwater, K., Foreman, M. G. G. (2013). Projected impacts of climate change on marine fish and fisheries. *ICES Journal of Marine Science, 70*, 1023–1037.

Holt, C. A., & Michielsens, C. G. (2020). Impact of time-varying productivity on estimated stock-recruitment parameters and biological reference points. *Canadian Journal of Fisheries and Aquatic Sciences, 77*, 836–847.

Hoyle, S. D., Huang, H., Kim, D. N., Lee, M. K., Matsumoto, T., & Walter, J. (2019). Collaborative study of bigeye tuna CPUE from multiple Atlantic Ocean longline fleets in 2018. *Collect. Vol. Sci. Pap. ICCAT, 75*, 2033–2080.

Hsu, J., Chang, Y. J., Brodziak, J., Kai, M., & Punt, A. E. (2024). On the probable distribution of stock-recruitment resilience of Pacific saury (*Cololabis saira*) in the Northwest Pacific Ocean. *ICES Journal of Marine Science, 81*, 748-759.

doi:10.6342/NTU202500253

Hsu, J., Chang, Y. J., Kitakado, T., Kai, M., Li, B., Hashimoto, M., & Park, K. J. (2021). Evaluating the spatiotemporal dynamics of Pacific saury in the Northwestern Pacific Ocean by using a geostatistical modelling approach. *Fisheries Research, 235*, 105821.

Hua, C., Li, F., Zhu, Q., Zhu, G., & Meng, L. (2020). Habitat suitability of Pacific saury (*Cololabis saira*) based on a yield-density model and weighted analysis. *Fisheries Research, 221*, 105408.

Hua, C. X., Tian, S. Q., & Shi, Y. C. (2023). Standardized CPUE of Pacific saury by China's stick-held dip net fishery up to 2022. *NPFC-2023-SSC PS11-WP04*.

Huang, W. B., Chang, Y. J., & Hsieh, C. H. (2021). Standardized CPUE of Pacific saury (*Cololabis saira*) caught by the Chinese Taipei stick-held dip net fishery up to 2020. *NPFC-2021-SSC PS07-WP14*.

Huang, W. B., Lo, N. C., Chiu, T. S., & Chen, C. S. (2007). Geographical distribution and abundance of Pacific saury, *Cololabis saira* (Brevoort) (Scomberesocidae), fishing stocks in the northwestern Pacific in relation to sea temperatures. *Zoological Research, 46*, 705.

Huang, W. B., Chang, Y. J., & Hsieh, C. H. (2023). Standardized CPUE of Pacific saury (*Cololabis saira*) caught by the Chinese Taipei stick-held dip net fishery up to 2022. *NPFC-2023-SSC PS11-WP02*.

Hubbs, C. L., & Wisner, R. L. (1980). Revision of the sauries (Pisces, Scomberesocidae) with descriptions of two new genera and one new species. *Fish Bulletin, 77*, 521-566.

Huret, M., Tsiaras, K., Daewel, U., Skogen, M. D., Gatti, P., Petitgas, P., & Somarakis, S. (2019). Variation in life-history traits of European anchovy along a latitudinal gradient: a bioenergetics modelling approach. *Marine Ecology Progress Series, 617*, 95–112.

Ichii, T., Nishikawa, H., Mahapatra, K., Okamura, H., Igarashi, H., Sakai, M., & Okada, Y. (2018). Oceanographic factors affecting interannual recruitment variability of Pacific saury (*Cololabis saira*) in the central and western North Pacific. *Fisheries Oceanography, 27*, 445–457.

Ichii, T., Nishikawa, H., Mahapatra, K., Okamura, H., Igarashi, H., Sakai, M., et al. (2018). Oceanographic factors affecting interannual recruitment variability of Pacific saury (Cololabis saira) in the central and western North Pacific. *Fisheries Oceanography, 27*, 445–457.

Ichinokawa, M., & Brodziak, J. (2010). Using adaptive area stratification to standardize catch rates with application to North Pacific swordfish (*Xiphias gladius*). *Fisheries Research, 106*, 249–260.

doi:10.6342/NTU202500253

Ichinokawa, M., Okamura, H., & Kurota, H. (2017). The status of Japanese fisheries relative to fisheries around the world. *ICES Journal of Marine Science, 74*, 1277–1287.

IOC-IHO-BODC, A. (2003). Centenary Edition of the GEBCO Digital Atlas. The Intergovernmental Oceanographic Commission, The International Hydrographic Organization and the British Oceanographic Data Centre, Liverpool, UK.

Ito, S. I., Okunishi, T., Kishi, M. J., & Wang, M. (2013). Modelling ecological responses of Pacific saury (*Cololabis saira*) to future climate change and its uncertainty. *ICES Journal of Marine Science, 70*, 980–990.

Iwahashi, M., Isoda, Y., Ito, S. I., Oozeki, Y., & Suyama, S. (2006). Estimation of seasonal spawning ground locations and ambient sea surface temperatures for eggs and larvae of Pacific saury (*Cololabis saira*) in the western North Pacific. *Fisheries Oceanography, 15*(2), 125–138.

Kai, M. (2019). Spatio-temporal changes in catch rates of pelagic sharks caught by Japanese research and training vessels in the western and central North Pacific. *Fisheries Research, 216*, 177–195.

Kai, M., Thorson, J. T., Piner, K. R., & Maunder, M. N. (2017). Spatiotemporal variation in size-structured populations using fishery data: an application to shortfin mako (*Isurus oxyrinchus*) in the Pacific Ocean. *Canadian Journal of Fisheries and Aquatic Sciences, 74*, 1765–1780.

Kakehi, S., Hashimoto, M., Naya, M., Ito, S. I., Miyamoto, H., & Suyama, S. (2022). Reduced body weight of Pacific saury (*Cololabis saira*) causes delayed initiation of spawning migration. *Fisheries Oceanography, 31*, 319–332.

Kaplan, I.C., Gaichas, S.K., Stawitz, C.C., Lynch, P.D., Marshall, K.N., Deroba, J.J., et al. (2021). Management strategy evaluation: allowing the light on the hill to illuminate more than one species. *Frontiers in Marine Science, 8*, 624355.

Kapur, M. S., Siple, M. C., Olmos, M., Privitera-Johnson, K. M., Adams, G., Best, J., et al. (2021). Equilibrium reference point calculations for the next generation of spatial assessments. *Fisheries Research, 244*, 106132.

Kaufman, L., & Rousseeuw, P.J. (1990). Finding Groups in Data: An Introduction to Cluster Analysis. Wiley, New Jersey.

Koenigstein, S., Jacox, M. G., Pozo Buil, M., Fiechter, J., Muhling, B. A., Brodie, S., & Tommasi, D. (2022). Population projections of Pacific sardine driven by ocean warming and changing food availability in the California Current. *ICES Journal of Marine Science, 79*, 2510–2523.

doi:10.6342/NTU202500253

Kosaka, S. (2000). Life history of the Pacific saury *Cololabis saira* in the northwest Pacific and considerations on resource fluctuations based on it. *Bulletin of the Tohoku National Fisheries Research Institute, 63*, 1–96. (Japanese with English abstract).

Kristensen, K., Nielsen, A., Berg, C. W., Skaug, H., & Bell, B. M. (2016). TMB: Automatic differentiation and Laplace approximation. *Journal of Statistical Software, 70*, 1–21.

Kristensen, K., Thygesen, U.H., Andersen, K.H., & Beyer, J.E. (2014). Estimating spatiotemporal dynamics of size-structured populations. *Canadian Journal of Fisheries and Aquatic Sciences, 71*, 326–336.

Kulik, V., Katugin, O., & Baitaliuk, A. (2021). Standardized CPUE of Pacific saury (*Cololabis saira*) caught by the RUSSIA's stick-held dip net fishery up to 2021. *NPFC-2023-SSC PS11-WP03*.

Kuriyama, P. T., Zwolinski, J. P., Hill, K. T., & Crone, P. R. (2020). Assessment of the Pacific sardine resource in 2020 for US management in 2020-2021.

Kuroda, H., & Yokouchi, K. (2017). Interdecadal decrease in potential fishing areas for Pacific saury off the southeastern coast of Hokkaido, Japan. *Fisheries Oceanography, 26*, 439–454.

Kuroda, H., & Yokouchi, K. (2017). Interdecadal decrease in potential fishing areas for Pacific saury off the southeastern coast of Hokkaido, Japan. *Fisheries Oceanography, 26*, 439−454.

Kurota, H., Szuwalski, C. S., & Ichinokawa, M. (2020). Drivers of recruitment dynamics in Japanese major fisheries resources: Effects of environmental conditions and spawner abundance. *Fisheries Research, 221*, 105353.

Lee, H.H., Maunder, M.N., Piner, K.R., et al. (2012). Can steepness of the stock–recruitment relationship be estimated in fishery stock assessment models? *Fisheries Research, 125-126*, 254–261.

Lee, H.-H., Piner, K. R., Methot Jr, R. D., & Maunder, M. N. (2014). Use of likelihood profiling over a global scaling parameter to structure the population dynamics model: An example using blue marlin in the Pacific Ocean. *Fisheries Research, 158*, 138–146.

Lindgren, F., Rue, H., & Lindström, J. (2011). An explicit link between Gaussian fields and Gaussian Markov random fields: the stochastic partial differential equation approach. *Journal of the Royal Statistical Society: Series B (Statistical Methodology), 73*, 423–498.

Liu, S., Liu, Y., Fu, C., Yan, L., Xu, Y., Wan, R., & Tian, Y. (2019). Using novel spawning ground indices to analyze the effects of climate change on Pacific saury abundance. *Journal of Marine Systems, 191*, 13−23.

doi:10.6342/NTU202500253

Mace, P. M., & Doonan, I. J. (1988). A generalised bioeconomic simulation model for fish population dynamics. *New Zealand Fisheries Assessment Research Document, 88/4*. Fisheries Research Centre, MAFFish, POB, 297.

Maechler, M., Rousseeuw, P., Struyf, A., Hubert, M., & Hornik, K. (2014). Cluster: Cluster Analysis Basics and Extensions R Package Version 1.15.2.

Mangel, M., Brodziak, J., & DiNardo, G. (2010). Reproductive ecology and scientific inference of steepness: a fundamental metric of population dynamics and strategic fisheries management. *Fish and Fisheries, 11*, 89–104.

Mangel, M., MacCall, A. D., Brodziak, J., Dick, E. J., Forrest, R. E., Pourzand, R., & Ralston, S. (2013). A perspective on steepness, reference points, and stock assessment. *Canadian Journal of Fisheries and Aquatic Sciences, 70*, 930–940.

Matsuda, H., Wada, T., Takeuchi, Y., & Matsumiya, Y. (1992). Model analysis of the effect of environmental fluctuation on the species replacement pattern of pelagic fishes under interspecific competition. *Research on Population Ecology, 34*, 309−319.

Maunder, M. N., & Punt, A. E. (2013). A review of integrated analysis in fisheries stock assessment. *Fisheries Research, 142*, 61–74.

Maunder, M. N., & Punt, A. E. (2004). Standardizing catch and effort data: a review of recent approaches. *Fisheries Research, 70*, 141–159.

Maunder, M. N., Sibert, J. R., Fonteneau, A., Hampton, J., Kleiber, P., & Harley, S. J. (2006). Interpreting catch per unit effort data to assess the status of individual stocks and communities. *ICES Journal of Marine Science, 63*, 1373–1385.

Maunder, M. N., Thorson, J. T., Xu, H., Oliveros-Ramos, R., Hoyle, S. D., Tremblay-Boyer, L., Lee, H. H., Kai, M., Chang, S.-K., Kitakado, T., Albertsen, C. M., Minte-Vera, C. V., Lennert-Cody, C. E., Aires-da-Silva, A. M., Piner, K. R. (2020). The need for spatiotemporal modeling to determine catch-per-unit effort based indices of abundance and associated composition data for inclusion in stock assessment models. *Fisheries Research, 229*, 105594.

McClatchie, S., Hendy, I. L., Thompson, A. R., & Watson, W. (2017). Collapse and recovery of forage fish populations prior to commercial exploitation. *Geophysical Research Letters, 44*, 1877–1885.

McCoy, M. W., & Gillooly, J. F. (2008). Predicting natural mortality rates of plants and animals. *Ecology Letters*.

McGowan, D. W., Branch, T. A., Haught, S., & Scheuerell, M. D. (2021). Multi-decadal shifts in the distribution and timing of Pacific herring (*Clupea pallasii*) spawning in

doi:10.6342/NTU202500253

Prince William Sound, Alaska. *Canadian Journal of Fisheries and Aquatic Sciences, 78*, 1611–1627.

McGurk, M. D. (1986). Natural mortality of marine pelagic fish eggs and larvae: the role of spatial patchiness. *Marine Ecology Progress Series, 34*, 227–242.

Methot Jr, R. D., & Wetzel, C. R. (2013). Stock synthesis: a biological and statistical framework for fish stock assessment and fishery management. *Fisheries Research, 142*, 86–99.

Miller, T. J., & Brooks, E. N. (2021). Steepness is a slippery slope. *Fish and Fisheries, 22*, 634–645.

Miyabe, N., & Takeuchi, Y. (2003). Standardized bluefin CPUE from the Japanese longline fishery in the Atlantic and Mediterranean Sea up to 1999. *Collective Volume of Scientific Papers, International Commission for the Conservation of Atlantic Tunas (ICCAT), 52*, 1130–1144.

Miyamoto, H., Suyama, S., Vijai, D., Kidokoro, H., Naya, M., Fuji, T., & Sakai, M. (2019). Predicting the timing of Pacific saury (*Cololabis saira*) immigration to Japanese fishing grounds: a new approach based on natural tags in otolith annual rings. *Fisheries Research, 209*, 167–177.

Miyamoto, H., Vijai, D., Kidokoro, H., Tadokoro, K., Watanabe, T., Fuji, T., & Suyama, S. (2020). Geographic variation in feeding of Pacific saury (*Cololabis saira*) in June and July in the North Pacific Ocean. *Fisheries Oceanography, 29(6)*, 558–571.

Moosa, N., & Butterworth, D. S. (2024). Investigating the influence of minor krill-predators on the krill-predator dynamics of the Antarctic ecosystem in the International Whaling Commission's Management Area II. *Canadian Journal of Fisheries and Aquatic Sciences, 81(8)*, 1066–1080.

Morgan, A. L., Thompson, K. D., Auchinachie, N. A., & Migaud, H. (2008). The effect of seasonality on normal haematological and innate immune parameters of rainbow trout *Oncorhynchus mykiss* L. *Fish and Shellfish Immunology, 25*, 791–799.

Myers, R. A., Bowen, K. G., & Barrowman, N. J. (1999). Maximum reproductive rate of fish at low population sizes. *Canadian Journal of Fisheries and Aquatic Sciences, 56*, 2404–2419.

Nakagawa, S., & Schielzeth, H. (2013). A general and simple method for obtaining R^2 from generalized linear mixed-effects models. *Methods in Ecology and Evolution, 4*, 133–142.

doi:10.6342/NTU202500253

Nakano, H. (1998). Stock status of Pacific swordfish, *Xiphias gladius*, inferred from CPUE of the Japanese longline fleet standardized using general linear models. *US National Marine Fisheries Service, NOAA Technical Report, 142*, 195–209.

Nakaya, M., Morioka, T., Fukunaga, K., Murakami, N., Ichikawa, T., Sekiya, S., & Suyama, S. (2010). Growth and maturation of Pacific saury *Cololabis saira* under laboratory conditions. *Fisheries Science, 76*, 45–53.

Nakaya, M., Morioka, T., Fukunaga, K., Murakami, N., Ichikawa, T., Sekiya, S., & Shimizu, A. (2011). Verification of growth-dependent survival in early life history of Pacific saury *Cololabis saira* using laboratory experiment. *Environmental Biology of Fishes, 92*, 113–123.

Nakayama, S.-I., Suyama, S., Fuji, T., Hashimoto, M., & Oshima, K. (2019). A trial calculation of natural mortality estimators for Pacific saury. *NPFC-2019-SSC PS05-WP18*.

NPFC (2019). Technical Working Group on Pacific Saury Stock Assessment 2019. 4th Meeting Report. *NPFC-2019-TWG PSSA04-Final Report*. 50 pp. (Available at www.npfc.int)

NPFC (2023a). Compiled data on Pacific saury catches in the Northwestern Pacific Ocean. *NPFC-2023-SSC PS11-WP01(Rev 1)*.

NPFC (2023b). Small Scientific Committee on Pacific Saury. (2023). 12th Meeting Report. *NPFC-2023-SSC PS12-Final Report*. 61 pp. (Available at www.npfc.int)

NPFC (2024a). Conservation and Management Measure for Pacific Saury. *CMM 2024-08*. (Available at www.npfc.int)

NPFC (2024b). Report of the 5th Meeting of the Joint SC-TCC-COM Small Working Group on Management Strategy Evaluation for Pacific Saury (SWG MSE PS). *NPFC-2024-SWG MSE PS05-Final Report*. 18-20 January 2024. Niigata, Japan.

Ono, K., Punt, A. E., & Hilborn, R. (2015). Think outside the grids: An objective approach to define spatial strata for catch and effort analysis. *Fisheries Research, 170*, 89–101.

Oozeki, Y., Watanabe, Y., & Kitagawa, D. (2004). Environmental factors affecting larval growth of Pacific saury, *Cololabis saira*, in the northwestern Pacific Ocean. *Fisheries Oceanography, 13*, 44–53.

Ortiz, M., & Arocha, F. (2004). Alternative error distribution models for standardization of catch rates of non-target species from a pelagic longline fishery: Billfish species in the Venezuelan tuna longline fishery. *Fisheries Research, 70*, 275–294.

doi:10.6342/NTU202500253

Patterson, K., Cook, R., Darby, C., Gavaris, S., Kell, L., Lewy, P., et al. (2001). Estimating uncertainty in fish stock assessment and forecasting. *Fish and Fisheries, 2(2)*, 125–157.

Pella, J. J., & Tomlinson, P. K. (1969). A generalized stock production model. *Inter-American Tropical Tuna Commission Bulletin, 13*, 416–497.

Pérez-Rodríguez, A., Umar, I., Goto, D., Howell, D., Mosqueira, I., & González-Troncoso, D. (2022). Evaluation of harvest control rules for a group of interacting commercial stocks using a multispecies Management Strategy Evaluation (MSE) framework. *Canadian Journal of Fisheries and Aquatic Sciences, 79*, 1–19.

Perretti, C.T., & Thorson, J.T. (2019). Spatiotemporal dynamics of summer flounder (*Paralichthys dentatus*) on the Northeast US shelf. *Fisheries Research, 215*, 62–68.

Pikitch, E., Boersma, P. D., Boyd, I., Conover, D., Cury, P., Essington, T., et al. (2018). The strong connection between forage fish and their predators: A response to Hilborn et al. (2017). *Fisheries Research*, 198, 220–223.

Pikitch, E.K., Rountos, K.J., Essington, T.E., Santora, C., Pauly, D., Watson, R., et al. (2014). The global contribution of forage fish to marine fisheries and ecosystems. *Fish and Fisheries*, 15, 43–64.

Piner, K. R., Lee, H. H., Maunder, M. N., & Methot, R. D. (2011). A simulation-based method to determine model misspecification: Examples using natural mortality and population dynamics models. *Marine and Coastal Fisheries*, 3, 336–343.

Pinheiro, J. C., & Bates, D. M. (2000). Linear mixed-effects models: Basic concepts and examples. In *Mixed-effects models in S and S-Plus* (pp. 3–56).

Punt, A. E. (2019). Spatial stock assessment methods: A viewpoint on current issues and assumptions. *Fisheries Research*, 213, 132–143.

Punt, A. E., A'mar, T., Bond, N. A., Butterworth, D. S., de Moor, C. L., De Oliveira, J. A., & Szuwalski, C. (2014). Fisheries management under climate and environmental uncertainty: Control rules and performance simulation. *ICES Journal of Marine Science*, 71, 2208–2220.

Punt, A. E., & Hilborn, R. A. Y. (1997). Fisheries stock assessment and decision analysis: The Bayesian approach. *Reviews in Fish Biology and Fisheries*, 7, 35–63.

Punt, A. E., Butterworth, D. S., de Moor, C. L., De Oliveira, J. A., & Haddon, M. (2016). Management strategy evaluation: Best practices. *Fish and Fisheries*, 17, 303–334.

Punt, A. E., Dalton, M. G., Adams, G. D., Barbeaux, S. J., Cheng, W., Hermann, A. J., ... & Rovellini, A. (2024). Capturing uncertainty when modelling environmental drivers

doi:10.6342/NTU202500253

of fish populations, with an illustrative application to Pacific Cod in the eastern Bering Sea. *Fisheries Research*, 272, 106951.

Punt, A. E., Walker, T. I., Taylor, B. L., & Pribac, F. (2000). Standardization of catch and effort data in a spatially-structured shark fishery. *Fisheries Research*, 45, 129–145.

Quinn II, T. J., Hoag, S. H., & Southward, G. M. (1982). Comparison of two methods of combining catch-per-unit-effort data from geographic regions. *Canadian Journal of Fisheries and Aquatic Sciences*, 39, 837–846.

R Core Team. (2021). R: A language and environment for statistical computing [online]. R Foundation for Statistical Computing, Vienna, Austria. Available from http://www.R-project.org/.

Rademeyer, R. A., Plagányi, É. E., & Butterworth, D. S. (2007). Tips and tricks in designing management procedures. *ICES Journal of Marine Science*, 64(4), 618–625.

Ricard, D., Minto, C., Jensen, O.P., et al. (2012). Examining the knowledge base and status of commercially exploited marine species with the RAM Legacy Stock Assessment Database. *Fish and Fisheries*, 13, 380–398.

Ricker, W. E. (1975). Computation and interpretation of biological statistics of fish populations. *Bulletin of the Fisheries Research Board of Canada*, Bulletin 191, Ottawa.

Rose, G. A., & Kulka, D.W. (1999). Hyperaggregation of fish and fisheries: How catch-per-unit-effort increased as the northern cod (*Gadus morhua*) declined. *Canadian Journal of Fisheries and Aquatic Sciences*, 56, 118–127.

Rose, G. A., & Leggett, W.C. (1991). Effects of biomass range interactions on catchability of migratory demersal fish by mobile fisheries—An example of Atlantic cod (*Gadus morhua*). *Canadian Journal of Fisheries and Aquatic Sciences*, 48, 843–848.

Safina, C., Rosenberg, A. A., Myers, R. A., Quinn II, T. J., & Collie, J. S. (2005). US ocean fish recovery: Staying the course. *Science*, 309, 707–708.

Saitoh, S.I., Kosaka, S., & Iisaka, J. (1986). Satellite infrared observations of Kuroshio warm-core rings and their application to study of Pacific saury migration. *Deep-Sea Research Part I: Oceanographic Research Papers*, 33, 1601–1615.

Salvatteci, R., Field, D., Gutierrez, D., Baumgartner, T., Ferreira, V., Ortlieb, L., et al. (2018). Multifarious anchovy and sardine regimes in the Humboldt Current System during the last 150 years. *Global Change Biology*, 24, 1055–1068.

Savage, V.M., Gillooly, J.F., Brown, J.H., West, G.B., & Charnov, E.L. (2004). Effects of body size and temperature on population growth. *American Naturalist*, 163, 429–441.

doi:10.6342/NTU202500253

Schiano, S., Nesslage, G. M., Drew, K., Schueller, A. M., Woodland, R. J., & Wilberg, M. J. (2023). Evaluation of alternative harvest policies for striped bass and their prey, Atlantic menhaden. *Canadian Journal of Fisheries and Aquatic Sciences*.

Sculley, M. L., & Brodziak, J. (2020). Quantifying the distribution of swordfish (*Xiphias gladius*) density in the Hawaii-based longline fishery. *Fisheries Research*, 230, 105638.

Shelton, A. O., Thorson, J. T., Ward, E. J., & Feist, B. E. (2014). Spatial semiparametric models improve estimates of species abundance and distribution. *Canadian Journal of Fisheries and Aquatic Sciences*, 71, 1655–1666.

Shono, H. (2014). Application of support vector regression to CPUE analysis for southern bluefin tuna (*Thunnus maccoyii*), and its comparison with conventional methods. *Fisheries Science*, 80, 879–886.

Sibert, J., & Hampton, J. (2003). Mobility of tropical tunas and the implications for fisheries management. *Marine Policy*, 27, 87–95.

Siple, M. C., Essington, T. E., & Plagányi, É. (2019). Forage fish fisheries management requires a tailored approach to balance trade-offs. *Fish and Fisheries*, 20, 110–124.

Siple, M. C., Koehn, L. E., Johnson, K. F., Punt, A. E., Canales, T. M., Carpi, P., ... & Zimmermann, F. (2021). Considerations for management strategy evaluation for small pelagic fishes. *Fish and Fisheries*, 22, 1167–1186.

Song, H. (2023). Standardized CPUE of Pacific saury (*Cololabis saira*) caught by the Korean's stick-held dip net fishery up to 2022. *NPFC-2023-SSC PS11-WP05(Rev 1)*.

Stow, C. A., Jolliff, J., McGillicuddy, D. J., Doney, S. C., Allen, J. I., Friedrichs, M. A., Rose, K. A., & Wallhead, P. (2009). Skill assessment for coupled biological/physical models of marine systems. *Journal of Marine Systems*, 76, 4–15.

Subbey, S., Devine, J. A., Schaarschmidt, U., & Nash, R. D. (2014). Modelling and forecasting stock-recruitment: Current and future perspectives. *ICES Journal of Marine Science*, 71, 2307–2322.

Suyama, S. (2002). Study on the age, growth, and maturation process of Pacific saury (*Cololabis saira*) in the North Pacific. *Bulletin of the Fish Research Agency*, 5, 68–113 (Japanese with English abstract).

Suyama, S., Morioka, T., Nakaya, M., Nakagami, M., & Ueno, Y. (2006). The study of the maturation process of the Pacific saury, *Cololabis saira*: The role of the rearing experiments. *Bulletin of the Fish Research Agency*, 4, 173–180.

doi:10.6342/NTU202500253

Suyama, S., Nakagami, M., Naya, M., & Ueno, Y. (2012). Comparison of the growth of age-1 Pacific saury (*Cololabis saira*) in the Western and the Central North Pacific. *Fisheries Science*, 78, 277–285.

Suyama, S., Nakagami, M., Naya, M., Kato, Y., Shibata, Y., & Sakai, M. (2015). Stock assessment and evaluation for the western Pacific stock of Pacific saury fiscal year 2015. In *Marine fisheries stock assessment and evaluation for Japanese waters (fiscal year 2015)* (pp. 283–336). Fisheries Agency and Fisheries Research Agency of Japan.

Suyama, S., Kurita, Y., & Ueno, Y. (2006). Age structure of Pacific saury (*Cololabis saira*) based on observations of the hyaline zones in the otolith and length frequency distributions. *Fisheries Science*, 72, 742–749.

Swain, D. P., & Sinclair, A. F. (1994). Fish distribution and catchability: What is the appropriate measure of distribution? *Canadian Journal of Fisheries and Aquatic Sciences*, 51, 1046–1054.

Szuwalski, C. S., & Hollowed, A. B. (2016). Climate change and non-stationary population processes in fisheries management. *ICES Journal of Marine Science*, 73, 1297–1305.

Szuwalski, C. S., Britten, G. L., Licandeo, R., Amoroso, R. O., Hilborn, R., & Walters, C. (2019). Global forage fish recruitment dynamics: A comparison of methods, time-variation, and reverse causality. *Fisheries Research*, 214, 56–64.

Szuwalski, C. S., Hollowed, A. B. (2016). Climate change and non-stationary population processes in fisheries management. *ICES Journal of Marine Science*, 73, 1297–1305.

Szuwalski, C. S., & Hilborn, R. (2015). Environment drives forage fish productivity. *Proceedings of the National Academy of Sciences*, 112, E3314–E3315.

Tadokoro, K., Chiba, S., Ono, T., Midorikawa, T., & Saino, T. (2005). Interannual variation in *Neocalanus* biomass in the Oyashio waters of the western North Pacific. *Fisheries Oceanography*, 14, 210–222.

Takasuka, A., Kuroda, H., Okunishi, T., Shimizu, Y., Hirota, Y., Kubota, H., Sakaji, R., Kimura, R., Ito, S. I., & Oozeki, Y. (2014). Occurrence and density of Pacific saury (*Cololabis saira*) larvae and juveniles in relation to environmental factors during the winter spawning season in the Kuroshio Current system. *Fisheries Oceanography*, 23(4), 304–321.

Takasuka, A., Nishikawa, K., Kuroda, H., Okunishi, T., Shimizu, Y., Sakaji, H., & Oozeki, Y. (2016). Growth variability of Pacific saury (*Cololabis saira*) larvae under contrasting environments across the Kuroshio axis: Survival potential of minority versus majority. *Fisheries Oceanography*, 25(4), 390–406.

doi:10.6342/NTU202500253

Takasuka, A., Oozeki, Y., Kubota, H., & Lluch-Cota, S. E. (2008). Contrasting spawning temperature optima: Why are anchovy and sardine regime shifts synchronous across the North Pacific? *Progress in Oceanography*, 77, 225–232.

Thorson, J. T., Ward, E. J. (2013). Accounting for space–time interactions in index standardization models. *Fisheries Research*, 147, 426–433.

Thorson, J. T., Shelton, A. O., Ward, E. J., & Skaug, H. J. (2015). Geostatistical delta-generalized linear mixed models improve precision for estimated abundance indices for West Coast groundfishes. *ICES Journal of Marine Science*, 72, 1297–1310.

Thorson, J. T., Barnett, L. A. (2017). Comparing estimates of abundance trends and distribution shifts using single- and multispecies models of fishes and biogenic habitat. *ICES Journal of Marine Science*, 74, 1311–1321.

Thorson, J. T., Fonner, R., Haltuch, M. A., Ono, K., & Winker, H. (2017). Accounting for spatiotemporal variation and fisher targeting when estimating abundance from multispecies fishery data. *Canadian Journal of Fisheries and Aquatic Sciences*, 74(11), 1794–1807.

Thorson, J. T., Ianelli, J. N., Kotwicki, S. (2017). The relative influence of temperature and size-structure on fish distribution shifts: A case-study on Walleye pollock in the Bering Sea. *Fisheries Fisheries*, 18, 1073–1084.

Thorson, J. T. (2019). Guidance for decisions using the Vector Autoregressive Spatio-Temporal (VAST) package in stock, ecosystem, habitat, and climate assessments. *Fisheries Research*, 210, 143–161.

Thorson, J. T. (2020). Predicting recruitment density dependence and intrinsic growth rate for all fishes worldwide using a data-integrated life-history model. *Fish and Fisheries*, 21, 237–251.

Tian, Y., Akamine, T., & Suda, M. (2003). Variations in the abundance of Pacific saury (*Cololabis saira*) from the northwestern Pacific in relation to oceanic-climate changes. *Fisheries Research*, 60, 439–454.

Tian, Y., Ueno, Y., Suda, M., & Akamine, T. (2004). Decadal variability in the abundance of Pacific saury and its response to climatic/oceanic regime shifts in the northwestern subtropical Pacific during the last half century. *Journal of Marine Systems*, 52, 235–257.

Tseng, C. T., Sun, C. L., Yeh, S. Z., Chen, S. C., Su, W. C., & Liu, D. C. (2011). Influence of climate-driven sea surface temperature increase on potential habitats of the Pacific saury (*Cololabis saira*). *ICES Journal of Marine Science*, 68, 1105–1113.

doi:10.6342/NTU202500253

Tseng, C. T., Su, N. J., Sun, C. L., Punt, A. E., Yeh, S. Z., Liu, D. C., & Su, W. C. (2013). Spatial and temporal variability of the Pacific saury (*Cololabis saira*) distribution in the northwestern Pacific Ocean. *ICES Journal of Marine Science*, 70, 991–999.

Tseng, C. T., Sun, C. L., Belkin, I. M., Yeh, S. Z., Kuo, C. L., & Liu, D. C. (2014). Sea surface temperature fronts affect distribution of Pacific saury (*Cololabis saira*) in the Northwestern Pacific Ocean. *Deep-Sea Research Part II: Topical Studies in Oceanography*, 107, 15–21.

Watanabe, Y., & Lo, N. C. (1989). Larval production and mortality of Pacific saury, *Cololabis saira*, in the Northwestern Pacific Ocean. *Collected Reprints*, 2(3), 555.

Watanabe, Y. (1991). Possible density-dependent dynamics of larval and juvenile saury population in the northwestern Pacific Ocean. *Report of Fish Research Investigation*, Japan Government, 27, 79–89 (in Japanese).

Watanabe, Y., Kurita, Y., Noto, M., Oozeki, Y., & Kitagawa, D. (2003). Growth and survival of Pacific saury (*Cololabis saira*) in the Kuroshio-Oyashio transitional waters. *Journal of Oceanography*, 59, 403–414.

Wilberg, M. J., Thorson, J. T., Linton, B. C., & Berkson, J. (2010). Incorporating time-varying catchability into population dynamic stock assessment models. *Reviews in Fish Biology and Fisheries*, 18, 7–24.

Wiff, R., Flores, A., Neira, S., & Caneco, B. (2018). Estimating steepness of the stock-recruitment relationship in Chilean fish stocks using meta-analysis. *Fisheries Research*, 200, 61–67.

Wildermuth, R. P., Tommasi, D., Kuriyama, P., Smith, J., & Kaplan, I. (2023). Evaluating robustness of harvest control rules to climate-driven variability in Pacific sardine recruitment. *Canadian Journal of Fisheries and Aquatic Sciences*.

Winker, H., Kerwath, S. E., & Attwood, C. G. (2013). Comparison of two approaches to standardize catch-per-unit-effort for targeting behaviour in a multispecies hand-line fishery. *Fisheries Research*, 139, 118–131.

Xu, H., Lennert-Cody, C. E., Maunder, M. N., & Minte-Vera, C. V. (2019). Spatiotemporal dynamics of the dolphin-associated purse-seine fishery for yellowfin tuna (*Thunnus albacares*) in the eastern Pacific Ocean. *Fisheries Research*, 213, 121–131.

Yamamoto, M., & Katayama, S. (2012). Interspecific comparisons of feeding habits between Japanese anchovy (*Engraulis japonicus*) and Japanese sardine (*Sardinops melanostictus*) in eastern Hiuchi-nada, central Seto Inland Sea, Japan, in 1995. *Bulletin of the Japanese Society of Fisheries Oceanography*.

doi:10.6342/NTU202500253

Yasuda, I., & Watanabe, Y. (1994). On the relationship between the Oyashio front and saury fishing grounds in the north-western Pacific: A forecasting method for fishing ground locations. *Fisheries Oceanography*, 3, 172–181.

Yatsu, A. (2019). Review of population dynamics and management of small pelagic fishes around the Japanese Archipelago. *Fisheries Science*, 85, 611–639.

Zhou, S., Campbell, R. A., & Hoyle, S. D. (2019). Catch per unit effort standardization using spatio-temporal models for Australia's Eastern Tuna and Billfish Fishery. *ICES Journal of Marine Science*, 76, 1489–1504.

doi:10.6342/NTU202500253

Tables

Table 1.1. Mean values of the life history parameters used to calculate distributions of stock-recruitment steepness for the Pacific saury in the Northwestern Pacific Ocean.

Code of population model (PM)	Description	Model	Parameters	Symbol	Value	Unit	Reference
PM01	Growth^{Lc}	$L_t = L_{\inf} \exp(-\exp(-K(Age - t_0)))$	Asymptotic length Growth coefficient Time at inflection	$L_{\inf}$ K t_0	30.58 0.01196 112.1	cm day^{-1} day	Suyama et al. (2015)
PM02	Weight-length relationship^{Lc}	$W_t = aL_t^b$	Scale parameter Exponent parameter	a b	2.2×10^{-3} 3.23	- -	Suyama et al. (2015)
PM03	Reproductive ecology parameters^{L}	$P = 1/1 + \exp(r(L_t - L_{50}))$	Female length at 50% maturity Shape parameter Average time between spawning events Batch fecundity Number of spawning seasons	L_{50} r T_B E_G SL	25.8 -0.66 4 300 5	cm - day eggs/g months	Kosaka (2000) Suyama et al. (2006) Suyama et al. (2009)
PM04	Annual natural mortality^{G}	$M(0,1) = 1.73L_{0,1}^{-1.61}L_{\inf}^{1.44}K_{vb}$	Length at the end of the early-life phase (120 days) (L_0) = 12 cm KnL; and the length at age-1 (485 days) (L_1) = 26.77 cm KnL was derived from the growth model. K_{vb} is the Brody growth coefficient of the von Bertalanffy growth model (Nakayama *et al.*, 2019. K_{vb} = 1.55 year^{-1}	M_0 M_1	6.82 1.88	year^{-1} year^{-1}	Gislason et al. (2010) Nakayama et al. (2019)
PM05	Early-life stage and early-life mortality parameters^{L}	$M_{EL}(d) = M_{ELa}dw_{ELS}(d)^{M_{ELb}}$ $M_J(d) = M_{Ja}dw_{ELS}(d)^{M_{Jb}}$	The daily mortality rates for the egg and larval stage (M_{EL}) and the juvenile stage (M_J) are based on the dry weight, whether it is below or above the critical weight. dw_{ELS} is the dry weight of fish during the early-life phase. $dw_{ELS} = 0.2W_{ELS}$	M_{EJa} M_{EJb} M_{Ja} M_{Jb}	2.2×10^{-4} -0.85 5.26×10^{-3} -0.25	-	McGurk (1986)

**Lc* indicates that correlation among the parameters is accounted for. *L* and *G* represent the parameters modeled using respectively the lognormal and gamma distributions.

doi:10.6342/NTU202500253

Table 1.2. Amount by which the mean values for main life history parameters are multiplied by and their coefficient of variation (CV) for the five scenarios for the Pacific saury in the Northwestern Pacific Ocean.

Main life history parameters	Scenario 1: Prevailing environmental condition (CV=0.2)	Scenario 2: Normal variation in a favorable environmental condition (CV=0.2)	Scenario 3: High variation in a favorable environmental condition (CV=0.4)	Scenario 4: Normal variation in an unfavorable environmental condition (CV=0.2)	Scenario 5: High variation in unfavorable environmental conditions (CV=0.4)	References
Growth ($L_{inf,}$ K, t_0)	1	1.05	1.05	0.95	0.95	Kosaka (2000); Kurita et al. (2004); Suyama et al. (2006);
Length-weight relationship (a, b)	1	1.05	1.05	0.95	0.95	Kakehi et al. (2021)
Maturity (L_{50}, r)	1	0.95	0.95	1.05	1.05	Kosaka (2000); Kurita (2006); Fuji et al. (2021)
Survival of early-life stage (M_{EJa}, M_{EJb}, M_{Ja}, M_{Jb})	1	0.95	0.95	1.05	1.05	Oozeki and Watanabe (2000); Watanabe et al. (2003); Oozeki et al. (2009)
Annual natural mortality (M_0, M_1)	1	0.95	0.95	1.05	1.05	Zwolinski and Demer (2013)

doi:10.6342/NTU202500253

Table 2.1. Summary statistics of Ad hoc, Binary, Spatial 1, Spatial 0.1 GLMMs, and VAST fitted to Pacific saury CPUE data from Northwestern Pacific Ocean during 1997 – 2019. The conditional R^2 denotes the conditional explained residuals, the ΔAIC is the difference between the conditional AIC and that of the best model. The mean conditional R^2 is the explained value of the training data, and the rho value (ρ) is the Pearson's correlation coefficient of the training and testing data sets from the five-fold cross-validations by repeated 10 times. The CV represents the coefficients of variation for the conditional R^2 and ρ from the five-fold cross-validations, respectively.

Model	Goodness-of-fit			Cross-validations			
	conditional R^2	conditional AIC	Δ AIC	mean conditional R^2	CV	mean ρ	CV
Ad hoc	0.27	534365	14063	0.25	0.023	0.43	0.014
Binary	0.34	529145	8843	0.32	0.018	0.48	0.016
Spatial 1	0.37	525713	5411	0.36	0.011	0.52	0.014
Spatial 0.1	0.39	524864	4562	0.39	0.015	0.53	0.017
VAST	0.68	520302	0	0.65	0.005	0.54	0.008

doi:10.6342/NTU202500253

Table 2.2. Summary of the explanatory power (in conditional R^2) and overall influence (from zero to one) for each variable considered in the Ad hoc, Binary, Spatial 1, Spatial 0.1 GLMMs, and VAST by using the Pacific saury data in Northwestern Pacific Ocean during 1997 – 2019.

Model	Variable	Conditional R^2	Overall influence
Ad hoc	*Year*	0.052	-
	SST+*SST*^{2}	0.028	0.017
	Vessel	0.087	0.169
	Area	0.042	0.152
	Year×*Area*	0.065	0.259
Binary	*Year*	0.047	-
	SST+*SST*^{2}	0.045	0.017
	Vessel	0.104	0.170
	Area	0.082	0.135
	Year×*Area*	0.064	0.301
Spatial1	*Year*	0.045	-
	SST+*SST*^{2}	0.021	0.017
	Vessel	0.098	0.169
	Area	0.121	0.122
	Year×*Area*	0.087	0.221
Spatial0.1	*Year*	0.040	-
	SST+*SST*^{2}	0.017	0.017
	Vessel	0.094	0.170
	Area	0.154	0.140
	Year×*Area*	0.087	0.225
VAST	*Year*	0.040	-
	SST+*SST*^{2}	0.032	0.017
	Vessel	0.091	0.169
	Spatial	0.230	0.128
	Spatio-temporal	0.288	0.252

doi:10.6342/NTU202500253

Table 3.1. Mechanisms and quantitative tests of each hypothesized driver that may affect the distribution of Pacific saury in the Northwestern Pacific Ocean.

Hypothesized drivers	Description of mechanism	Quantitative test for the hypothesis
Single local or regional environmental variable	Variation in a single regional (e.g., SST) or regional environmental variable drives interannual changes in distribution	1. Fixing the intercepts at their average values across years: $\bar{\beta}=n_t^{-1}\sum_{t=1}^{n_t}\beta(t)$; 2. Retaining the residual spatial variation: $\omega(s)$; 3. Fixing the residual spatio-temporal variation at zero: $\varepsilon(s,t)=0$; 4. Retaining the coefficient of a single local (e.g., SST) or regional environmental variable and fixing the impact of subset local/regional environmental variable at zero.
Multiple local and regional environmental variables	Variation in all local and regional environmental variables drives interannual changes in distribution	1. Fixing the intercepts at their average values across years: $\bar{\beta}=n_t^{-1}\sum_{t=1}^{n_t}\beta(t)$; 2. Retaining the residual spatial variation: $\omega(s)$; 3. Fixing the residual spatio-temporal variation at zero: $\varepsilon(s,t)=0$; 4. Retaining the coefficients of all local and regional environmental variables.
Unmodelled variable	Otherwise unmodelled processes (e.g., the shift in the spatial distribution of predators or food availability) drive interannual changes in distribution	1. Fixing the intercepts at their average values across years: $\bar{\beta}=n_t^{-1}\sum_{t=1}^{n_t}\beta(t)$; 2. Retaining the residual spatial variation: $\omega(s)$; 3. Retaining the residual spatio-temporal variation; 4. Fixing the coefficients of all local and regional environmental variables at zero: $\sum_{i=1}^{n=5}\gamma_i(s,t)=0$.

doi:10.6342/NTU202500253

Table 4.1. Descriptions of fisheries catch, abundance indices, and length composition data included in the model for the Pacific saury stock assessment in the Northwestern Pacific Ocean (WNPO) including reference code, members, description, unit, time-period, and data sources.

Fleet No	**Reference code**	**Members**	**Catch unit**	**Source**
F1	F1_JPN_late	Japan	B	NPFC (2023a)
F2	F2_TWN	Taiwan	B	NPFC (2023a)
F3	F3_KOR	Korea	B	NPFC (2023a)
F4	F4_RUS	Russia	B	NPFC (2023a)
F5	F5_CHN	China	B	NPFC (2023a)
F6	F6_VAN	Vanuatu	B	NPFC (2023a)
F7	F7_JPN_early	Japan	B	NPFC (2023a)
Abundance No	**Reference code**	**Description**	**Time-series**	**Source**
S1	S1_JPN_early	Japanese early fishery	1980 – 1993	Kazuhiro et al. (2018)
S2	S2_JPN_late	Japan late fishery	1994 – 2022	Hashimoto et al. (2023a)
S3	S3_TWN	Taiwan	2001 – 2022	Huang et al. (2023)
S4	S4_KOR	Korea	2001 – 2022	Song. (2023)
S5	S5_RUS	Russia	1994 – 2022	Kulik et al. (2023)
S6	S6_CHN	China	2013 – 2022	Hua et al. (2023)
S7	S7_JPN_bio	Japanese scientific survey	2007 – 2022	Hashimoto et al. (2023b)
Length composition data No	**Reference code**	**Members**	**Time series**	**Source**
F1	F1_JPN	Japan	1994 – 2022	NPFC (2023a)
F2	F2_TWN	Taiwan	2007 – 2022	NPFC (2023a)

doi:10.6342/NTU202500253

Table 4.2. Key life history and recruitment parameters used for the Pacific saury assessment model in the Northwestern Pacific Ocean.

Parameter	Value	Comments	Reference
Reference age (a1)	0	Fixed parameter	Suyama et al. (2015)
Maximum age (a2)	2	Fixed parameter	Suyama et al. (2015)
Length at a1 (L1)	0.66	Fixed parameter	Refit Suyama et al. (2015)
Length at a1 (L2)	31.45	Fixed parameter	Refit Suyama et al. (2015)
Growth rate (*K*)	2.02	Fixed parameter	Refit Suyama et al. (2015)
CV of L1	0.20	Fixed parameter	
CV of L2	0.20	Fixed parameter	
Wtlen_1_Fem	2.44e-06	Fixed parameter	Fuji et al. (2019)
Wtlen_2_Fem	3.34694	Fixed parameter	Fuji et al. (2019)
Size-at-50% Maturity	28.7	Fixed parameter	Suyama (2006)
Slope of maturity ogive	-0.80	Fixed parameter	Suyama (2006)
Natural mortality (*M*)	2.18	Fixed parameter	Nakayama et al. (2019)
Fecundity	Proportional to spawning biomass	Fixed parameter	Fuji et al. (2019)
Spawning season	February	Model structure	Fuji et al. (2020)
Spawner-recruit relationship	Beverton-Holt	Model structure	
R_0	-	Estimated	
Steepness (*h*)	0.82	Fixed parameter	Hsu et al. (2024)
Recruitment variability (σ_R)	0.6	Fixed parameter	

doi:10.6342/NTU202500253

Table 4.3. Fishery-specific selectivity assumptions for the Pacific saury stock assessment in in the Northwestern Pacific Ocean. The selectivity curves for fleets lacking length composition data were assumed to be the same as (i.e., mirror) closely related fisheries or fisheries operating in the same area.

Fleet	Selectivity function
F1_JPN	Double normal
F2_TWN	Double normal
F3_KOR	Mirror F2
F4_RUS	Mirror F1
F5_CHN	Mirror F1
F6_VAN	Mirror F2
S1_JPN_early	Mirror F1
S2_JPN_late	Mirror F1
S3_TWN	Mirror F2
S4_KOR	Mirror F2
S5_RUS	Mirror F1
S6_CHN	Mirror F2
S7_JPN_bio	Mirror F1

doi:10.6342/NTU202500253

Table 4.4. Estimated reference points derived from the Stock Synthesis model for Pacific saury in the Northwestern Pacific Ocean, where F is the instantaneous annual fishing mortality rate, SSB is spawning stock biomass, and $SSB_{F=0}$ indicates the average 5-year SSB_0 estimate, and MSY is the maximum sustainable yield reference point.

	Estimate	SD
$SSB_{F=0}$	284868	32104.4
SSB_{MSY}	42611.80	4798.96
SSB_{2022}	25809.90	4299.01
$SSB_{2020\text{-}2022}$	31655.40	4677.77
MSY	540217.00	61258.70
F_{MSY}	2.61	0.04
F_{2022}	1.42	0.22

doi:10.6342/NTU202500253

Table 4.5. Projected results of Pacific saury spawning stock biomass (SSB, mt) and catch (mt) in 2023 – 2027 under deterministic projection.

SSB			
Year	$0.5F_{MSY}$	$0.75F_{MSY}$	F_{MSY}
2023	53157.95	70998.39	52591.4
2024	80318.76	69807.83	51709.5
2025	95182.12	70176.24	51982.4
2026	102037.8	70093.62	51921.2
2027	104405.1	70124	51943.7

Catch			
Year	$0.5F_{MSY}$	$0.75F_{MSY}$	F_{MSY}
2023	48747.05	60933.81	88631
2024	135971	169963.8	247220
2025	173369.4	216711.7	315217
2026	221160.5	276450.6	402110
2027	222264.9	277831.1	404118

doi:10.6342/NTU202500253

Table 4.6. Projected results of Pacific saury spawning stock biomass (SSB, mt) and catch (mt) in 2023 – 2027 under stochastic projection.

	Prob ($SSB>SSB_{MSY}$)		
Year	$0.5F_{MSY}$	$0.75F_{MSY}$	F_{MSY}
2023	100	84.9	54.9
2024	100	85.8	75.8
2025	100	83.7	57.6
2026	100	77.7	50.5
2027	100	75.5	53.5

	$Catch_{2023-2027}$		
	$0.5F_{MSY}$	$0.75F_{MSY}$	F_{MSY}
Median	321453	608786	616513
SD	80813	162236	157870
10th percentile	110230	514423	420604
90th percentile	741252	929473	834757

doi:10.6342/NTU202500253

Figures

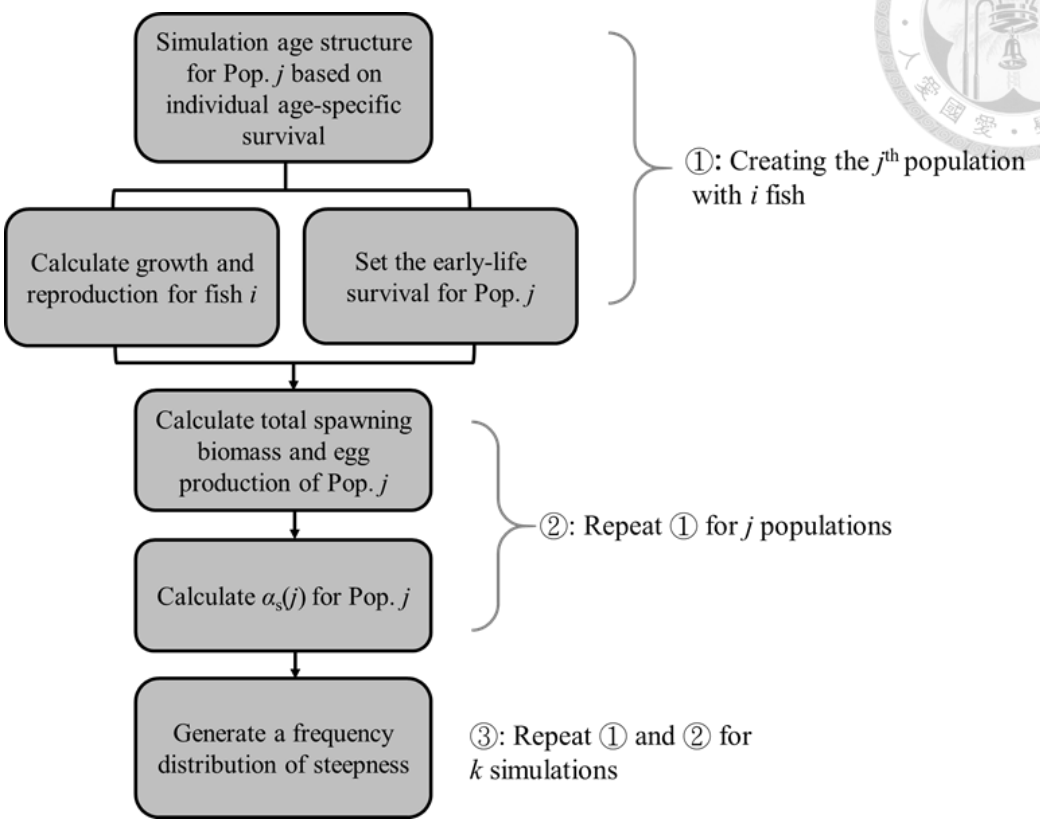

Figure 1.1. General design of the simulation study. Pop. *j* represents the *j* population.

doi:10.6342/NTU202500253

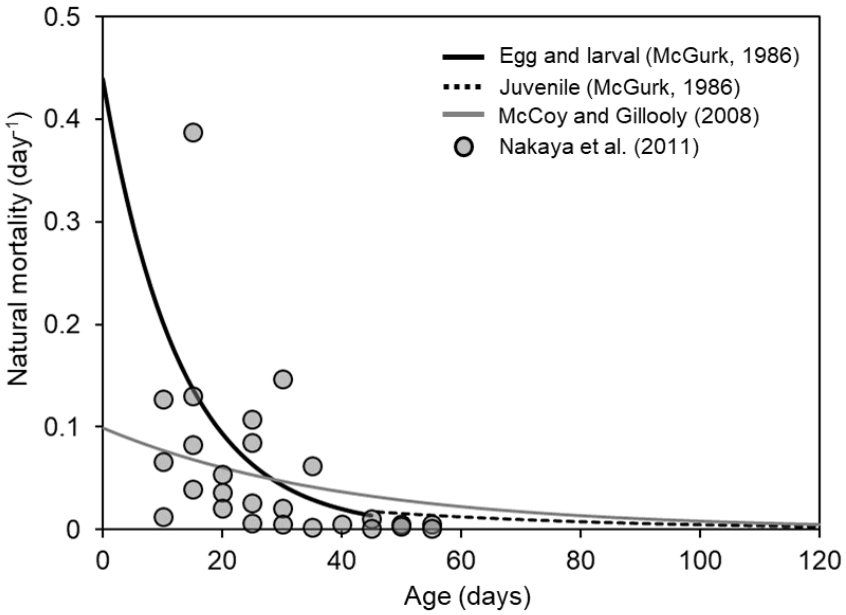

Figure 1.2. The daily natural mortality of fish in the early-life phase derived by McGurk (1986) (egg and larval stages: solid lines; juvenile: dashed lines), and McCoy and Gillooly (2008) (grey solid line). The grey circles represent the daily natural mortality for the Pacific saury from the rearing experiment from Nakaya et al. (2011).

doi:10.6342/NTU202500253

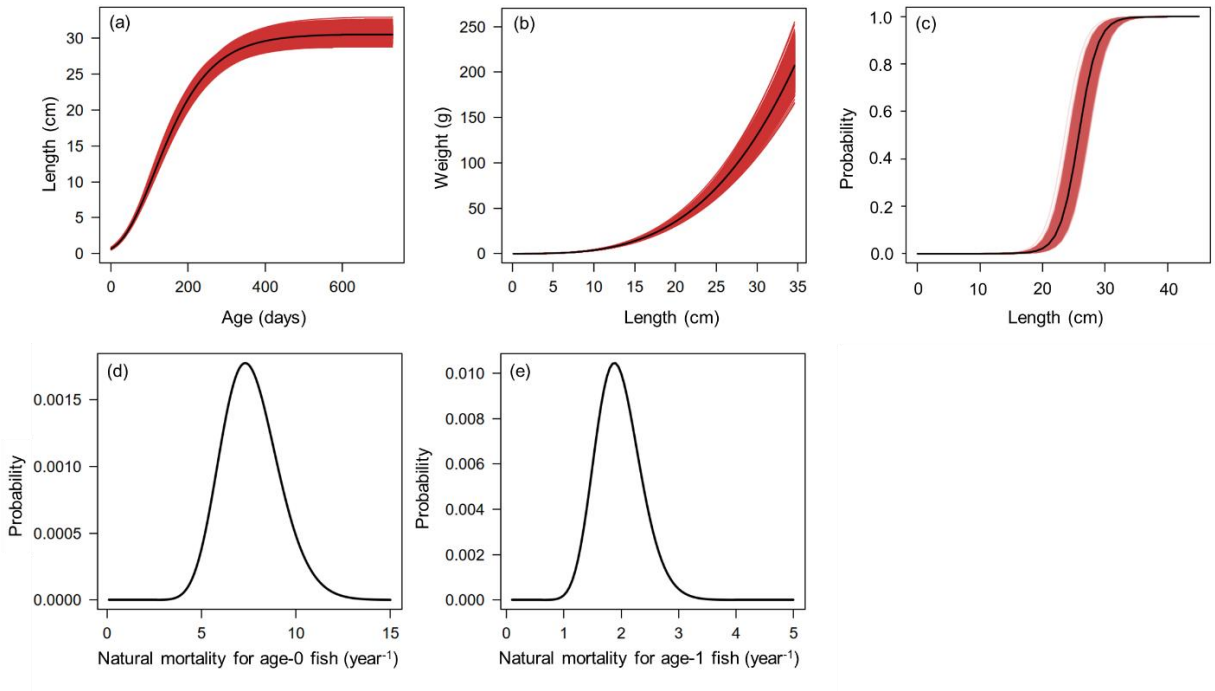

Figure 1.3. The biological information for the (a) growth (b) weight-at-length and (c) maturity and the annual natural mortality of the (d) age-0 and (e) age-1 fish, respectively are used to derive the distribution of steepness for the Pacific saury in the Northwest Pacific Ocean.

doi:10.6342/NTU202500253

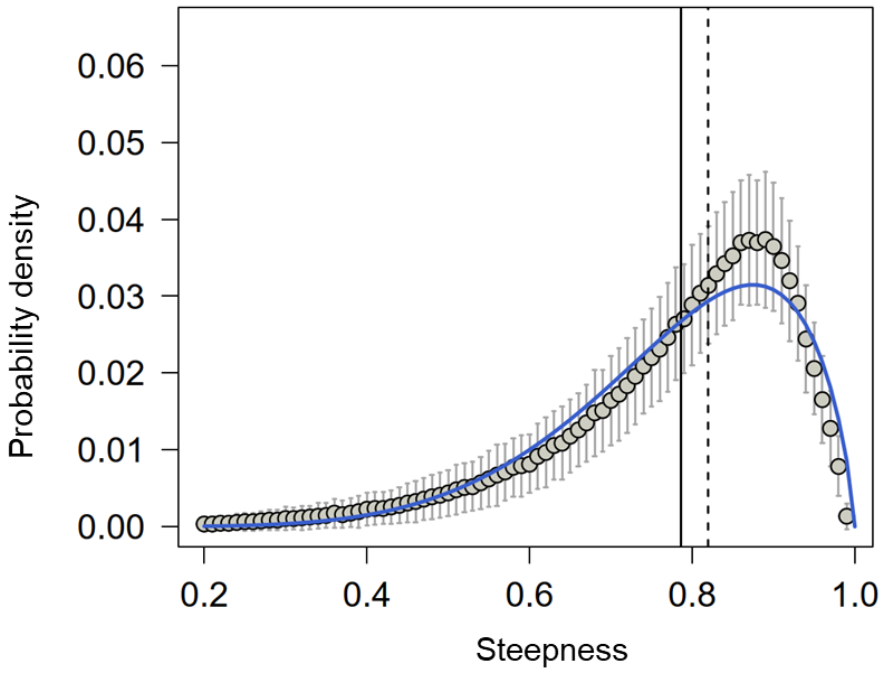

Figure 1.4. Empirical probability density distribution of stock-recruitment steepness for Pacific saury along with fitted beta density (in blue line). The solid and dashed black vertical lines denote the mean and median values for steepness, respectively. The black circle denotes the mean steepness value for each steepness interval (0.01) while the vertical bars indicate on standard deviation are shown for the empirical distribution.

doi:10.6342/NTU202500253

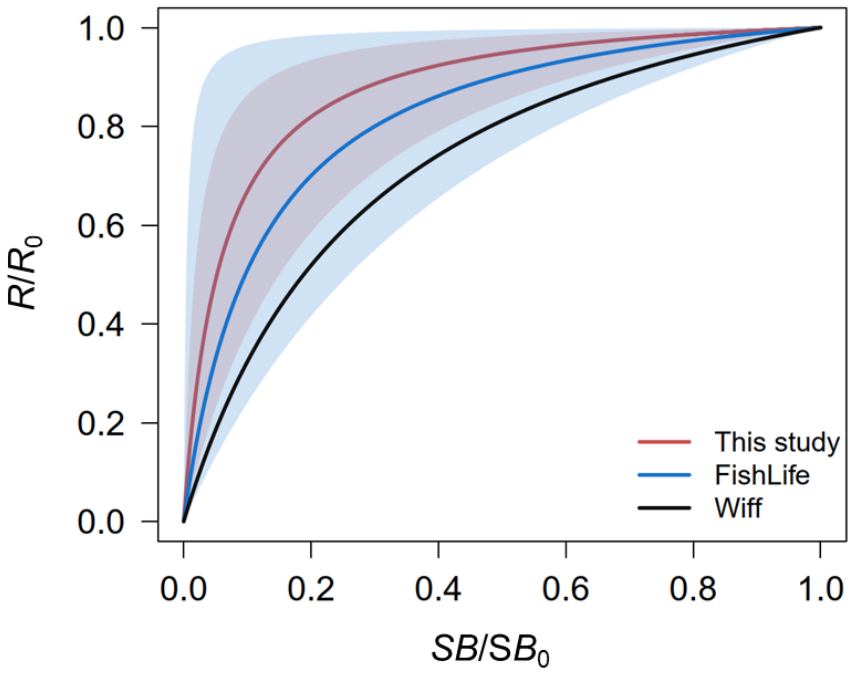

Figure 1.5. Estimated stock-recruitment curve of Pacific saury derived from the mean steepness value calculated by this study (red line), compared to those derived from the mean steepness value from the *FishLife* (in blue line) and Wiff et al. (2018) (in black line), respectively. Polygons denote the 80% intervals. Relative recruits (R) indicate recruitment/unfished recruitment (R_0), and relative biomass indicate biomass (B)/unfished biomass (B_0).

doi:10.6342/NTU202500253

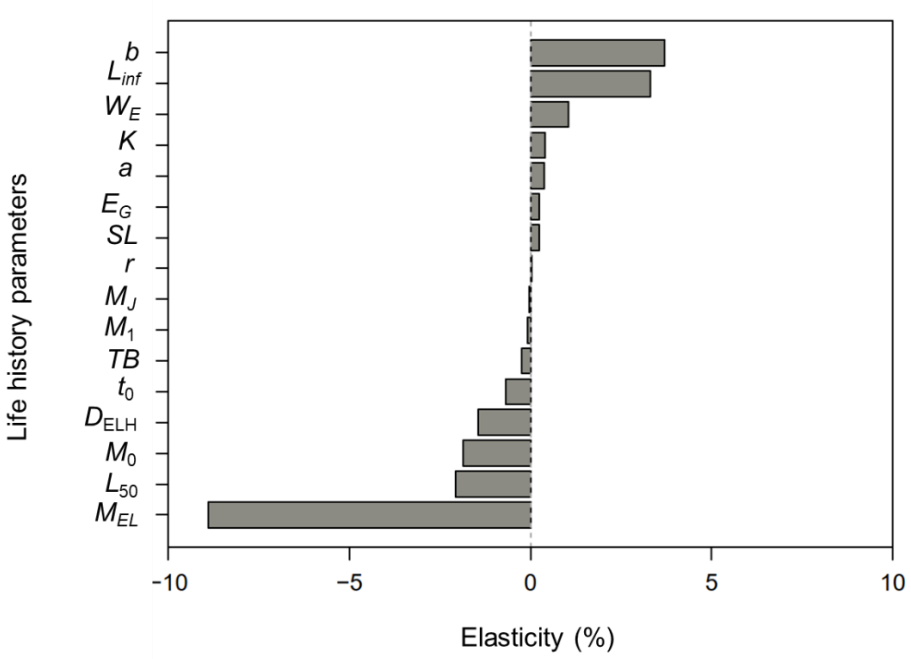

Figure 1.6. The elasticity of steepness for baseline life-history parameter values. The specific names of each life history parameter provided in **Table 1.1**.

doi:10.6342/NTU202500253

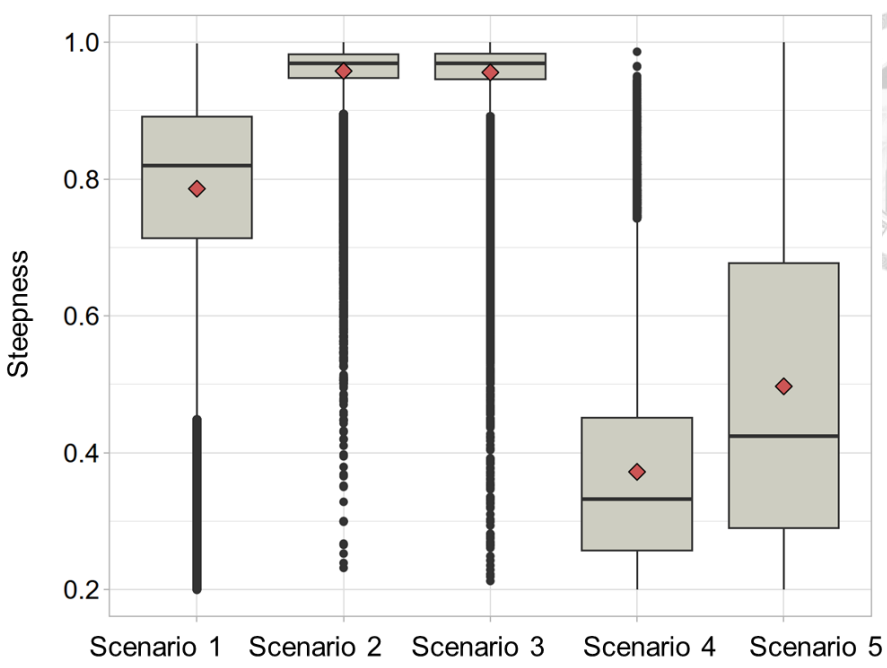

Figure 1.7. Boxplots of steepness for the Pacific saury for the five environmental scenarios. Scenario 1 involves prevailing environmental conditions and a coefficient of variation (CV) of 0.2 for the life history parameters. Scenarios 2 and 3 involve favorable environmental conditions and CVs of 0.2 and 0.4, respectively, and Scenarios 4 and 5 involve unfavorable environmental conditions and CVs of 0.2 and 0.4, respectively.

doi:10.6342/NTU202500253

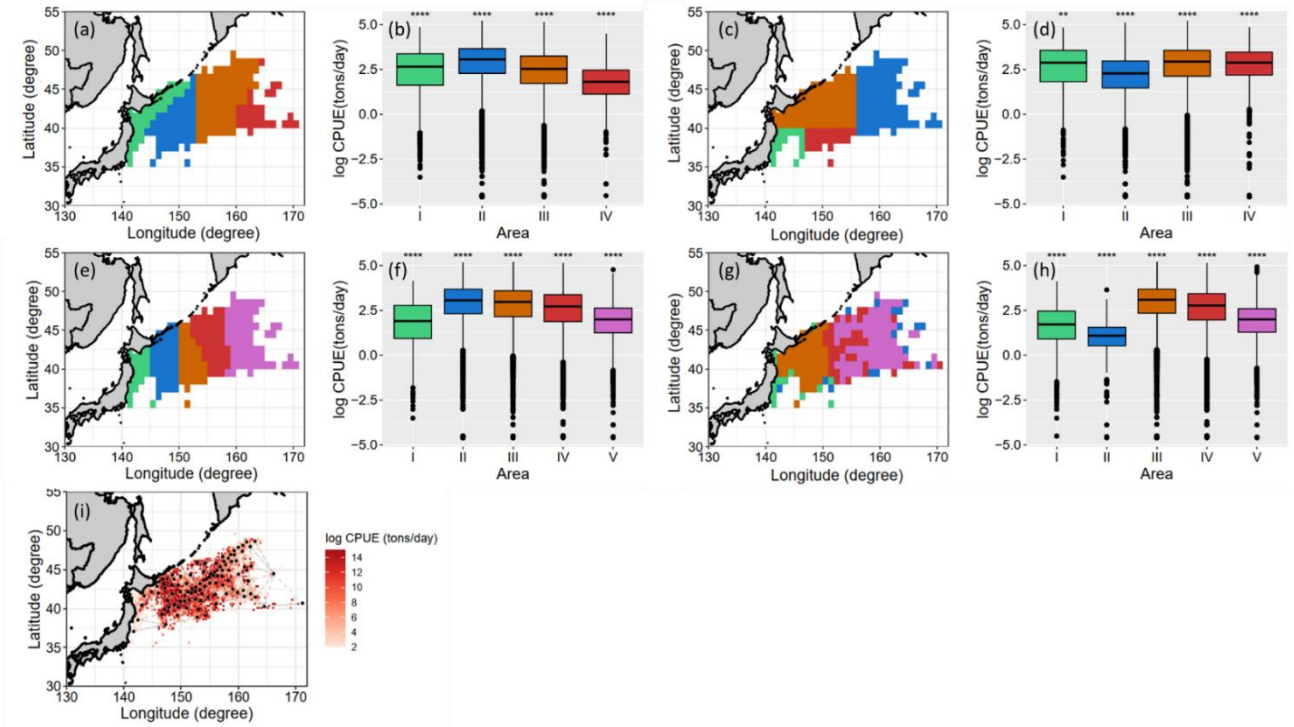

Figure 2.1. The resulting area stratifications with boxplots of observed CPUEs for each area strata are determined by (a-b) the Ad hoc approach (four area strata), (c-d) the Binary approach (four area strata), (e-f) the Spatial 1 (five area strata), (g-h) the Spatial 0.1 (five area strata); and the (i) knot (in black points) configuration of VAST with the observed CPUE (in red colors) by using the Pacific saury data in Northwestern Pacific Ocean during 1997 – 2019. Star symbols on boxplot represent the significance levels with the overall mean of observed CPUEs (****: $p <= 0.0001$, ***: $p <= 0.001$, **: $p <= 0.01$) by using the ANOVA test.

doi:10.6342/NTU202500253

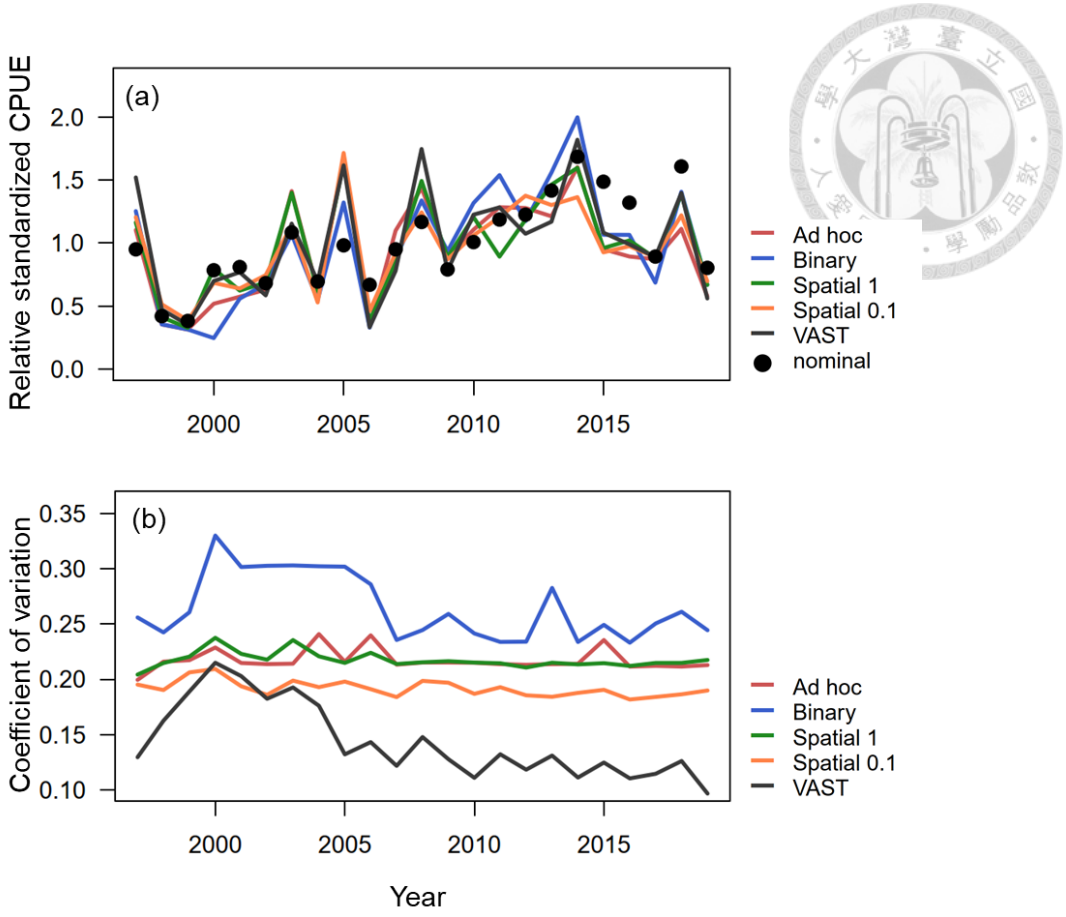

Figure 2.2. Annual trends of (a) the relative standardized abundance indices without area-weighting (relative to mean), and (b) the coefficient of variation of standardized CPUE indices without area-weighting for the Ad hoc, Binary, Spatial 1, Spatial 0.1 GLMMs, and VAST for Pacific saury in the Northwestern Pacific Ocean during 1997 – 2019. Solid black points represent the annual nominal CPUEs for Pacific saury.

doi:10.6342/NTU202500253

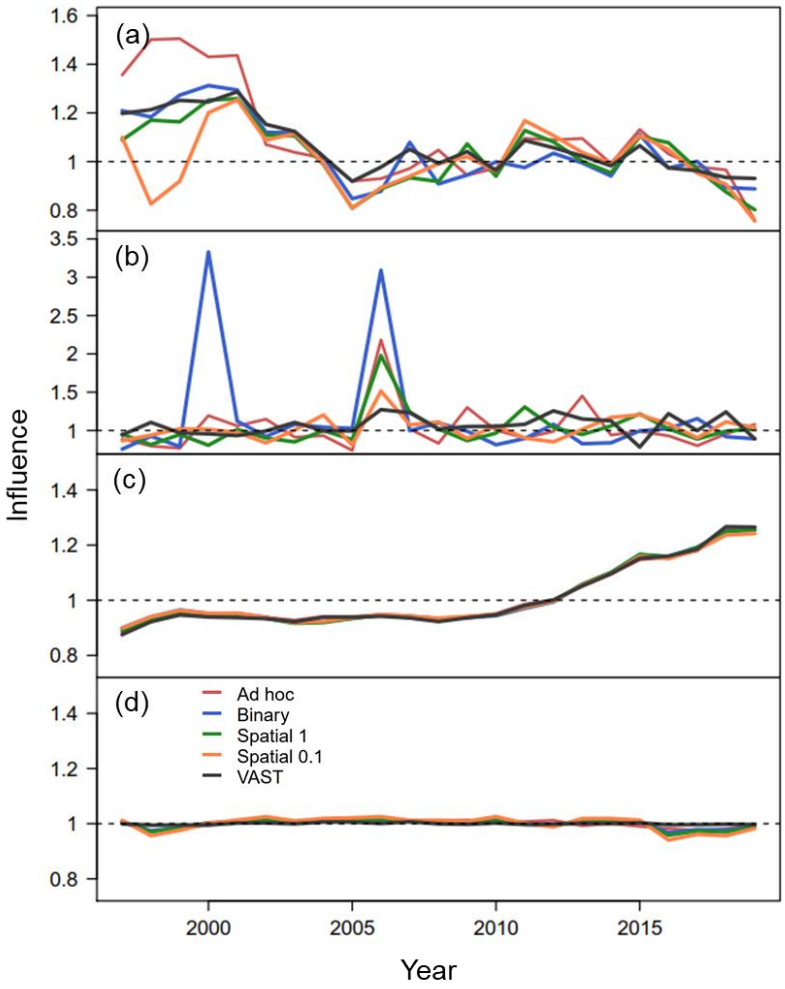

Figure 2.3. The annual influence of (a) spatial, (b) interaction of year and spatial/spatio-temporal random effect, (c) vessel, and (d) quadratic water temperature effects for Ad hoc, Binary, Spatial 1, Spatial 0.1 GLMMs, and VAST for Pacific saury in the Northwestern Pacific Ocean during 1997 – 2019.

doi:10.6342/NTU202500253

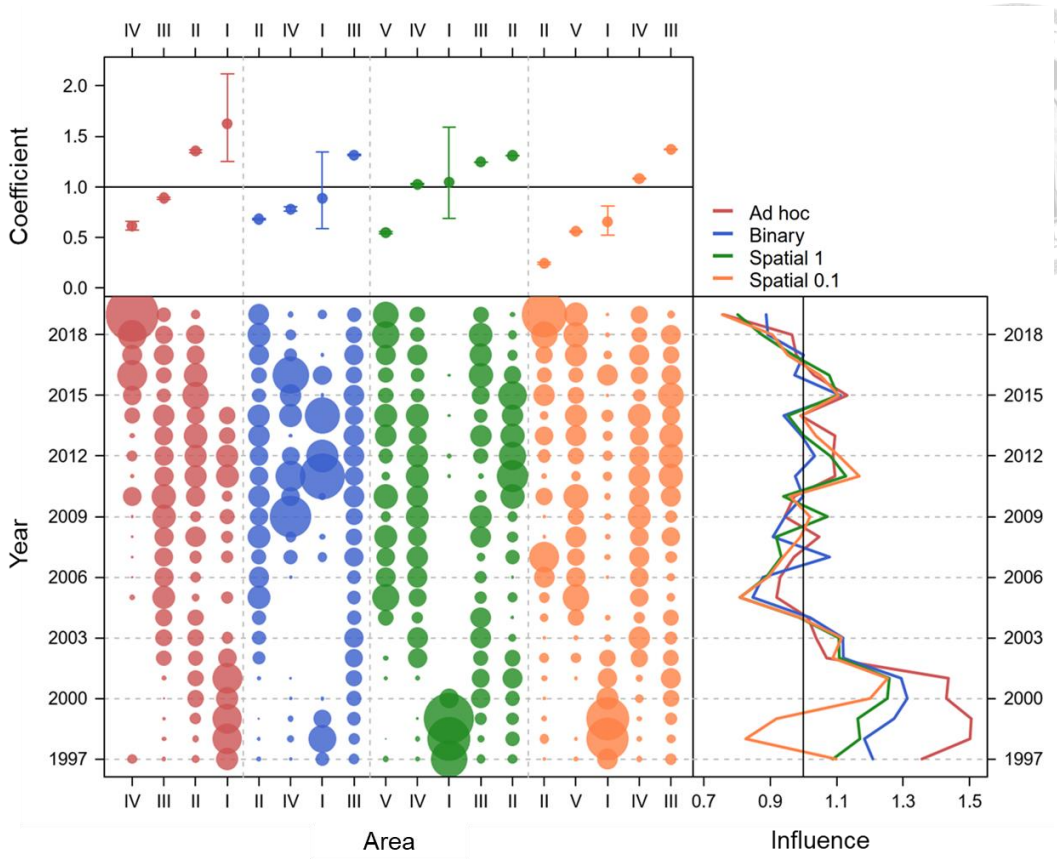

Figure 2.4. The coefficient-distribution-influence (CDI) plot of the spatial effect for Ad hoc, Binary, Spatial 1 and Spatial 0.1 GLMMs for Pacific saury in the Northwestern Pacific Ocean during 1997 – 2019. The top panel of the CDI plot provides the normalized coefficients and their standard errors for each area stratum (four area strata for Ad hoc, Binary GLMMs, and five area strata for Spatial 1 and Spatial 0.1 GLMMs). In the bottom left panel, the bubbles indicate the annual distribution of observed CPUEs from each area stratum in each year. The bottom right panel shows the annual value of influence for the spatial effect.

doi:10.6342/NTU202500253

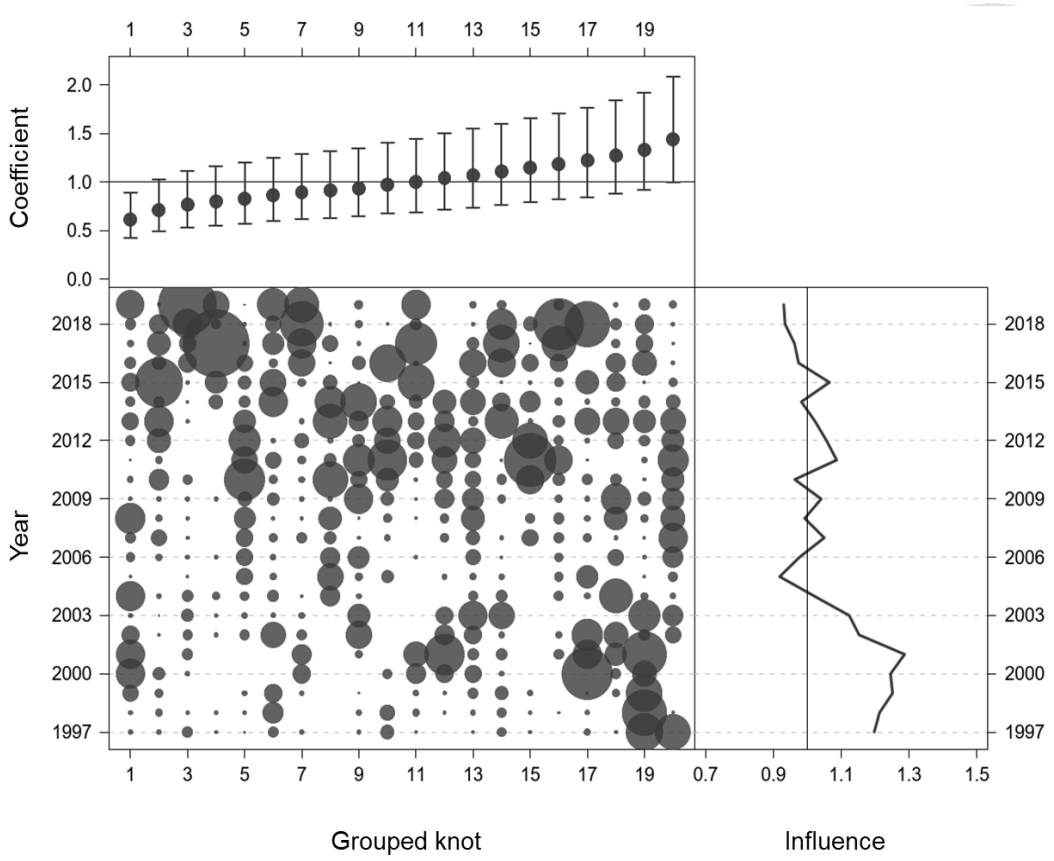

Figure 2.5. The coefficient-distribution-influence (CDI) plot of the spatial random effect for the VAST model for Pacific saury in the Northwestern Pacific Ocean during 1997 – 2019. The top panel of the CDI plot provides the normalized coefficients and their standard errors. In the bottom left panel, bubbles indicate the annual distribution of observed CPUEs from each grouped knot (every five knots) in each year. The bottom right panel shows the annual value of influence for the spatial random effect.

doi:10.6342/NTU202500253

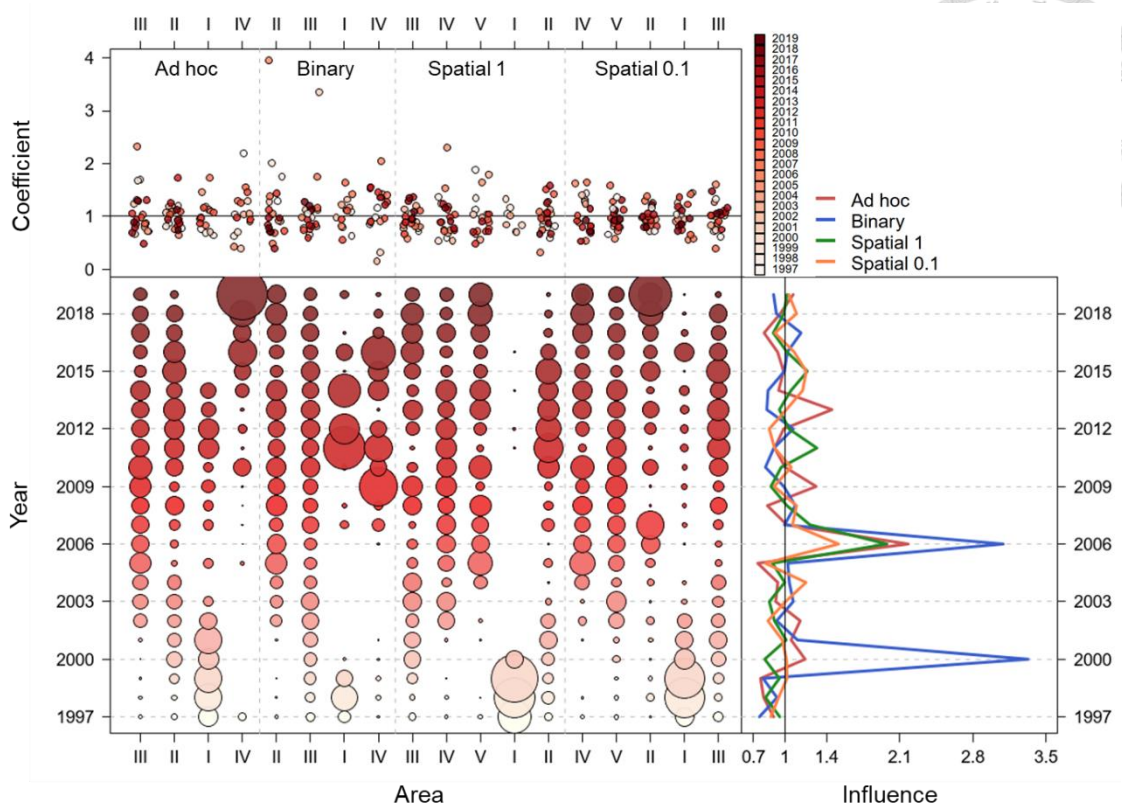

Figure 2.6. The coefficient-distribution-influence (CDI) of the year × spatial interaction random effect for the Ad hoc, Binary, Spatial 1, and Spatial 0.1 GLMMs for Pacific saury in the Northwestern Pacific Ocean during 1997 – 2019. The top panel of the plot provides the boxplots of normalized coefficients for each area stratum (four area strata for Ad hoc, Binary GLMMs, and five area strata for Spatial 1 and Spatial 0.1 GLMMs). The solid color points represent the coefficient for each year. The area coefficient in each year was jittered with small random noise for graphical visualization. In the bottom left panel, bubbles indicate the annual distribution of observed CPUEs from each area stratum in each year. The bottom right panel shows the annual value of influence for the year × spatial interaction random effect.

doi:10.6342/NTU202500253

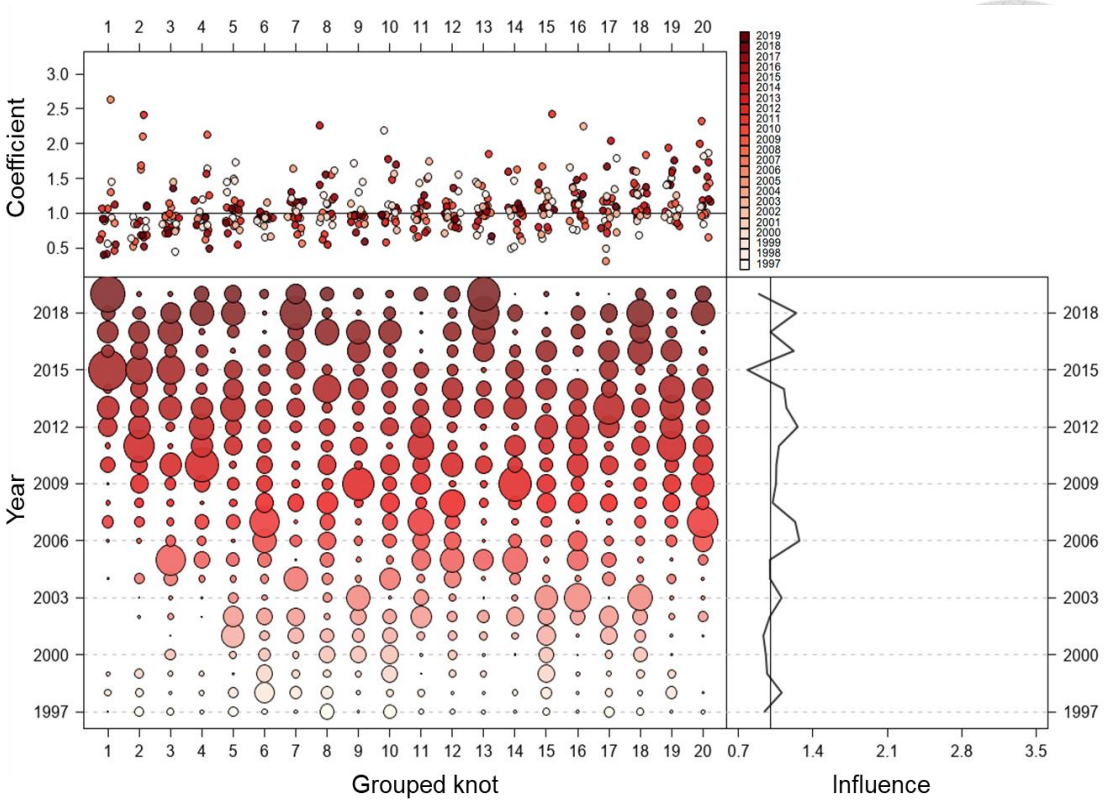

Figure 2.7. The coefficient-distribution-influence (CDI) plot of spatio-temporal random effect for the VAST model for Pacific saury in the Northwestern Pacific Ocean during 1997 – 2019. The top panel of the plot provides the boxplots of the normalized coefficient for each combined knot (every five knots). The solid color points represent the coefficient for each year. The grouped knots coefficient in each year was jittered with small random noise for graphical visualization. In the bottom left panel, bubbles indicate the annual distribution of observed CPUEs from each stratified area in each year. The bottom right panel shows the annual value of influence for the spatio-temporal random effect.

doi:10.6342/NTU202500253

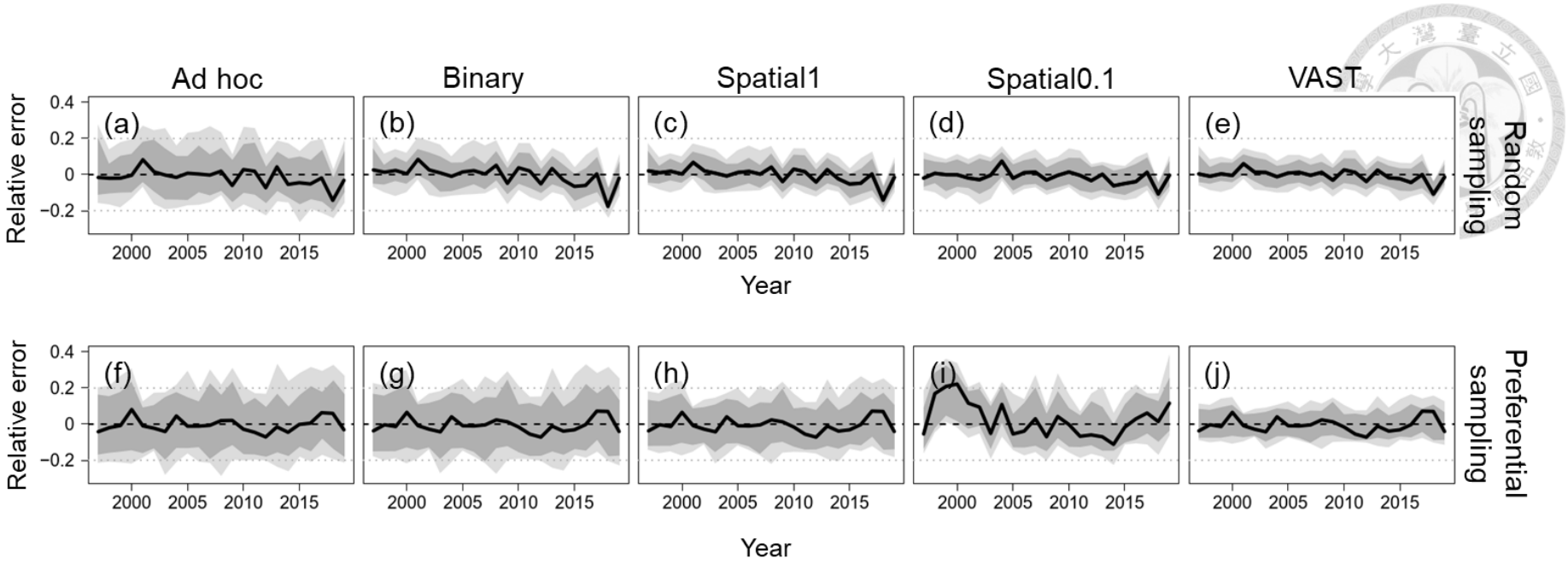

Figure 2.8. Time series of relative error (RE) in the index of abundance. The dark and light grey polygon represents the 80% and 95% confidence interval, respectively. RE is calculated for Ad hoc, Binary, Spatial 1 and Spatial 0.1 GLMMs, and VAST with the two sampling scenarios (random, and preferential samplings). The grey horizontal dashed line is the reference line (the relative error is 0.2) for the relative errors.

doi:10.6342/NTU202500253

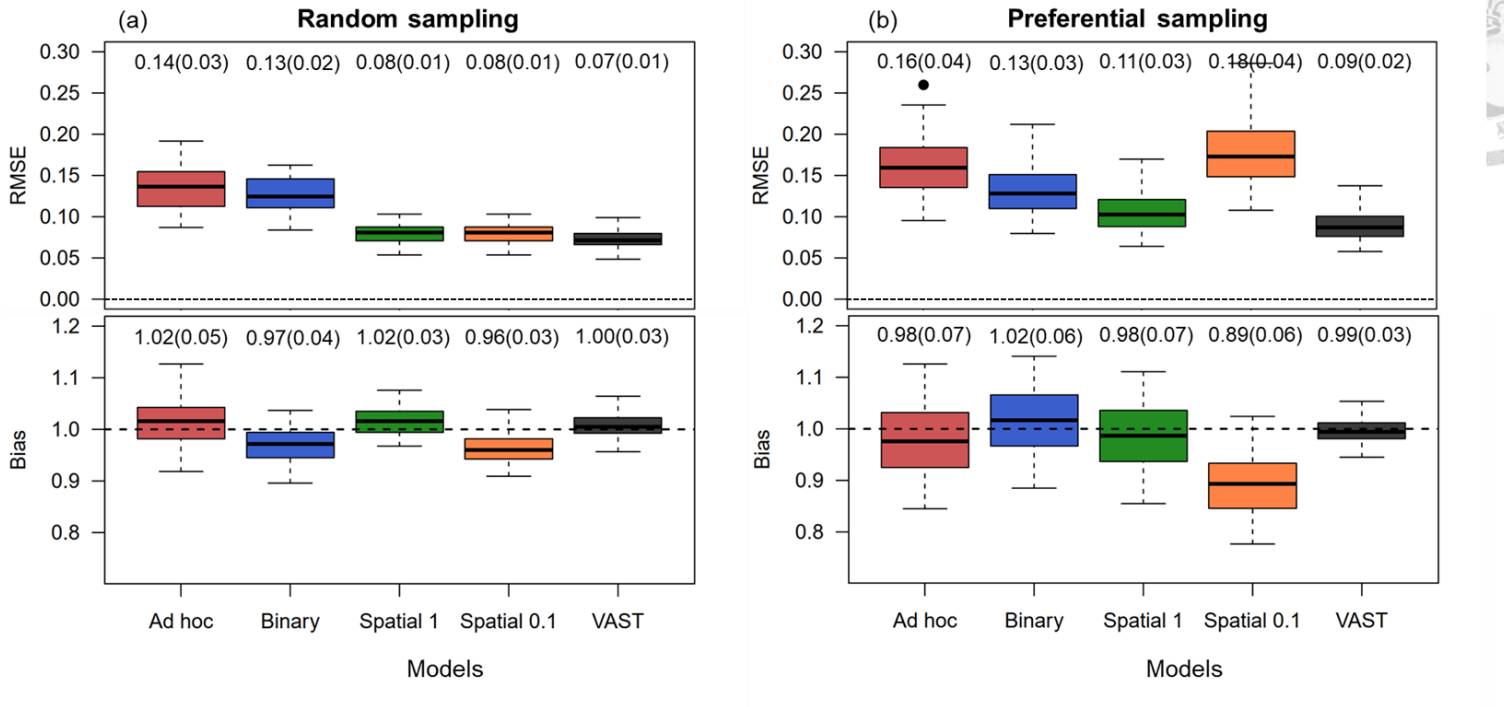

Figure 2.9. The boxplots of performance metrics for the (a,b) root mean squared error (RMSE) and (c,d) bias metrics calculated across all replicates under the two spatial sampling scenarios (random and preferential samplings) for the Ad hoc, Binary, Spatial 1, Spatial 0.1 GLMMs and VAST. The numbers above the boxplots indicate the mean value of RMSE and bias metrics. Values in the parentheses are the standard deviations. The horizontal dashed line is the reference line for the bias metrics (one represents no bias).

doi:10.6342/NTU202500253

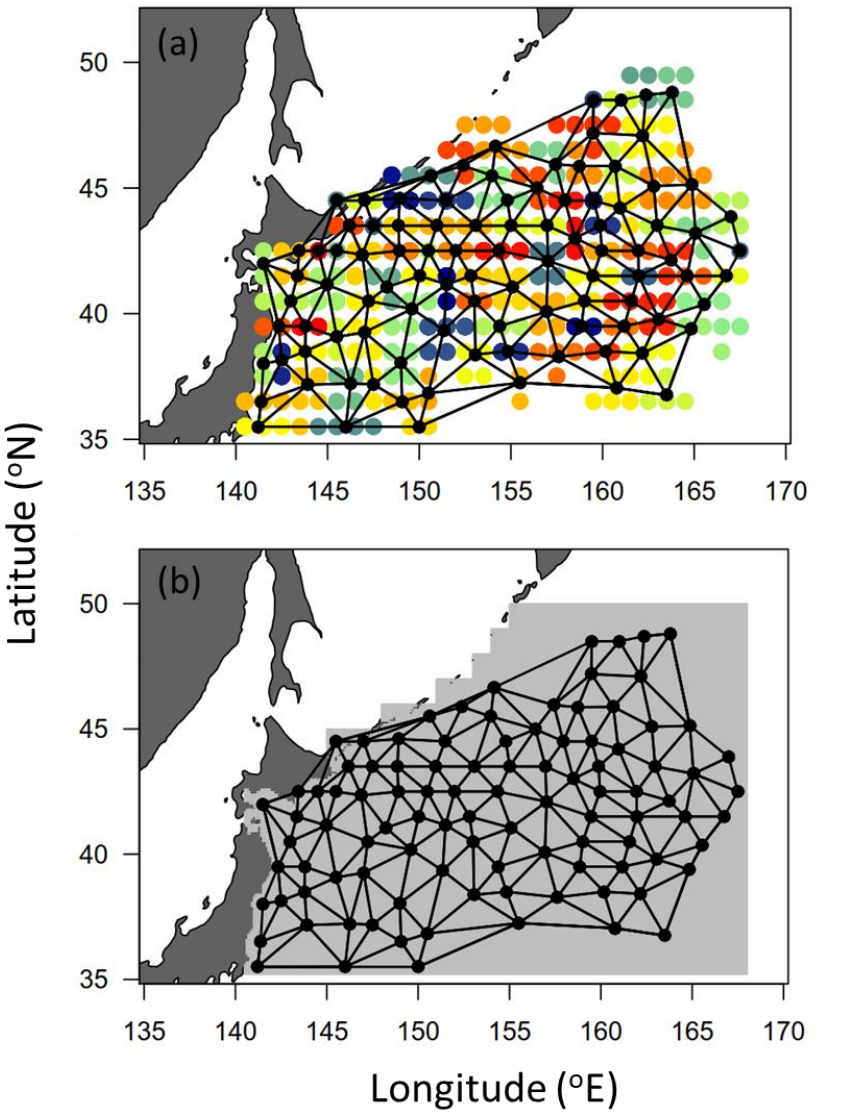

Figure 3.1. The spatial distribution of knots and mesh used to fit the spatio-temporal model; (a) an effect is estimated for each of the 100 knots (black solid circles) in the spatio-temporal model. The colored circles grouped by knots indicate the locations of spatial observations from 2001 to 2017 within the 1°×1° grid; (b) the spatial domain (grey polygon) for predicting Pacific saury density (unit: mass of fish in metric ton per day per square degree) in this study.

doi:10.6342/NTU202500253

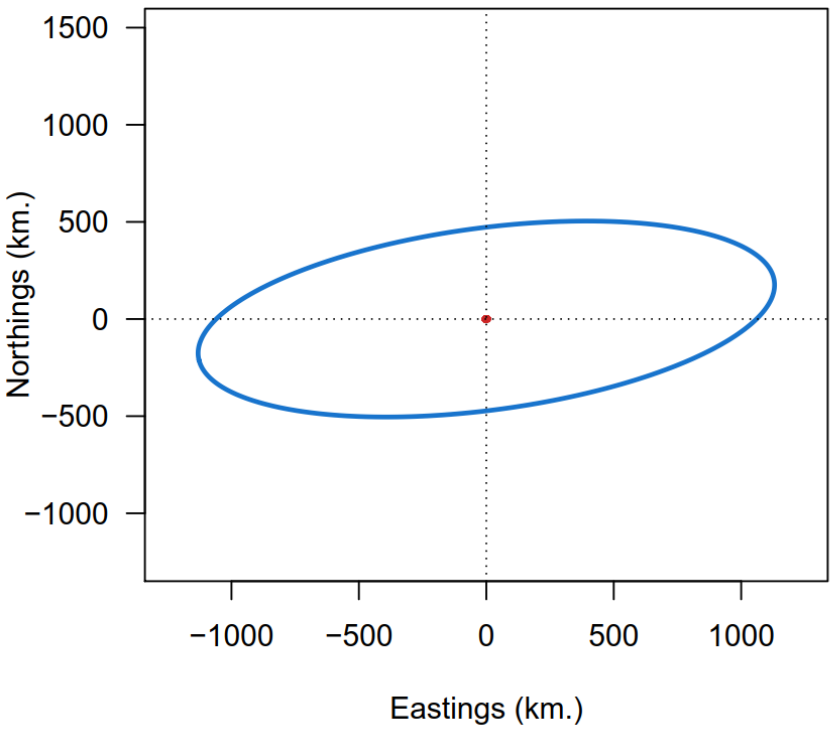

Figure 3.2. The magnitude of 2-dimensional spatial autocorrelation for Pacific saury distribution. The ellipse signifies the distance (from a point located at position (0,0)), where the correlation drops to 10 %. For example, an ellipse that is stretched East-West signifies that the predicted density is correlated over a longer distance moving East-West than North-South.

doi:10.6342/NTU202500253

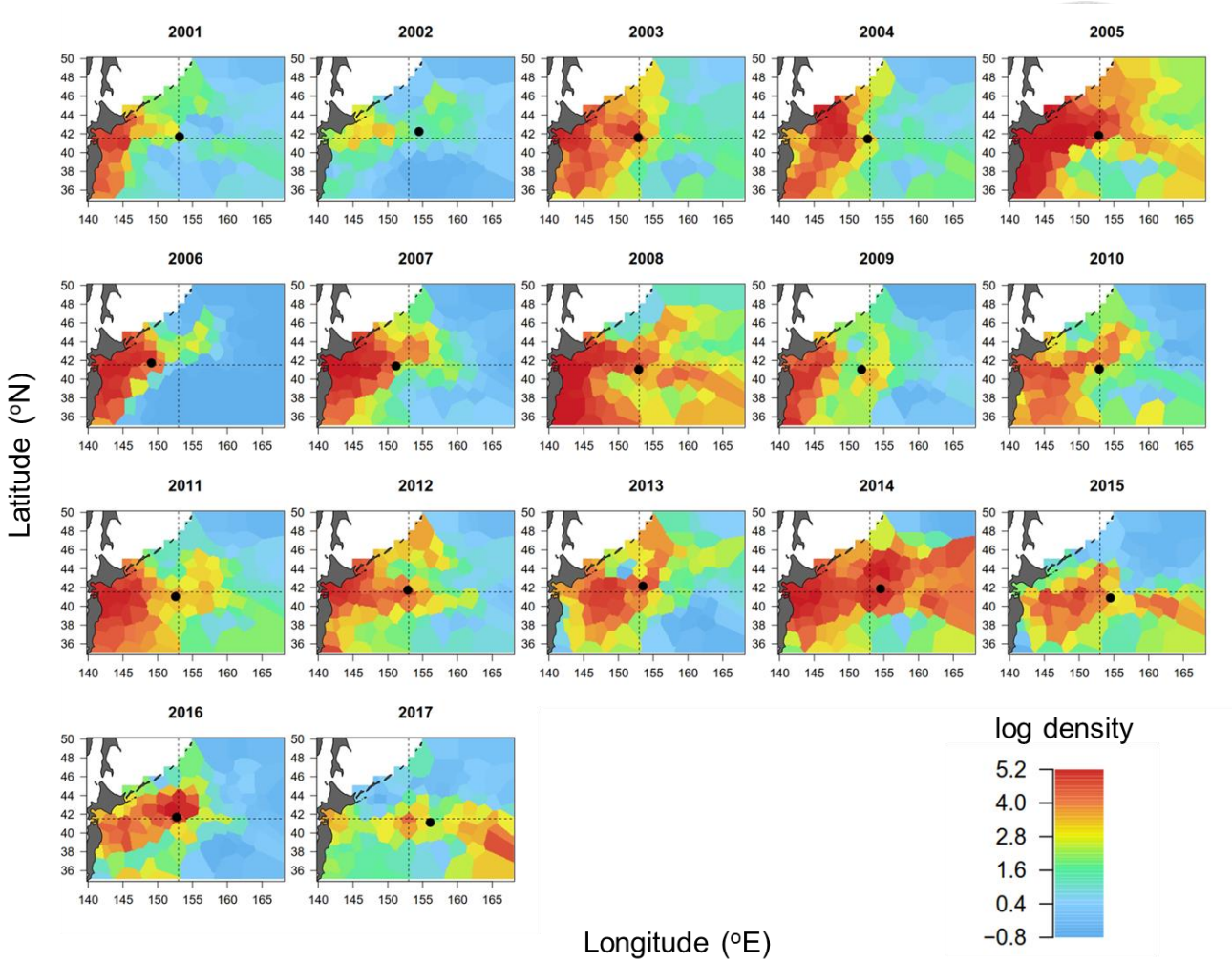

Figure 3.3. Spatiotemporal distributions of the log-transformed density of Pacific saury (unit: mass of fish in metric ton per day per square degree) from 2001 to 2017. The black circle is the location of the estimated centroid of gravity (COG). The dashed line represents the average location of the estimated centroid of gravity (COG).

doi:10.6342/NTU202500253

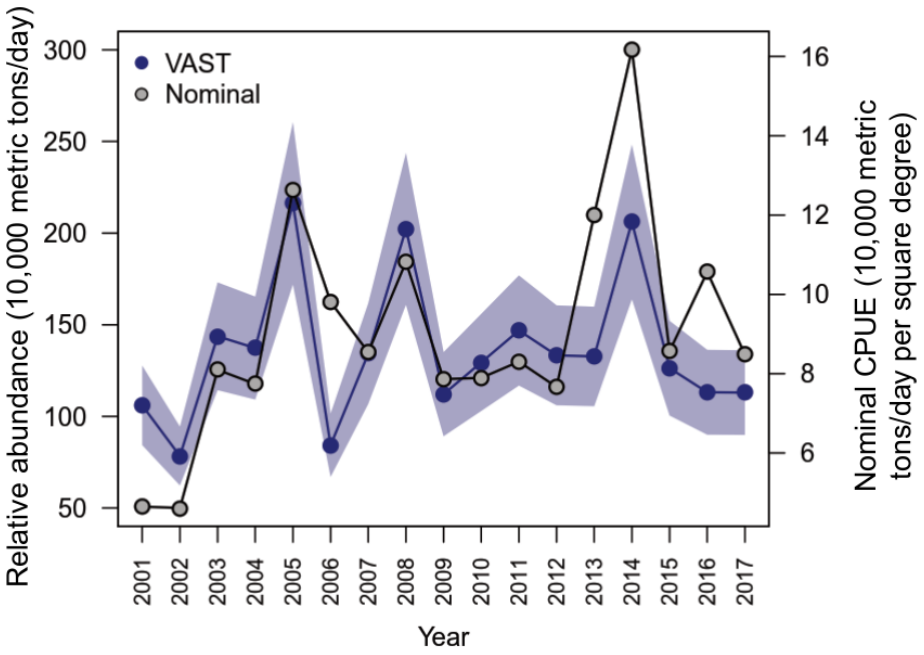

Figure 3.4. The time-series of the index of relative abundance (metric ton/day) from VAST for Pacific saury in the Northwestern Pacific Ocean during 2001 – 2017. The blue polygon represents the 95% confidence interval. The grey circle represents the nominal catch-per-unit-effort, CPUE (metric ton/day per square degree).

doi:10.6342/NTU202500253

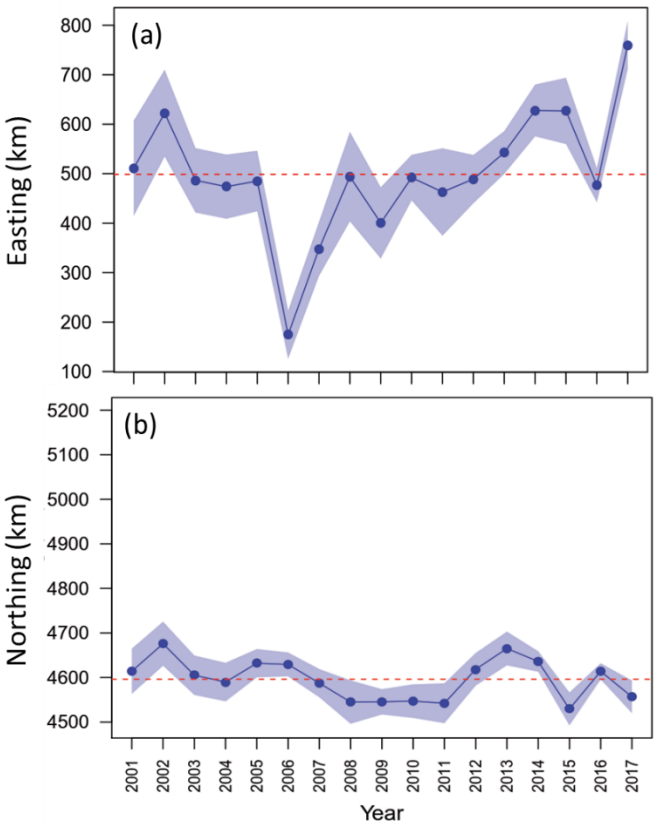

Figure 3.5. The time-series of the estimated centroids of gravities (COGs) in the (a) easting and (b) northing directions from the spatio-temporal model during 2001 – 2017. The red dashed line represents the average COG over the year; the blue polygon represents the 95% confidence interval.

doi:10.6342/NTU202500253

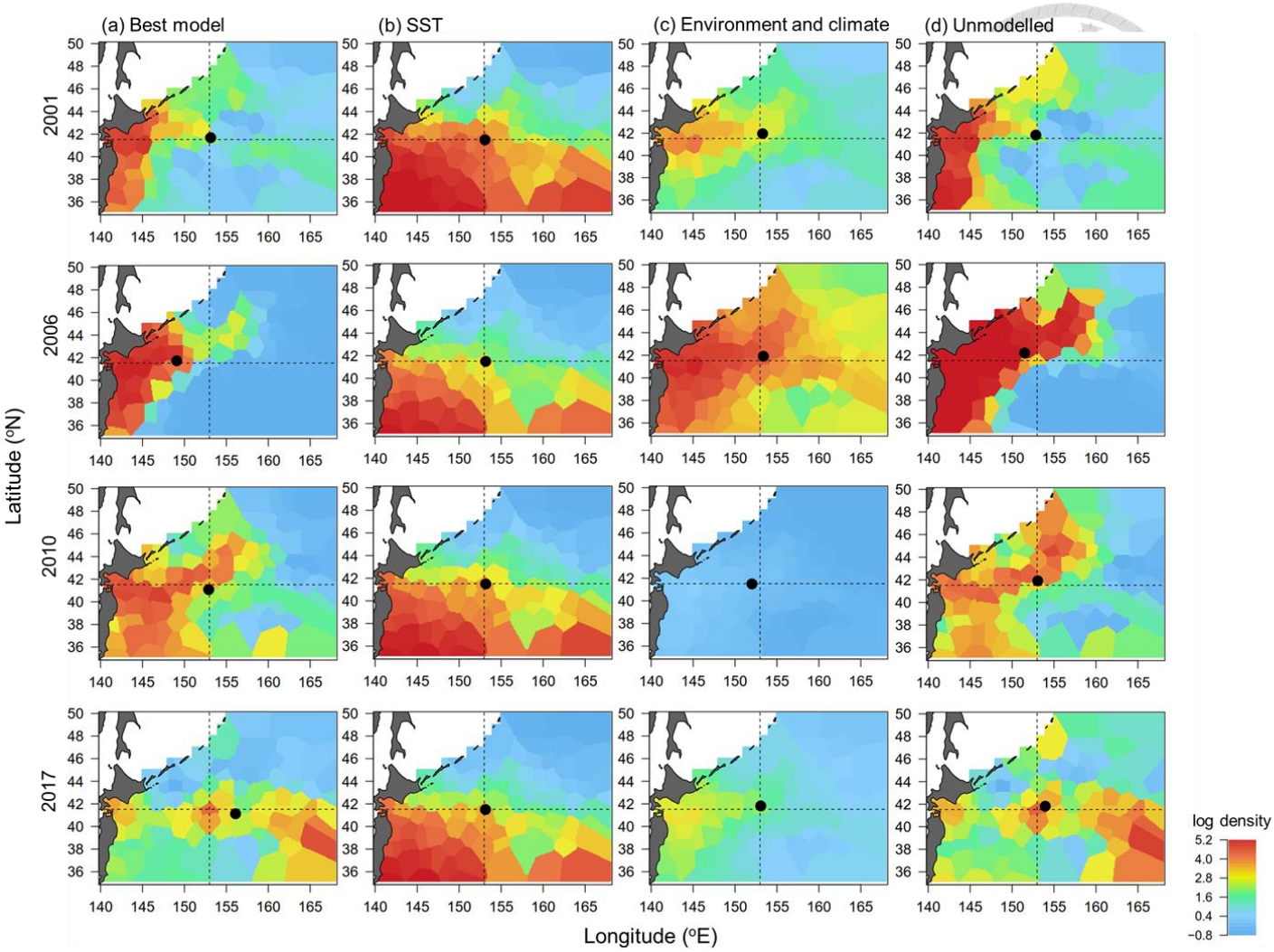

Figure 3.6. Estimated log-density (unit: mass of fish in metric ton per day per square degree) in 2001, 2006, 2010, and 2017 for the Pacific saury from the best model (a). Each hypothesized driver that eliminates all causes for variation in distribution except the SST (b), the multiple local and regional environmental variables (c), and the unmodelled variable (d). The black circle represents the location of the estimated centroid of gravity (COG) for each model. The dashed line represents the average location of the estimated centroid of gravity (COG) from the best model.

doi:10.6342/NTU202500253

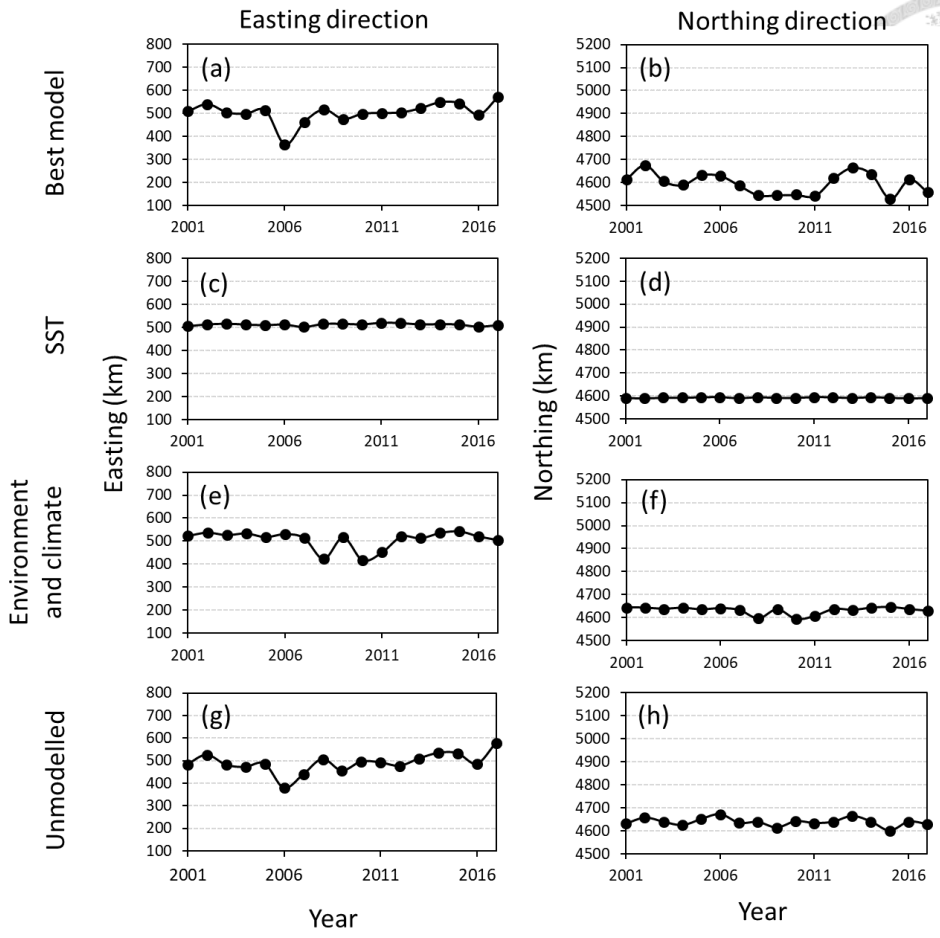

Figure 3.7. The estimated centroids-of-gravity (COGs) during 2001 – 2017 for the Pacific saury from the best model (a, b) in easting and northing directions, compared to those from each hypothesized driver that eliminates all causes for variation in distribution except SST (c, d), the multiple local and regional environmental variables (e, f), and the unmodelled variable (g, h).

doi:10.6342/NTU202500253

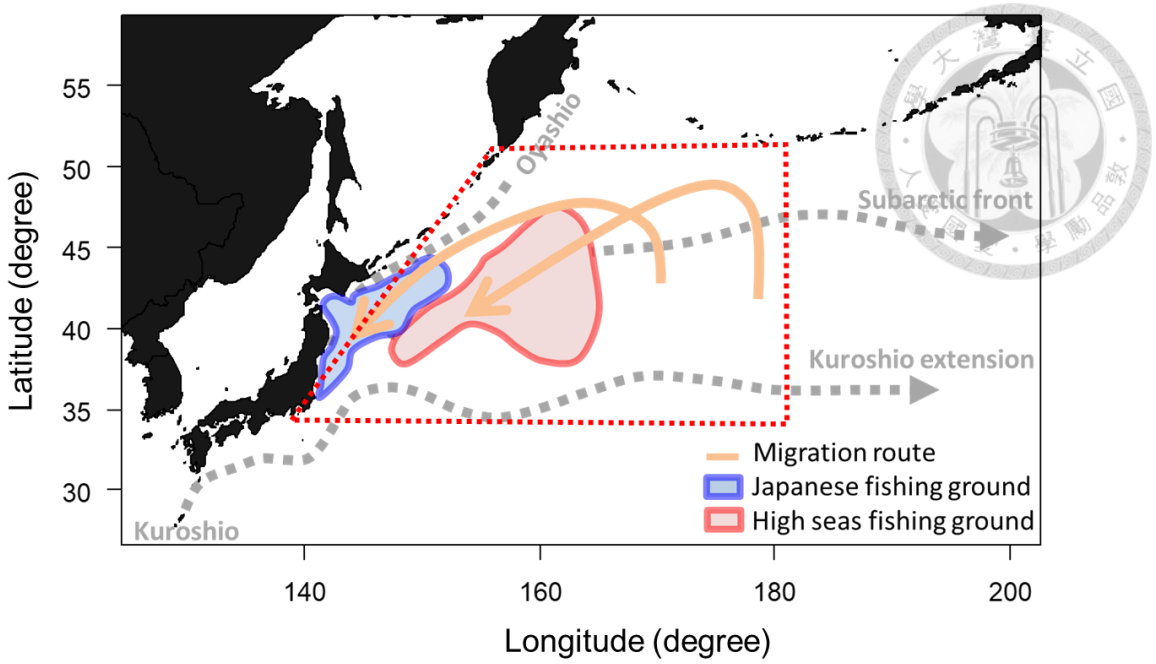

Figure 4.1. The spatial boundary of Pacific saury assessment in the Northwestern Pacific Ocean.

doi:10.6342/NTU202500253

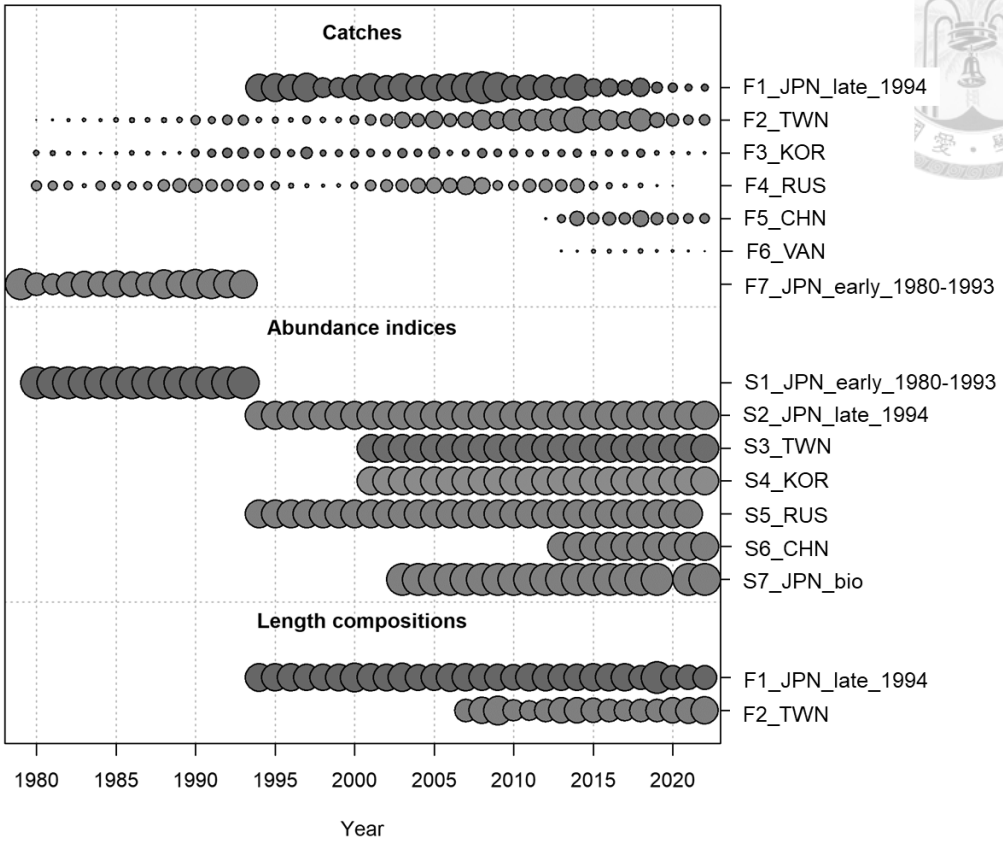

Figure 4.2. Catches, abundance indices, and length composition data included in the Pacific saury stock assessment in the Northwestern Pacific Ocean.

doi:10.6342/NTU202500253

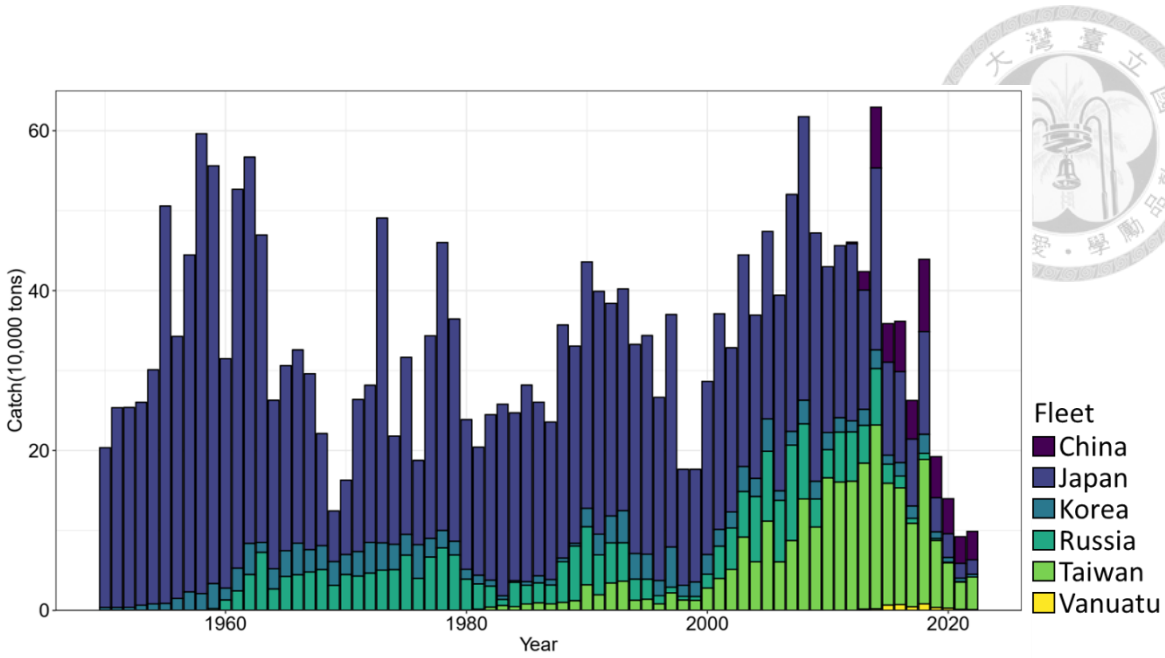

Figure 4.3. Time-series of catches (in metric tons) of the Pacific saury in Northwestern Pacific Ocean from 1980 to 2022 by the fleets.

doi:10.6342/NTU202500253

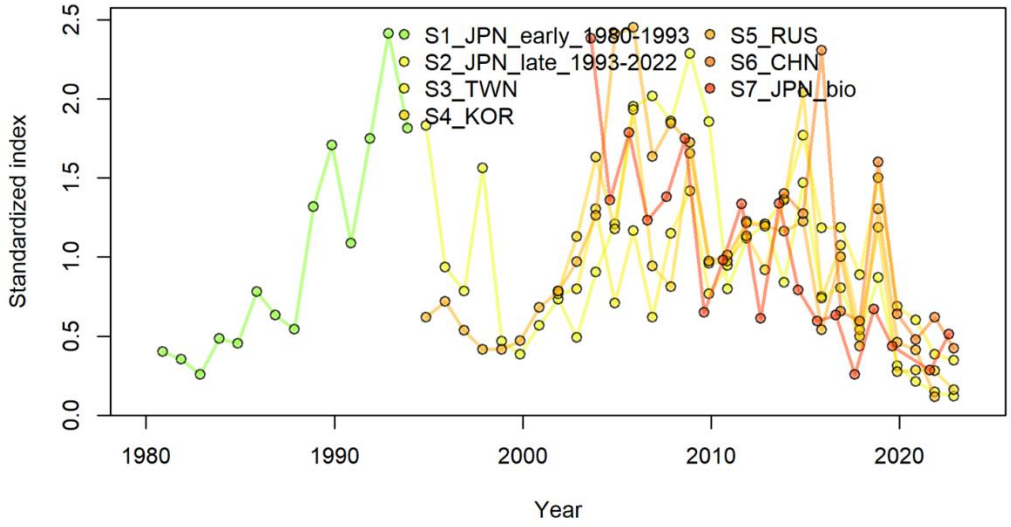

Figure 4.4. Time-series of Pacific saury relative standardized CPUEs (relative to mean) from early Japan (S1_JPN_early), late Japan (S2_JPN_late), Taiwan (S3_TWN), Korea (S4_KOR), Russia (S5_RUS), China (S6_CHN) stick-held dip net fisheries and biomass survey index of Japan (S7_JPN_bio) during 1980 – 2022 in the Northwestern Pacific Ocean.

doi:10.6342/NTU202500253

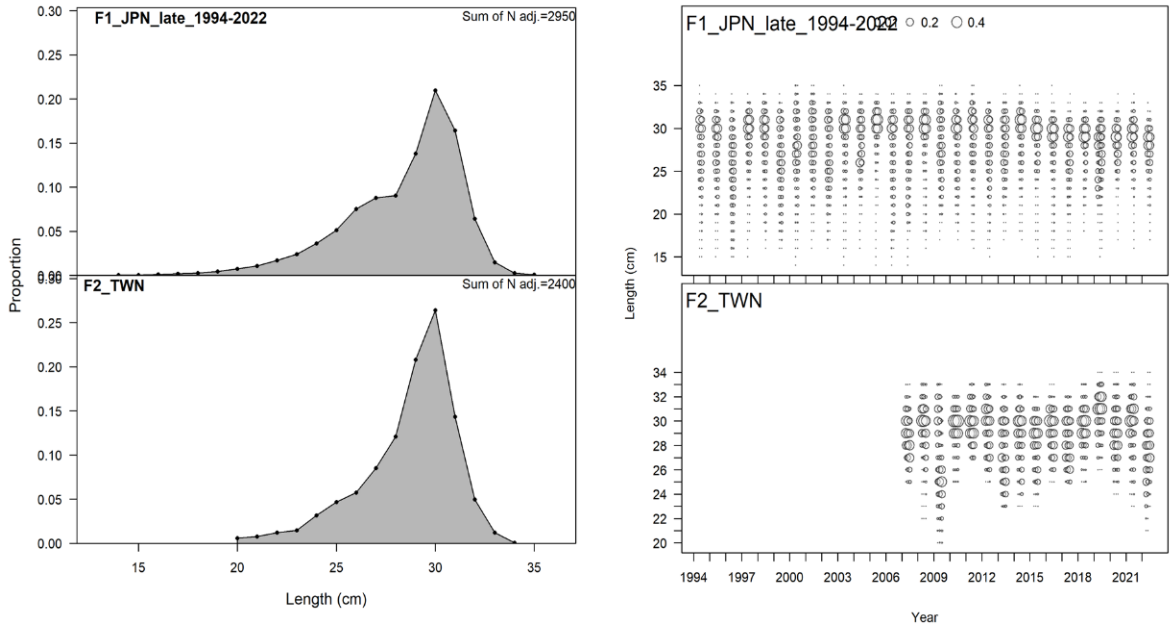

Figure 4.5. Length composition data is available in 1-cm size bins by fisheries for the Pacific saury stock assessment in the Northwestern Pacific Ocean.

doi:10.6342/NTU202500253

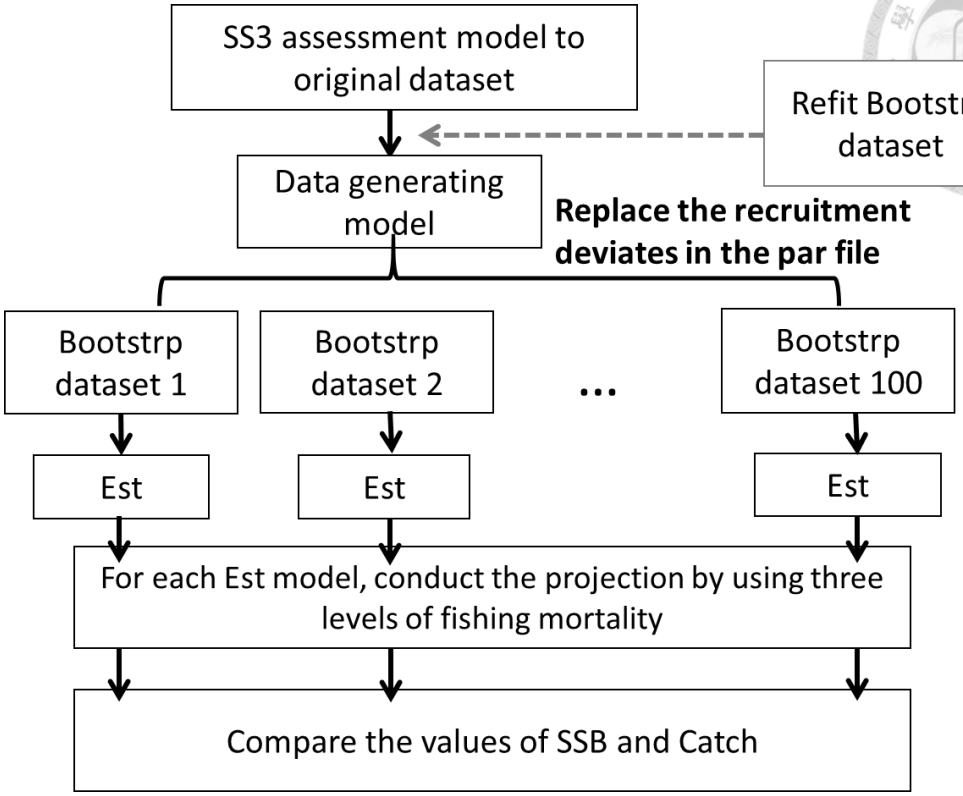

Figure 4.6. The flowchart of the stochastic projection for the Pacific saury.

doi:10.6342/NTU202500253

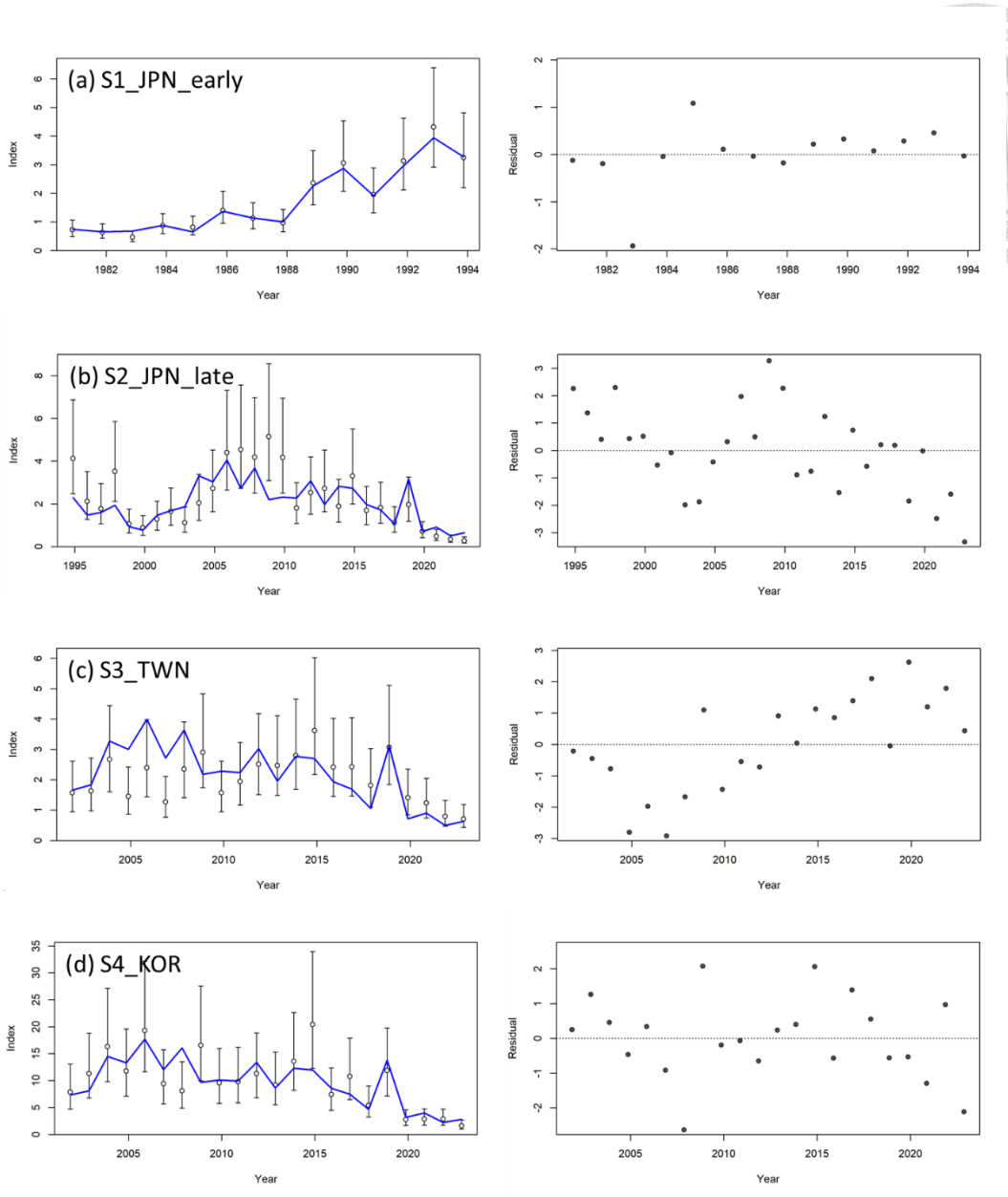

Figure 4.7. Fit to the early and late Japan indices (S1_JPN_early and S2_JPN_late), Taiwan index (S3_TWN) and Korea (S4_KOR) for the WNPO Pacific saury stock assessment. Left is the input CPUE with CV and the model fit CPUE (blue line). Right is the annual residuals of that fit.

doi:10.6342/NTU202500253

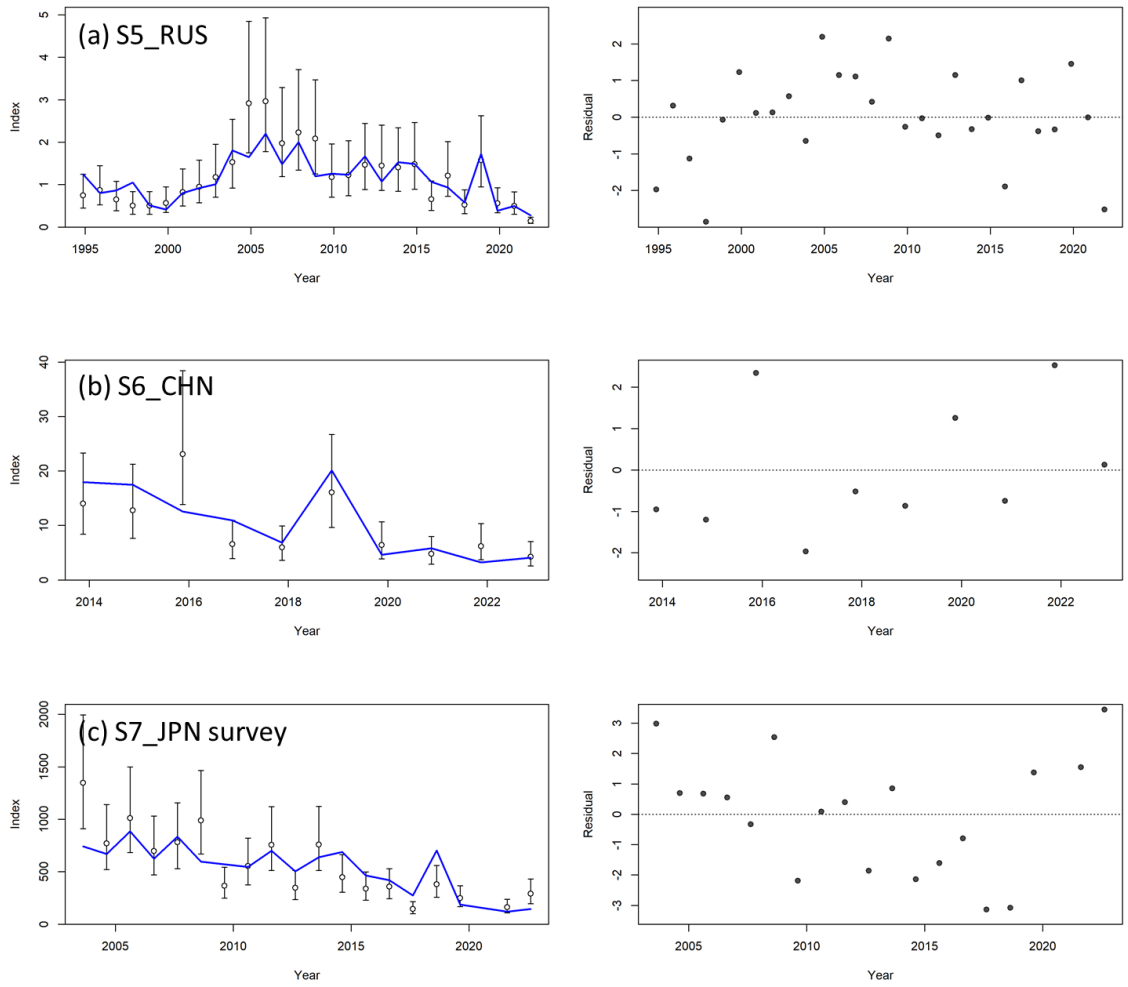

Figure 4.8. Fit to Russia (S5_RUS), China (S6_CHN) and Japanese biomass survey (S7_JPN_bio) indices for the WNPO Pacific saury stock assessment. Left is the input CPUE with CV and the model fit CPUE (blue line). Right is the annual residuals of that fit.

doi:10.6342/NTU202500253

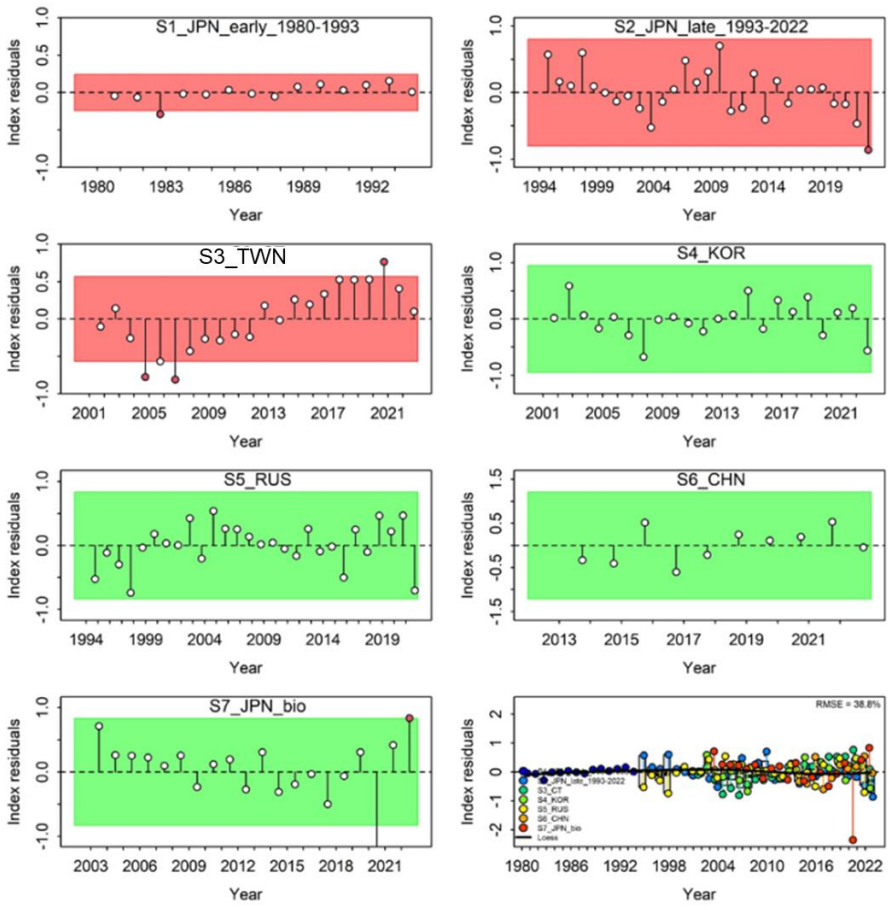

Figure 4.9. Results from a runs test for each CPUE index. Red shade indicates the index failed the test (residuals are not random), green shade indicates the index passed the test. Red circles indicate the residuals hit a boundary of 3 times of sigma (residual standard deviations).

doi:10.6342/NTU202500253

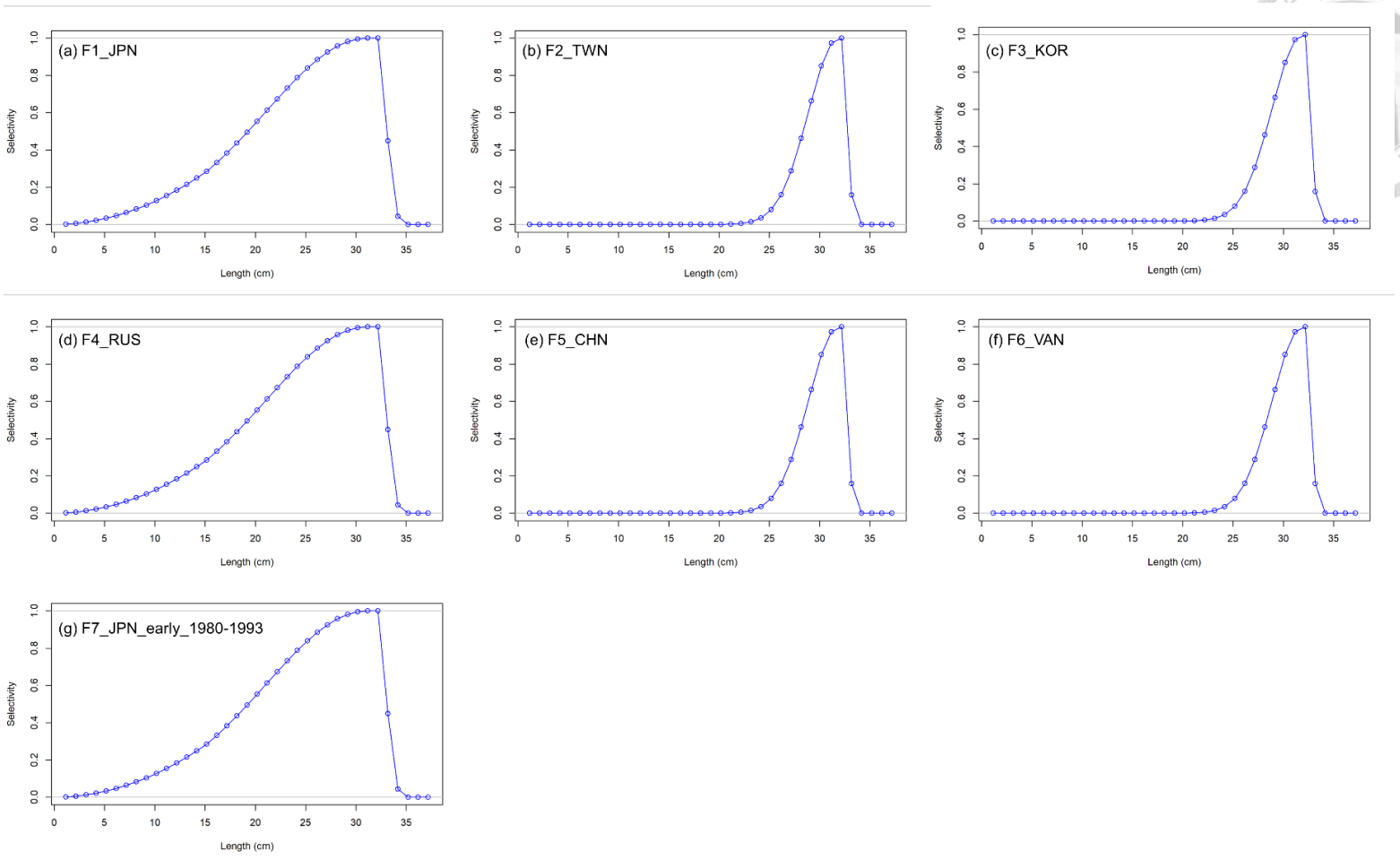

Figure 4.10. The estimated selectivity curve for each fleet in the Pacific saury stock assessment. See **Table 4.1** for the reference code.

doi:10.6342/NTU202500253

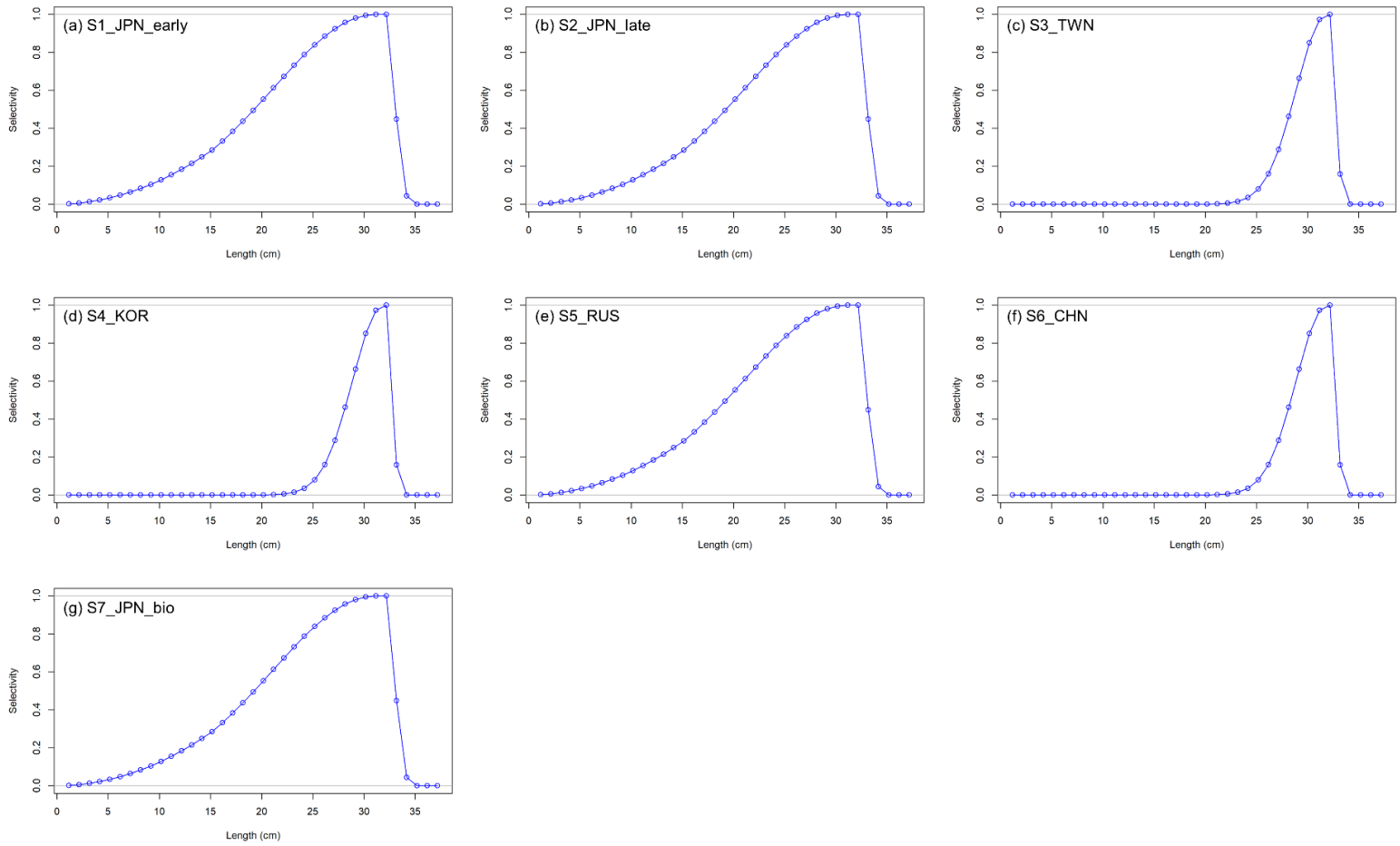

Figure 4.11. The estimated selectivity curve for each survey in the Pacific saury stock assessment. See **Table 4.1** for the reference code.

doi:10.6342/NTU202500253

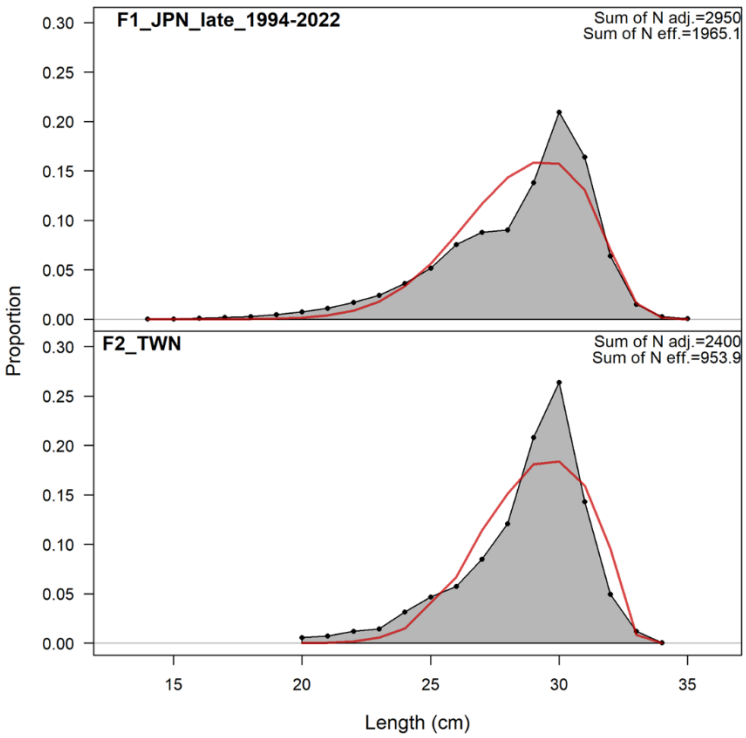

Figure 4.12. Aggregate length composition data is available for the Pacific saury stock assessment in the Northwestern Pacific Ocean, grey shading indicates observed data, and red line indicates expected distribution based upon the estimated selectivity.

doi:10.6342/NTU202500253

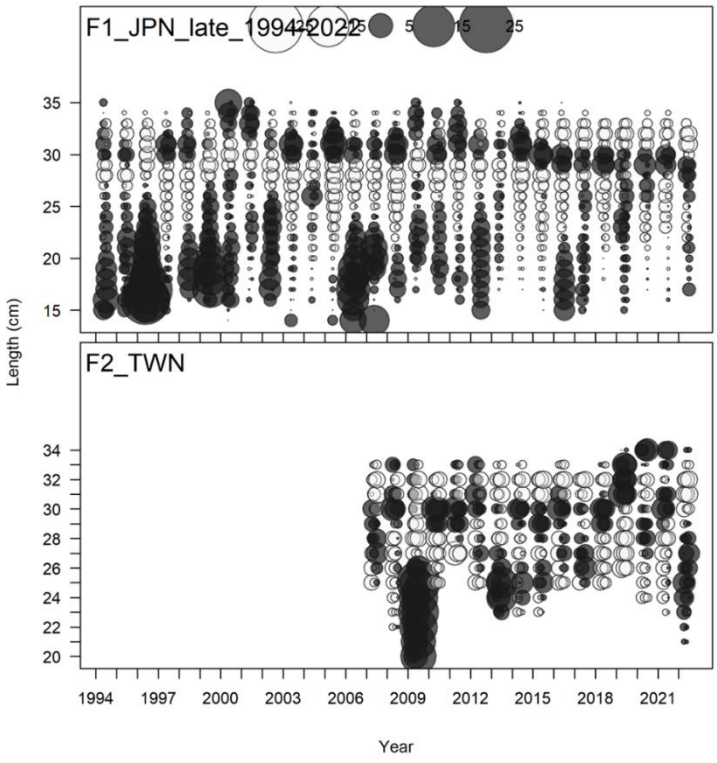

Figure 4.13. Fits to the quarterly residuals for Japan (F1_JPN, top) and Taiwan (F2_TWN, bottom) length composition data. Open circles indicate negative residuals and closed circles indicate positive residuals.

doi:10.6342/NTU202500253

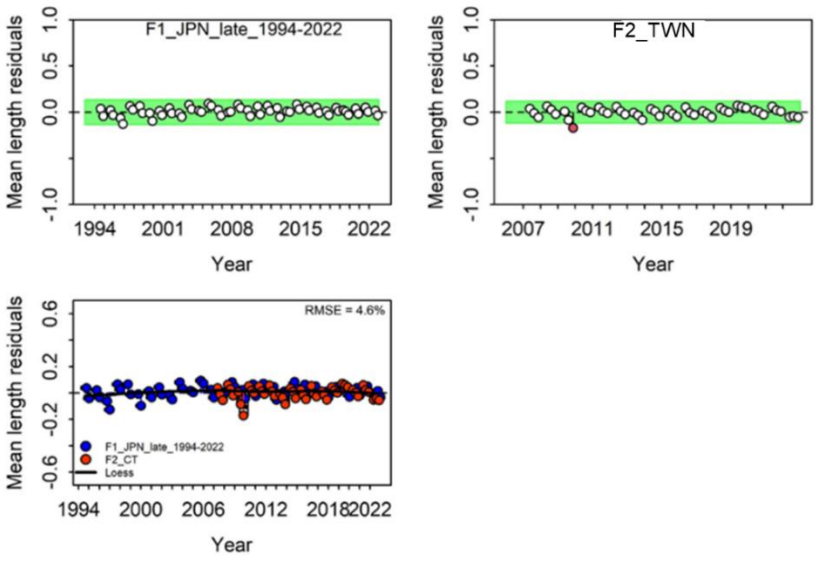

Figure 4.14. Results from a runs test for each length composition time series. Red indicates the data failed the test (residuals are not random), green indicates the data passed the test. Red circles indicate the residuals hit a boundary of 3 times of sigma (residual standard deviations).

doi:10.6342/NTU202500253

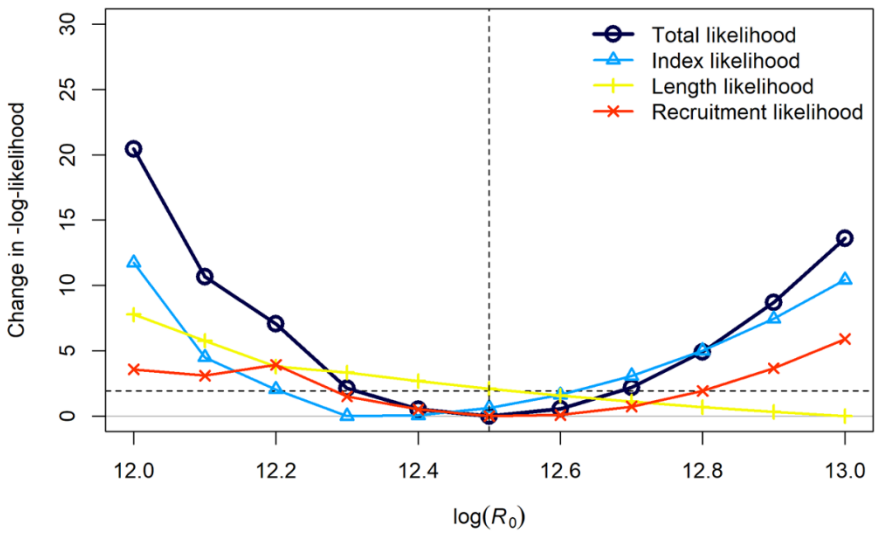

Figure 4.15. Profiles of the relative-negative log likelihoods by different likelihood components for the virgin recruitment in log-scale (log(R_0)) of the Pacific saury assessment model in the Northwestern Pacific Ocean.

doi:10.6342/NTU202500253

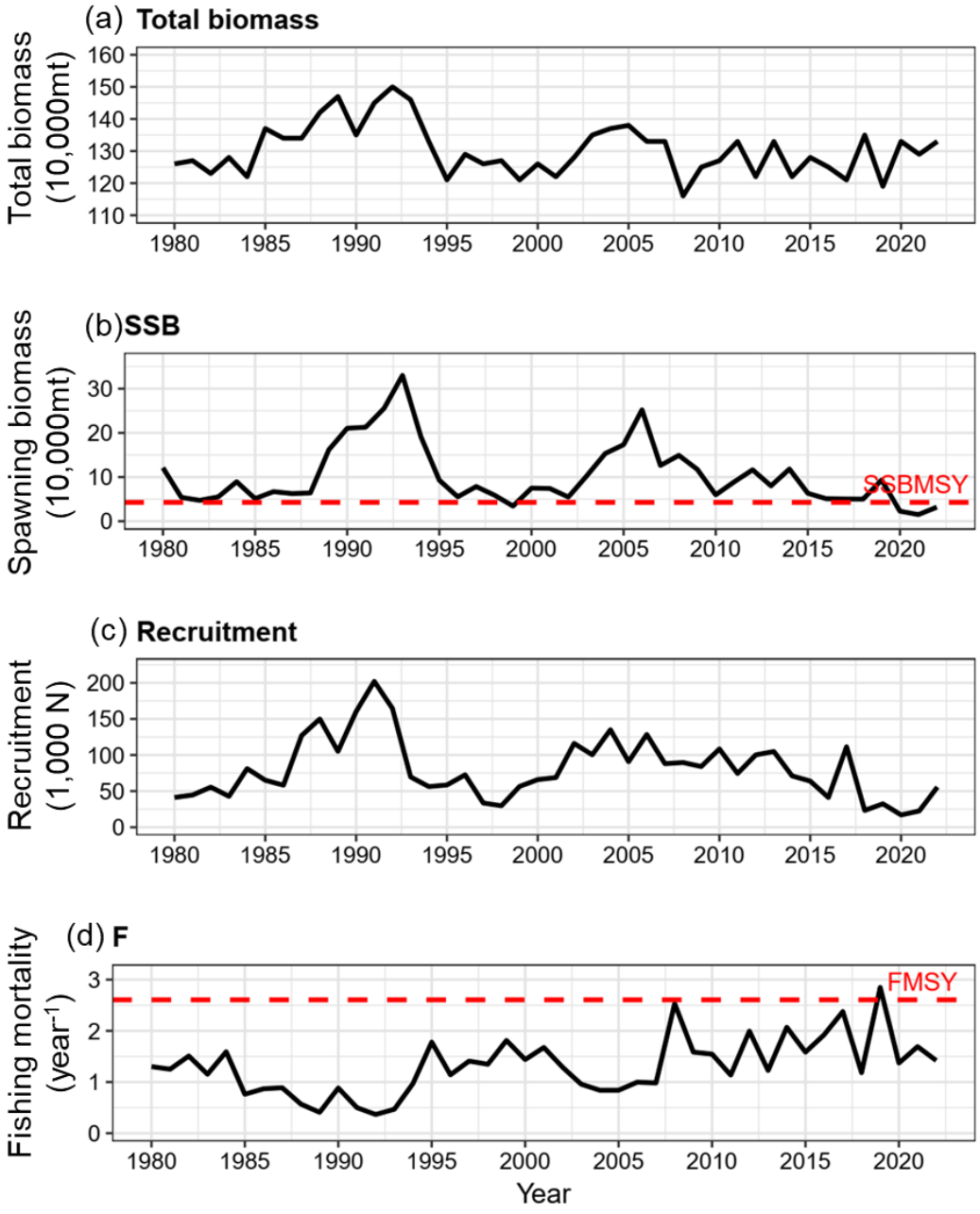

Figure 4.16. Estimated time-series of (a) total biomass (age-1 and older), (b) spawning biomass, (c) age-0 recruitment, and (d) instantaneous fishing mortality ($year^{-1}$) for the Pacific saury during the studied period in the Northwestern Pacific Ocean. The red horizontal dash line indicated the SSB_{MSY} and F_{MSY}.

doi:10.6342/NTU202500253

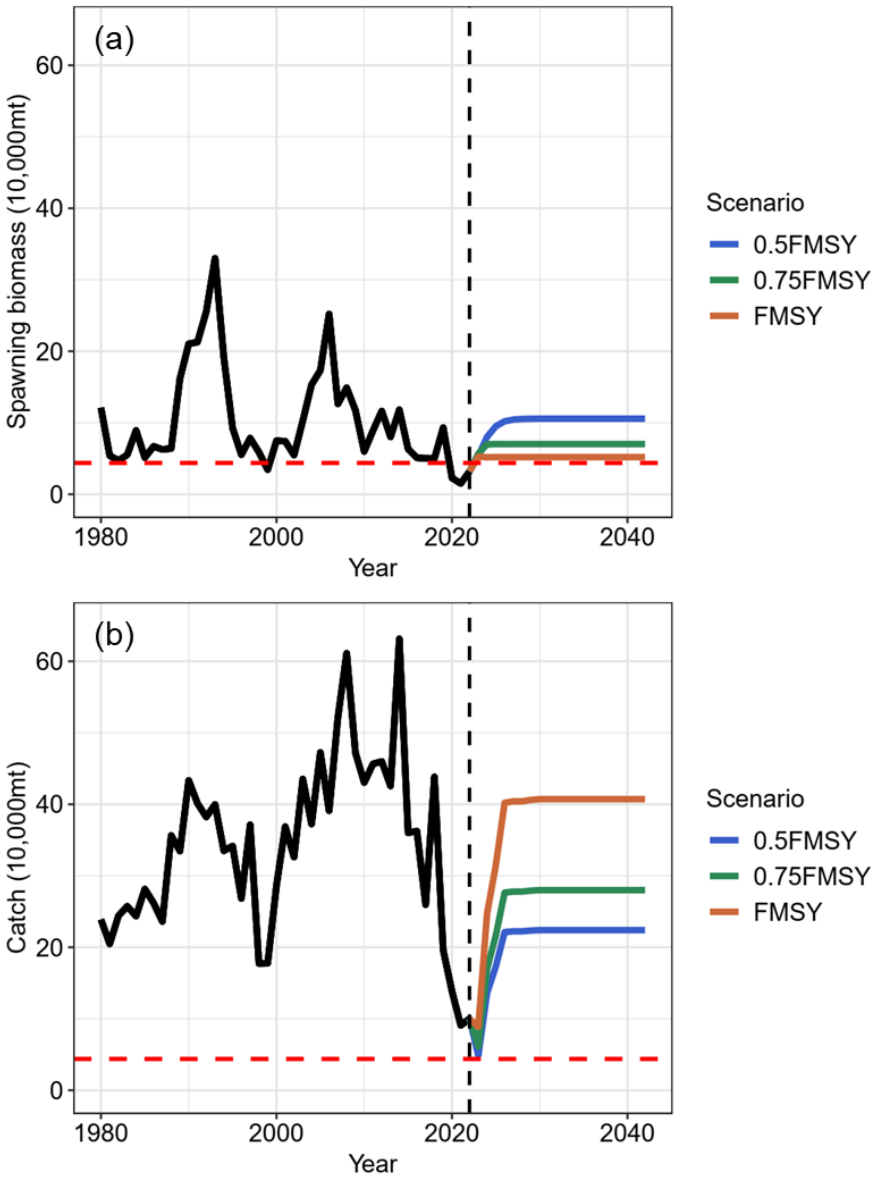

Figure 4.17. Forecasted (a) spawning biomass and (b) catch under three fishing mortality scenarios ($0.5F_{MSY}$, $0.75F_{MSY}$ and F_{MSY}) using a deterministic approach from 2023 – 2042 for Pacific saury. The dashed red lines in each panel represent the SSB_{MSY} and MSY, respectively.

doi:10.6342/NTU202500253

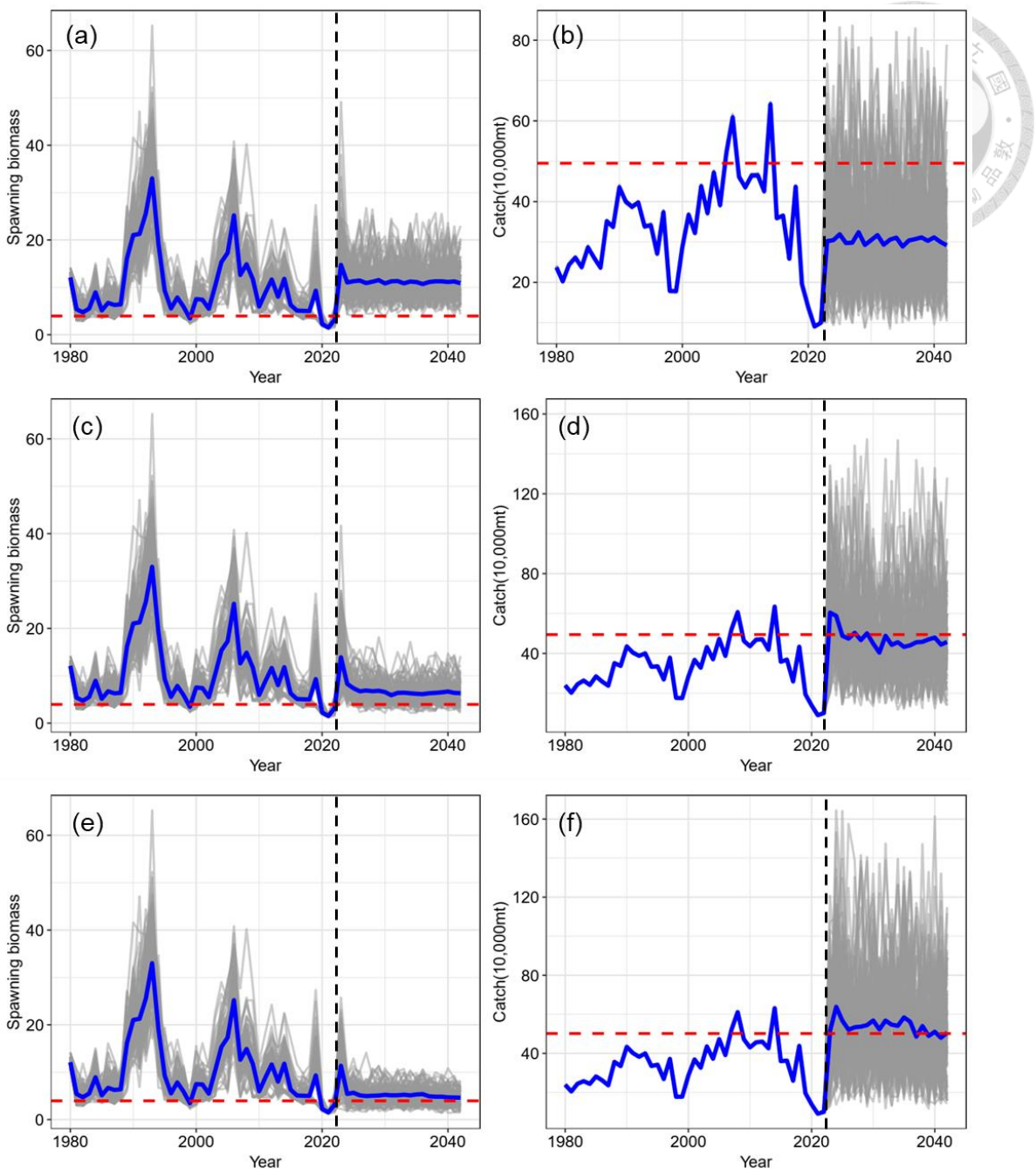

Figure 4.18. Forecasted spawning biomass (left) and catch (right) under three fishing mortality scenarios ($0.5F_{MSY}$, $0.75F_{MSY}$ and F_{MSY}) using a stochastic approach from 2023 – 2042 for Pacific saury. The dashed red lines in each panel represent the SSB_{MSY} and MSY, respectively.

doi:10.6342/NTU202500253

Appendix tables

Table S1.1. Parameters of the distribution for stock-recruitment steepness under the five scenarios for Pacific saury in the Northwestern Pacific Ocean. *CV* denoted the coefficient of variation. 80% P.I. represented the 80% probability interval for steepness.

Scenario	Estimated steepness			
	Mean	Median	*CV*	80% P.I.
1	0.79	0.82	0.18	0.59, 0.93
2	0.96	0.97	0.05	0.91, 0.99
3	0.95	0.97	0.08	0.88, 0.99
4	0.37	0.33	0.39	0.22, 0.59
5	0.50	0.42	0.49	0.23, 0.91

doi:10.6342/NTU202500253

Table S2.1. Summary of model selection information on Pacific saury data by using the likelihood ratio test for each explanatory variable included in the Ad hoc, Binary, Spatial 1, Spatial 0.1 GLMMs and VAST for Pacific saury in the Northwestern Pacific Ocean during 1997 – 2019.

Model	Variables	Deviance	Number of parameters	*p*-value
Ad hoc	-*Area*	286992	28	<0.001
	-*SST*+*SST*^{2}	287179	29	<0.001
	-*Vessel*	290535	30	<0.001
	-*Year*×*Area*	289624	30	<0.001
	Full	284748	31	<0.001
Binary	-*Area*	281147	28	<0.005
	-*SST*+*SST*^{2}	281159	29	<0.001
	-*Vessel*	284923	30	<0.001
	-*Year*×*Area*	285834	30	<0.001
	Full	280846	31	<0.001
Spatial 1	-*Area*	278613	28	<0.001
	-*SST*+*SST*^{2}	278628	30	<0.001
	-*Vessel*	282355	31	<0.001
	-*Year*×*Area*	283293	31	<0.001
	Full	278420	32	<0.001
Spatial 0.1	-*Area*	277783	28	<0.001
	-*SST*+*SST*^{2}	277622	30	<0.001
	-*Vessel*	281343	31	<0.001
	-*Year*×*Area*	281157	31	<0.001
	Full	275648	32	<0.001
VAST	-*Spatial*	1064595	45	<0.001
	-*SST*+*SST*^{2}	1064501	45	<0.001
	-*Vessel*	1066833	44	<0.001
	-*Spatio-temporal*	1071044	44	<0.001
	Full	1050998	46	<0.001

doi:10.6342/NTU202500253

Table S3.1. Results of parsimonious backward search based on the Akaike Information Criterion. Omega is the spatial variation; epsilon is the spatio-temporal variation; sst is the sea surface temperature; sst^2 is temperature-quadratic equation; ssh is the sea surface height; chl*a* is the concentration of chlorophyll-*a*; pdo(N) and pdo(E) is the Pacific Decadal Oscillation index (PDO) with northing and easting direction, respectively; soi(N) and soi(E) is the Southern Oscillation Index with northing and easting direction, respectively; and *q* is the catchability (fleets). The AIC denotes the resultant value after removing each variable. Smaller AIC value indicates the most parsimonious model, and the larger value in the table indicates the larger impact after removing the variable.

Backward batch	ID	Variables	AIC value
Batch 1		NULL	--
	1	-omega	60532.47
	2	-epsilon	--
	3	-sst	60499.58
	4	-sst^2	60499.42
	5	-ssh	--
	6	-chl*a*	60498.88
	7	-pdo(N)	--
	8	**-pdo(E)**	**60497.26**
	9	-soi(N)	--
	10	-soi(E)	--
	11	-*q*	60749.16
Batch 2	1	-omega	60530.47
	2	-epsilon	--
	3	-sst	60495.65
	4	-sst^2	60495.48
	5	-ssh	--
	6	-chl*a*	--
	7	**-pdo(N)**	**60494.44**
	8	-soi(N)	60526.44
	9	-soi(E)	60513.86
	10	-*q*	60745.31
Batch 3	1	-omega	--
	2	-epsilon	--
	3	-sst	60493.11
	4	-sst^2	60492.99
	5	**-ssh**	**60486.9**
	6	-chl*a*	60491.04
	7	-soi(N)	--
	8	-soi(E)	60519.14
	9	-*q*	60742.21
Batch 4	1	-omega	60522.85
	2	-epsilon	61116.74
	3	-sst	60513.41
	4	-sst^2	60498.93
	5	-chl*a*	60487.75
	6	-soi(N)	60488.14
	7	-soi(E)	60561.54
	8	-*q*	60738.58

doi:10.6342/NTU202500253

Appendix figures

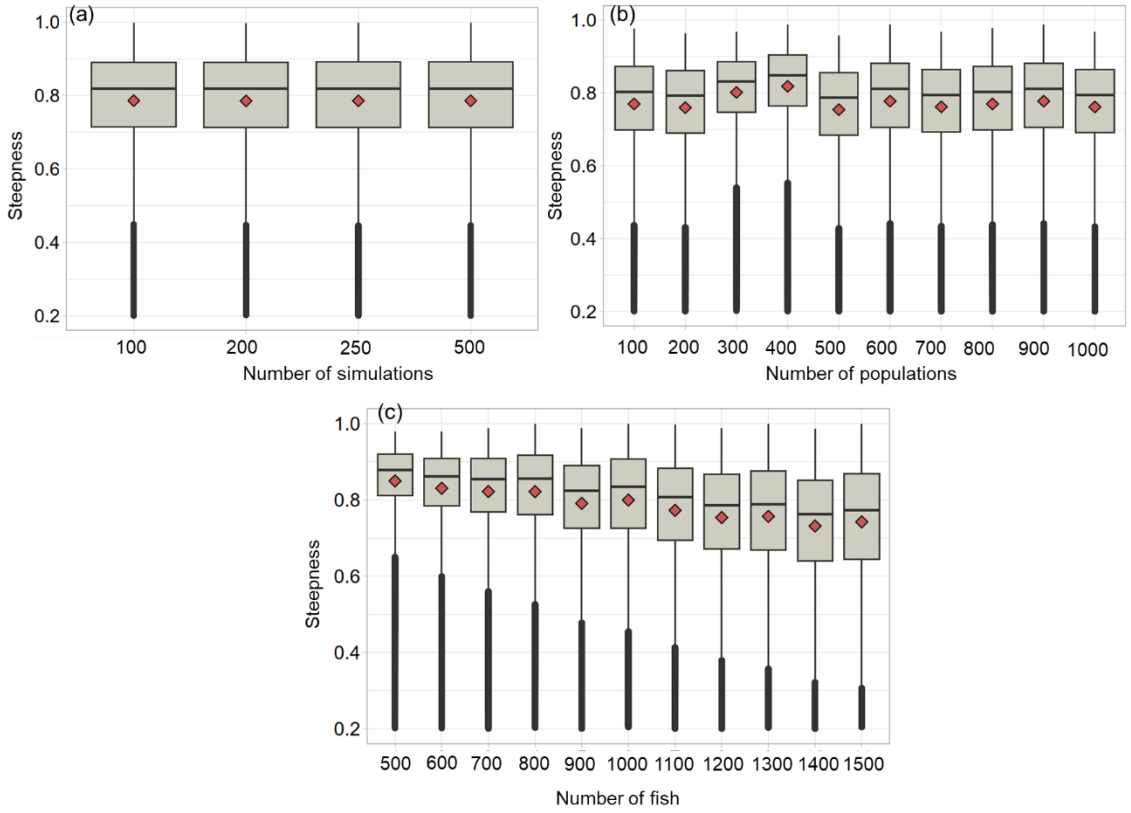

Figure S1.1. Boxplots of summaries of steepness values for Pacific saury in the Northwestern Pacific Ocean as a function of (a) the number of simulations (100, 200, 250, 500); (b) the number of populations (100, 200, 300, 400, 500, 600, 700, 800, 900, 1000); and (c) the number of fish per population (500, 600, 700, 800, 900, 1000, 1100, 1200, 1300, 1400, 1500). Red diamonds indicated the mean values.

doi:10.6342/NTU202500253

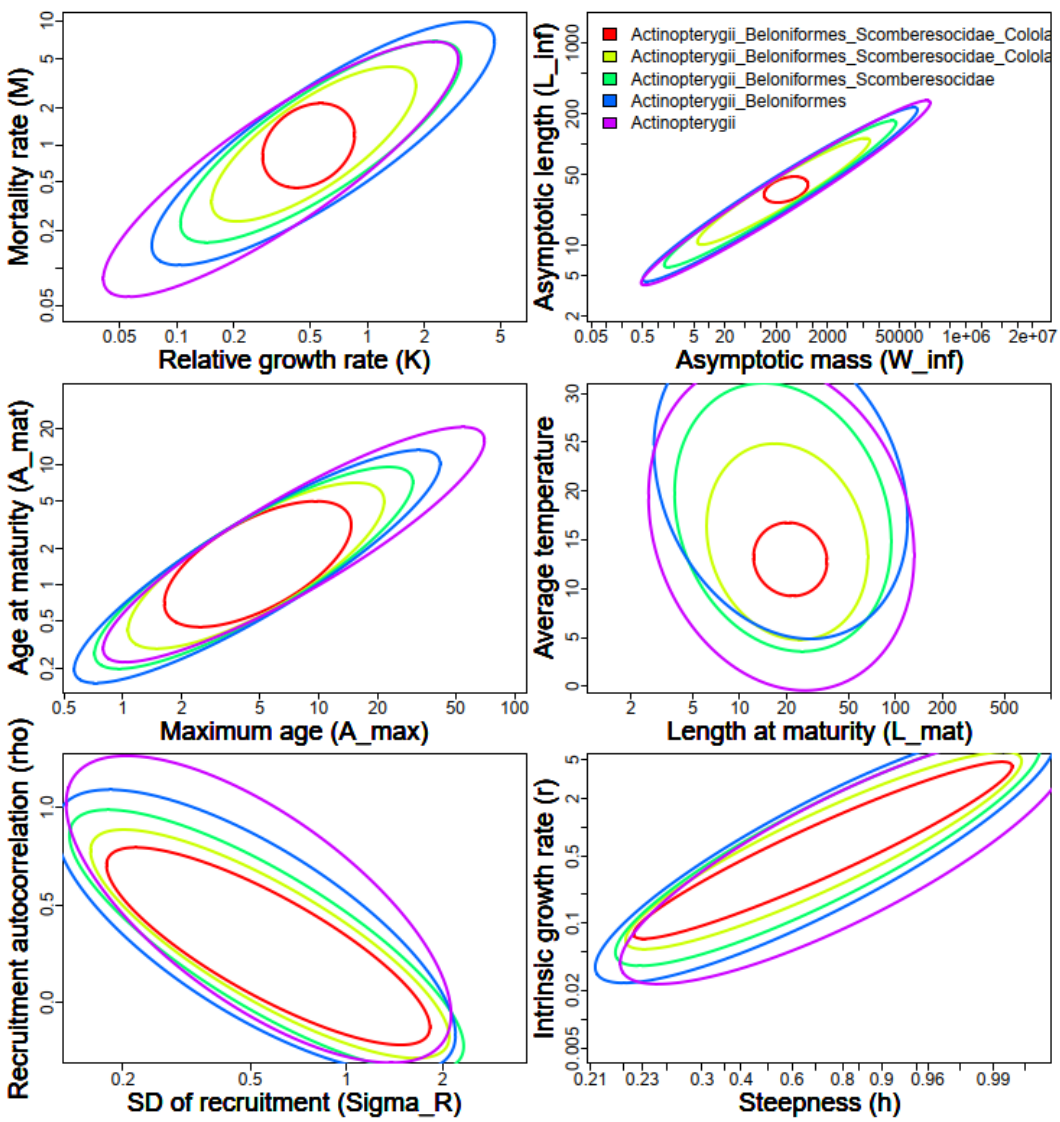

Figure S1.2. Predictive distribution for selected life-history and stock-recruit parameters for Pacific saury from the R package of *FishLife* (Thorson, 2019).

doi:10.6342/NTU202500253

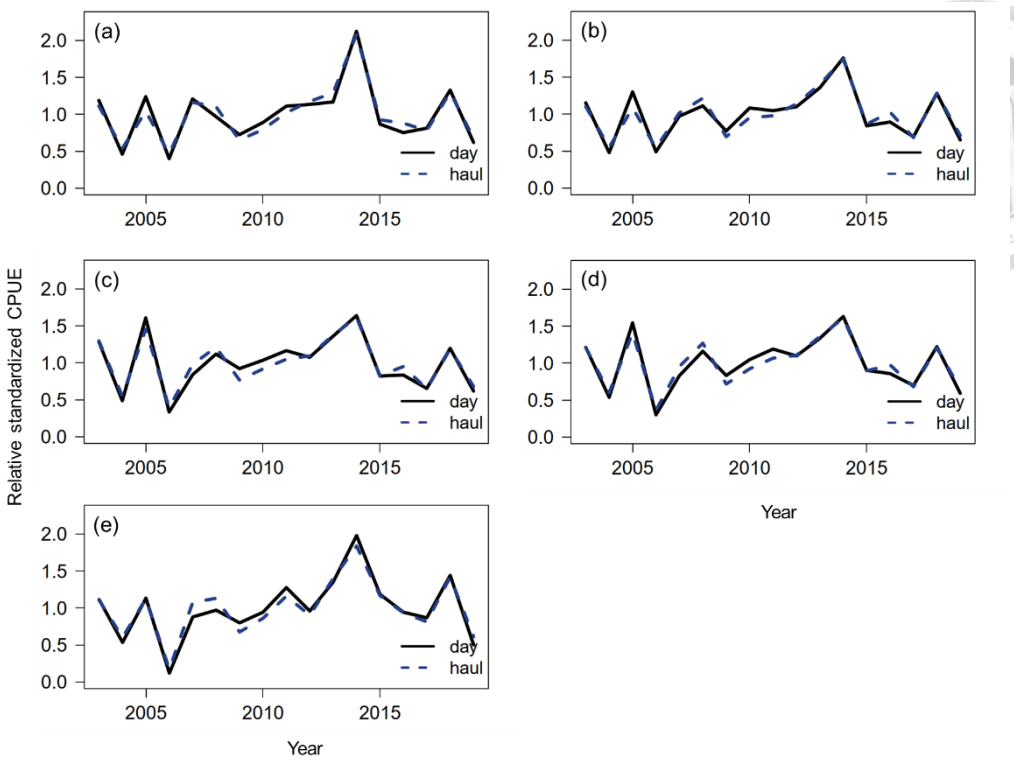

Figure S2.1. Annual trends of the relative standardized abundance indices (normalized to their mean) calculated by using the effort metrics of fishing day (in black line), and haul (dashed line) for (a) Ad hoc, (b) Binary, (c) Spatial 1, (d) Spatial 0.1 GLMMs and (e) VAST for Pacific saury in the Northwestern Pacific Ocean during 1997 – 2019.

doi:10.6342/NTU202500253

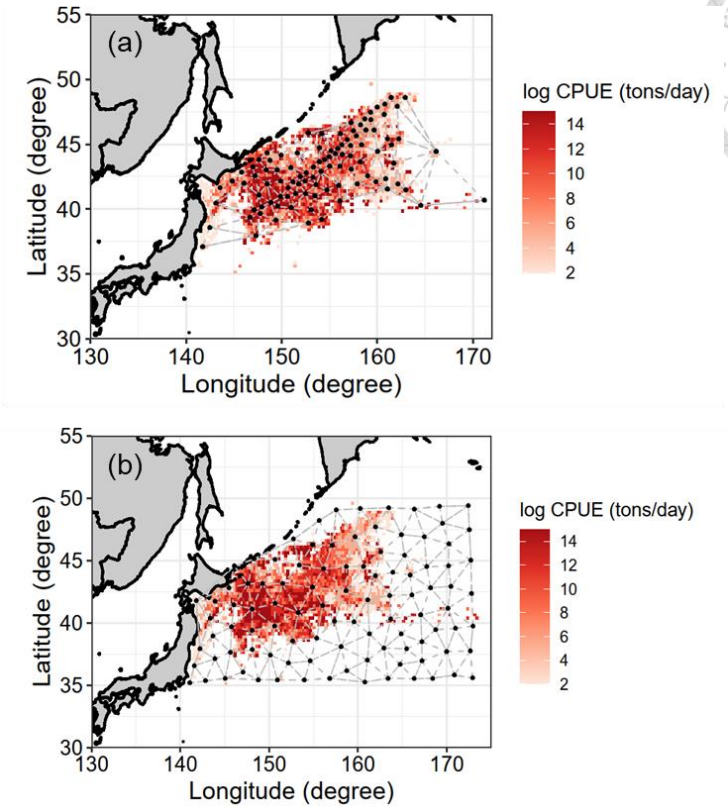

Figure S2.2. The defined spatial distribution of knots (in black points) based on (a) the *k*-means algorithm and (b) uniform allocation (in red colors) for the Pacific saury data in the Northwestern Pacific Ocean during 1997 – 2019.

doi:10.6342/NTU202500253

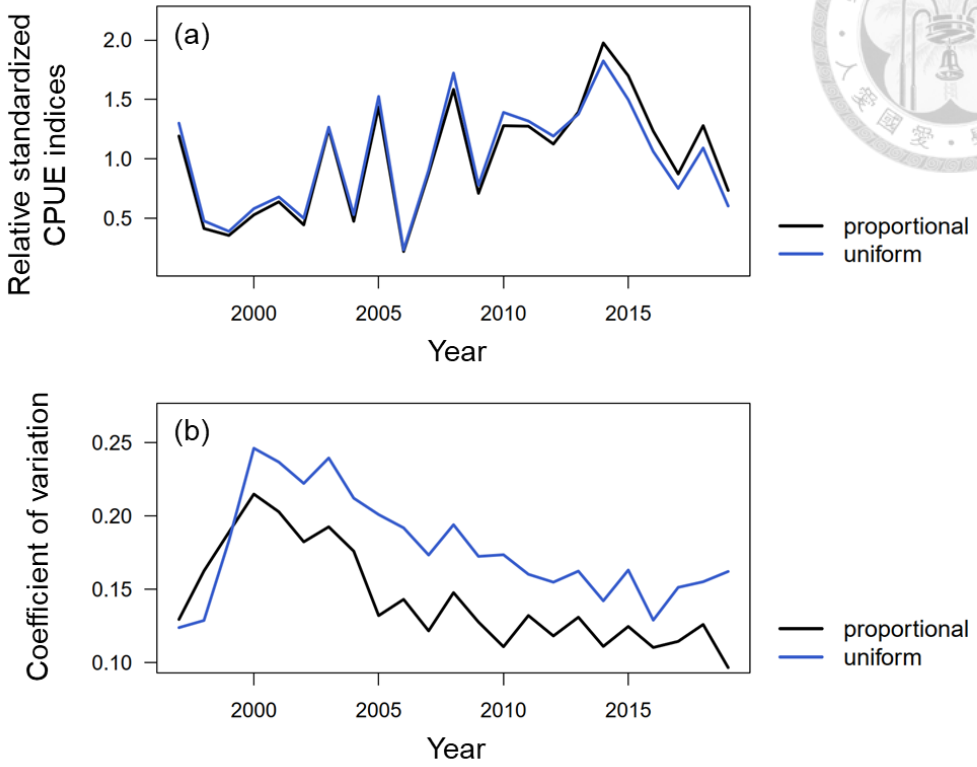

Figure S2.3. Results of (a) standardized CPUEs (normalized to their mean) and (b) coefficient of variations derived from VAST with proportional knot distribution (in black line) and the uniform knot distribution (in blue line).

doi:10.6342/NTU202500253

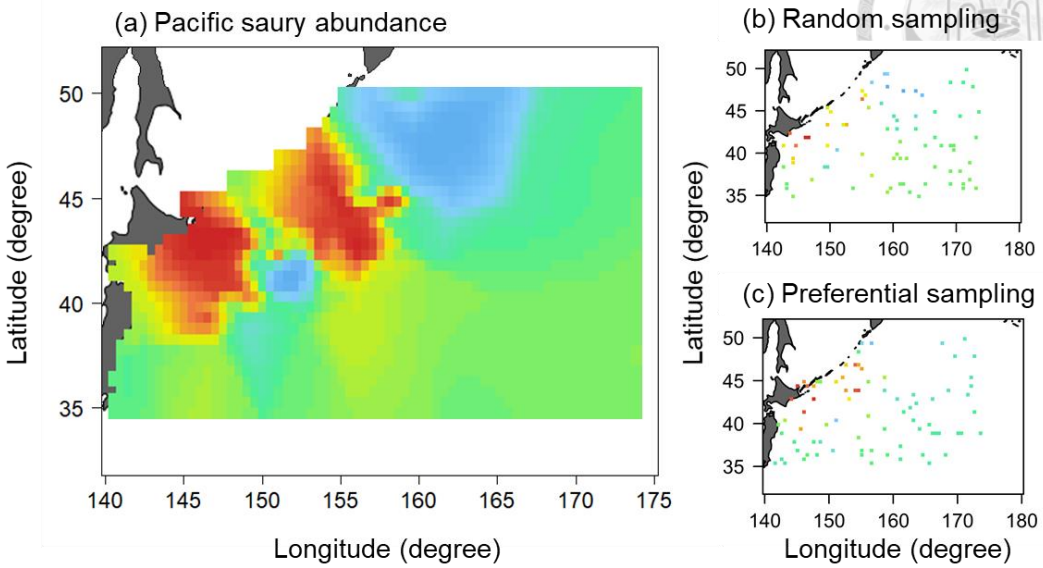

Figure S2.4. (a) Simulated spatial distribution of Pacific saury abundance in the Northwestern Pacific Ocean. Red (blue) colors indicate greater (smaller) levels of abundance. The simulated distributions of fishery data for the Pacific saury with (b) random sampling and (c) preferential sampling scenarios.

doi:10.6342/NTU202500253

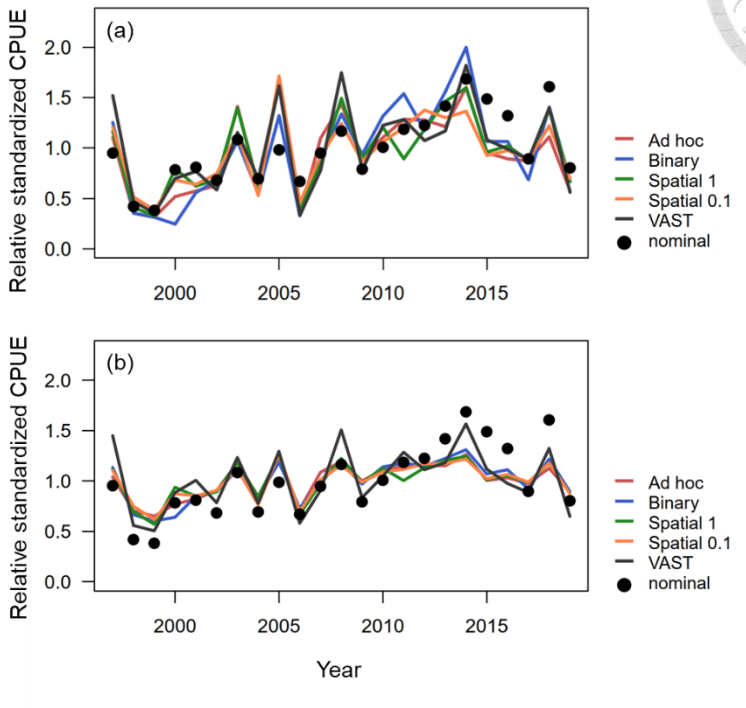

Figure S2.5. Annual trends of (a) the relative standardized abundance indices (normalized to their mean) without area-weighting, and (b) with area-weighting for the Ad hoc, Binary, Spatial 1, Spatial 0.1 GLMMs, and VAST for Pacific saury in the Northwestern Pacific Ocean during 1997 – 2019. Solid black points represent the annual nominal CPUEs for Pacific saury.

doi:10.6342/NTU202500253

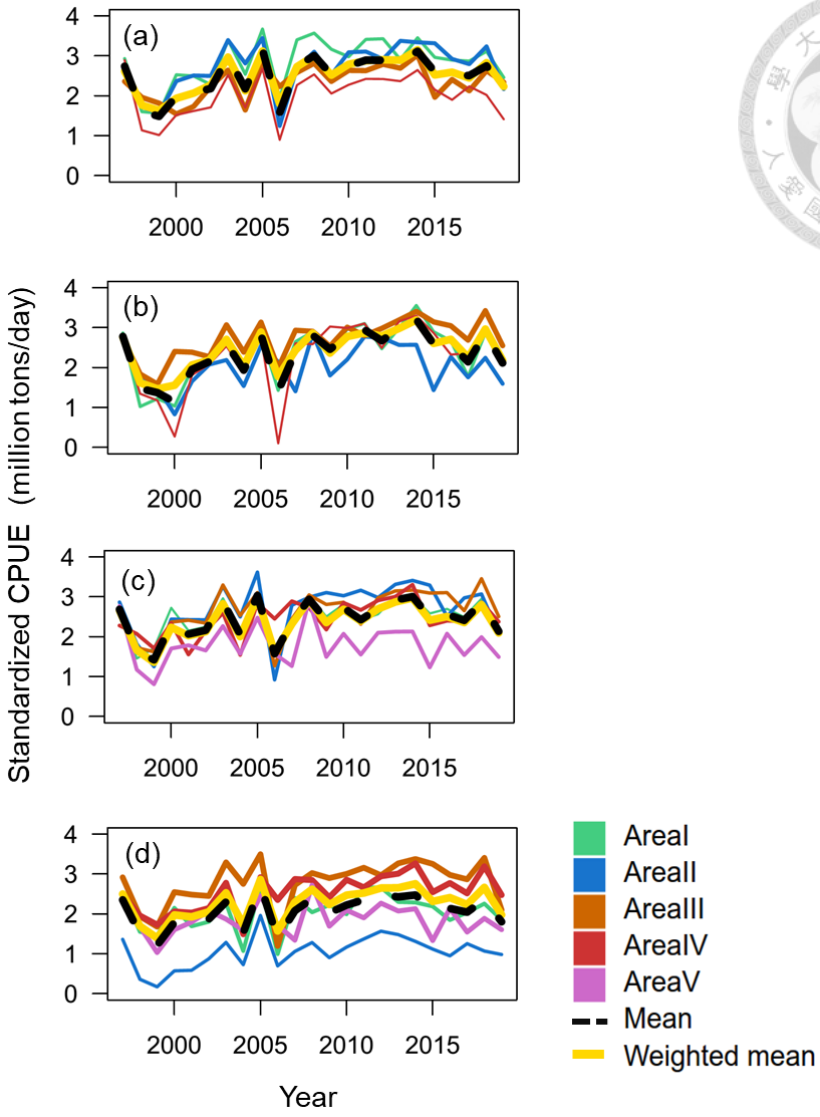

Figure S2.6. Time series of the standardized abundance indices for each area derived from the (a) Ad hoc, (b) Binary, (c) Spatial1 and (d) Spatial 0.1 GLMMs for Pacific saury in the Northwestern Pacific Ocean during 1997 – 2019. Black dash line represents the arithmetic mean of standardized abundance over areas. Yellow solid line represents the weighted mean of standardized abundance over areas. Thickness of line represents the size of the surface area for each area strata (a larger surface area has a thicker line).

doi:10.6342/NTU202500253

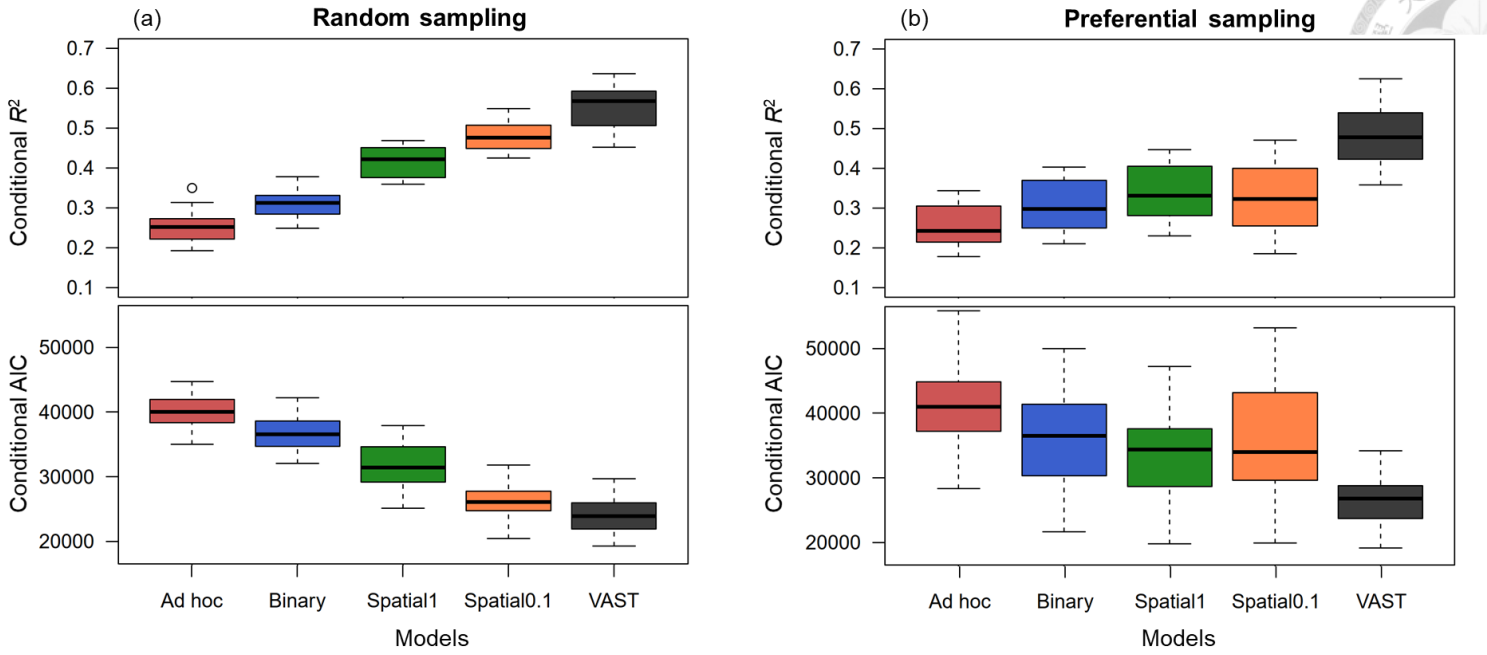

Figure S2.7. The boxplots of model selection criteria for the conditional R^2 and conditional AIC derived from all replicates under the (a) random and (b) preferential sampling scenarios for the Ad hoc, Binary, Spatial 1, Spatial 0.1 GLMMs and VAST.

doi:10.6342/NTU202500253

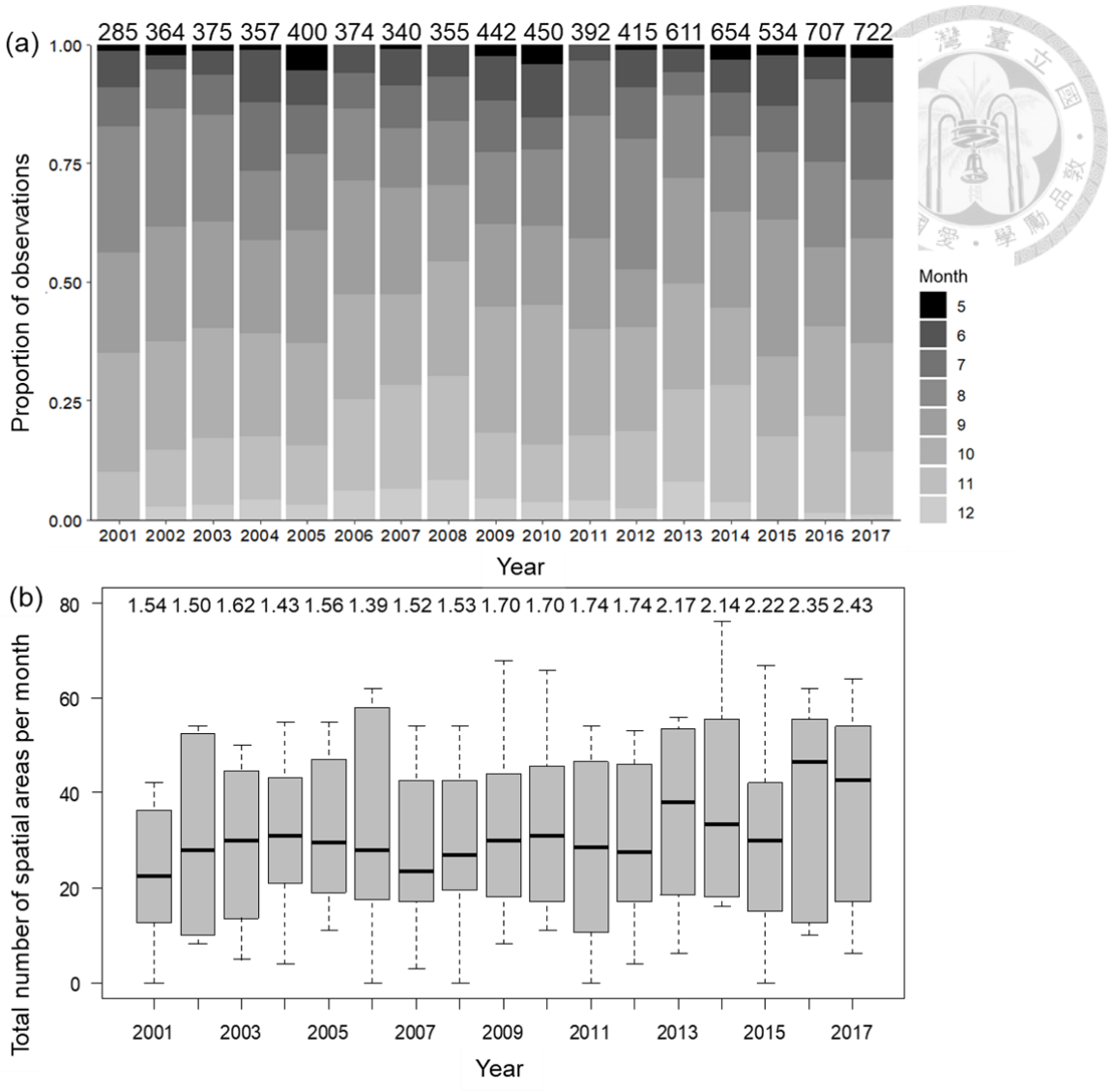

Figure S3.1. The monthly composition of the spatial grid (1°×1° grid) in proportions (a) and the boxplot of total number of spatial areas per month (i.e., the number of unique grids for each month) for the Pacific saury fishery-dependent data from all members of NPFC collected in the fishing season (May to December) during 2001 and 2017. The numbers above panel (a) and (b) are the total number of observations and the average sample size per spatial grid, respectively.

doi:10.6342/NTU202500253

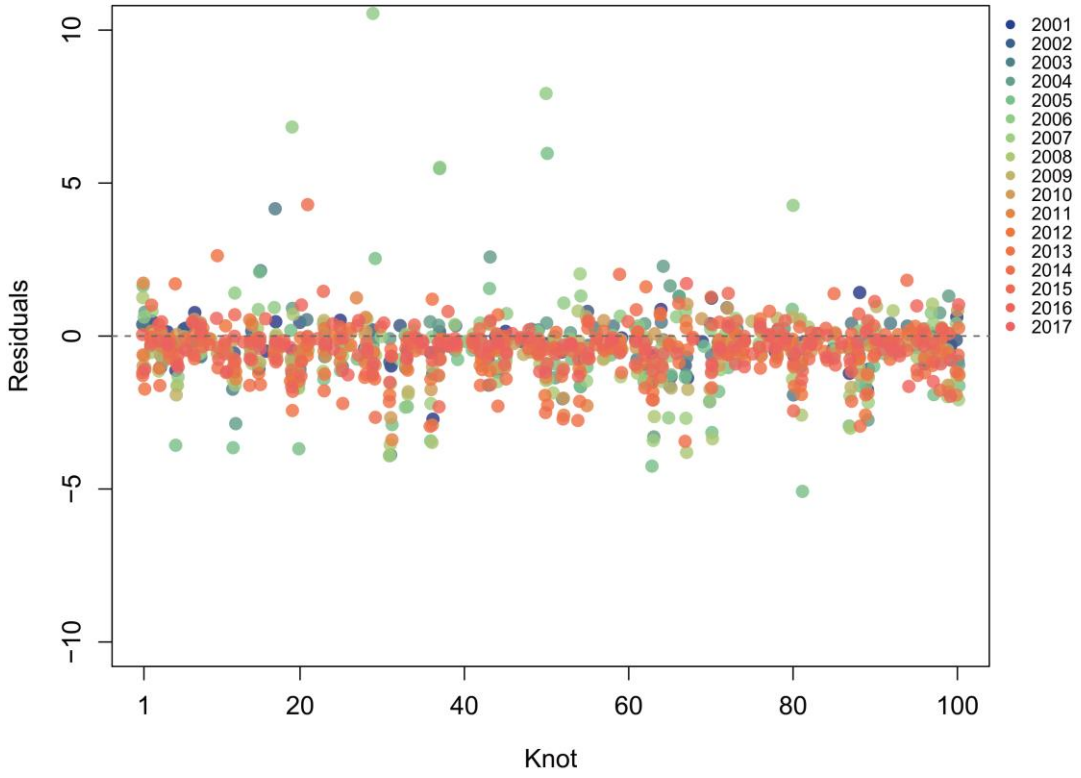

Figure S3.2. Time-series of model residuals (unit: mass of fish in metric ton per day per square degree) for each knot. Color circles indicated the residuals from 2001 to 2017.

doi:10.6342/NTU202500253

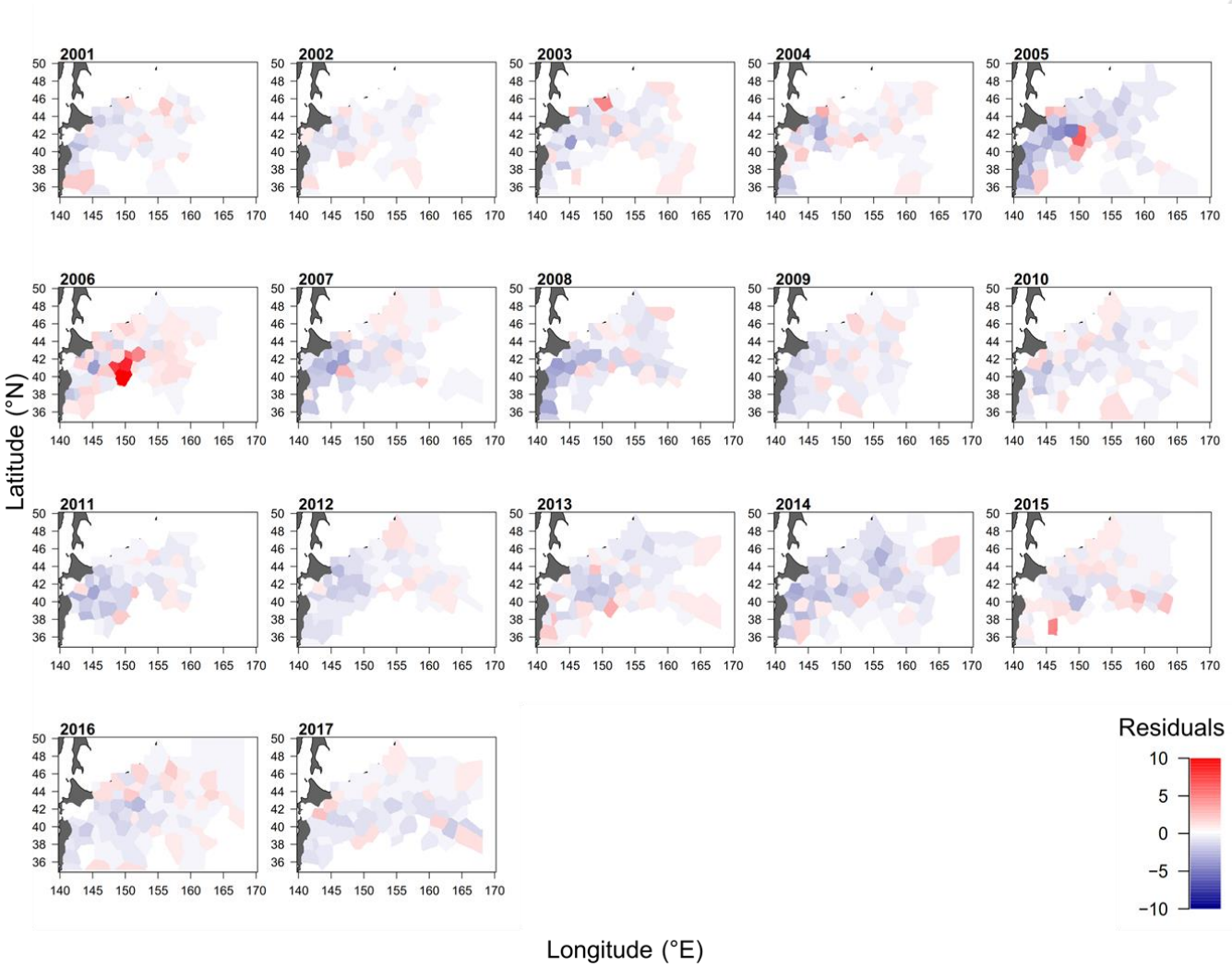

Figure S3.3. Spatial distribution of model residuals (unit: mass of fish in metric ton per day per square degree) from 2001 to 2017.

doi:10.6342/NTU202500253

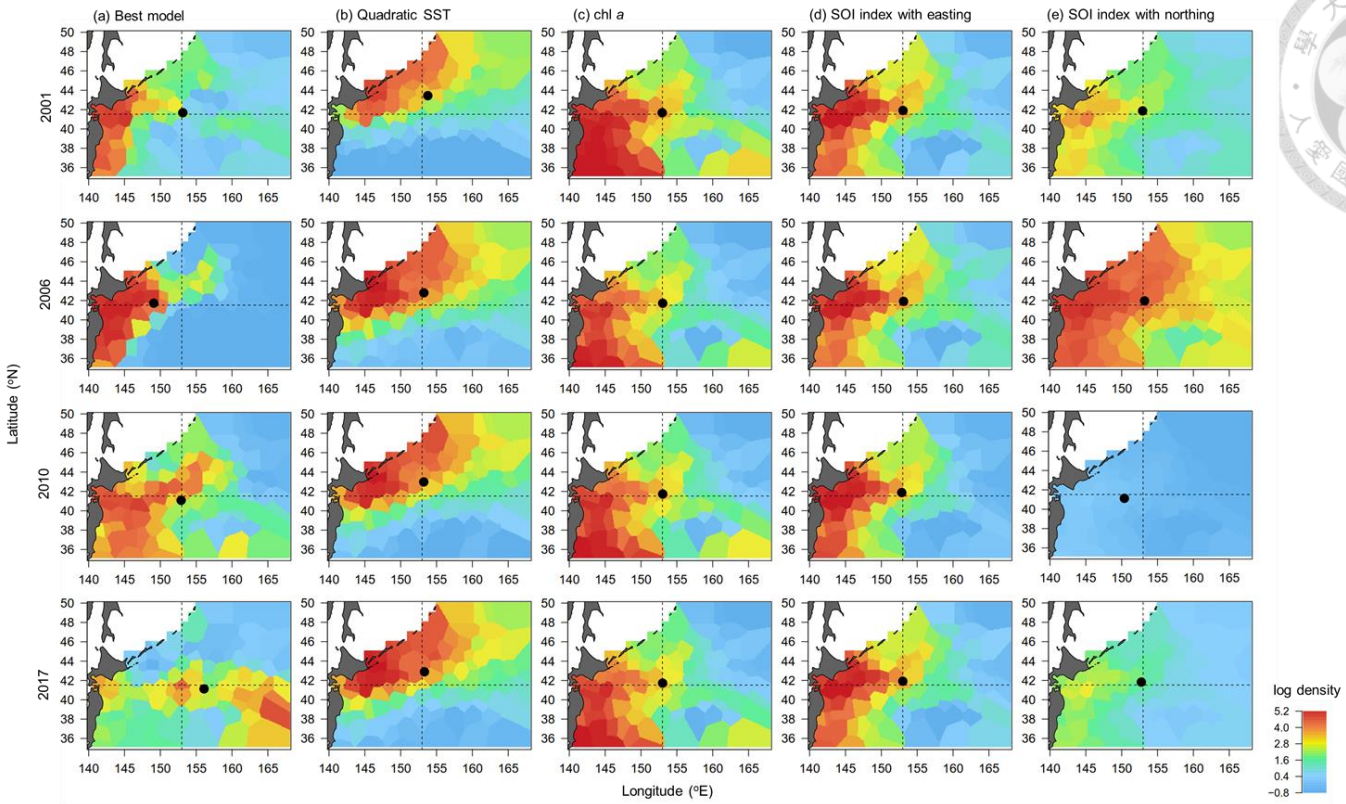

Figure S3.4. Estimated logarithm density (unit: mass of fish in metric ton per day per square degree) in 2001, 2006, 2010 and 2017 of the Pacific saury from the best model (a), compared with each hypothesized driver that eliminates all causes for variation in distribution except the quartic SST (b), chl-*a* (c), SOI index with easting (d), and SOI index with northing (e). The black circle represents the location of the estimated centroid of gravity (COG) for each model. The dashed line represents the average location of the estimated centroid of gravity (COG) from the best model.

doi:10.6342/NTU202500253

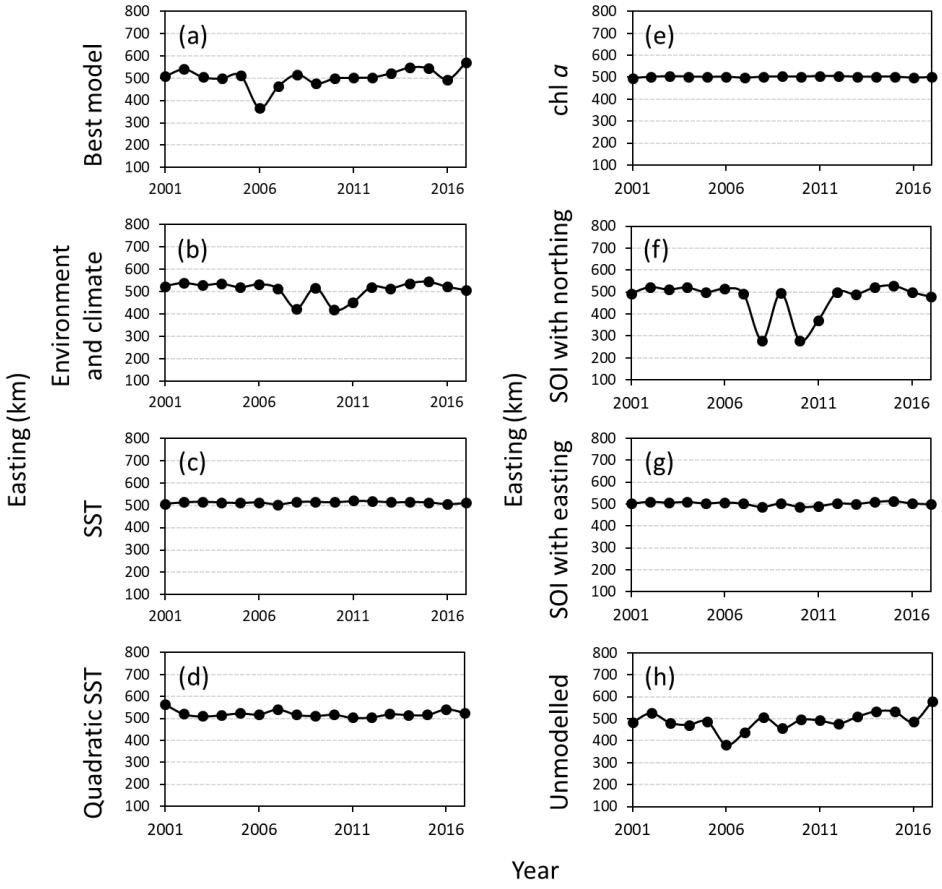

Figure S3.5. The estimated centroid-of-gravities (COGs) during 2001 – 2017 from the best model (a) in easting direction compared with each hypothesized driver that eliminates all causes for variation in distribution except the multiple environmental variables and climatic indices (b), SST (c), quadratic SST (d), chl-*a* (e), SOI index with northing and easting (f, g), and the unmodelled variable (h).

doi:10.6342/NTU202500253

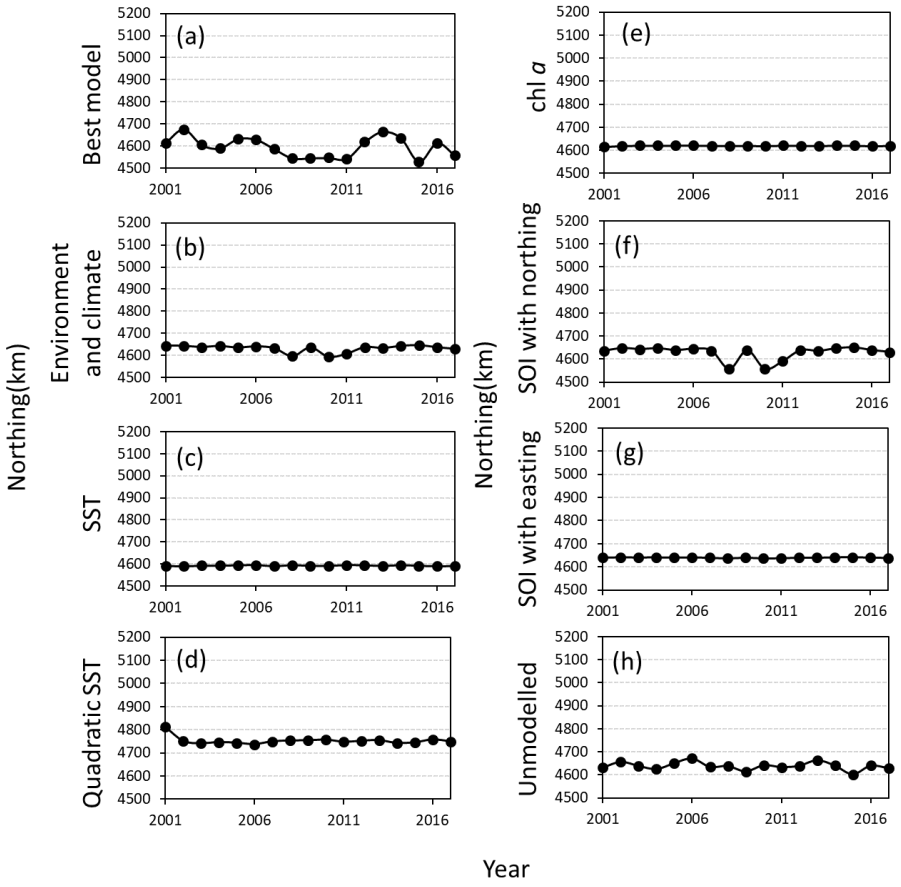

Figure S3.6. The estimated centroid-of-gravities (COGs) during 2001 – 2017 from the best model (a) in northing direction compared with each hypothesized driver that eliminates all causes for variation in distribution except the multiple environmental variables and climatic indices (b), SST (c), SST-squared (d), chl-*a* (e), the SOI index with northing and easting (f, g), and the unmodelled variable (h).

doi:10.6342/NTU202500253

Curriculum Vitae

JHEN HSU

Email: jhenhsu@ntu.edu.tw; jhene.hsu@gmail.com

Room 413, Institute of Oceanography, National Taiwan University,

No.1, Sec. 4, Roosevelt Road, Taipei, Taiwan

EDUCATION

Ph. D. Student Institute of Oceanography, National Taiwan University, Taiwan (2019 – 2025)

M.S. Institute of Fisheries, National Taiwan University, Taiwan (2016 – 2018)

B.S. Department of Environmental Biology & Fisheries Science, National Taiwan Ocean University (2012 – 2016)

RESEARCH EXPERIENCE

2019 Sep – present: Modelling scientist in a stock assessment of Pacific saury (*Cololabis saira*) in the North Pacific Ocean. The stock assessment was conducted by the NPFC Small Scientific Committee on Pacific Saury, chaired by Dr. Toshihide Kitakado.

2019 Nov – present: Developing the joint CPUE index of the Pacific saury in the Northwest Pacific Ocean by using the spatio-temporal approach. The joint CPUE standardization work was conducted by the NPFC Small Scientific Committee on Pacific Saury, chaired by Dr. Toshihide Kitakado.

2019 Dec – present: Analyzing Taiwanese longline fisheries statistics and assisting in the standardization of catch rate analysis for the billfish and albacore by using the spatio-temporal approach. The Billfish Working Group (BILLWG) and Albacore Working Group (ALBWG) of the International Scientific Committee for Tuna and Tuna-like Species in the North Pacific Ocean (ISC), chaired by Dr. Michelle Sculley and Dr. Sarah Hawkshaw.

JOURNAL ARTICLES (Peer-reviewed journals)

1. **Hsu, J.**, Chang, Y. J., Brodziak, J., Kai, M., and Punt, A. E. (2024). On the probable distribution of stock-recruitment resilience of Pacific saury (*Cololabis saira*) in the

doi:10.6342/NTU202500253

Northwest Pacific Ocean. *ICES Journal of Marine Science, 81*, 748-759.
2. Hung, W. C., **Hsu, J**., Chang, Y. J., Huang, W. B., Hsieh, C. H., and Chung, M. T. (2023). Spatiotemporal variations and influential factors affecting reproductive dynamics of Pacific saury in the Northwest Pacific during fishing season. *Journal of Fish Biology*, *103*, 1335-1346.
3. **Hsu, J**., Chang, Y. J., and Ducharme-Barth, N. D. (2022). Evaluation of the influence of spatial treatments on catch-per-unit-effort standardization: A fishery application and simulation study of Pacific saury in the Northwestern Pacific Ocean. Fisheries Research, 255, 106440.
4. Chang, Y. J., **Hsu, J.**, Lai, P. K., Lan, K. W., and Tsai, W. P. (2021). Evaluation of the Impacts of Climate Change on Albacore Distribution in the South Pacific Ocean by Using Ensemble Forecast. Frontiers in Marine Science, 1404.
5. Shiao, J. C., **Hsu, J.**, Cheng, C. C., Tsai, W. Y., Lu, H. B., Tanaka, Y., and Wang, P. L. (2021). Contribution rates of different spawning and feeding grounds to adult Pacific bluefin tuna (*Thunnus orientalis*) in the northwestern Pacific Ocean. Deep Sea Research Part I: Oceanographic Research Papers, 169, 103453.
6. **Hsu, J.**, Chang, Y. J., Kitakado, T., Kai, M., Li, B., Hashimoto, M., Hsieh, C-H., Kulik, V., Park, K. J. (2021). Evaluating the spatiotemporal dynamics of Pacific saury in the Northwestern Pacific Ocean by using a geostatistical modelling approach. Fisheries Research, 235, 105821.
7. Chang, Y. J., Winker, H., Sculley, M., and **Hsu, J**. (2020). Evaluation of the status and risk of overexploitation of the Pacific billfish stocks considering non-stationary population processes. Deep Sea Research Part II: Topical Studies in Oceanography, 175, 104707.
8. Chang, Y. J., **Hsu, J.**, Shiao, J. C., and Chang, S. K. (2019). Evaluation of the effects of otolith sampling strategies and ageing error on estimation of the age composition and growth curve for Pacific bluefin tuna *Thunnus orientalis*. Marine and Freshwater Research, 70, 1838-1849.
9. Chang, Y. J., Lan, K. W., Walsh, W. A., **Hsu, J.**, and Hsieh, C. H. (2019). Modelling the impacts of environmental variation on habitat suitability for Pacific saury in the Northwestern Pacific Ocean. Fisheries Oceanography, 28, 291-304.
10. Shiao, J. C., Lu, H. B., **Hsu, J.**, Wang, H. Y., Chang, S. K., Huang, M. Y., and Ishihara, T. (2017). Changes in size, age, and sex ratio composition of Pacific bluefin tuna (*Thunnus orientalis*) on the northwestern Pacific Ocean spawning grounds. ICES Journal of Marine Science, 74, 204-214.

doi:10.6342/NTU202500253

GRADUATE RESEARCH EXPERIENCE

Area of Specialization: Fisheries Biology, Quantitative Modelling in Fish Population Dynamics. Good knowledge in R and TMB. Excellent experience with Bayesian surplus production models, Stock Synthesis and spatio-temporal modeling (R packages: VAST)

PROFESSIONAL SOCIETIES

ICES training course: Advanced stock assessment with RTMB (Nanaimo, Canada, 2024; NPFC funding support)

North Pacific Fisheries Commission (NPFC) (Since 2019)

International Scientific Committee for Tuna and Tuna-like Species in the North Pacific Ocean (ISC) (Since 2019)

AWARD & SCHOLARSHIP

Best oral presentation, PICES 2022 Annual Meeting, Busan, Korea

Third place in Oral Contest, 2021 Oceanographic Society of the Republic of China.

Scholarship, Graduate Students Study Abroad Program, National Science and Technology Council (2023 – 2024) - Visiting student in the Prof. Punt's lab in University of Washington, Seattle, WA, USA

Scholarships of Fishery Development Foundation of the Fisheries Agency of the Council of Agriculture of Taiwan (2019 – 2020).

doi:10.6342/NTU202500253